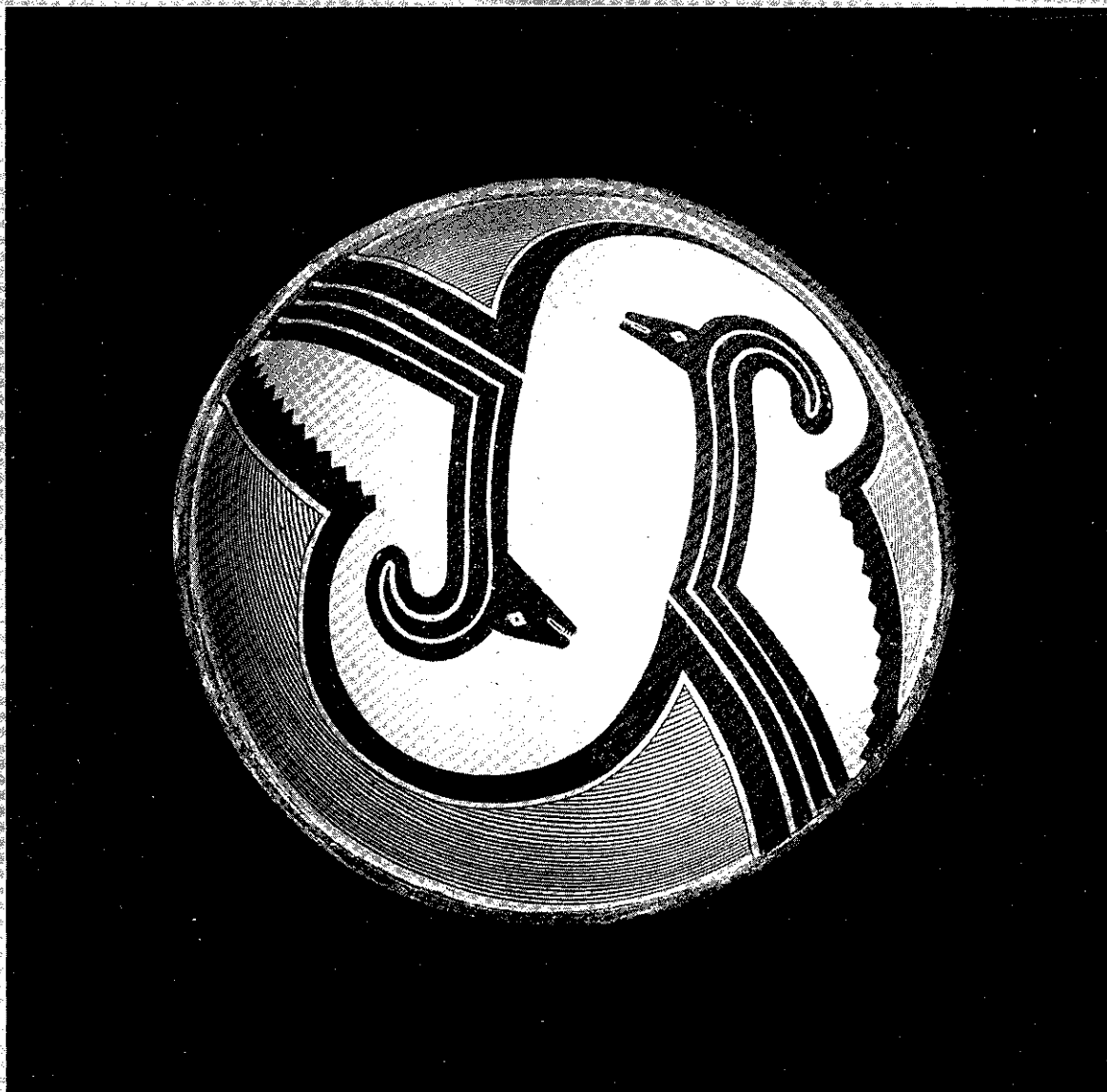


Chun C. Lin

# G E C 9 1

44TH ANNUAL GASEOUS ELECTRONICS CONFERENCE

22-25 OCTOBER, 1991, ALBUQUERQUE, NEW MEXICO



THE UNIVERSITY OF NEW MEXICO

# 44<sup>th</sup> Annual Gaseous Electronics Conference

22-25 October 1991 • Albuquerque, New Mexico

## PROGRAM AND ABSTRACTS

A Sponsored Conference  
of the  
American Physical Society,  
Division of Atomic, Molecular, and Optical Physics

Hosted by:  
Department of Chemical & Nuclear Engineering  
Center for High Technology Materials  
The University of New Mexico

### EXECUTIVE COMMITTEE

Chun C. Lin Chairman University of Wisconsin	Harold M. Anderson Secretary University of New Mexico
Pablo Vicharelli Secretary-elect GTE Laboratories	W. Lowell Morgan Treasurer Kinema Research
Russell A. Bonham Indiana University	Herbert H. Sawin Massachusetts Institute of Technology
Kurt H. Becker City College of New York	John F. Waymouth Marblehead, MA
John Heidenreich IBM - T. J. Watson	Joseph T. Verdeyen University of Illinois
James B. Gerardo Sandia National Laboratories	

### LOCAL COMMITTEE:

Ken Greenberg Sandia National Laboratories	William Moeny Tetra Corporation
Charles Fleddermann University of New Mexico	

*Front cover* : Mimbres Classic Black on White Bowl  
C 1000 - 1150 A. D.

This bowl is on display at the Maxwell Museum of Anthropology at the University of New Mexico.

On the bowl two mountain sheep are shown in a highly stylized fashion. Since these sheep are not portrayed as they would have been found in the natural world, it may be that this design had a special symbolic meaning, although we do not know what that meaning might have been.

*Cover Design*: Steve Rhodes  
UNM Publications  
Office of Public Affairs

*Photography* : Michael Mouchette

*Printing* : UNM Printing Services

## **ACKNOWLEDGEMENTS**

The Gaseous Electronics Conference gratefully acknowledges the support of the Department of Chemical and Nuclear Engineering, the Center for High Technology Materials (CHTM) and its business office, the College of Engineering and the Administration of the University of New Mexico for assistance with local arrangements. Financial support for the Gaseous Electronics Conference has been provided by:

### **GOVERNMENT AGENCIES**

**The National Science Foundation**

**The Army Research Office**

**The Air Force Office of Scientific Research**

### **MAJOR CORPORATE SPONSORS**

**IBM – International Business Machines Corporation**

**GTE Incorporated**

**The General Electric Company**

**Coherent, Incorporated**

The Gaseous Electronic Conference is sponsored by the American Physical Society, Division of Atomic, Molecular and Optical Physics

## ADDITIONAL SUPPORT

The Gaseous Electronics Conference gratefully acknowledges the following corporations for participating in the GEC '91 Scientific Equipment and Literature Exhibit.

<b>American Institute of Physics</b>	<b>IBM</b>
<b>Balzers</b>	<b>IOP Publishing</b>
<b>Chromex</b>	<b>Key High Vacuum</b>
<b>Coherent Laser Group</b>	<b>Lucas Laboratories</b>
<b>Comdel, Inc.</b>	<b>MCNC</b>
<b>Commonwealth Scientific</b>	<b>MDC Vacuum Products Corporation</b>
<b>CVI Laser Corporation</b>	<b>Melles Griot</b>
<b>EG&amp;G Instruments, Inc.</b>	<b>MKS Instruments</b>
<b>EEV, Inc.</b>	<b>Norcal</b>
<b>ENI</b>	<b>Princeton Instruments</b>
<b>Extrel</b>	<b>Springer Verlag New York, Inc.</b>
<b>Granville-Phillips Company</b>	<b>Tektronix</b>
<b>Huntington Mechanical Laboratories</b>	<b>THT</b>

The educational outreach activities (Science Teacher's Day) conducted in conjunction with GEC '91 were also provided financial support from:

The American Physical Society  
American Vacuum Society: New Mexico Chapter

Particular thanks are to be given to:

Cheryl Brozena – UNM-ChNE Staff Assistant for Special Projects  
Maryanne Danfelser – Teacher's Day and Guest Program Coordinator  
Sophia Garcia – Registration Coordinator  
Mary Mackie – Hotel, Food and Beverage Coordinator  
Roland Wildman – UNM-CHTM Business Office  
Tom Wintrich – Exhibit Manager

## CONTENTS

ACKNOWLEDGMENTS .....	I
PREFACE .....	IV
TECHNICAL PROGRAM .....	1
SESSIONS	
AA. Glows I.....	27
AB. Multiphoton Processes and Negative Ions .....	32
BA. Particulates in RF Discharges.....	36
BB. Collision Processes in Discharges .....	41
CA. Comparison Session on High Density Plasmas .....	46
CB. Dissociation and Heavy Particle Collisions .....	51
D. Posters.....	56
DA. Diagnostics.....	57
DB. GEC Reference Cell and Related RF Discharge Measurements/Modelling .....	61
EA. Cathodes in Discharges: A Review .....	76
EB. Ionization and Electron Collisions .....	79
F. PLENARY LECTURE.....	84
H. Posters.....	86
HA. Transport.....	87
HB. Electron and Photon Collisions.....	93
HC Lamps .....	101
J. Posters.....	107
JA Optical and Probe Diagnostics.....	108
JB Glows .....	114
JC Particles in Plasmas.....	122
K Workshop – GEC Reference Cell Issues.....	126
LA. Lamps and Cathodes.....	127
LB. Electron Excitation and Ionization.....	132
M. Posters.....	137
MA. Glows .....	138
MB. Plasma Surface Interactions.....	146
MC. Heavy Particles and Negative Ions.....	149
NA. Alternative Applications for Plasma Processing .....	157
NB. Discharge Models .....	161
P. Posters.....	166
PA. Collisions in Plasmas.....	167
PB. Emission Spectroscopy.....	172
PC. Pulsed Power.....	178
PD. Alternative Applications for Plasma Processing.....	183
QA. Ionized Gas Physics in Pulsed Power.....	187
QB. Glows II.....	190
RA. Lasers and Switching.....	195
RB. ECR and Induction Plasmas .....	200
Scientific and Literature Exhibit Program.....	205/
Science Teacher's Day Program .....	212/
Index of Authors.....	214

## PREFACE

The decade of the 1990's is opening for the Gaseous Electronics Conference with precedent setting growth. The technical program comprises 110 oral presentations and 191 poster presentations for a total of 301 papers. The total number of authors are 582. Two timely workshops will be held dealing with:

- GEC Reference Cell Issues
- Comparison Session on High Density Plasma Processing

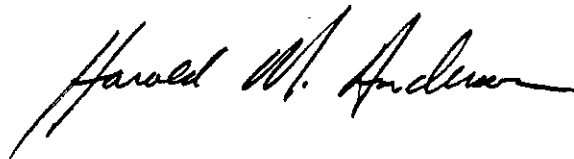
Other arranged sessions deal with:

- Particulates in RF Discharges
- Cathodes in Discharges: A Review
- Electron and Atom Collision Related Phenomena
- New and Alternative Applications for Plasma Processing
- Ionized Gas Physics in Pulsed Power Applications

The plenary session features Dr. Pace Van Devender of Sandia National Laboratories who will present his talk "Plasma Physics Issues for Inertial Fusion with Light Ion Beams." As is customary in the GEC, we anticipate the entire program will provoke lively and spirited discussion about processes occurring in plasmas.

Regular attendees at the GEC will notice several innovative changes in the 1991 meeting. For the first time in our 44 year history the conference will feature a Scientific Equipment and Literature Exhibit. The response to this new feature has exceeded our greatest expectations with 26 corporations exhibiting at the conference. Also in a truly unique experiment, the GEC is proud to announce its first ever educational outreach initiative. The program is designed to provide teachers with information and access to new materials and innovative "hands on" instructional strategies for teaching high school physics and chemistry.

The University of New Mexico and our colleagues throughout the State welcome the attendees of the 44th Gaseous Electronics Conference. Despite the intense demands of the conference agenda, we hope you will find the time to enjoy a few moments appreciating "our land of enchantment."



Harold M. Anderson  
Secretary GEC '91

**TECHNICAL PROGRAM**  
**FORTY FOURTH ANNUAL**  
**GASEOUS ELECTRONICS CONFERENCE**

**REGISTRATION AND RECEPTION**

6:30 - 9:30 PM, Tuesday, October 22, 1991  
 Doubletree Hotel, Ulam Ballroom Albuquerque, NM

1992  
 6:00 - 9:50 PM Monday,  
 Stambro

**SESSION AA. GLOWS I**

8:00 - 10:00 AM, Tuesday, October 22, Ballroom A  
 Chair: C. Fleddermann, University of New Mexico

- |              |      |  |
|--------------|------|--|
| 8:00 - 8:15  | AA-1 | Electron and Metastable Measurements in Helium RF Discharges<br>G.A. Hebner and K.E. Greenberg   |
| 8:15 - 8:30  | AA-2 | Plasma Parameter and EEDF Measurements in Low Pressure Argon and Nitrogen RF Discharges<br>M.B. Hopkins and J.V. Scanlan   |
| 8:30 - 8:45  | AA-3 | Electrical Characteristics of Parallel Plate RF Discharges at 13.56 MHz in Helium and Argon<br>V.A. Godyak, R.B. Piejak, and B.M. Alexandrovich                            |
| 8:45 - 9:00  | AA-4 | Transition From a Capacitive to a Resistive Regime in a RF Discharge in Silane: Experimental and Numerical Diagnostics<br>P. Belenguer, J.P. Boeuf, C. Bohm, and J. Perrin |
| 9:00 - 9:15  | AA-5 | Numerical Analysis of RF Glow Discharges in HCl by RCT Model<br>N. Nakano, T. Makabe, and N. Shimura   |
| 9:15 - 9:30  | AA-6 | Electron Beam - Sheath Interaction in RF Discharges<br>B.P. Wood, M.A. Lieberman, and A.J. Lichtenberg   |
| 9:30 - 9:45  | AA-7 | Ion Energy Distributions in a Simulated RF Plasma with Unequal Area Electrodes<br>R. Boswell and H. Smith  |
| 9:45 - 10:00 | AA-8 | Monte Carlo-Fluid Hybrid Model of RF Glow Discharges in Various Gas Mixtures<br>T.J. Sommerer and M.J. Kushner   |

**SESSION AB. MULTIPHOTON PROCESSES AND NEGATIVE IONS**

8:00 - 10:00 AM, Tuesday, October 22, Ballroom B  
 Chair: B. Stumpf, University of Idaho

- |             |      |   |
|-------------|------|---|
| 8:00 - 8:30 | AB-1 | Atoms and Molecules in Intense Laser Fields<br>H. Helm  |
| 8:30 - 8:45 | AB-2 | Two-Photon Ionization of Trimethylamine using KrF Laser Radiation<br>P.W. Werner and E. Schamiloglu |



- 8:45 - 9:15 AB-3 Progress in  $H^-$  Spectroscopy  
H.C. Bryant
- 9:15 - 9:30 AB-4 Motivation for New  $H^-$  Double Photodetachment Threshold Studies at LAMPF  
J.R. Friedman, X.Q. Guo, K.H. Becker, and M.S. Lubell
- 9:30 - 9:45 AB-5 Enhanced Electron Attachment to Superexcited States of Nitric Oxide  
L.A. Pinnaduwege and L.G. Christophorou
- 9:45 - 10:00 AB-6 Cross Sections for the Formation of Negative Ions by Electron Impact on  $F_2$  and  $SF_6$   
M.V.V.S. Rao and S.K. Srivastava

### SESSION BA. PARTICULATES IN RF DISCHARGES

10:15 - 12:15 PM, Tuesday, October 22, Ballroom A

Chair: J. Heindenreich, IBM - T. J. Watson

- 10:15 - 10:45 BA-1 Particulates in Plasmas: An Astrophysical View  
C.K. Goertz
- 10:45 - 11:00 BA-2 Mapping of the Electrical Properties of Contamination Particle Traps in a Sputter Plasma  
R.N. Carlile and S. Geha
- 11:00 - 11:15 BA-3 The Dependence of the Electrical Properties of Particle Traps and the Plasma Sheath on the Material and Topography of the Wafer Electrodes  
S. Geha, R.N. Carlile and S.E. Beck
- 11:15 - 11:30 BA-4 Simulation of Particulate ("Dust") Transport in RF Glow Discharges  
T.J. Sommerer, J.J. McCaughey and M.J. Kushner
- 11:30 - 11:45 BA-5 Time Evolution of Particle Size in Ar-SiH<sub>4</sub> Plasma, Influence on External Electrical Parameters and Spectral Emissions  
L. Boufendi, A. Bouchoule, J. Ph. Blondeau, A. Plain, C. Laure and M. Toogood
- 11:45 - 12:00 BA-6 Macroscopic Particle Behavior in a Parallel Plate Discharge  
D.B. Graves, J.E. Daugherty, M.D. Kilgore and R.K. Porteous
- 12:00 - 12:15 BA-7 The Transport of Dust Particles in Glow Discharge Plasmas  
J.H. Keller, M.S. Barnes, J.C. Forster, J.A. O'Neill and D.K. Coultas

## SESSION BB. COLLISION PROCESSES IN DISCHARGES

10:15 - 12:15 PM, Tuesday, October 22, Ballroom B

Chair: C. De Joseph, Jr., Wright-Patterson AFB

- 10:15 - 10:30 BB-1 The Effects of Excited State Densities on the Radially Resolved Electron Energy Distribution  
M.J. Hartig and M.J. Kushner
- 10:30 - 10:45 BB-2 Relating Scattering Cross-sections to Transport Data  
E. Kunhardt
- 10:45 - 11:00 BB-3 A Hydrodynamic Model of the Negative Ion Source  
F.A. Haas, A.J.T. Holmes and E. Surrey
- 11:00 - 11:15 BB-4 Surface-Wave-Sustained Plasma Source of a Supersonic Beam of Argon Metastables  
M. Bannister, J.L. Cecchi, and G. Scholes
- 11:15 - 11:30 BB-5 Assessing Reactions in a Discharge in N<sub>2</sub>O from the Light Emission  
T.H. Teich and W. Blumer
- 11:30 - 11:45 BB-6 Interference of Lightning in the Nightglow of Venus  
D.L. Huestis and T.G. Slanger
- 11:45 - 12:00 BB-7 Collisional Processes in Pulsed Laser Deposition of High Temperature Superconducting YBa<sub>2</sub>Cu<sub>3</sub>O<sub>7-8</sub> Thin Films  
N.S. Nogar, R.C. Dye, S.R. Foltyn, R.E. Muenshausen and X.D. Wu
- 12:00 - 12:15 BB-8 Effect of Ion-Ion Collisions on Plasma Flow in the Downstream Region of an ECR Plasma Etching Reactor  
M. Hussein, G.A. Emmert and N. Hershkowitz

## SESSION CA. COMPARISON SESSION ON HIGH DENSITY PLASMAS

1:30 - 3:30 PM, Tuesday, October 22, Ballroom A

Chair: J.H. Keller, IBM - East Fishkill

- 1:30 - 1:42 CA-1 Electron Cyclotron Resonance Plasma Etching  
T.D. Mantei
- 1:42 - 1:54 CA-2 Evaluation of a Permanent Magnet, Ring Multicusp, Etch Chamber with a Remote ECR Plasma Source  
J.R. Trow and J.M. Cook
- 1:54 - 2:06 CA-3 Recent Results from Helicon Reactors  
R.W. Boswell, A.J. Perry and D. Henry
- 2:06 - 2:18 CA-4 Status and Future of Helicon Sources  
F.F. Chen

- 2:18 - 2:30 CA-5 Application of Helicon-Diffusion Reactors for Dry Processing  
R. Van Os, N.M.P. Benjamin and B.N. Chapman
- 2:30 - 2:42 CA-6 High Density Plasma Source for Etching Aluminum Thin Films  
G. Kovall, A. Lamm, and C. Chen
- 2:42 - 2:54 CA-7 The Transformer Coupled Plasma (TCP) Source  
D. Gates, E. Peltzer, H. Nguyen, and J. Holland
- 2:54 - 3:06 CA-8 High Density Plasma Processing Comparison Session - RF Induction  
Multipole  
J.H. Keller and J.C. Forster
- 3:06 - 3:30 DISCUSSION

An open discussion is encouraged on the above topics and any other relevant issues, but the key to a workshop success lies in the contributions from the floor. Spirited and free flowing interjections from the floor are encouraged, as are contributed insights and suggestions. Topics that should be raised include: Are there inherent limitations to the application of any of these plasma sources to plasma etch processing? How do the various systems compare? What are the future challenges to high density plasma systems?

## SESSION CB. DISSOCIATION AND HEAVY PARTICLE COLLISIONS

1:30 - 3:30 PM, Tuesday, October 22, Ballroom B  
Chair: D.J. Eckstrom, SRI International

- 1:30 - 2:00 CB-1 Slow Collisions of Ions with Rydberg Atoms  
K.B. MacAdam
- 2:00 - 2:15 CB-2 Effect of Enhanced Collision Energy on Product Vibrational Excitation for  
the Proton Transfer Reaction:  $O^- + HF \rightarrow F^- + OH(v = 0.1)$   
K. Knutsen, V.M. Bierbaum, and S.R. Leone
- 2:15 - 2:30 CB-3  $NH A \rightarrow X$  and  $OH A \rightarrow X$  Chemiluminescence on  $O^+ - N_2H_4$  Collisions at  
Suprathermal Energies  
J.A. Gardner, R.A. Dressler, R.H. Salter and E. Murad
- 2:30 - 2:45 CB-4 Electron-Impact Dissociation of  $H^+_3$   
A.E. Orel
- 2:45 - 3:00 CB-5 Energetics of the  $O^- + CH_4$  Ion-Molecule Reaction  
H.H. Michels, R.H. Hobbs, A.A. Viggiano, R.A. Morris and  
J.F. Paulson
- 3:00 - 3:15 CB-6 Charge Transfer Reactions of Slow  $He^{++}$  Ions with Molecules  
R.E. Tosh and R. Johnsen

- 3:15 - 3:30 CB-7 The Reactions of  $\text{Si}^+$  Ions with  $\text{CH}_3\text{SiH}_3$ ,  $\text{CH}_3\text{SiD}_3$ ,  $\text{C}_2\text{H}_6$ , and  $\text{CH}_3\text{CHD}_2$   
K.P. Lim and F.W. Lampe

## SESSION D. POSTERS

3:30 - 5:30, Tuesday, October 22, Ballroom C (All poster papers should be posted before the start of the session in the appropriate location, preferably by 1:30 PM, Tuesday, October 22)

### DIAGNOSTICS

- DA-1 Laser Induced Fluorescence Studies of Ion Dynamics in an ECR Etcher  
E.A. Den Hartog, H. Persing, J.S. Hamers, and R.C. Woods
- DA-2 Infrared Diode Laser Absorption Studies in an Electron Cyclotron Resonance Plasma Etching Tool  
R.C. Woods, R.L. McClain, and L.J. Mahoney
- DA-3 Dependence of Optogalvanic Signal on Laser Excitation Region in a Low Power Neon RF Discharge  
D. Kumar and S.P. McGlynn
- DA-4 Mole Fractions of H,  $\text{CH}_3$  and Other Species During Filament-Assisted Diamond Growth  
W.L.-Hsu
- DA-5 A New Pitch-Angle Diagnostic for Magnetized Plasmas  
S.W. Lam and N. Hershkowitz
- DA-6 Characterization of ECR Plasmas Optimized for the Deposition of Polycrystalline Diamond Films  
D.L. Youchison, C.R. Eddy, Jr., and B.D. Sartwell
- DA-7 A Tessellated Probe for Plasma Process Development  
N.M.P. Benjamin, B.N. Chapman, G.T. Grover and K.R. Kreig
- DA-8 Measurement of  $\text{CF}_3$  Radical in RF Excited  $\text{CHF}_3$  Plasma Using Infrared Diode Laser Absorption Spectroscopy  
T. Goto, A. Sakai, M. Naito and N. Itabashi

### GEC REFERENCE CELL AND RELATED RF DISCHARGE MEASUREMENTS AND MODELLING

- DB-1 An Alternative Approach to Identifying Discharge Conditions in the GEC Reference Cell  
V.A. Godyak
- DB-2 A Comparison of Electrical Discharge Characteristics Measured in a Symmetric RF System and in the GEC Reference Cell  
V.A. Godyak, R.B. Piejak and B.M. Alexandrovich

- DB-3 Particle Simulation of Low-Pressure Radio Frequency Discharges  
M.M. Turner
- DB-4 Comparison of Continuum Model Predictions to Results from a Well-Defined Parallel-Plate Reactor  
G.L. Huppert and H.H. Sawin
- DB-5 A Comparison of PIC/MC RF Discharge Simulations to Experimental Measurements  
D.B. Graves, T.E. Nitschke and M. Surendra
- DB-6 Comparison of Fluid and Particle-in-Cell Simulations of RF Glow Discharges  
D.B. Graves, T.E. Nitschke and M. Surendra
- DB-7 Particle-in-Cell/Monte-Carlo Simulations of RF Parallel Plate Discharges: A Parametric Study  
M. Surendra and D.B. Graves
- DB-8 A Bounded Particle in Cell Code With an Atomic Physics Model for Simulating Processing Plasmas  
V. Vahedi, M.A. Lieberman, G. Dipeso, C.K. Birdsall, T.D. Rognlien, J.R. Hiskes and R.H. Cohen
- DB-9 A Comparison of PIC Simulation and Experimental Results in a Capacitive RF Discharge  
P. Mirrashidi, B.P. Wood, V. Vahedi, M.A. Lieberman and C.K. Birdsall
- DB-10 Heating by RF Sheaths  
B.P. Wood, M.A. Lieberman and A.J. Lichtenberg
- DB-11 Heating of Electrons by RF Sheaths  
A.E. Wendt and W.N.G. Hitchon
- DB-12 A Two-Coupled-Sheath Model for the Conduction of Current Through Asymmetric Parallel Plate RF Discharges  
A.H. Sato and M.A. Lieberman
- DB-13 A Computational Investigation of the GEC RF Reference Cell Using a Monte Carlo-Fluid Hybrid Model  
T.J. Sommerer and M.J. Kushner
- DB-14 Three Electron Transport Models by Particle-in-Cell Method for RF Glow Discharge  
C.Li and C. Wu
- DB-15 Nonequilibrium Transport Effects in Space-Time Varying Electric Fields  
J.H. Tsai and C. Wu
- DB-16 Simulations of the GEC RF-Driven Plasma Reactor with He  
M.E. Riley, P. Drallos and R. McGrath
- DB-17 Electrical Isolation of RF Plasma Discharges  
P.A. Miller, H. Anderson and M.P. Splichal

- DB-18 Spectral Signature Analysis and Parallel Optical Emission Spectroscopy for Discharge Characterization  
M.P. Splichal, H.M. Anderson and J.L. Mock
- DB-19 Etching Results from the GEC RF Reference Cell  
P.D. Pochan and P.A. Miller
- DB-20 Impedance Characteristic of the GEC Reference Cell  
J.T. Verdeyen and P.A. Miller
- DB-21 Two-Dimensional Helium Metastable Density Profiles in a GEC RF Reference Cell  
K.E. Greenberg and G.A. Hebner
- DB-22 Confinement and Transient Effects in the GEC Reference Reactor  
P. Bletzinger, A. Garscadden and F.V. Wells
- DB-23 Optical Emission and Electrical Measurements on the NIST GEC RF Reference Cell  
J.R. Roberts, S. Djurovic, J.K. Olthoff and M.A. Sobolewski
- DB-24 Accurate Electrical Measurements of RF Glow Discharges in the NIST GEC Reference Cell  
M.A. Sobolewski, J.K. Olthoff, J.R. Whetstone and J. Roberts
- DB-25 Ion Kinetic Energy Distributions in the GEC Reference Cell  
J.K. Olthoff, R.J. Van Brunt and M.A. Sobolewski
- DB-26 Measurements on the Michigan GEC Reference Cell  
M.L. Brake, M. Passow, J. Pender, A. Lujan, M. Buie, P. Ventzek and M. Elta
- DB-27 Spatial and Temporal Resolution of Plasma-Induced Emission Measurements  
M.J. Colgan and D.E. Murnick
- DB-28 Modeling and Diagnostics of RF Glow Discharges in Ar  
T. Makabe, N. Nakano, F. Tochikubo and S. Kakuta
- DB-29 Electrical Measurements and Analysis of Ar and SF<sub>6</sub> RF Discharges  
H. Shan, J. McVittie and S. Self
- DB-30 The Parametric and Time Dependencies of Negative Ions from Pulsed RF Discharges  
L.J. Overzet, L. Luo and Y. Lin

### **SESSION EA. CATHODES IN DISCHARGES: A REVIEW**

8:00 - 10:00 AM, Wednesday, October 23, Ballroom A  
Chair: J.F. Waymouth

- 8:05 - 8:35 EA-1 Diagnostics and Modeling of the Cathode Fall and Negative Glow Regions of Cold Cathode Discharges  
J.E. Lawler and W.N.G. Hitchon

- 8:35 - 9:05 EA-2 Diagnostics and Modelling of the Sheath and Negative Glow of Hot-Cathode Discharges  
V. Godyak and R. Lagushenko
- 9:05 - 9:35 EA-3 Diagnostics and Modeling of the Cathode Temperature Profile in Hot-Cathode Discharges  
A.K. Bhattacharya and T.F. Soules
- 9:35 - 10:00 EA-4 Electron Emission in Hot-Cathode Discharges: Modelling and Paucity of Good Diagnostic Methods  
J.F. Waymouth

## SESSION EB. IONIZATION AND ELECTRON COLLISIONS

8:00 - 10:00 AM, Wednesday, October 23, Ballroom B

Chair: R.A. Bonham, Indiana University

- 8:00 - 8:15 EB-1 Partial Electron Ionization Cross Sections for Molecules  
M. Foltin, C. Winkler, V. Grill, D. Margreiter, H.U. Poll and T.D. Mark
- 8:15 - 8:30 EB-2 Cross Sections for the Production of Positive Ions by Electron Impact on F<sub>2</sub>  
S.K. Srivastava and M.V.V.S. Rao
- 8:30 - 8:45 EB-3 Electron-Impact Ionization of Atoms and Molecules Using The Fast-Beam-Technique  
V. Tarnovsky and K. Becker
- 8:45 - 9:00 EB-4 Why are Multicharged Partial Ionization Cross Sections so Hard to Measure? An Analysis of Time-of-Flight Techniques  
M.R. Bruce and R.A. Bonham
- 9:00 - 9:15 EB-5 Electron-H<sub>2</sub>S Collisions in an Exact Exchange Plus Parameter-Free Polarization Model  
A. Jain and K.L. Baluja
- 9:15 - 9:30 EB-6 Metastable Fragmentation of Rare Gas Cluster Ions Initiated by Excimer Decay  
M. Foltin, G. Walder and T.D. Mark
- 9:30 - 9:45 EB-7 Low Energy e-Ar Momentum Transfer Cross-Section  
M.J. Brennan
- 9:45 - 10:00 EB-8 Elastic Scattering of Low Energy Electrons from Ammonia  
D.T. Alle, R.J. Gulley, M.J. Brunger and S.J. Buckman

### WELCOME

10:15 AM - 10:30 AM, Wednesday October 23

Ballroom A

Richard E. Peck, President  
The University of New Mexico

**SESSION F. PLENARY LECTURE**

10:30 - 11:30 AM, Wednesday, October 23, Ballroom A  
 Chair: J. Gerardo, Sandia National Laboratories

10:30 - 11:30 F-1 Plasma Physics Issues for Inertial Fusion with Light Ion Beams  
 J.P. VanDevender

**SESSION G. BUSINESS MEETING**

11:30 AM - 12:00 NOON, Wednesday, October 23, Ballroom A

**SCIENTIFIC EQUIPMENT and LITERATURE EXHIBIT**

1:30 - 5:30 PM, Wednesday, October 23, Ballroom C  
 (Exhibits will be on display continuously through 5:30 PM, Thursday October 24)

**EXHIBITORS:**

American Institute of Physics

Balzers

Chromex

Coherent Laser Group

Comdel, Inc.

Commonwealth Scientific

CVI Laser Corporation

EG&G Instruments, Inc.

EEV, Inc.

ENI

Extrel

Granville-Phillips Company

Huntington Mechanical Laboratories

IBM

IOP Publishing

Key High Vacuum

Lucas Laboratories

MCNC

MDC Vacuum Products Corporation

Melles Griot

MKS Instruments

Norcal

Princeton Instruments

Springer Verlag New York, Inc.

Tektronix

THT (representing Astex and other mfr's)

UNM Center for High Technology Materials

UNM College of Engineering

**SESSION H. POSTERS**

1:30 - 3:30, Wednesday, October 23, Ballroom C (All poster papers should be posted before the start of the session in the appropriate location, preferably by 1:30 PM, Tuesday, October 22)

**TRANSPORT**

HA-1 Nonequilibrium Electron Transport: A Comparison of Approaches Based on a Finite Set of Moment Equations  
 J.H. Ingold and E. Kunhardt



- HA-2 Self-Consistent Monte Carlo Simulation of RF Glow Discharges  
J.H. Tsai and C. Wu
- HA-3 Nonequilibrium Electron Transport Near Absorbing Boundaries  
J. Ingold
- HA-4 Time Dependence of Swarm Parameters of Electrons in Argon  
A.A. Sebastian and J.M. Wadehra
- HA-5 Departures from Thermodynamic Equilibrium in Particle-Beam Generated Molecular Oxygen Plasma  
N. Peyraud-Cuenca
- HA-6 Multigroup Treatment of Electron Transport in Gases  
E. Kunhardt
- HA-7 An Analysis of Position-Dependent Electron Swarm Behavior in Steady-State Townsend Discharges  
Y. Sakai, H. Sugawara and H. Tagashira
- HA-8 An Ion Transport Model for the Afterglow of Radio-Frequency Discharges  
L.J. Overzet and L. Luo
- HA-9 Velocity Distributions of Na<sup>+</sup> Ions in Ne  
M.J. Hogan, P.P. Ong and K.Y. Lam
- HA-10 Radial Distribution of the Plasma Density in the Positive Column of the High Current Stationary Glow Discharge  
L. Pekker
- HA-11 Monte-Carlo Simulation of Electron Properties in an Electron Cyclotron Resonance Microwave Discharge  
S.C. Kuo and E.E. Kunhardt

### ELECTRON and PHOTON COLLISIONS

- HB-1 Angular Distribution of Electrons Elastically Scattered from Water Vapor  
A. Grafe and T.W. Shyn
- HB-2 Electron CF<sub>4</sub> Scattering at Low and Intermediate Energies  
H. Tanaka, L. Boesten, H. Sata, M. Dillon, D. Spence and M. Kimura
- HB-3 Electron Scattering on NO<sub>2</sub>: Vibrational Excitation at Low Energy (0.3 - 3eV)  
R. Abouaf and C. Benoit
- HB-4 The Absolute Electron Impact Cross Sections for Double Cation Formation in CF<sub>4</sub>  
M.R. Bruce, C. Ma, and R.A. Bonham
- HB-5 Direct Measurement of Ionization-Excitation Branching Ratios for N<sub>2</sub> using a Coincidence Ionization Technique  
J.P. Doering and L. Goembel

- HB-6 Selective Detection of  $O^1S$  by XeO Formation Following Electron Impact  
Dissociation of  $O_2$  and  $N_2O$   
L.R. LeClair, J.J. Corr and J.W. McConkey
- HB-7 Production of Excited Helium Atoms in the Singlet Levels by Electron Collisions  
with Metastable Helium Atoms  
R.B. Lockwood, F.A. Sharpton, L.W. Anderson, J.E. Lawler and C.C. Lin
- HB-8 Threshold Behavior in Electron Excitation of Na  
B.Marinkovic, P. Wang and A. Gallagher
- HB-9 Dissociative Photoionization Processes in Isolated Weakly-Bound Small Molecular  
Clusters  
E.A. Walters, J.R. Grover, J.T. Clay, G. Hagenow and P. Cid-Aguero
- HB-10 Subexcitation Electrons in an  $O_2$  and  $N_2$  Mixture  
M. Kimura, M.A. Ishii and M. Inokuti
- HB-11 The Mass Dependence of Cross Sections for Vibrational Excitation of Diatomic  
Molecules by Electron Impact  
D.E. Atems and J.M. Wadehra
- HB-12 Non Franck-Condon Effects in the Molecular Electronic Excitation of  $O_2$  and CO  
M. Dillon, D. Spence, M. Kimura, R.J. Buenker, L. Chantranupong and  
G. Hirsch
- HB-13 A First Born Approximation Data Base for Excited State-Excited State Electron  
Impact Transitions in Alkali Atoms  
U. Krishnan and B. Stumpf
- HB-14 Differential Cross Sections for Electron Collisions from  $H_2O$  and  $NH_3$  Molecules at  
1-200 eV in a Multi-Potential Hybrid Approach  
K.L. Baluja and A. Jain
- HB-15 Low Energy Electron-Ethylene Scattering  
T.N. Rescigno, B.H. Lengsfeld and B.I. Schneider

#### LAMPS

- HC-1 Argon Metastables in the Negative Glow of a Fluorescent Lamp Like Discharge  
K. Mitsuhashi, R.C. Wamsley and J.E. Lawler
- HC-2 Measuring Ion Current to the Cathode of a Mercury-Rare-Gas Discharge  
J.F. Waymouth
- HC-3 Self-Consistent Cathode Fall Study Including Negative Glow Electrons  
M. Dalvie, S. Hamaguchi and R. Farouki
- HC-4 Model Calculations of the Isotope Effect in Hg-Ar Discharges  
M. Duffy and J. Ingold

- HC-5            On the Importance of the Hg\*/Hg\* Inelastic Scattering in the Modeling of the Low Pressure Hg-Ar Discharges  
G. Zissis, V. Plagnol and J.J. Damelincourt
- HC-6            On the Influence of the Physical Plasma Parameters in the Modelling of the Low Pressure Hg-Ar Discharges  
V. Plagnol, G. Zissis, I. Bernat
- HC-7            Characteristics of HgBr in a Dielectric Barrier Discharge  
H.P. Popp and A. Beying
- HC-8            Constricted High Power Microwave Excited Krypton Arc Lamp  
G. Lohmann, H.P. Popp, M. Neiger and H. Merkel
- HC-9            Chemical Nonequilibrium in a 0.1 Bar Hydrogen Arc  
T.L. Eddy
- HC-10           Effect of Hollow Cathode Cooling on Plasma Plume Emission Characteristics  
W.L. Collett, S.M. Mahajan and C.A. Ventrice
- HC-11           Some Important Properties of Arc Core  
Z. Li
- HC-12           A Model for Interaction of Arc and Gas Flow  
Z. Li

## SESSION J. POSTERS

3:30 - 5:30, Wednesday, October 23, Ballroom C (All poster papers should be posted before the start of the session in the appropriate location, preferably by 1:30 PM, Tuesday, October 22)

### OPTICAL and PROBE DIAGNOSTICS

- JA-1            What Determines Ion Energy at an Unbiased Wafer in an ECR Etching Tool  
N. Hershkowitz, S.W. Lam, M. Hussein, H. Persing, and E. Den Hartog
- JA-2            The Use of Faraday Rotation to Measure the Thickness and Polarization of an Alkali Vapor  
M. Dulick, D.R. Swenson, D. Tupa, R.L. York, W.D. Cornelius and O.B. van Dyck
- JA-3            Wafer Temperature Measurement During Process by IR-Interferometry  
C.F. Van Os and B.N. Chapman
- JA-4            Laser Induced Fluorescence Temperature Measurements in a CH<sub>4</sub>-H<sub>2</sub> Discharge During the Growth of Diamond  
H.N. Chu, E.A. Den Hartog, A.R. Lefkow, L.W. Anderson, M.G. Lagally and J.E. Lawler
- JA-5            Spatial Profiles of Absolute H-Atom Concentration in RF Discharges  
A.D. Tserepi, J.R. Dunlop, B.L. Preppernau and T.A. Miller

- JA-6 RF Sheath Characteristics in a Plasma Sputtering System  
K.F. Al-Assadi and N.M.D. Brown
- JA-7 A Micro-Machined Sensor for In Situ Characterization of Plasma Sheath Potentials and Ion Energy Distributions  
R. Jewett, M. Blain, H.M. Anderson and B. Smith
- JA-8 Mass Spectra of Hydrocarbon DC Arcjet Plasmas used in the Deposition of Polycrystalline Diamond  
K.R. Stalder and W. Homsí
- JA-9 Measurement of Electron Density in Methane/Hydrogen/Oxygen Plasma  
H. Snyder and C.B. Fleddermann
- JA-10 Langmuir Probe Characterization of Drifting Electrons  
T.E. Sheridan
- JA-11 Spatially Resolved Ion Velocity Distributions in Chlorine Electron Cyclotron Resonance Plasmas  
T. Nakano, N. Sadeghi, D.J. Trevor, R.A. Gottscho and R.W. Boswell
- JA-12 Spatial Vibrational Population Profiles of the Ground State of N<sub>2</sub> in a Compact, Wall-Less DC Glow Discharge using Coherent Anti-Stokes Raman Spectroscopy  
P.P. Yaney and M.W. Millard

### GLOWS

- JB-1 Self-Consistent DC Glow Discharge Simulations Applied to Diamond Film Deposition Reactors  
M. Surendra, D.B. Graves and L.S. Plano
- JB-2 An Efficient Algorithm for the Study of Non-Equilibrium Dynamics of Electrons from the Solution of Boltzmann Equation  
S. Shankar and K.F. Jensen
- JB-3 Breakdown Characteristics of Non-Planar Plasma Sheaths  
A. Syljuasen, E.E. Kunhardt, J. Bentson, S. Popovic and S. Barone
- JB-4 Hydrogenated Amorphous Silicon Thin Film Deposition using an Electron Beam Generated Disc Plasma  
D.M. Shaw, T.Y. Sheng, Z. Yu, G.J. Collins and N. Adachi
- JB-5 Analytical Expression of the Ionization Source Term in Argon, Helium and Nitrogen  
I. Peres, N. Ouadoudi, L.C. Pitchford and J.P. Boeuf
- JB-6 Recombination Peaks in Pulsed Noble Gas-Cu Hollow Cathode Afterglow  
G. Rubin, M. Janossy, P. Mezei, P. Apai and K. Rozsa
- JB-7 Monte Carlo Study of the Electron Swarm in a He Disc Plasma  
B. Shi, T. Sheng, Z. Yu and G.J. Collins

- JB-8 Ionization and Excitation Rate Coefficients in Argon and Helium Over a Wide Range of E/N  
P.J. Drallos, G.N. Hays and M.E. Riley
- JB-9 Modeling of Magnetron Discharges  
M. Meyyappan and T.R. Govindan
- JB-10 A Collisional-Radiative Model for Low-Pressure Microwave Discharges in Helium  
L.L. Alves, G. Gousset and C.M. Ferrerira
- JB-11 Optical Emission-Based Measurements of Electric Fields in the Cathode Fall Region of He and CF<sub>4</sub>/He DC Glow Discharges  
H. Shan, S.A. Self and M.A. Cappelli
- JB-12 Particle-in-Cell Simulation of Plasma Immersion Ion Implantation  
R.W. Boswell and M.A. Jarnyk
- JB-13 Incorporation of Plasma Effects in the Modelling of Chemical Vapor Deposition of Diamond  
E. Meeks and M.A. Cappelli
- JB-14 Pressure Gradients and Flow Patterns in the DC Positive Column  
D.W. Ernie and L. Pekker
- JB-15 Analysis of the Transition to Chaos in a Glow Discharge  
D. Hudson
- JB-16 Simulations of Energetic Neutral Generation in Plasma Sheaths  
J. Rey and J. McVittie

#### PARTICLES IN PLASMAS

- JC-1 Particle Detection and Electrostatic Trapping in Plasma Processes  
J.E. Heidenreich and G.S. Selwyn
- JC-2 Simulation of Particle Confinement and Flux Penetration in DC Discharges  
S.J. Choi, M.J. McCaughey, T.J. Sommerer and M.J. Kushner
- JC-3 Model for Charging and Confinement of Particulates in a Plasma  
J. Goree
- JC-4 Dust in RF Plasmas  
B.N. Ganguly, P.D. Haaland, P. Bletzinger and A. Garscadden
- JC-5 Modeling 2-D Electric Field Variations in a Parallel Plate RF Discharge using Particle-in-Cell Monte Carlo Techniques  
R.C. Sierocinski, H.M. Anderson, R.K. Keinigs and T.A. Oliphant
- JC-6 Rotational Relaxation Molecules N<sub>2</sub> in Free Jet Expansion  
R.E. Mukhametzianov

- JC-7                    Process Induced Particulate Generation and Deposition During Single Wafer  
Reactive Ion Etching  
                          P.J. Resnick, H.M. Anderson and N.E. Brown

## SESSION K    WORKSHOP – GEC REFERENCE CELL ISSUES

7:00 - 9:00 PM, Wednesday, October 23, Ballroom A

Co-Facilitators:    J. Gerardo, Sandia National Labs  
                          H. Sawin, MIT

- K-1                    Summary of the Status of Reference Cell Measurements and Modelling by Various  
Groups  
                          J. Gerardo, H. Sawin

An open discussion is encouraged on comparisons between model predictions of RF discharge systems and calibration measurements made on standardized cells such as the GEC Reference Cell, as well as any other relevant issues regarding standardized cell design, experiment and measurement. The tone of the workshop will be set by the contributed papers of the Tuesday afternoon poster session on GEC Reference Cell and related systems results. The key to a workshop lies in the contributions from the floor. Spirited and free flowing interjections from the floor are encouraged, as are contributed insights and suggestion. A sign-up sheet for workshop presentations (two overheads and a five minute time limit) will be made available during the pre-workshop poster session.

## SESSION LA. LAMPS and CATHODES

8:00 - 10:00 AM, Thursday, October 24, Ballroom A

Chair: J. Ingold, General Electric, Nela Park

- |             |      |   |
|-------------|------|---|
| 8:00 - 8:15 | LA-1 | X-Ray Measurement of Spatial Distribution of Mercury Gas Density and Temperature in Operating HID Lamps<br>T. Fohl, J. Lester and P.A. Vicharelli       |
| 8:15 - 8:30 | LA-2 | Time Dependent x-Ray Measurements of Mercury Density in HID Lamps<br>J. Lester, J. Kramer and T. Fohl   |
| 8:30 - 8:45 | LA-3 | Time Dependent Electron Energy Distribution Effects in the Low-Pressure Hg-Ar Positive Column<br>J.T. Dakin   |
| 8:45 - 9:00 | LA-4 | Current Dependence of Hg <sup>+</sup> Densities in the Cathode Region of a Hg-Ar Discharge<br>R.C. Wamsley, T.R. O'Brien, K. Mitsuhashi and J.E. Lawler |
| 9:00 - 9:15 | LA-5 | Voltage-Current Characteristics in the Hot Cathode Glow Discharge<br>W.W. Byszewski, Y.M. Li, P.D. Gregor and A.B. Budinger                             |
| 9:15 - 9:30 | LA-6 | Nonequilibrium Cathode Fall Models<br>Y.M. Li   |

- 9:30 - 9:45 LA-7 Investigation of the Arc Spot Formation on Cold Cathodes in Dependence on the Electrode Material  
R. Bayer and J. Mentel
- 9:45 - 10:00 LA-8 Continuous Phase Transition Model of an Arc Cathode Region at Atmospheric Pressure  
H. Minoo, A. Kaddani, C. Delalondre and O. Simonin

### SESSION LB. ELECTRON EXCITATION and IONIZATION

8:00 - 10:00 AM, Thursday, October 24, Ballroom B  
Chair: Tom Rescigno, Lawrence Livermore National Laboratory

- 8:00 - 8:15 LB-1 Electron Scattering at the Threshold Region, 2-4 eV, of Resonant Transition in Sodium  
C.H. Ying, L. Vuskovic and B. Bederson
- 8:15 - 8:30 LB-2 Electron Impact Excitation of the Rare Gases  
M.A. Khakoo, T. Tran and D. Bordelon
- 8:30 - 8:45 LB-3 Non-Statistical Branching Ratios for Excitation of Metastable States in Noble Gases  
K. Bartschat, D.H. Madison and P. Burke
- 8:45 - 9:00 LB-4 Electron Impact Excitation of Higher Rubidium States  
C. Flynn, Z. Wei and B. Stumpf
- 9:00 - 9:15 LB-5 Electron Impact Excitation of the Copper Resonance Lines  
C. Flynn, Z. Wei and B. Stumpf
- 9:15 - 9:30 LB-6 VUV Emission Cross Sections for OI Resonance Lines Following Electron Impact on Atomic Oxygen  
S. Wang and J.W. McConkey
- 9:30 - 9:45 LB-7 Electron-Impact Excitation from the Metastable States of Helium  
D.C. Cartwright and G. Csanak
- 9:45 - 10:00 LB-8 Comparison of Electron and Positron Results for Scattering from Hydrogen  
D.H. Madison, M. Woodward and V. Bubelev

### NEW FRONTIERS IN PHYSICS AND CHEMISTRY: SCIENCE TEACHER'S DAY

8:00 AM - 3:30 PM

Picuris Room - Lower Level Convention Center

Attendance is limited to those participants who have preregistered for the High School Science Teacher's Day Program. Attendees of the GEC technical program wishing to take part in the Teacher's day program **must** contact the registration desk prior to Wednesday at noon. Space for the talks presented at the teachers program is limited and we would appreciate your cooperation. However, teachers will be present for the Thursday afternoon Poster Session and we encourage dialogue between teachers and scientists attending the GEC. The agenda for the Teacher's Day Program is included at the end of the technical abstracts.

## SCIENTIFIC EQUIPMENT and LITERATURE EXHIBIT

10:15 - 12:15 PM, Thursday, October 24, Ballroom C (Exhibits will be on display continuously through 5:30 PM, Thursday October 24 - see Exhibitors Program for listings)

### SESSION M. POSTERS

10:15 AM - 12:15 PM, Thursday, October 24, Ballroom C  
(All poster papers should be posted before the start of the session in the appropriate location, preferably by 1:30 PM, Tuesday, October 22)

#### GLOWS

- |       |  |
|-------|--|
| MA-1  | Wide Area Near After Glow Oxygen Radical and VUV Source for Photoresist Ashing<br>Z. Yu, G.J. Collins, S. Hattori, D. Sugimoto, M. Saita and J.D. Meyer                                |
| MA-2  | Voltage Current Characteristics of Low Pressure Argon Discharges<br>I. Peres, L.C. Pitchford, J.P. Boeuf, H. Gielen and P. Postma  |
| MA-3  | Multi-Dimensional Modeling of the Discharge Excited XeCl Laser<br>M.M. Turner  |
| MA-4  | High Voltage Hollow Cathode Magnetron Discharge<br>K. Rozsa, L. Li, G.J. Collins and P. Apai   |
| MA-5  | An Analytic Model of the Ion Angular Distribution Function in a Highly Collisional Sheath<br>M.A. Lieberman, V. Vahedi and R.A. Stewart  |
| MA-6  | Monte Carlo Study of Both Electron and Hydrogen Atom Swarms in A Hydrogen Molecule Disc Discharge System<br>B. Shi, T.Y. Sheng, Z. Yu and G.J. Collins                                 |
| MA-7  | A Phenomenologically Developed Surface Kinetic Model for CF <sub>4</sub> and CF <sub>4</sub> /O <sub>2</sub> Etch of SiO <sub>2</sub><br>V. Singh, A.K. Varnas and R.R. Rhinehart      |
| MA-8  | Potential and Ion Energy Distribution in the Sheath<br>K.U. Riemann  |
| MA-9  | Electrical Breakdown in Partially Enclosed Structures<br>E.E. Kunhardt, S. Barone, J. Bentson and S. Popovic   |
| MA-10 | Plasma Stoichiometry and Reaction Rate Constants in a Continuous Flow Stirred-Tank Reactor<br>F.V. Wells, R. Rodriguez, D. Warner and P. Woodward                                      |
| MA-11 | Investigation of Discharge Impedance and Spectral Emission in a Cylindrical Magnetron with an Internal Axial Anode Grid<br>L. Li, Z. Yu, B. Shi, G.J. Collins, K. Rozsa and J.D. Meyer |



- MA-12            The Solar Array Module Plasma Interactions Experiment (SAMPIE)  
                  G.B. Hillard
- MA-13            Dissociation and Chemiluminescence of Silane in Active Nitrogen  
                  C.A. DeJoseph, Jr.
- MA-14            Particle Simulation of a Narrow-Gap Symmetric Malter Gas Diode  
                  R.W. Schmieder, R.T. McGrath and R.B. Campbell
- MA-15            Kinetics of Polythiophene Deposition in an Argon Afterglow  
                  P. Haaland and J. Targove
- MA-16            New Hollow Cathode Contours for Superior Performance  
                  W.L. Collett and S.M. Mahajan

### PLASMA SURFACE INTERACTIONS

- MB-1            Efficient Sputtering and Deposition by a Flat-Cathode DC Glow Discharge  
                  K. Rozra, G. Stutzin and A. Gallagher
- MB-2            Surface Charge Deposition and its Influence on the Stochastic Behavior of  
Pulsating Dielectric Barrier Discharges  
                  R.J. Van Brunt and E.W. Cernyar
- MB-3            Vibrational Relaxation and Dissociation of D<sub>2</sub>(vj) on Cu(111)  
                  M. Cacciatore, P. De Felice, M. Capitelli and G.D. Billing
- MB-4            Evidence for Above- and Sub-Surface Neutralization During Interactions of Highly  
Charged Ions with a Metal Surface  
                  F.W. Meyer, S.H. Overbury, C.C. Havener, P.A. Zeijlmans Van  
Emmichoven and D.M. Zehner
- MB-5            Electron Scattering as a Probe of Adsorbate/Surface Interactions: Low-Energy  
*e*-BeCO and *e*-Be<sub>3</sub>CO Elastic Scattering  
                  J.A. Sheehy and W.M. Huo
- MB-6            LIF Characterization of a Magnetron Discharge Used in Preparing High  
Temperature Superconducting Thin Films  
                  W.G. Graham, B.F. Burns and T. Morrow

### HEAVY PARTICLES and NEGATIVE IONS

- MC-1            Ar<sub>2</sub> Second Continuum Emission in a Pulsed Discharge Excited Pulsed Supersonic  
Gas Expansion  
                  M.F. Masters, J.E. Tucker, B.L. Wexler and S.K. Searles
- MC-2            Visible Emissions Produced in the Reaction of 8 km/s O/O<sup>+</sup> with H<sub>2</sub>O  
                  D.M. Sonnenfroh and G.E. Caledonia
- MC-3            Ion Motion in an Ion Cyclotron Resonance Trap  
                  K. Riehl, D. Determan, L. Pachter and P. Haaland

- MC-4 Rotational Excitation of  $N_2^+$  in Collisions with  $N_2$   
J. Borysow and A.V. Phelps
- MC-5 Radiative and Nonradiative Charge Transfer in  $He^+ + H_2$  Collisions in the meV Regime  
M. Kimura and N.F. Lane
- MC-6 Diatomic Interaction Potentials for Rare Gas-Rare Gas and Rare Gas-Halide Systems  
E.J. Mansky
- MC-7 Vibrational Energy Exchanges in  $H_2$  and  $D_2$  Collisions: The Effect of Rotational Coupling  
M. Cacciatore, R.A. Caporusso and G.D. Billing
- MC-8 Calculations of Fine-Structure Changing Collisions of Excited Xe  
A.P. Hickman, D.L. Huestis and R.P. Saxon
- MC-9 Temporary Negative Ion States of CN-Bearing Compounds  
P.D. Burrow, A.E. Howard, A.R. Johnston and K.D. Jordan
- MC-10 Dissociative Attachment in Monochloroalkanes  
D.M. Pearl and P.D. Burrow
- MC-11 Photodetachment of  $Ca^-$  Near the  $Ca(1P)$  Threshold  
C.W. Walter and J.R. Peterson
- MC-12 Extraction of Negative Ions from a Pulsed Modulated Volume Source  
K.N. Mellon and M.B. Hopkins
- MC-13 The Optically Pumped Polarized  $H^-$  Ion Source at LAMPF  
R.L. York, D. Tupa, D.R. Swenson and O.B. van Dyck
- MC-14 Dissociative Recombination of  $N_4^+$  Ions with Electrons  
Y.S. Cao and R. Johnsen
- MC-15 Dissociative Recombination of TMAE Ions  
K.R. Stalder, D.J. Eckstrom and R.J. Vidmar
- MC-16 Product States of  $Ar_2^+$  Dissociative Recombination  
J.R. Peterson

#### SESSION NA. ALTERNATIVE APPLICATIONS FOR PLASMA PROCESSING

1:30 - 3:30 PM, Thursday, October 24, Ballroom A

Chair: M. Moisan, Universite de Montreal

- 1:30 - 2:00 NA-1 Review of Thermal Plasma Chemical Vapor Deposition  
J.V.R. Heberlein

- 2:00 - 2:30 NA-2 Plasma and their Adaptation to Biomedical Applications: The Example of Sterilizations  
J. Pelletier
- 2:30 - 2:45 NA-3 Radical Production in Coronal Discharges for Air Cleaning  
B.M. Penetrante, J.N. Bardsley, P.A. Vitello, G.E. Vogtlin and W.W. Hofer
- 2:45 - 3:00 NA-4 Magnetron Enhanced Reactive Ion Etching of GaAS  
M. Meyyappan and G.F. McLane
- 3:00 - 3:15 NA-5 Characterization of a Compact RF Induction Plasma Source and the Extracted Neutral Beam  
L. Chen and A. Sekiguchi
- 3:15 - 3:30 NA-6 Investigation of ECR Discharge Mechanisms Based on the Study of Surface-Wave Sustained Magnetoplasmas: A Systematic Approach  
J. Margot and M. Moisan

### SESSION NB. DISCHARGE MODELS

1:30 - 3:30 PM, Thursday, October 24, Ballroom B

Chair: J.P. Boeuf, CNRS, Toulouse

- 1:30 - 1:45 NB-1 Model Calculations of Hot F Atom Energy Distribution in Low Pressure Plasma Reactors  
A.S. Clarke and B. Shizgal
- 1:45 - 2:00 NB-2 Charging of Pattern Features During Plasma Etching  
J.C. Arnold and H.H. Sawin
- 2:00 - 2:15 NB-3 Transient and Steady-State Hollow Cathode Discharges: Model  
L.C. Pitchford and J. P. Boeuf
- 2:15 - 2:30 NB-4 Steady State and Transient Hollow Cathode Discharges: Experiments  
J.P. Booth, M.P. Alberta and J. Derouard
- 2:30 - 2:45 NB-5 Temporal Relaxation of Electrons in Nitrogen  
E.E. Kunhardt and P. Hui
- 2:45 - 3:00 NB-6 Electron Drift Velocity and Net Ionization Coefficient at High E/N in SiH<sub>4</sub>  
L.E. Kline and D.K. Davies
- 3:00 - 3:15 NB-7 Comparison Between Nonequilibrium and Equilibrium Fluid Models of RF Glow Discharges  
F. Young and C. Wu
- 3:15 - 3:30 NB-8 The Bohm Criterion and the Ion Acoustic Sound Barrier  
K.U. Riemann

## SCIENTIFIC EQUIPMENT and LITERATURE EXHIBIT

3:30 - 5:30 PM, Wednesday, October 23, Ballroom C  
(Exhibits will be on display continuously through 5:30 PM, Thursday October 24 - see Exhibitors Program for Listing)

### SESSION P. POSTERS

3:30 - 5:30 PM, Thursday, October 24, Ballroom C (All poster papers should be posted before the start of the session in the appropriate location, preferably by 1:30 PM, Tuesday, October 22)

#### COLLISIONS IN PLASMAS

- PA-1 Stark Broadening in Laser-Produced Oxygen Plasma  
L.S. Dzelzhalns, W.A.M. Blumberg, V. Eccles and R.A. Armstrong
- PA-2 CH Emission from Low Current, CH<sub>4</sub> - Ar Discharges at High E/n  
Z. Lj. Petrovic and A.V. Phelps
- PA-3 Breakdown Delay Times in Photo-Triggered Discharges  
M. Legentil, S. Pasquiers, V. Puech and R. Riva
- PA-4 Electron Excitation Temperature and Density Measurements in Non-Equilibrium, Low-Pressure, Cs-Ar Plasma  
S.D. Marcum and T.M. Ciferno
- PA-5 Characterization of a Flowing Afterglow in an Electronegative Plasma  
D.E. Bell and Wm.F. Bailey
- PA-6 Modeling of Magnetic Multicusp Deuterium Plasmas for Negative Ion Production  
C. Gorse, M. Capitelli and M. Bacal
- PA-7 Oscillations in Pulsed, Parallel-Plane Hydrogen Discharges  
B.M. Jelenkovic, Z.Lj. Petrovic, K. Rozsa and A.V. Phelps
- PA-8 Excitation by Fast Hydrogen Atoms in H<sub>2</sub> Discharges at High E/n  
Z.Lj. Petrovic, B.M. Jelenkovic and A.V. Phelps
- PA-9 Model Simulations of He RF Discharges and the Importance of Including Ionization from Metastables  
R.C. Sierocinski and H.M. Anderson
- PA-10 Boundary Dominated High Field Low Pressure Deuterium Discharges  
B.N. Ganguly and A. Garscadden

#### EMISSION SPECTROSCOPY

- PB-1 CT Measurement of DC-Magnetron Discharges in Ar  
A. Itoh, N. Shimura, T. Koike and T. Makabe

- PB-2 Spectroscopic Determination of Level Populations in a Positive Column HeSe<sup>+</sup> Laser  
R. Nentwig and J. Mentel
- PB-3 Study of Optical Emission Spectra in the Microwave Plasma Assisted Diamond Deposition Environment  
S.C. Kuo and E.E. Kunhardt
- PB-4 Dependence of O(<sup>1</sup>S) Ar Decaytime on O<sub>2</sub> Content  
K. Yuasa
- PB-5 Vacuum Ultraviolet (VUV) Measurements on an ECR Plasma using CF<sub>4</sub> and CHF<sub>3</sub>  
J.S. Jenq and J.W. Taylor
- PB-6 Measurement of X-Rays Emitted from ECR Processing Plasma  
J.L. Shohet, T.J. Castagna, K.A. Ashtiani and N. Hershkowitz
- PB-7 Study of the Soft X-Ray Emission from Carbon Plasma Excited by Fast Capillary Discharges  
B. Szapiro, J.J. Rocca, M.C. Marconi, D. Cortazar and F. Tomasel
- PB-8 Time Resolved Electric Field Measurements in Hydrogen RF Plasma by Stark Emission Spectroscopy  
J.P. Booth, J. Derouard and N. Sadeghi
- PB-9 Comparison of the Stark Broadening of Hydrogen Balmer and Neutral Helium Lines in a High Pressure, Low Electron Temperature Helium Plasma  
L.W. Downes, S.D. Marcum, W.E. Wells, and J. Stevefelt
- PB-10 Optical Absorption Spectroscopy Study of the Role of Plasma Chemistry in YBCO Pulsed Laser Deposition  
W.G. Graham, H.F. Sakeek, T. Morrow and D.G. Walmsley
- PB-11 Time and Space Resolved Optical Emission and Electron Energy Distribution Function Measurements in RF Plasma  
W.G. Graham, C.A. Anderson and K.R. Stalder
- PB-12 Elementary Processes in He-N<sub>2</sub> RF Pulsed Discharges  
S. De Benedictis, G. Dilecce and M. Simek

#### PULSED POWER

- PC-1 Glow Voltage Reduction by Gas Kinetics Engineering in Atmospheric Pressure Pulsed Glow Discharges for Pulsed Power Switches  
W.M. Moeny, J.M. Elizondo, A.E. Rodriguez and M.G. White
- PC-2 Ionization Coefficients and Sparking Potentials in Ternary Mixtures of SF<sub>6</sub>-CCl<sub>2</sub>F<sub>2</sub>-N<sub>2</sub> and SF<sub>6</sub>CCl<sub>2</sub>F<sub>2</sub>-CO<sub>2</sub>  
G.R. Venkateshaiah and M.S. Naidu
- PC-3 Time-Dependent Boltzmann Analysis of Relaxation of Kinetic Coefficients in Air  
A.E. Rodriguez

- PC-4            Non-Equilibrium Electron Transport in Dry Air  
                  A.E. Rodriguez
- PC-5            The Effect of Water Vapour on Impulse Breakdown of Air  
                  J. Dutton, A.J. Davies, M. Matallah and R. Waters
- PC-6            Interaction of Microwaves with Gaseous Plasma formed by Abrupt Laser-Induced  
Ionization  
                  P.R. Bolton and J.E. Swain
- PC-7            Cathode Heating Mechanisms in Hollow Cathode Pseudospark Thyratrons  
                  T.J. Sommerer, H. Pak and M.J. Kushner
- PC-8            Glow Discharge Opening and Closing Plasma Switch Scheme  
                  J.J. Rocca, F. Gonzalez and K. Floyd
- PC-9            Kinetic Model of a Thermionic Direct Energy Converter  
                  W.N.G. Hitchon, J.E. Lawler, G.J. Parker and J.B. McVey

#### ALTERNATIVE APPLICATIONS FOR PLASMA PROCESSING

- PD-1            Experimental Study of Magnetoplasmas Sustained by Electromagnetic Guided  
Waves at or Close to Electron Cyclotron Resonance (ECR)  
                  J. Margot, M. Moisan and R. Grenier
- PD-2            Contamination by Sputtering in Mirror Field Electron Cyclotron Resonance  
Microwave Ion Plasma  
                  S.M. Gorbatkin and L.A. Berry
- PD-3            An Improved Spiral Loop Antenna for Inductively Coupled Plasma Sources  
                  T. Intrator, J. Menard and N. Hershkowitz
- PD-4            Experimental Characterization of a Chlorine Helicon Plasma  
                  T. Nakano, N. Sadighi, D.J. Trevor, R.A. Gottscho, R.W. Boswell,  
J. Margot-Chaker and A. Perry
- PD-5            Simple and Inexpensive Microwave Plasma Assisted CVD Facility  
                  M.A. Brewer, I.G. Brown, M.R. Dickinson, J.E. Galvin, R.A. MacGill and  
M.C. Salvadori
- PD-6            A Recirculating Coronal Discharge System for Air Cleaning  
                  G.E. Vogtlin, W.W. Hofer, B.M. Penetrante and J.N. Bardsley
- PD-7            Multidipole-RF Electrode Experiments  
                  R. Breun, C. Lai, N. Hershkowitz, A. Wendt and C. Woods

**SOCIAL HOUR AND BANQUET THURSDAY, OCTOBER 24****SOCIAL HOUR**

6:30 - 7:30 PM

Hyatt Regency Mezzanine

**BANQUET**

7:30 - 9:30 PM

Hyatt Regency Grand Pavilion

**SESSION QA. IONIZED GAS PHYSICS IN PULSED POWER**

8:00 - 10:00 AM, Friday, October 25, Ballroom A

Chair: W. M. Moeny, Tetra Corp.

- |              |      |  |
|--------------|------|--|
| 8:00 - 8:30  | QA-1 | Modeling a KrF Laser - Triggered SF <sub>6</sub> Spark Gap<br>A.E. Rodriguez   |
| 8:30 - 9:00  | QA-2 | Magnetic Control of Hollow Cathode Discharges<br>K.H. Schoenbach, G.A. Gerdin, T. Tessnow, J. Piekarek<br>and R. Joshi                           |
| 9:00 - 9:30  | QA-3 | Hollow and Super-Emissive Cathode Processes in the Pseudospark and<br>Back-Lighted Thyatron<br>M.A. Gundersen, G. Kirkman and W. Hartmann        |
| 9:30 - 10:00 | QA-4 | The Tacitron, A Low Noise Thyatron Capable of Current Interruption by<br>Grid Action...40 Years Later<br>G. McDuff, T.R. Burkes and V. Kaibeshev |

**SESSION QB. GLOWS II**

8:00 - 10:00 AM, Friday, October 25, Ballroom B

Chair: M. Lieberman, University of California, Berkeley

- |             |      |  |
|-------------|------|--|
| 8:00 - 8:15 | QB-1 | A Plasma Kinetics and Surface Deposition Model for the Deposition of<br>SiO <sub>2</sub> from O <sub>2</sub> /TEOS RF Discharges<br>M.J. Kushner, P.J. Stout and T.J. Sommerer |
| 8:15 - 8:30 | QB-2 | Nonequilibrium Plasma Destruction of Hazardous Organic Compounds<br>using Silent Electrical Discharges<br>L.A. Rosocha and W.H. McCulla  |
| 8:30 - 8:45 | QB-3 | Modeling and Simulation of Plasma Enhanced Chemical Vapor Deposition<br>M.M. Islamraja, C. Chang, J.P. McVittie, M.C. Cappelli<br>and K.C. Saraswat                            |
| 8:45 - 9:00 | QB-4 | Optimization of Deposition Fluxes in Remote Plasma Enhanced Chemical<br>Vapor Deposition<br>M.J. Kushner   |

- 9:00 - 9:15      QB-5      Chemistry and Kinetics of Plasma Deposition of SiO<sub>2</sub> Films from TEOS and Mixtures of TEOS with O<sub>2</sub> and Rare Gases  
C. Charles, P. Garcia and Y. Catherine
- 9:15 - 9:30      QB-6      Variation of Voltage, Ion Flux, and Other Plasma Properties as a Function of Pressure and Power in a Confined Argon Discharge  
J. Liu and H.H. Sawin
- 9:30 - 9:45      QB-7      A Study of Collisions in the Cathode Fall of Glow Discharges from a Numerical Solution of the Boltzmann Equation for Electrons  
S. Shankar and K.F. Jensen
- 9:45 - 10:00     QB-8      Toroidal Discharges in Superimposed Electrical and Magnetic Fields  
S. Popovic, E. Kunhardt, J. Bentson, and S. Barone

### SESSION RA. LASERS and SWITCHING

10:15 AM - 12:15 PM, Friday, October 25, Ballroom A  
Chair: C. Young, Tetra Corp

- 10:15 - 10:30     RA-1      Characterization of the Fission-Fragment Excited Helium/Argon Laser at 1.79  $\mu\text{m}$   
G.A. Hebner and G.N. Hays
- 10:30 - 10:45     RA-2      Long Pulse (100  $\mu\text{s}$ ) Ar-Xe Laser Pumped by an Electron-Beam-Controlled Discharge  
T.T. Perkins and J.H. Jacob
- 10:45 - 11:00     RA-3      Modeling of the Microwave and Discharge Excited Atomic Xe Laser  
J.W. Shon and M.J. Kushner
- 11:00 - 11:15     RA-4      Visible Recombination Laser using Electron Beam Pumping  
R.L. Rhoades and J.T. Verdeyen
- 11:15 - 11:30     RA-5      Modeling of a Low Pressure Cesium-Barium Discharge for Switch Applications  
C.M. Young and A.E. Rodriguez
- 11:30 - 11:45     RA-6      Simulation of Holdoff in Nonplanar Geometries and Hollow Cathode Switches  
H. Pak and M.J. Kushner
- 11:45 - 12:00     RA-7      Ion Source Spectroscopy on PBFA II  
J.E. Bailey, A.L. Carlson, A.B. Filuk, T. Nash and Y. Maron
- 12:00 - 12:15     RA-8      Radial Structure of Kilobar-Pressure Plasma Discharges  
S.N. Kempka and D.A. Benson



**SESSION RB. ECR and INDUCTION PLASMAS**

10:15 AM - 12:00 PM, Friday, October 25, Ballroom B

Chair: M. Barnes, IBM - East Fishkill

- |               |      |  |
|---------------|------|--|
| 10:15 - 10:30 | RB-1 | Electron Densities in the Diffusion Space of a Helical Resonator Plasma<br>P. Bletzinger   |
| 10:30 - 10:45 | RB-2 | Microwave Impedance Matching in an ECR Plasma Etch Tool<br>J.E. Stevens and J.L. Cecchi  |
| 10:45 - 11:00 | RB-3 | Relative Fluorine Concentrations in RF and (ECR) Microwave/RF Hybrid Glow Discharges<br>J. Pender, M. Passow, K. Sung, Y. Liu, S. Pang, M. Brake and M. Elta |
| 11:00 - 11:15 | RB-4 | Depositing Thick SiO <sub>2</sub> Layers with the Helicon Diffusion Reactor<br>R. Boswell, A Durandet, G. Giroult-Matlakowski and H. Persing                 |
| 11:15 - 11:30 | RB-5 | A Network Model of the Helical Resonator<br>K. Niazi, D.L. Flamm and M.A. Lieberman  |
| 11:30 - 11:45 | RB-6 | 2D Modeling of a Low Pressure Plasma in a Non-Uniform Magnetic Field<br>R.K. Porteous and D.B. Graves  |
| 11:45 - 12:00 | RB-7 | A WKB Approach to Electron Transport Problems<br>L. Demeio and B. Shizgal  |

**SESSION AA**

8:00AM - 10 AM, Tuesday, October 22

Ballroom A

**GLOWS I**

Chair: C. Fleddermann, University of New Mexico

**AA-1** Electron and Metastable Measurements in Helium RF Discharges. \* G. A. HEBNER and K. E. GREENBERG, Sandia National Laboratories--Electron and metastable density measurements have been performed in the GEC RF Reference Cell at 0.5 and 1.0 Torr of helium with both cw and pulse-modulated rf input. CW electron densities determined using microwave interferometry indicate that the line integral of the electron density varies between  $0.6 \times 10^{10}$  and  $1.8 \times 10^{12} \text{ cm}^{-2}$  for rf powers from 0.25 to 12 W at 1.0 Torr. For these same conditions, absorption measurements show the upper limit on the  $2^3\text{S}$  metastable density varies between  $2.0 \times 10^{11}$  and  $5.5 \times 10^{11} \text{ cm}^{-3}$ . The  $2^1\text{S}$  metastable density was approximately a factor of three less than the  $2^3\text{S}$  density. Modulation of the applied rf power can result in a three fold increase in the electron density in the afterglow under certain operating conditions. A time-dependent afterglow model which balances electron production and loss processes was used to calculate the metastable density and yielded good agreement with the values determined by absorption spectroscopy. Time-resolved LIF measurements of the  $2^3\text{S}$  metastable level show that the metastable population density reaches steady state faster than the electron density when the discharge is pulsed on. Implications for the time evolution of the electron energy distribution and for the modeling of helium rf discharges will be discussed.

\*This work was performed at Sandia National Laboratories and supported by the U.S. Department of Energy under DE-AC04-76DP00789.

**AA-2** PLASMA PARAMETER AND EEDF MEASUREMENTS IN LOW PRESSURE ARGON AND NITROGEN RF DISCHARGES

M.B. Hopkins, J.V. Scanlan, Dublin City University, Dublin 9, Ireland.

Plasma parameters, including the electron energy distribution function (eefd), have been measured in 13.56MHz argon and nitrogen discharges as a function of pressure and position using a tuned Langmuir probe. The eefd measurements demonstrate that the argon rf plasma can be sustained entirely by single step ionization whereas in the case of nitrogen, another source of ionization is necessary to account for the plasma production rate [1]. The eefd's measured over a range of pressures in argon are approximately bi-Maxwellian, whereas the nitrogen eefd becomes highly non-Maxwellian at high gas pressures. The low pressure eefd's display an isotropic group of ionizing electrons despite the fact that their mean free paths exceed the chamber dimension [2]. A model which explains this persistence of rf plasmas at low pressures has been developed and is supported by the spatial measurements.

[1] J.V. Scanlan, M.B. Hopkins, submitted for publication.

[2] J.V. Scanlan, M.B. Hopkins, ICPIG XX, Pisa, 1991.

**AA-3** Electrical Characteristics of Parallel Plate rf Discharges at 13.56 MHz in Helium and Argon. V. A. Godyak, R. B. Piejak and B. M. Alexandrovich, GTE Laboratories Incorporated -- Electrical characteristics have been measured for symmetrically driven rf discharges in helium over a pressure range between 0.03 Torr and 3 Torr and compared with previous measurements in argon made in the same parallel plate discharge system at the same electrode spacing (6.7 cm). As expected, in general the qualitative behavior of discharges is the same for both gases, of course, numerically, the discharge characteristics differ. Measured electrical parameters, such as discharge voltage, phase shift, ohmic voltage, equivalent resistance and effective sheath capacitance will be presented as a function of discharge current density ranging between .1 and 10 mA/cm<sup>2</sup>. This data is useful to modelers interested in comparing their results with experimental measurements over a wide range of parameter space.

**AA-4** TRANSITION FROM A CAPACITIVE TO A RESISTIVE REGIME IN A RF DISCHARGE IN SILANE: EXPERIMENTAL AND NUMERICAL DIAGNOSTICS. P. BELENGUER, J.P. BOEUF, C. BOHM\* AND J. PERRIN\* CNRS, Centre de Physique Atomique, Toulouse, FRANCE, \*Ecole Polytechnique, Palaiseau, FRANCE. Electrical and optical measurements in a symmetric, isothermal 13.56 MHz silane discharge have been performed at 55 and 185 mtorr (200°C). Power dissipation, current-voltage phase shift and time averaged emission profiles have been measured as a function of the applied rf voltage. These measurements have been compared with results from selfconsistent fluid and particle models of the discharge. The experimental results show that for a given pressure, the power dissipation presents an abrupt increase above a critical voltage. Detailed comparisons between experiments and models suggest that the observed phenomenon is due to an increase of the charged particle loss in the plasma. This transition could be related to a larger electron attachment on silane radicals, but more probably to the formation of powders in the plasma.

**AA-5** Numerical Analysis of RF Glow Discharges in HCl by RCT Model N.Nakano, T.Makabe and N.Shimura, Keio Univ.

— HCl gas is frequently used for dry etching of crystal and poly-Si. Reactive ion etching in HCl is operated in RF glow discharges at 13.56MHz under a relatively high pressure, 0.1~0.5Torr. The electron swarm parameter is given over a wide range of E/N from the numerical analysis of Boltzmann equation by Finite Element Method. Discharge structures with and without DC-bias voltage have been investigated by RCT model. Double layer is formed in front of the instantaneous anode as appeared in typical electronegative gases, since HCl has large cross section for electron attachment. The RF discharge is the system with positive and negative ions as a majority, including the active minority, electrons. As a result, the electric field in a bulk plasma increases and the phase-shift between both electrodes decreases, as compared with electropositive gases. The Influence of DC-bias voltage and dissipated power on the structure is discussed in terms of sheath width and the positive ion energy.

**AA-6** Electron Beam - Sheath Interaction in RF Discharges. \* B.P. WOOD, M.A. LIEBERMAN, and A.J. LICHTENBERG, U.C. Berkeley  
- Capacitively coupled rf discharges used for materials processing are typically operated at 1-100 mTorr with 50-1000 v applied at 13.56 MHz in a parallel plate chamber. Using PDP1, a 1d3v PIC simulation code,<sup>1</sup> we find that an electron beam is generated by the expanding sheath. At low pressure this beam can cross the discharge to interact with the opposite sheath. Depending on the phase of the opposite sheath, the beam may be lost to the electrode or reflected back into the discharge with either a higher or lower energy. This strongly affects the ionization rate and discharge power balance. The phase of the opposite sheath when the electron beam arrives is a sensitive function of the discharge length. By changing the discharge length a resonant effect can be observed in the simulation.

---

\*Work supported in part by the NSF and DOE.

<sup>1</sup>Available from C.K. Birdsall, Plasma Theory and Simulation Group, EECS Dept., U.C. Berkeley.

**AA-7** Ion Energy Distributions in a Simulated rf Plasma with Unequal Area Electrodes. R. Boswell, H. Smith, Plasma Research Laboratory, Research School of Physical Sciences and Engineering, The Australian National University, Canberra, ACT 2601, Australia -

A particle-in-cell (PIC) code is used to simulate a capacitive rf plasma with unequal area electrodes. The ratio of the sheath voltages as a function of the electrode area ratio is determined, and compared to experimental and theoretical results. The voltages which develop on the electrodes are shown to be highly dependent on the state of equilibrium of the plasma. The ion energy distributions at the electrodes are shown to be determined by the sheath potential, and the shape of the distribution by the sheath width. Electron energy distributions within the plasma are found for various times during the rf cycle.

**AA-8** Monte Carlo-Fluid Hybrid Model of rf Glow Discharges in Various Gas Mixtures. Timothy J. Sommerer and Mark J. Kushner, University of Illinois, Department of Electrical and Computer Engineering, Urbana, IL 61801

\* - A hybrid Monte Carlo fluid model for rf glow discharges has been developed. A fluid simulation (FS) is used to describe charged particle transport to obtain densities and to solve Poisson's equation for the electric field. Electron impact rates and transport coefficients are separately obtained by iteratively running a Monte Carlo electron simulation with the FS using the electric field and species densities calculated from the fluid model. In this manner the non-equilibrium nature of the EED is well represented. Typically, 10 rf cycles are calculated sequentially in each model until all quantities converge. The rapid convergence of the simulation (30 mins - 8 hours on a laboratory computer) allows neutral and charged particle plasma chemistry to be simultaneously included in the hybrid model. Results will be presented from a selection of gas mixtures (He, He/O<sub>2</sub>, He/N<sub>2</sub>, CF<sub>4</sub>/O<sub>2</sub>, Ar/N<sub>2</sub>, SiH<sub>4</sub>/NH<sub>3</sub>, He/O<sub>2</sub>/N<sub>2</sub>/H<sub>2</sub>O) and operating conditions including the GEC Reference Cell.

\* Work supported by IBM E. Fishkill, NSF and SRC.

**SESSION AB**

8:00AM - 10 AM, Tuesday, October 22

Ballroom B

**MULTIPHOTON PROCESSES & NEGATIVE IONS**

Chair: B. Stumpf, University of Idaho

**AB-1** Atoms and Molecules in Intense Laser Fields,\* Hanspeter Helm, SRI International --We will review experiments on gas-phase multiphoton ionization and multiphoton dissociation using intense laser sources in the picosecond and subpicosecond regime. The examination of kinetic energy and angular distributions of photoelectrons and fragment ions shows directly the modification of the excited state structure due to the presence of the intense electromagnetic field. The most important effect is that energy levels are shifted into resonance with the laser wavelength at certain laser intensities, thereby enhancing the rate of multiphoton excitation. Theoretical predictions and models for excitation, ionization, and dissociation will be compared with experimental results.

\*Work supported by NSF and AFOSR.

**AB-2** Two-Photon Ionization of Trimethylamine Using KrF Laser Radiation,\* P. W. WERNER and E. SCHAMILOGLU, University of New Mexico and Sandia National Laboratories—The efficiency of two-photon ionization of trimethylamine (TMA) using KrF laser radiation has been measured in both the low flux and high flux limits of laser intensity. A TMA fill pressure of about  $3 \times 10^{-5}$  Torr (lower than that used by previous researchers), and laser energies from about 0.5–7.0 J were used. The electron density produced by the laser ionization was measured using a microwave resonator probe.<sup>1,2</sup> This technique allows for very accurate, spatially and temporally resolved measurements. The electron density was found to depend on the square of the laser intensity in the low flux limit and was approximately linear with intensity in the high flux limit. The low flux limit results are in good agreement with calculations of the two-photon process.

\* Work supported by SDIO/DOE through NSWC and SNL under DOE contract DE-AC04-76DPP007898.

1. R. L. Stenzel, *Rev. Sci. Instrum.* **47**, 603 (1976).
2. P. W. Werner and E. Schamiloglu, *Proceedings of the 14<sup>th</sup> International Symposium on Discharges and Electrical Insulation in Vacuum* (Santa Fe, NM, 1990), p. 759.



**AB-3** Progress in H<sup>-</sup> Spectroscopy, \*H.C. Bryant, The University of New Mexico--Unlike helium, H<sup>-</sup> has no excited states between its ground state and the one-electron continuum beginning in the infrared at 0.7542eV. Nevertheless, like helium, this simplest of negative ions has a rich structure of doubly - excited, autoionizing states in the vacuum ultraviolet. I will tell you about some recent measurements<sup>1</sup> in which several manifolds of states have been addressed using a Doppler-shifted laser beam. In addition, these states have been further probed by imposed electric fields. An interesting pattern is emerging in which the two highly-correlated electrons behave as a quasiparticle orbiting the proton. These levels can be described by a modified Rydberg formula<sup>2</sup> in which the quantum defect arises from an internal degree of freedom of the quasiparticle.

\*Work supported by Division of Chemical Services, B.E.S., Office of Energy Research, U.S. DOE.

<sup>1</sup> P.G. Harris, H.C. Bryant, A.H. Mohagheghi, R.A. Reeder, C.Y. Tang, J.B. Donahue, C.R. Quick, *Phys. Rev. A* 42, 6443 (1990)

<sup>2</sup> H.R. Sadeghpour, *Phys. Rev. A* 43, 5821 (1991)

**AB-4** Motivation for New H<sup>-</sup> Double Photodetachment Threshold Studies at LAMPF. J.R. FRIEDMAN, X.Q. GUO, K.H. BECKER, M.S. LUBELL, City College of CUNY. — The results of spin-asymmetry studies carried out for electron impact ionization of hydrogen<sup>1</sup> revealed significant deviations from the prediction of the Wannier threshold law for double escape. Detailed statistical analyses of four other previously published threshold studies, all of which had originally claimed consistency with the Wannier law, now provide additional evidence for difficulties with the conventional theory.<sup>2</sup> In contrast to the corollary of the ergodic hypothesis that only the asymptotic form of the wave function need be considered for threshold escape, it appears that three-body dynamics must actually be taken into account if the problem is to be described properly. As earlier investigations at LAMPF have shown,<sup>3</sup> double photodetachment of the negative hydrogen ion provides an excellent method for investigating the threshold behavior of two-electron escape. The application of new laser technologies, combined with substantial improvements in LAMPF operation achieved in recent years, should significantly enhance the accuracy with which such measurements can be made.

<sup>1</sup> X.Q. Guo *et al.*, *Phys. Rev. Lett.* 65, 1857 (1990).

<sup>2</sup> J.R. Friedman *et al.*, submitted to *Phys. Rev. Lett.*

<sup>3</sup> J.B. Donahue *et al.*, *Phys. Rev. Lett.* 48, 1538 (1982).

**AB-5** Enhanced Electron Attachment to Super-excited States of Nitric Oxide\*; L.A.PINNADUWAGE and L.G.CHRISTOPHOROU, Oak Ridge National Lab. and Univ. of Tenn., Knoxville-We report the observation of slow electron attachment to laser-produced superexcited states (SES)--states lying above the first ionization threshold--of NO using a new experimental technique developed for the measurement of electron attachment to short-lived (lifetime  $< 10^{-8}$  s) excited species. The SES of NO were produced in multiphoton excitation processes via, i) real and virtual states, and ii) only virtual states. For slow electron (electron energy  $< 3$  eV) attachment to the SES, we estimate electron attachment cross sections  $> 10^{-10}$  cm<sup>2</sup> which are more than 8 orders of magnitude larger compared to that for the ground electronic state of NO.

\*Work supported by OHER, DOE and NSF.

1. L.A.Pinnaduwege, L.G.Christophorou and A.P. Bitouni, J.Chem.Phys. (in press, 1990).
2. L.A.Pinnaduwege and L.G.Christophorou, submitted to Chem. Phys. Letters.

**AB-6** Cross Sections for the Formation of Negative Ions by Electron Impact on F<sub>2</sub> and SF<sub>6</sub>\*: M.V.V.S. Rao# and S.K. Srivastava, Jet Propulsion Laboratory, California Institute of Technology - Normalized values of cross sections for the formation of negative ions by electron impact on F<sub>2</sub> and SF<sub>6</sub> have been obtained by employing a crossed electron beam-molecular beam collision geometry and the relative flow technique. It has been shown previously<sup>1</sup> that F<sup>-</sup> from F<sub>2</sub> appears at about 0 eV electron impact energy. We also find this and observe an additional, much weaker, peak at about 5.5 eV. The polar dissociation process begins at about 15 eV. In the case of SF<sub>6</sub> the following negative ions are observed: SF<sub>6</sub><sup>-</sup>, SF<sub>5</sub><sup>-</sup>, SF<sub>4</sub><sup>-</sup>, SF<sub>3</sub><sup>-</sup>, SF<sub>2</sub><sup>-</sup>, F<sub>2</sub><sup>-</sup>, and F<sup>-</sup>. Energies, at which they appear, have been measured for both the dissociative attachment process and the polar dissociation process. Present cross section values are compared with previous two measurements with whom the overall agreement is poor.

\*Work supported in part by Air Force Wright Aeronautical Laboratories and in part by the Los Alamos Scientific Laboratory.  
#NRC-NASA Research Associate.

1. A. Chutjian and S. H. Alajajian, Phys. Rev. A35, 4512(1987).

**SESSION BA**

10:15 AM - 12:15 PM, Tuesday, October 22

Ballroom A

**PARTICULATES IN RF DISCHARGES**

Chair: J. Heindenreich, IBM - T.J. Watson

**BA-1** Particulates in Plasmas: An Astrophysical View, C. K. GOERTZ, Dept. of Physics & Astronomy, Univ. of Iowa - The processes that lead to charging of dust grains in a plasma are briefly reviewed. Whereas for single grains the results have been long known, the reduction of the average charge on a grain by "Debye screening" has only recently been discovered. This reduction can be important in the Jovian ring and in the rings of Uranus. The emerging field of gravitoelectrodynamics which deals with the motion of charged grains in a planetary magnetosphere is then reviewed. Important mechanisms for distributing grains in radial distance are due to stochastic fluctuations of the grain charge and a systematic variation due to motion through plasma gradients. The electrostatic levitation model for the formation of spokes is discussed, and it is shown that the radial transport of dust contained in the spokes may be responsible for the rich radial structure in Saturn's rings. Finally, collective effects in dusty plasmas are discussed which affect various waves, such as density waves in planetary rings and low-frequency plasma waves. The possibility of charged grains forming a Coulomb lattice is briefly described.

**BA-2** Mapping of the Electrical Properties of Contamination Particles Traps in a Sputter Plasma,\* R.N. CARLILE and S. GEHA, Univ. of Arizona - Clouds of contamination particles have been observed by several workers suspended in process plasmas. We report in this work on the electrical properties of particle clouds, which we call particle traps, in an argon sputter plasma with a substrate which is a graphite disk upon which is placed a silicon wafer. We have used a tuned Langmuir probe to map the time-averaged plasma potential as well as other plasma parameters throughout the region of the plasma that contains a trap. We find that the trap is as much as 5 volts higher in time-averaged plasma potential than that of the surrounding plasma. Elementary electrostatics must then dictate that the trap is a region of net positive charge with an electric field being directed outward from the trap. Thus, negatively charged particles will flow into the trap. The electrostatic plasma potential rises so rapidly at a trap boundary that a double layer may exist there.

\*Work supported by Sematech

**BA-3** The Dependence of the Electrical Properties of Particle Traps and the Plasma Sheath on the Material and Topography of the Wafer Electrodes,\* S. GEHA, R.N. CARLILE, and S.E. BECK, Univ. of Arizona- We have found that the electrical properties of contamination particle traps are highly dependent on the material and topography of the wafer electrode. For an argon plasma, particle traps will occur for all material configurations that we have so far investigated: silicon (50 mm) on graphite (100 mm), silicon on silicon, stainless on silicon, aluminum on silicon, and silicon on aluminum. Using a tuned Langmuir probe, we have mapped the time-averaged plasma potential for the region of the plasma occupied by the traps. We find very repeatable results which are significantly different for each material combination. The topography of the 0.6 mm thick 50 mm Si wafer sitting on a 100 mm wafer itself will create a trap! The Langmuir probe is an effective tool for mapping the interface between the plasma and the sheath to within  $\pm 0.5$  mm; the interface follows the topography on the wafer electrode, although there are exceptions.

\*Work supported by Sematech

**BA-4** Simulation of Particulate ("Dust") Transport in rf Glow Discharges. Timothy J. Sommerer, Michael J. McCaughey, and Mark J. Kushner, University of Illinois, Department of Electrical and Computer Engineering, Urbana, IL 61801 \* - The transport of particulate contamination ("dust") in rf glow discharges as used in microelectronic fabrication has been modeled using a hybrid Monte Carlo- fluid simulation. We find that dust transport is dominated by viscous ion drag<sup>1</sup> arising from Coulomb interactions between the charged dust and the charged ions drifting and diffusing in the plasma. Dust accumulates where the ion drag force is balanced by the electrostatic force from the strong sheath fields, in qualitative agreement with experiments. We also find that the Debye shielding of the charged dust is disrupted in the strong oscillating sheath fields. The results show that dust segregates by size with larger particles being closer to the electrodes, in agreement with experiments. Calculations in electronegative gas mixtures suggest that, while potential wells may exist at the same location as the maximum in dust density, they are not required for the accumulation of dust.

\* Work supported by IBM E. Fishkill, NSF and SRC.

<sup>1</sup> M. S. Barnes, et al. to be published.

**BA-5** Time evolution of particle size in Ar-SiH<sub>4</sub> plasma, influence on external electrical parameters and spectral emissions, \*L. BOUFENDI, A. BOUCHOLE, J. Ph. BLONDEAU, A. PLAIN, C. LAURE, M. TOOGOOD, GREMI Université d'Orléans France- The temporal variation of the size of the particles, generated in an Ar/SiH<sub>4</sub> (1 to 4%) plasma is studied over the range 0.5 to 300s by transmission electronic microscopy (TEM). The results show a linear increase in particle diameter for the first five seconds of about 100Å/s, and indicate narrow size distribution at all times. At longer times, spatial variation of the particle distribution is observed. The presence of particles causes a significant variation of the phase shift between the plasma current  $I_p(t)$  and the RF voltage  $V_{rf}(t)$  leading to a more resistive plasma. This change is also indicated by the emission intensity of argon lines as SiH<sub>4</sub> is added to a pure argon plasma. The phase variation is observed at the start of particle nucleation. Thus the phase shift can be used as a sensitive diagnostic for the presence of particle in the plasma. Their presence has also been detected by spectral diagnostic technics. The time evolution of the SiH\* ( $A^2\Delta \rightarrow X^2\Pi$   $\lambda = 414$  nm) and Ar\* ( $1S_2 \rightarrow 2P_1$   $\lambda = 7503$  Å) emission intensities show a dramatic decrease as the particles appear.

**BA-6** Macroscopic Particle Behavior in a Parallel Plate Discharge, D.B.GRAVES, J.E.DAUGHERTY, M.D.KILGORE, and R.K.PORTEOUS, U.C. Berkeley - The behavior of macroscopic particles in a parallel plate RF discharge is examined using a one-dimensional fluid model. The particle spatial distribution is influenced by electrostatic, gravitational, and thermophoretic forces as well as by ion momentum transfer. Plasma screening plays an important role in the particle behavior. Investigations for the case of low particle density - such that the particles have negligible influence on the plasma - show that forces may balance at multiple positions in the interelectrode gap. In particular, the spatial particle density profile has narrow peaks at the sheath edges and may have a peak at midgap depending on particle size and conditions. As the particle density becomes high, the particle influence on the plasma becomes important via ion-electron recombination on the particle surface and contribution to the macroscopic potential.

**BA-7**     The Transport of Dust Particles in Glow Discharge Plasmas, by John H. Keller, Michael S. Barnes, John C. Forster, James A. O'Neill and D. Keith Coultas, IBM East Fishkill Facility, Route 52, B/300, Z/48A, Hopewell Junction, NY 12533-0999.

A theory is presented for the transport of dust particles in glow discharge plasmas. The forces which act on the negatively charged dust particles are examined and estimated. The potential difference between the dust particle and the plasma can be estimated using the thick sheath probe theory developed by Langmuir and Mott-Smith. Thermal as well as monoenergetic ion currents are used in this model. The five forces discussed are: ion drag, electrostatic, neutral drag, gravitational and relaxation forces. The dominant force is shown to be dependent upon the particle size and location within the discharge. Particles (on the order of one micron) hover above wall surfaces when the ion drag and electrostatic forces are in balance.

**SESSION BB**

10:15 AM - 12:15 PM, Tuesday, October 22

Ballroom B

**COLLISION PROCESSES IN DISCHARGES**

Chair: C. De Joseph Jr., Wright-Patterson AFB



**BB-1** The Effects of Excited State Densities on the Radially Resolved Electron Energy Distribution, Michael J. Hartig and Mark J. Kushner, University of Illinois, Department of Electrical and Computer Engineering, Urbana, IL 61801 \* - In cylindrical low pressure glow discharges the shape of the radially resolved electron energy distribution (RREED) is determined by the disparity in mean free paths of electrons as a function of energy, and by the radial ambipolar electric field. Transport of excited states of the gas, however, can provide a "nonlocal" power input to the RREED by superelastic relaxation from locations where the RREED provides a higher rate of excitation. We have developed a model for the RREED taking into account energy resolved drift and diffusion in the ambipolar field, and applied it to the study of the effects of excited state densities on the RREED. In our example system (He/Hg) we found that the RREED, normally cooled by the ambipolar field near the walls, is heated by superelastic relaxation from excited states generated near the axis.

\* Work supported by Sandia National Laboratory, and the National Science Foundation.

**BB-2** Relating Scattering Cross-sections to Transport Data, E.E. KUNHARDT, Webster Research Institute, Polytech University - Farmingdale, NY - A reduced formulation for the inverse problem of electron kinetics, namely, that of obtaining the electron-atom scattering cross-sections from swarm data, is presented. An equation for the electron density is obtained from which the equations relating the experimental data and the scattering cross-sections are established. These equations are derived from a modal expansion of the distribution in terms of eigenfunctions of an extended collision operator and from an asymptotic analysis of the resulting dispersed relation. A case study is presented using Nitrogen as the background gas. The direct problem of the use of transport data for the modeling of discharges will also be discussed.

**BB-3** A Hydrodynamic Model of the Negative Ion Source, F A HAAS, A J T HOLMES and E SURREY, Culham Lab. UK - Unlike atomic and molecular processes in ion sources, the macroscopic properties have received little attention. Here, 'hydrodynamic' equations are used to investigate the electron, positive and negative ion properties of a bucket source. The source is assumed to be two-dimensional with the filter magnetic field (~ 30G) in the ignorable direction. The momentum equations include elastic collision processes between neutrals, electrons and both species of ions. Negative ions are produced by dissociative attachment, and destroyed by electron detachment and mutual neutralisation. Estimates based on charge exchange suggest that the positive ion and neutral temperatures are similar, whilst ion-ion Coulomb collisions indicate that the negative ion temperature is also of a similar order. Results from the Culham source suggest that the electron density along the axis falls exponentially. Assuming that the positive ion temperature also falls exponentially, then analysis leads to exponential forms for the electron temperature and electrostatic potential - in good agreement with experiment, as is the calculated axial profile for the negative ion density.

**BB-4** Surface-Wave-Sustained Plasma Source of a Supersonic Beam of Argon Metastables. M. BANNISTER, J. L. CECCHI, G. SCOLES, Princeton University.--- Argon plasmas sustained by 2.45 GHz electromagnetic surface waves are expanded into vacuum through a simple converging nozzle to produce supersonic beams of metastable argon atoms. The speed distribution of metastables in the beam has been investigated as a function of discharge parameters with a time-of-flight detector. Metastable fluxes up to  $6.0 \times 10^{14} \text{ s}^{-1} \text{ sr}^{-1}$  have been measured with parallel speed ratios in the range 4.1-8.0. Plasma electron density axial profiles measured by an interferometric technique will also be presented. The metastable beam could serve as an excitation source for processing applications where charged particles are undesirable.

**BB-5** Assessing reactions in a discharge in N<sub>2</sub>O from the light emission. T.H. TEICH and W. BLUMER, Swiss Federal Institute of Technology, Zürich. -In order to elucidate some reactions in discharges in flue gas mixtures (DeNO<sub>x</sub> experiments), the previously suggested method of studying the time dependence of light output from a short duration and low current Trichel pulse discharge\* - using synchronized single photon counting - has been expanded and refined. It has once more been applied to a discharge in N<sub>2</sub>O or in N<sub>2</sub>O with a small admixture of N<sub>2</sub> to serve as an "electron tracer". *Time gated* recording of the emission spectra reduces dark current counts and helps to separate overlapping spectral bands of differing origins. In pure N<sub>2</sub>O, the emission from N<sub>2</sub>O<sup>+</sup> (368 nm) is used to assess the short-lived electron population generating the primary reactant which then produces excitation of the NO(B) state, most intense emissions from v' = 0 and v' = 1. The v' = 1 population is found to decay considerably faster than that with v' = 0. To assess the reaction rates involved, a fitting routine to the direct readout from the MCA accumulating the single photon counts is being set up. This looks promising as the analytic solutions for the excited state populations present themselves as double exponential functions.

\* T.H. Teich, 42<sup>nd</sup> GEC abstracts, paper RB-1, p. 209 (1989)

**BB-6** Inference of Lightning in the Nightglow of Venus\* D. L. Huestis and T. G. Slinger, SRI International--The two published spectra of the nightglow emissions of Venus are attributed to NO C→X and A→X from 180 to 280 nm<sup>1</sup> and O<sub>2</sub> c→X from 400 to 700 nm<sup>2</sup>, due apparently to N + O and O + O recombination. Presumably the N and O atoms are formed by photodissociation of CO<sub>2</sub> and N<sub>2</sub> on the dayside and diffuse to the nightside. We have been reanalyzing the uv spectra taken by Pioneer Venus<sup>1</sup>. The majority of the scans contain only a few photons (0-10), summing to a characteristic N + O recombination spectrum with nine bands. There are a few bright scans with 25-65 photons showing only one or two spectrally adjacent NO bands. We interpret these bright truncated spectra as due to strong spatial or temporal variability, possibly due to lightning.

\* Supported by NASA

1. A. I. Stewart and C. A. Barth, *Science* **205**, 59 (1979).
2. V. A. Krasnopolsky, *Venus*, D. M. Hunten, L. Colin, T. M. Donahue, V. I. Moroz, Eds. (University of Arizona Press, Tucson, 1983).

**BB-7** Collisional Processes in Pulsed Laser Deposition of High Temperature Superconducting  $\text{YBa}_2\text{Cu}_3\text{O}_{7-\delta}$  Thin Films. N. S. NOGAR, R. C. DYE, S. R. FOLTYN, R. E. MUENCHHAUSEN AND X. D. WU, LANL. - Collisional processes are known to have a significant effect on laser deposition of  $\text{YBa}_2\text{Cu}_3\text{O}_{7-\delta}$  thin films, due both to the high density of material desorbed<sup>1</sup>, and to the presence of an oxidizing process gas<sup>2</sup>. We have examined these processes experimentally, through a combination of real-time optical and mass spectrometric<sup>3</sup> diagnostics and post-deposition analysis, and by modeling, through a combination of Monte Carlo and hydrodynamic methods. Knudsen layer formation is found to significantly effect the plume shape, while reactive collisions dominate the chemistry.

1. R. E. Muenchausen, K. M. Hubbard, S. Foltyn, R. C. Estler, N. S. Nogar, C. Jenkins, *Appl. Phys. Lett.* **56**, 578 (1990).
2. R. C. Dye, R. E. Muenchausen, N. S. Nogar, *Chem. Phys. Lett.* in press, (1991).
3. R. C. Estler, N. S. Nogar, *J. Appl. Phys.* **69**, 1654 (1991).

**BB-8** Effect of Ion-Ion Collisions on Plasma Flow in the Downstream Region of an ECR Plasma Etching Reactor\*, MAKAREM HUSSEIN, G. A. EMMERT and N. HERSHKOWITZ, U. of Wisconsin-Madison--In a previous work<sup>1</sup>, ion-neutral collisions were shown to have a significant effect in reducing the ion energy and the electrostatic potential drop in the downstream region of an ECR plasma etching system. In this work, we concentrate on studying the effect of ion-ion collisions on the ion parallel and perpendicular energy spectra. A kinetic simulation of plasma flow in the downstream region of an ECR etching reactor, in which ion-ion collisions are included using a Monte Carlo collision algorithm based on a binary collision model developed by Takizuka and Abe<sup>2</sup>, will be presented. Results show that ion-ion collisions play an important role in gaining back some of the ion perpendicular energy lost into the parallel direction because of the divergence of the magnetic field.

\* Supported by the Engineering Research Center for Plasma-Aided Manufacturing at the University of Wisconsin under NSF grant # ECD-8721545.

<sup>1</sup> M. Hussein, G. Emmert and N. Hershkowitz, *Collisional Effects on the Ion Energy and Angular Distributions in ECR Plasmas*, submitted to *J. Vac. Sc. Technol. A*.

<sup>2</sup> T. Takizuka and H. Abe, *J. Computational Phys.* **25**, 205 (1977).

**SESSION CA**

1:30 PM - 3:30 PM, Tuesday, October 22

Ballroom A

**COMPARISON SESSION ON HIGH DENSITY PLASMAS**

Chair: J.H. Keller, IBM - East Fishkill

**CA-1** Electron Cyclotron Resonance Plasma Etching,  
T. D. Mantei, University of Cincinnati- A microwave electron cyclotron resonance (ECR) reactor has been developed for selective anisotropic etching of gate polysilicon over oxide. The system uses Cl<sub>2</sub>-O<sub>2</sub> chemistry, and handles 150 mm wafers with He backside cooling and vacuum load-locked wafer entry. At an input power density of  $\approx 5$  W/cm<sup>2</sup>, an etch rate of 4000 Å/min is obtained in undoped polysilicon, using 100 sccm Cl<sub>2</sub>, 0.6% O<sub>2</sub>, 4 mTorr pressure, and zero applied rf bias. The poly-oxide selectivity is 100 to 300, and the poly-resist selectivity is 15 to 20. Half-micron gates etched with no applied bias are anisotropic (>88-89° wall angle), and etched surfaces are residue free.

**CA-2** Evaluation of a Permanent Magnet,  
Ring Multicusp, Etch Chamber with a Remote ECR  
Plasma Source, J. R. TROW and J. M. COOK,  
Applied Materials Inc. - Results from etching poly silicon wafers with chlorine, in a large volume, high flow plasma chamber will be presented. Plasma confinement was enhanced by a set of permanent magnets arranged to form magnetic multicusp rings. This novel magnet configuration has several advantages over the line multicusps commonly used. These include circular symmetry, easy matching to sources with strong solenoidal magnetic fields, and direct wafer access. Almost any remote plasma source could be accommodated by this multicusp device; however, so far we have utilized a 6" ECR source exclusively. This device was developed as part of an effort to evaluate alternative plasma processing technologies.

**CA-3** Recent results from Helicon Reactors R. W. BOSWELL A.J. PERRY Space Plasma and Plasma Processing P.R.L. Research School of Physical Sciences and Engineering Australian National University Canberra, Australia. D.HENRY CNET Meylan France. Results of etching using helicon reactors in Australia, Europe and the USA are summarized. All reactors have a 15 cm diameter source and a 30 cm diameter diffusion chamber where the substrate is situated. Some use solenoidal confinement and some a hybrid scheme with solenoidal source confinement and multipole diffusion chamber confinement. Photoresist with  $O_2$  on 6 inch wafers has been investigated. Silicon etching has been done using  $BCl_3$ ,  $BCl_3/O_2$ ,  $HB_r$ ,  $SF_6$ , the last two with cooled substrates ( $-70^\circ C$ ).

**CA-4** Status and Future of Helicon Sources. FRANCIS F. CHEN, UCLA - Plasma generators based on Landau damping of helicon waves have several advantages for materials processing: they are electrodeless, efficient, dense, and uniform, and have small dc magnetic and electric fields. But the situation is much more complicated than originally thought, and agreement with theory is not easily achieved. Densities of  $10^{14} \text{ cm}^{-3}$  have been reported with peaked profiles, and  $> 10^{12} \text{ cm}^{-3}$  with broad profiles. We believe that high efficiency is caused by continuous wave acceleration of primary electrons and give experimental evidence for this. At low B fields of 10-50 G, we have found a second density peak which we think is a type of ECR discharge at rf frequencies. At low fields, electrostatic confinement of primaries is an important effect, as in capillary discharges. At high fields (100-800 G) burnout of neutrals along the axis and radiation pressure from the antenna could be important. In addition, there is non-resonant inductive ionization, which shows up clearly in our measurements. To produce the ideal plasma source, these factors, together with antenna design, gas feed, and field shape, have to be understood and optimized; and we think that this can be done.

**CA-5** Application of Helicon-Diffusion Reactors for Dry Processing, R. VAN OS, N. M. P. BENJAMIN, B. N. CHAPMAN, Lucas Labs, Sunnyvale, CA 94086 - Helicon plasma sources operating at 13.56MHz in low B fields ( $<100G$ ), which have already been shown to be effective in generating high intensity plasmas with low intrinsic bias, are now commercially available. The use of diffusion reactors based upon this technology is still relatively immature, such that a "library" of application work does not yet exist in the way that it does for diode reactors. In this paper we present some of the early work on process development, both performed in house, and by colleagues at other institutions. The applications surveyed are primarily for precision etching, where rate control, uniformity, and the independence of induced self-bias are imperative.

**CA-6** High Density Plasma Source for Etching Aluminum Thin Films. G. Kovall, A. Lamm, C. Chen, Lam Research Corp. High density plasmas comparable to ECR and Helicon have been generated at pressures of 5 to 30 mTorr using a flat, spiral, transformer coupled plasma (TCP) source. This plasma source inductively couples energy to the plasma at an RF Frequency of 13.56MHz. Argon ion densities of  $10^{11}/cm^3$  and corresponding ion current densities of  $40 mA/cm^2$  have been measured for input powers of 300W using a Langmuir probe. The ion current density was highest below the center of the spiral and by diffusion created a Gaussian shaped distribution. With RF bias on the wafer, aluminum submicron sandwich films have been etched anisotropically at rates of 8500 Angstroms/minute on 6" and 8" wafers using a  $Cl_2/BCl_3$  chemistry.



**CA-7** The Transformer Coupled Plasma (TCP) Source, Duane Gates, Eric Peltzer, Huong Nguyen, John Holland, Lam Research Corporation, 4650 Cushing Pkwy., Fremont, CA.

A planar inductive approach to achieving high density plasmas for use in low pressure processing of thin films has been developed. The Transformer Coupled Plasma source operates by coupling radio frequency currents within a planar inductor to a processing chamber. The coupling between the currents of the source coil and the currents within the plasma creates a high density plasma which can be sustained over a large range of pressures (1-500 mTorr). Furthermore, the planar geometry of the TCP source makes the resultant plasma ideal for wafer processing.

The TCP source is currently being developed for use in polysilicon, metal, and photoresist film processing. High etch rates with good selectivities to underlying layers have been achieved. Independent control of the source parameters (TCP) and the substrate parameters (RF Bias) enables the etch profile and the etch selectivities to be effectively controlled. Langmuir probe measurements have indicated that the TCP source can produce ion densities  $>10^{12}$  cm<sup>-3</sup> with low plasma potentials. Results for optical emission actinometry measurements suggest that this source can also be used for the efficient generation of reactive neutral species.

**CA-8** High Density Plasma Processing Comparison Session - RF Induction Multipole, John H. Keller and John C. Forster, IBM E. Fishkill, Z/48A, Hopewell Jct., NY. - Etch results will be presented for comparison with other with density systems: 1) A curve showing Photo Resist etch rate with an input plasma power of 4 Watts/cm<sup>2</sup>; an rf bias power 0.0, 1.0 and 2.0 watts/cm<sup>2</sup> and oxygen flow of .2 sccm/cm<sup>2</sup> of wafer surface, 2) a similar curve at higher power, 3) an SEM showing etch results, 4) plot of plasma density near the wafer vs power. This data will be compared to two ECR etch systems.

If possible chlorine/oxygen etch results will be given for etching of Poly Silicon.

**SESSION CB**

1:30 PM - 3:30 PM, Tuesday, October 22

Ballroom B

**DISSOCIATION & HEAVY PARTICLE COLLISIONS**

Chair: D.J. Eckstrom, SRI International

**CB-1** Slow Collisions of Ions with Rydberg Atoms. K.B. MacADAM,\* University of Kentucky.\*\* - New experimental results have been obtained in collisions of singly charged ions with Na Rydberg atoms. a) The distribution of final  $n$  states populated by electron capture shows non-monotonic variations of width with incident energy over the range 60-2100 eV. b) The total capture cross section for alkali ions on Rydberg targets shows peaks and dips over the same energy range, correlated with particular reduced velocities  $\bar{v}$  and the polarization of the exciting laser. c)  $\ell$ -Changing collisions of  $\text{Na}^+$  on  $\text{Na}(nd)$  targets,  $n=26$  and  $28$ , at low  $\bar{v}$  preferentially transfer multiple units  $\hbar$  of orbital angular momentum under single-collision conditions, despite very large impact parameters. d) Inelastic impacts of  $\text{Na}^+$  on  $\text{Na } 36s$  and  $30p$  states, perturbed by electric fields, populate a strongly field-dependent mixture of nearby Stark levels. A synopsis of recent progress will be given.

\*Visiting Fellow, JILA, U. Colorado/NIST, Boulder, CO, until August 1992.

\*Supported in part by NSF Grant No. PHY-8808022.

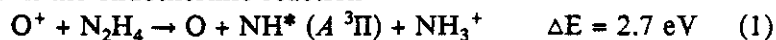
<sup>1</sup>S.B. Hansen, L.G. Gray, E. Horsdal-Pedersen and K.B. MacAdam, J. Phys. B (to be published).

**CB-2** Effect of Enhanced Collision Energy on Product Vibrational Excitation for the Proton Transfer Reaction:  $\text{O}^- + \text{HF} \rightarrow \text{F}^- + \text{OH}(v=0,1)$ .\* K. KNUTSEN, V. M. BIERBAUM, and S. R. LEONE,\*\* JILA, U. of Colorado and NIST. - Relative vibrational state populations are determined for the OH product of the reaction  $\text{O}^- + \text{HF} \rightarrow \text{F}^- + \text{OH}(v=0,1)$ , as a function of reactant center-of-mass collision energy in a flow-drift tube, using laser-induced fluorescence detection. Our results indicate that OH vibrational excitation increases with increasing collision energy at near-thermal energies. This is in direct contrast to the results of studies of neutral light-atom exchange systems. Theory and experiment suggest that the reaction behavior should be dominated by the kinematics of the mass ratio and be independent of the details of the potential energy surface. The results are considered in terms of the deep attractive well in the ion-molecule surface, which determines the reaction dynamics of this system.

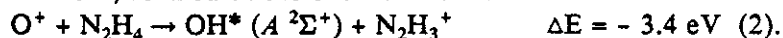
\* This work is supported by the Air Force Office of Scientific Research.

\*\* Staff Member, Quantum Physics Division, National Institute of Standards and Technology.

**CB-3** NH  $A \rightarrow X$  and OH  $A \rightarrow X$  Chemiluminescence in  $O^+ - N_2H_4$  Collisions at Suprathermal Energies, J. A. GARDNER, R. A. DRESSLER, R. H. SALTER, and E. MURAD, PhotoMetrics, Inc. (JAG) and PL/WSSI—Intense emissions at 335 nm have been observed in the space shuttle environment during thruster firings. These emissions are attributed to the NH ( $A \rightarrow X$ ) transition; however, the source of the excited NH is currently unknown. Chemiluminescence measurements are reported here for collisions between (the atmospheric ion)  $O^+$  and  $N_2H_4$  (a close relative of the thruster fuel MMH) at suprathermal energies ( $E_{c.m.} = 4$  to 50 eV). Emissions are observed that are attributable to two species: excited NH, most likely formed in the endothermic reaction



and excited OH, formed in the exothermic reaction



The intensity of the 335 nm NH band increases as  $E_{c.m.}$  is raised from 4 to 50 eV, and this band is the dominant spectral feature above  $E_{c.m.} = 13$  eV. In contrast, the 310 nm OH  $A \rightarrow X$  band intensity decreases rapidly with increasing center-of-mass collision energy (roughly proportional to  $E^{-0.75}$ ). The OH band is dominant below  $E_{c.m.} = 10$  eV, which is the energy range that is typical of the low Earth orbital environment.

**CB-4** Electron-Impact Dissociation of  $H_3^+$  A. E. OREL\*, Dept. of Applied Science, UC Davis--We have carried out a theoretical determination of the electron impact dissociation cross section of  $H_3^+$  from 15eV to 21eV via excitation of the two lowest ( $^3E$ ,  $^1E$ ) excited electronic states using the complex Kohn variational method. The calculations employed extensive multi-configuration target wave functions that accurately reproduced the energy levels and transition dipoles of the ground and excited states of the ions. All open channels were included explicitly in the scattering calculation. Closed channel effects were included via an *ab initio* optical potential. Modifications of the total excitation cross section due to the effect of zero-point nuclear motion of the target were found to be significant.

\* Work supported by NSF PHY-90-14845, and performed under the auspices of the US Department of Energy at Lawrence Livermore National Laboratory under contract number W-7405-ENG-48.

**CB-5** Energetics of the  $O^- + CH_4$  Ion-Molecule Reaction\*, H. H. Michels and R. H. Hobbs UTRC, and A. A. Viggiano, R. A. Morris and J. F. Paulson, AFPL, Geophysics Directorate---The reaction of  $O^-$  with  $CH_4$  is exothermic by 24.9 kJ/mol to form  $OH^-$  through hydrogen abstraction. Preliminary experimental data indicate that the rate of this reaction is substantially reduced by the substitution of deuterated methane. We have examined the minimum energy pathway for this reaction, along the  $^2A_1$  ground state surface, using the intrinsic reaction coordinate method of Schmidt, et al <sup>1</sup>. At the HF/6-31++G(d,p) level of theory, we find a classical barrier height of approximately 2 kJ/mol. Rovibrational energy quantum corrections have been applied to reactants, transition states and products for  $CH_4$  and the deuterated forms  $CH_2D_2$  and  $CD_4$ . The calculated barrier heights and overall exothermicity correlate with the observed relative reaction rates for the deuterated forms; an increased barrier height results in a slower rate for D abstraction compared to H abstraction. Correlated energy calculations at the MP2/6-31++G(d,p) level of theory have been carried out for reactants, products and at the geometry of the transition state. The effect of correlation is to lower the barriers heights uniformly. We find a broad barrier along the minimum energy reaction coordinate in the region of the transition state. This suggests that quantum tunneling effects are negligible for this system.

\*Supported in part by AFOSR under Contract F49620-89-C-0019.

<sup>1</sup>M. W. Schmidt, et al, JACS 107 p2585 (1985).

### CB-6

#### Charge Transfer Reactions of Slow $He^{++}$ Ions with Molecules.

R.E. TOSH and R. JOHNSEN, University of Pittsburgh--- We have measured rate coefficients and product-ion distributions for reactions of slow (0.01 to 1 eV)  $He^{++}$  ions with  $H_2$ ,  $N_2$ ,  $O_2$ ,  $CO$ ,  $CO_2$ , and  $H_2O$  molecules using a selected-ion drift tube. The reaction rates are close to the limiting induced-dipole or ADO rate coefficients and are essentially independent of ion energy, except in the case of  $H_2O$  where we find a very large thermal rate coefficient ( $10 \times 10^{-9} \text{ cm}^3/\text{s}$ ) that decreases with increasing energy. Singly and doubly-charged product ions are observed in several reactions indicating that both single and double charge transfer, and possibly transfer ionization occur simultaneously. Somewhat surprisingly, the reaction with  $CO_2$  produces a significant fraction of  $C^{++}$  ions in both the ground and first metastable state.

Work supported, in part, by NASA.

**CB-7 THE REACTIONS OF  $\text{Si}^+$  IONS WITH  $\text{CH}_3\text{SiH}_3$ ,  $\text{CH}_3\text{SiD}_3$ ,  $\text{C}_2\text{H}_6$  and  $\text{CH}_3\text{CHD}_2$ , K. P. Lim and F. W. Lampe\*, Department of Chemistry, The Pennsylvania State University, 152 Davey Laboratory, University Park, PA 16802**

The reactions of  $\text{Si}^+$  with  $\text{CH}_3\text{SiH}_3$ ,  $\text{CH}_3\text{SiD}_3$ ,  $\text{C}_2\text{H}_6$ , and  $\text{CH}_3\text{CHD}_2$  have been studied in a tandem mass spectrometric apparatus over the kinetic energy range of 1-10 eV (LAB). In all systems the major process is the formation of  $\text{SiCH}_3^+$ , as well as  $\text{SiCH}_2\text{D}^+$  and  $\text{SiCHD}_2^+$  in the case of the reaction with  $\text{CH}_3\text{CHD}_2$ . It is shown that in the reaction of  $\text{Si}^+$  with  $\text{CH}_3\text{SiH}_3$  and  $\text{CH}_3\text{SiD}_3$  the process is best described as a Walden inversion while in the reaction with  $\text{C}_2\text{H}_6$  and  $\text{CH}_3\text{CHD}_2$  the process appears to approximate the spectator stripping model or modified spectator stripping (polarization-reflection model). In the reaction with  $\text{CH}_3\text{CHD}_2$ , the slight preference of the  $\text{Si}^+$  to strip the  $\text{CH}_3$  radical rather than the  $\text{CHD}_2$  radical is shown to be in accord with a cross-sectional energy dependence of approximately  $E^{-1}$ .

**SESSION D**

3:30 PM - 5:30 PM, Tuesday, October 22

Ballroom C

**POSTERS**

**Diagnostics**

**GEC Reference Cell & Related RF Discharge  
Measurements & Modelling**

**DA-1** Laser Induced Fluorescence Studies of Ion Dynamics in an ECR Etcher, E. A. DEN HARTOG, H. PERSING, J. S. HAMERS, and R. CLAUDE WOODS, U. of Wisconsin-Madison- We have studied the axial and radial velocity distributions of  $N_2^+$  ions in the bulk plasma downstream of a divergent field ECR source in both pure  $N_2$  and in mixtures of  $N_2$  and He. The velocity distributions were determined from Doppler broadened and shifted lineshapes using laser induced fluorescence. Ions in an ECR device gain axial energy in the ambipolar drop in plasma potential between the source and downstream region ( $\Delta\phi$ ), but even at the relatively low pressures studied, the collision rates are sufficient to greatly attenuate this gain. The average axial ion energy is 3.6 eV at 0.3 mTorr (~18% of  $\Delta\phi$  ~ 20 V), and drops sharply with increased pressure to 0.11 eV at 4 mTorr (~2% of  $\Delta\phi$  ~ 5 V). Over the same pressure range the transverse ion temperature is found to vary from 0.42 eV to 0.18 eV. At pressures above 1 mTorr the axial ion velocities appear to agree well with drift velocities determined from mobility theory. This comparison assumes an electric field strength equal to  $\Delta\phi$  divided by the distance between source and downstream. Off axis the ions have a net outward radial drift velocity due to the ions following the diverging B-field as they drift downstream. In contrast to the ion translational energies, the  $N_2^+$  rotational temperature is near ambient at low pressure and rises with increased pressure.

\* work supported under NSF grant ECD-8721545

**DA-2** Infrared Diode Laser Absorption Studies in an Electron Cyclotron Resonance Plasma Etching Tool, \* R. CLAUDE WOODS, R.L. McCLAIN, L.J. MAHONEY, Engineering Research Center for Plasma-Aided Manufacturing, U. of Wisconsin-Madison- A high resolution infrared spectrometer has been used to investigate plasmas in the downstream region of a diverging field ECR etcher. The absorption spectrometer based on a Laser Analytics diode laser source employs a Herriott type multipass cell with the two gold coated mirrors recessed from the active plasma. Laser propagation is orthogonal to the axial magnetic field (plasma streaming) direction and typically 30 passes yield an effective path length of 9 m. Absorption lines of  $CF_2$ ,  $CF_3$ , and  $CF_4$  have been monitored in  $CF_4/O_2/CHF_3$  plasmas as gas composition, pressure (1 to 3 mTorr), and power (500 to 900 W) are changed. Absolute densities of  $CF_2$  are determined from the measured line intensity and our *ab initio* value of the line strength. The  $CF_2$  density varies from  $5 \times 10^{10} \text{ cm}^{-3}$  to  $7 \times 10^{11} \text{ cm}^{-3}$  over the range of plasma conditions studied.

\* This work was supported under grant ECD-8721545 from the National Science Foundation



**DA-3 Dependence of Optogalvanic Signal on Laser Excitation Region in a Low Power Neon rf Discharge.**  
**D. KUMAR, S. P. McGLYNN, Dept. of Chemistry, LSU, Baton Rouge, LA. 70803** - - - The regional dependence

of pulsed laser optogalvanic signals from some 1s<sub>j</sub> -> 2p<sub>k</sub> excitations in neon (~5 torr) in a low power ~30 MHz rf discharge has been investigated. A gradual transition to a drastically different temporal profile is observed as the excitation laser beam is displaced away from the main body of the plasma. These changes may be interpreted using a recently developed method which permits distinction between optogalvanic signals generated by (i), changes in the equilibrium ionization rates and (ii), the photoacoustic effect. The observed behavior can be explained as a laser induced modulation of (i), plasma resonance (electrical) characteristics and/or (ii), coupling between the plasma and the pick-up coil.

**DA-4 Mole Fractions of H, CH<sub>3</sub> and Other Species During Filament-Assisted Diamond Growth, \* W. L. Hsu, Sandia National Laboratories, Livermore, CA 94550**- Molecular beam mass spectrometry has been used to quantitatively analyze the composition of the gaseous environment in a hot-filament reactor under diamond-growth conditions. Low concentrations of free-radicals, with mole fractions of as low as 10<sup>-5</sup>, can be detected by using the threshold ionization technique. The absolute concentrations are determined by a combination of using the published ionization cross-sections and calibrating the instrument sensitivity. At a filament temperature of 2600 K, the H-atom concentration in the proximity of the growth surface was found to decrease with increasing addition of methane to the feed gas, dropping by more than an order of magnitude when the methane percentage was increased from 0.4% to 7.2%. Concurrent with this decrease, large changes in the concentration of the hydrocarbon species were observed. From the measured mole fractions, the reaction  $H+CH_4 \rightleftharpoons H_2+CH_3$  was found to be in nonequilibrium near the surface, with the reverse rate ranging from approximately three to sixteen times larger than the forward rate. We attribute the cause of this nonequilibrium to heterogeneous reactions on the surface of the substrate.

\*This work was supported by US DOE under contract #DE-AC0476DP00789 and DARPA/DSO-Material Science Program.

**DA-5** A New Pitch-Angle Diagnostic For Magnetized Plasmas—S.W. LAM AND N. HERSHKOWITZ, Engineering Research Center, University of Wisconsin-Madison—Directional etching in magnetized plasmas is determined by the ratio of the ion perpendicular temperature  $T_{i\perp}$  (perpendicular to the magnetic field) to the average ion parallel energy  $E_z$  (parallel to the magnetic field) at the wafer-plasma sheath boundary. An instrument, a Pitch-Angle Diagnostic (PAD), capable of measuring the ratio  $T_{i\perp}/E_z$  in a magnetized plasma is described. It consists of a collector, a plane stainless steel electrode with its axis parallel to magnetic flux line, which can be slid along the inside of a stainless steel cylindrical tube of radius  $R$ . The collector is insulated from the tube and is biased to a negative potential to collect ions. Theoretical analysis shows that the collected ion current only depends on the ratio of  $T_{i\perp}/E_z$  and is insensitive to the absolute value of  $T_{i\perp}$  and  $E_z$ . If  $E_z$  is known, PAD can provide a measurement of  $T_{i\perp}$ . It is found that the ion perpendicular temperatures derived from the PAD are comparable to those obtained from LIF (Laser Induced Fluorescence) measurement for nitrogen plasma.

\* Work supported in part by NSF Grant No. ECD-8721545 and in part by Varian Associates.

**DA-6** Characterization of ECR Plasmas Optimized for the Deposition of Polycrystalline Diamond Films, D.L. YOUCHISON,\* C.R. EDDY, Jr., and B.D. SARTWELL, Naval Research Laboratory - Optical emission spectroscopy, Langmuir probes, and  $\underline{B}$ -field probes have been used to characterize electron cyclotron resonance plasmas used in the deposition of polycrystalline diamond films. These plasmas were generated at 10 mTorr using various ratios of  $\text{CO}/\text{H}_2$  and  $\text{CH}_4/\text{O}_2/\text{H}_2$  to produce the highest quality films (i.e. high degree of faceting and intense Raman peak). Temperature, density, and  $\underline{B}$  field profiles obtained at optimum growth conditions will be presented. The best diamond films were produced with the ECR layer a distance of 7.6 cm in front of the substrate producing  $n_e = 2 \times 10^{11}$  and  $T_e = 5$  eV at the substrate. Actinometry was used to quantify the optical emission spectra. In the  $\text{CO}/\text{H}_2$  system, line intensity ratios of  $\text{H}_\gamma/\text{Ar}=9.4$ ,  $\text{CH}/\text{C}_2=2.4$ ,  $\text{H}_\gamma/\text{C}_2=2.5$ , and  $\text{O}/\text{C}_2=0.27$  were typical. Nearly identical films were produced in the  $\text{CH}_4/\text{O}_2/\text{H}_2$  system, with line intensity ratios of  $\text{H}_\gamma/\text{Ar}=12.4$ ,  $\text{CH}/\text{C}_2=2.8$ ,  $\text{H}_\gamma/\text{C}_2=2.7$ , and  $\text{O}/\text{C}_2=0.24$ . These results indicate that the feedgas composition is less important than the critical ratio of  $\text{C}/\text{O}/\text{H}_2$  in an ECR plasma.

\*Office of Naval Technology Postdoctoral Fellow

**DA-7** A Tessellated Probe for Plasma Process Development, N. M. P. BENJAMIN, B. N. CHAPMAN, G. T. GROVER and K. R. KRIEG, Lucas Labs, Sunnyvale, CA 94086 - A 200mm diameter insulating plate tiled with a hexagonal array of 121 electrostatic probe elements forms a tessellated probe capable of simulating a wafer and its chuck during processing. This tool is being used to make ion flux and spatial distribution measurements, to aid in process development for a helicon/diffusion reactor. Computer automated data acquisition, processing, storage and real time graphics are available, such that parameters can be conveniently derived and displayed.

**DA-8** Measurement of CF<sub>3</sub> radical in RF excited CHF<sub>3</sub> plasma using infrared diode laser absorption spectroscopy\*  
T. GOTO, A. SAKAI, M. NAITO and N. ITABASHI, Nagoya Univ., and E. HIROTA, Graduate Univ. for Advanced Studies --  
There are CF, CF<sub>2</sub> and CF<sub>3</sub> radicals in RF excited CH<sub>m</sub>F<sub>n</sub> plasmas used for etching process. The CF and CF<sub>2</sub> radicals were measured using laser induced fluorescence and infrared laser absorption methods. However the CF<sub>3</sub> radical has not ever been measured. In this work, with using infrared diode laser absorption spectroscopy (IRLAS), first the CF<sub>3</sub> radical was measured in the on-off modulated RF CHF<sub>3</sub> plasma. The RF chamber had plane parallel electrodes of 20 cm diameter and 3 cm separation, and the White type multireflection system for obtaining an absorption length of 12 m. The measurement was made using the  $\nu_3$  band in the wavelength region of  $\sim 8\mu$ . The spatial distribution of the CF<sub>3</sub> radical density between electrodes was measured at a RF power of 50 W and a CHF<sub>3</sub> pressure of 50 mTorr. It was shown to be almost flat, which is consistent with the long decay time constant of more than 10 ms observed in the transient absorption waveform. The H<sub>2</sub> pressure dependence of the CF<sub>3</sub> radical density was also measured.  
\*Supported by Grant-in-Aid for Scientific Research on Priority Areas of Education, Science and Culture.

**DB-1** An Alternative Approach to Identifying Discharge Conditions in the GEC Reference Cell, V.A. Godyak, GTE Laboratories Incorporated, Waltham MA -- The use of wire probes to identify discharge conditions is discussed in application to the GEC Reference Cell or to an industrial plasma reactor. Three kinds of probe diagnostics with differing levels of complexity and informativeness will be considered as an alternative to measuring the electrical discharge characteristics. While it is generally not easy to determine the discharge's electrical characteristics from the electrical characteristics of a plasma processing system, probe methods directly relate to the plasma parameters regardless of the power source (dc, rf or  $\mu$ wave) and particular hardware design (matcher, generator etc.). A probe based system promises the possibility of an in situ diagnostic with practically instant information display which could be included in a feed-back system to control plasma processing.

**DB-2** A Comparison of Electrical Discharge Characteristics Measured in a Symmetric rf System and in the GEC Reference Cell, V. A. Godyak, R. B. Piejak and B. M. Alexandrovich, GTE Laboratories Incorporated -- Electrical discharge characteristics (driving voltage and discharge power vs discharge current) have been measured in a radially confined, symmetrical rf discharge system driven at 13.56 MHz. Significant differences has been found between these measurements and those measurements made in the GEC Reference Cell under similar discharge conditions: argon gas, with the same electrode spacing, driving frequency, discharge voltage and gas pressure. Fundamental differences between the two discharge systems, as well as, measurement and analysis techniques used with the GEC Reference Cell, are believed to account for the observed discrepancy and these subjects will be discussed.

**DB-3** Particle Simulation of Low-Pressure Radio Frequency Discharges, M.M. TURNER, DCU - This paper will describe a hybrid particle-in-cell/Monte-Carlo simulation at a radio-frequency discharge in a low pressure gas. Results will be presented for a helium-like model gas, and comparisons with experimental measurements for pressure scaling will be made. The occurrence of a heating mode transition at a critical pressure<sup>1</sup> will be discussed.

I.V.A. Godyak and R.B. Piejak, *Phys. Rev. Lett.* 65(20), pp 996-999.

**DB-4** Comparison of Continuum Model Predictions to Results from a Well-defined Parallel-plate Reactor, G. L. Huppert and H. H. Sawin, *Department of Chemical Engineering, MIT, Cambridge, MA 02139*. Continuum discharge modeling has been implemented using a spectral element spatial discretization and optimized for vectorization on a CRAY-II computer. The model is extremely efficient, and produces accurate solutions with minimal computation time. One dimensional results will be presented for an argon plasma with a one inch gap at pressures of 0.5 and 1.0 torr, to be compared with similar data collected by Joanne Liu on a well-defined parallel-plate reactor. The model results for current versus voltage, power, ion flux, ion energy, and spatial and temporally resolved emission will be compared to experimental results.

**DB-5** A Comparison of PIC/MC RF Discharge Simulations to Experimental Measurements, D.B. GRAVES, T.E. NITSCHKE, and M. SURENDRA, U.C. Berkeley - Particle-in-cell / Monte Carlo simulations of rf discharges between parallel plate electrodes in helium have been compared to experimental measurements for a range of conditions. The simulation is conducted for an electrode separation of 6.7 cm, and it is assumed that the discharge may be treated as one dimensional. Voltage-current, plasma density, average electron energy and the distribution of electron energy, period-averaged in the center of the discharge are predicted and compared to experiment.

**DB-6** Comparison of Fluid and Particle-in-Cell Simulations of RF Glow Discharges, D.B. GRAVES, T.E. NITSCHKE, and M. SURENDRA, U.C. Berkeley - Particle-in-cell / Monte Carlo simulations of RF parallel plate electrode glow discharges are compared to fluid model simulations in helium and argon. The particle simulations have the advantage of being able to treat highly non-equilibrium, non-local phenomena, but they are relatively expensive computationally. For many future applications of discharge simulation, multiple spatial dimensions and neutral transport and chemistry will be important, and computational cost will become an issue. We explore the ability of a fluid model to treat discharges at pressures low enough that collisional mean free paths are not the smallest length scale. Comparisons to experimental measurements are made when possible.

**DB-7** Particle-in-cell/Monte-Carlo simulations of rf parallel plate discharges: A parametric study, M. SURENDRA and D. B. GRAVES, University of California, Berkeley - Self-consistent kinetic level simulations have been used to study the behavior of capacitive rf parallel plate discharges over a range of voltage, frequency and pressure. Results suggest simple scaling laws that are in broad agreement with analytic models and experimental measurements. Ion flux and plasma density are found to vary approximately linearly with voltage and quadratically with frequency at constant pressure and electrode spacing. Sheath thickness decreases with frequency but is almost independent of voltage. Furthermore, ion flux increases sublinearly with pressure, while sheath thickness decreases sublinearly with pressure. These studies indicate that low voltage discharges with high ion flux and low ion collisionality in sheaths are possible at very high frequencies (~ 100 MHz).

**DB-8** A Bounded Particle in Cell Code with an Atomic Physics Model for Simulating Processing Plasmas,<sup>1</sup> V. VAHEDI, M. A. LIEBERMAN, G. DIPESO, C. K. BIRDSALL, University of California, Berkeley, T. D. ROGNLIEN, J. R. HISKES, and R. H. COHEN, Lawrence Livermore National Laboratory- We are combining a particle-in-cell (PIC) model for particle and field dynamics with a Monte Carlo collision (MCC) scheme to model the collisions between the charged and neutral particles. The MCC model can also be extended to model Coulomb collisions between charged particles which tends to be significant at very low temperature discharges. These models are incorporated into PDP1, a bounded one dimensional plasma simulation code. As a specific example, we consider oxygen RF discharges at various neutral pressures and RF voltages. Electrons,  $O_2^+$ ,  $O^+$ , and  $O$  are evolved as particles. These models can be used to model other processing discharges.

- 
1. Work performed for USDOE by LLNL under contract W-7405-ENG-48; a portion of the UCB work performed for NSF under grant ECS-8910827.

**DB-9** A Comparison of PIC Simulation and Experimental Results in a Capacitive RF Discharge.<sup>1</sup> P. MIRRASHIDI, B. P. WOOD, V. VAHEDI, M. A. LIEBERMAN, and C. K. BIRDSALL, EECS Dept. University of California, Berkeley - Simulation results from PDP1, a 1d3v bounded particle-in-cell code,<sup>2</sup> are compared to recently published experimental results<sup>3</sup> over a pressure range of 10-100 mTorr and 100-1000 V applied RF voltage in a symmetric, parallel plate, argon discharge. We show that where similar results are obtained, the simulation allows insight into plasma parameters which are not experimentally accessible, such as details of the electron power sources and losses.

- 
1. Work supported in part by the ONR, DOE and NSF.
  2. Available from C. K. Birdsall, Plasma Theory and Simulation Group, EECS Dept., UC Berkeley.
  3. V. A. Godyak, and R. B. Piejak, and B. M. Alexandrovich, IEEE Trans. Plasma Sci., August 1991.

**DB-10** Heating by RF Sheaths.\* B.P. WOOD, M.A. LIEBERMAN, and A.J. LICHTENBERG, EECS Dept., U.C. Berkeley - Low pressure, capacitively coupled rf discharges used for materials processing are typically operated at 1-100 mTorr with 50-1000 v applied at 13.56 MHz in a parallel plate chamber. Under these conditions, electrons are stochastically heated. Previous derivations<sup>1</sup> of stochastic heating rates have assumed that the sheath motion is slow compared to the electron thermal velocity, and that the electrons are maxwellian. Using PDP1, a 1d3v PIC simulation code,<sup>2</sup> we find that these assumptions are not valid for many experimental parameter ranges. In particular, the electron distribution is two temperature, is warmer at the sheath edge than in the body of the plasma, and displays drifts which are of the order of the sheath velocity. Incorporating these changed assumptions into the existing theory, we show that the stochastic power delivered by the sheaths to the electrons is greatly enhanced, and that the scaling of the density and sheath thickness with r.f. driving voltage is increased. We compare these scalings to recently published experimental results.<sup>3</sup>

---

\*Work supported in part by the NSF and DOE.

<sup>1</sup>M.A. Lieberman, IEEE Trans. Plasma Sci. 16 638 (1988).

<sup>2</sup>Available from C.K. Birdsall, EECS Dept., U.C. Berkeley.

<sup>3</sup>V. A. Godyak, and R. B. Piejak, and B.M. Alexandrovich, IEEE Trans. Plasma Sci., August 1991.



**DB-11** Heating of Electrons by RF Sheaths\* A. E. Wendt and W.N.G. Hitchon, University of Wisconsin, Madison- This theoretical reexamination of the sheath heating process looks at its role for a variety of electron energy distributions and sheath conditions. The model assumes a sheath electric field which varies linearly with distance from the electrode and sinusoidally in time. We find that for typical sheath conditions, exact calculations of electron energy gain through sheath interaction, resolved in incoming phase and velocity, agree well with an "impulse" model, in which the change of electron velocity is simply twice the instantaneous velocity of the sheath edge at the time of interaction, except for those which actually strike the electrode. For electrons entering the sheath region with velocities greater than the maximum sheath velocity, energy loss due to electron escape to the electrode becomes important, so that only the colder electrons participate in net power input into the system. With our analytical impulse model of electron energy gain, scaling of power input will be calculated for various parameters. Application to discharge modelling will also be discussed.

\* Work supported under NSF Grant # ECD-8721545

**DB-12** A Two-Coupled-Sheath Model for the Conduction of Current Through Asymmetric Parallel Plate RF Discharges.\* A.H. SATO, M.A. LIEBERMAN. U.C., Berkeley .--- The effect of electrode area ratio on the current flowing through a parallel plate rf discharge is studied to gain qualitative understanding on how current continuity is maintained in asymmetric systems and how electrode asymmetry affects the harmonic spectrum of the current. A uniform ion density sheath model is used. The total current flowing through the powered electrode sheath is equated to that at the ground electrode sheath, and the external voltage is set equal to the sum of the voltage drops across each sheath. This results in a first order differential equation in one sheath voltage, which is integrated numerically. Some results are: (1) The current waveforms approach skewed sine waves with increasing rf amplitude. (2) Current continuity is accomplished by nonsinusoidal variations in the sheath voltages. (3) Increasing the area ratio induces a broadening of both conduction and displacement current frequency spectra. (4) At modest area ratios, the large, distinct conduction current spike is very weak. In this case, the coupling of two sheaths allows nonsinusoidal variations in the sheath voltages that broaden the conduction current wave form.

\* Work supported by NSF Grant ECS-8517363 and DOE Grant DE-FG03-87ER13727.

**DB-13** A Computational Investigation of the GEC rf Reference Cell Using a Monte Carlo-Fluid Hybrid Model.  
 Timothy J. Sommerer and Mark J. Kushner, University of Illinois, Department of Electrical and Computer

Engineering, Urbana, IL 61801 \* - Operating conditions of the Gaseous Electronics Conference rf reference cell have been investigated using a hybrid Monte Carlo fluid model for rf glow discharges. The model combines a Monte Carlo Simulation (MCS) to provide nonequilibrium excitation rates with a fluid simulation (FS) to provide species densities and electric fields. Discharges sustained in He, Ar, and N<sub>2</sub> have been modeled to compare with experimental measurements. In each case, the effects of multistep processes and Penning ionizations (when applicable) have been assessed. Additional simulations of electronegative gases and gas mixtures have been performed for purposes of comparison to the standard reference cell gases, including the effects of trace impurities (eg., He/O<sub>2</sub>/N<sub>2</sub>)

\* Work supported by IBM E. Fishkill, NSF and SRC.

**DB-14** Three Electron Transport Models by Particle-In-Cell Method for RF Glow Discharge.\* C. LI and C. WU, EE Auburn U.- Three self-consistent particle-in-cell models based on fluid and Poisson's equations for parallel-plate rf glow discharges have been developed. The electron transport is modeled by the equilibrium single-moment, and nonequilibrium two- and three- moment equations, respectively. In the analysis of electron power deposition for nonequilibrium model, the secondary electrons take time and distance to gain energy from space-charge fields to form a high-energy electron beam. Then, due to collisions and diffusion, these fast electrons lose energy and reach low-energy equilibrium states in the bulk of plasma. Because electrons need time and space to gain and lose energy, the nonlocal behavior is observed. Comparing with the equilibrium model, the sheath width and the peak ionization rate of nonequilibrium model are reduced by 13% and 78%, respectively, for the case that the rf amplitude is 40 v/cm at 1 torr. Comparisons among these three transport models are reported in this paper in terms of the densities, velocities and energy distributions, ionization rate and sheath width.

\* This work is supported by NSF under ECS-9009395 and CRAY Research Inc.

**DB-15** Nonequilibrium Transport Effects In Space-time Varying Electric Fields, \* J. H. TSAI and C. WU, Electrical Engineering Department, Auburn University, AL 36849. — The mechanisms of the nonequilibrium electron transport and the nonlocal phenomenon of the glow discharge have been studied in a space-time varying electric fields by Monte Carlo simulation. The nonequilibrium transport effect has been investigated by examining the electron energy distribution function and the electron currents of multiple energy groups. In addition, the trajectories of the electrons from the sheath region are simulated to demonstrate the nonequilibrium effects as a function of the rapidly space-time varying electric fields.

\*This work is supported by NSF under ECS-9009395 and CRAY Research Inc.

**DB-16** Simulations of the GEC RF-Driven Plasma Reactor with He,\* Merle E. Riley, Paul Drallos, and Robert McGrath, Sandia National Labs. We have developed a model of the electronic processes occurring in a He plasma entailing 12 electronic transitions, 5 levels (some composite), and trapped radiative decay of certain states. Along with surface scattering conditions, momentum transfer, charge transfer, and diffusion, these processes are incorporated into a 1D-2V electron Boltzmann equation (BE) code with time evolution alternating between BE and fluid equations (FE) dynamics. The FE electronic rates are obtained periodically from the BE. The ions and neutrals are completely FE. The BE-FE hybrid works well, enabling a study of the plasma and reaction kinetics to near steady state of the actual laboratory system.

\*Work performed at Sandia National Laboratories, supported by the US DOE under contract No. DE-AC04-76DP00789.

**DB-17** Electrical Isolation of RF Plasma Discharges,\* Paul A. Miller, Sandia National Laboratories, and Harold Anderson and Michael P. Splichal, University of New Mexico - Plasmas excited by radio-frequency (rf) power have nonlinear impedance characteristics. This causes the plasma state to depend on the nature of the circuitry that supplies electrical power to the plasma.<sup>1</sup> This dependency occurs because the harmonics of the drive frequency, which are generated by the plasma nonlinearity, interact with the impedance of the external circuitry at the harmonic frequencies. We describe the use of a low-pass rf filter in the power feed to the plasma in the GEC RF Reference Cell. The filter successfully isolates the plasma and eliminates its sensitivity to changes in the rf generator, cable plant, and matching network.

- \* Work supported by SEMATECH under contracts DE-FI04-89AL588772 and 88-MC-502, and by the U.S. Department of Energy under contract DE-AC04-76-DP00789.
1. K.E. Greenberg, P.J. Hargis, and P. A. Miller, "The GEC RF Reference Cell: Diagnostic Techniques and Initial Results", Sandia Report SETEC 90-013 (1990).

**DB-18** Spectral Signature Analysis and Parallel Optical Emission Spectroscopy for Discharge Characterization.

M. P. Splichal, H.M. Anderson, J. L. Mock, U. of New Mexico

New techniques for non-intrusive, in-situ measurement of discharge characteristics are critical to advanced control strategies for reactive ion etch plasma processing. This study reports on the development of rapid, spatially resolved optical emission spectroscopy tools and spectral "fingerprinting" techniques which can be used to precisely characterize discharge electrical features. Using the Reference Cell plasma reactor, systematic electrical probe measurements were made of the current and voltage waveform characteristics for Ar and fluorocarbon discharges while additionally collecting 3-channel optical emission spectra. It is shown that the broad optical emission spectral fingerprint of these plasmas contains information which directly correlates with I, V and bias measurements of the discharge to within the accuracy of the probe measurement itself. However, the amount of quantitative information contained in the spectral fingerprint is shown to have significant spatial dependence. Implications for reactive ion etch process control will be discussed.

**DB-19 Etching Results from the GEC RF Reference Cell,\*** P.D. Pochan, Geo-Centers, Inc., and P.A. Miller, Sandia National Laboratories - We report the first etching results from the GEC Cell which is evolving as a scientific reference system. Polysilicon etching was measured for both  $\text{Cl}_2$  and  $\text{Cl}_2/\text{HBr}$  plasmas. Wafers were 100-mm-diam p-doped ( $125 \Omega/\text{sq}$ ) silicon covered with 12 nm of oxide, 450 nm of polysilicon, and 500 nm of patterned photoresist. We used both scanning electron microscopy (SEM) and refraction (Nanospec) techniques to determine the etch parameters. Preliminary results for  $\text{Cl}_2$  are etch rates of 50 to 90 nm/min with 20 sccm  $\text{Cl}_2$  at 100 mtorr and 200  $V_{\text{p-p}}$  RF excitation (10 W) at 13.56 MHz. The  $\text{Cl}_2/\text{HBr}$  rates span 25 to 50 nm/min for 15 sccm  $\text{Cl}_2$ , 5 sccm HBr, 100 mtorr, and 200  $V_{\text{p-p}}$  excitation. These results are consistent with published data from other systems.<sup>1,2</sup> SEM profiles show that the addition of HBr changes the etch profile from isotropic to anisotropic.

\* Work supported by SEMATECH under contract DE-FI04-89AL588772

1. D. Economou and E. S. Aydil, *J. Appl. Phys.* **69**, 109 (1991).
2. S. C. McNevin, *J. Vac. Sci. Technol.* **B8**, 1185 (1990).

**DB-20 Impedance Characteristic of the GEC Reference Cell,\*** Joseph T. Verdeyen, University of Illinois, and Paul A. Miller, Sandia National Laboratories - One can make measurements of the electrical parameters (V, I, P) at the access terminals of a reactor, but it is more desirable to relate those parameters to that at the plasma terminals. Toward that end, we have made precision impedance measurements over the range of 1-108 MHz on the GEC RF Reference Cell with the plasma terminals open circuited, short circuited and inductively loaded. This enables us to infer an equivalent circuit which is consistent with the geometry of the cell and which agrees with the input measurements to a high degree of accuracy. Using this circuit, one can relate the plasma quantities to the terminal values with the standard ABCD matrix which is valid at all frequencies. The procedure for inferring this circuit and accounting for the resistive losses will be presented.

\*Work supported by SEMATECH under contract DE-FI04-89AL58872 and by the U.S. Department of Energy under contract DE-AC04-76-DP00789.

**DB-21** Two-Dimensional Helium Metastable Density Profiles in a GEC RF Reference Cell,\* K. E. Greenberg and G. A. Hebner, Sandia National Laboratories --

Optical absorption spectroscopy was used to measure  $2^3S$  and  $2^1S$  metastable densities in 13.56-MHz, helium discharges. Apertured light from a helium Geisler tube was expanded, collimated, and directed into a GEC Reference Cell through an 8-in viewport (6 inches clear optical access). The light exiting the cell through a similar viewport was focused and imaged, through a 0.5-mm aperture and bandpass filter, onto the intensifier of a CCD-array detector system. Spatially resolved absorption profiles (with approximately one millimeter resolution), extending from the center of the discharge to the edge of the viewport, were recorded for 1- to 15-W discharges at 0.5 and 1.0 Torr pressure. At 1.0 Torr, the metastable density profiles were peaked near the powered electrode with the  $2^1S$  profile reaching a maximum closer to the electrode than the  $2^3S$  profile. In addition, the metastable density dropped rapidly outside of the discharge region. At 0.5 Torr pressure, the metastable profiles were symmetric, peaking at the midpoint between the electrodes. Total metastable densities were on the order of  $10^{11}/\text{cm}^3$  for a 1-Torr discharge.

\*This work was performed at Sandia National Laboratories and supported by the U.S. Department of Energy under contract No. DE-AC04-76DP00789.

**DB-22** Confinement and Transient Effects in the GEC Reference Reactor. P. Bletzinger, A. Garscadden, Aero Propulsion and Power Directorate, WPAFB, Ohio and F. V. Wells, Idaho State University, Pocatello, ID.-- Measurements of electrical characteristics and electron densities ( $N_e$ ) in the GEC reference reactor were performed. To better define the dimensions of the plasma for electron density measurements with a microwave interferometer a pyrex cylinder with diameter equal to the electrode diameter was installed. Comparisons with the unconfined configuration were made.  $N_e$  varied little in Ar but increased strongly in He with pressure and decreased for both with confinement.  $N_e$  in  $N_2$  increased slightly with decreasing pressure. These characteristics are interpreted using a simple model which considers the relative importance of diffusion and recombination. Using pulsed rf excitation, a build-up time constant for the DC bias of 50 to 300  $\mu\text{s}$  for Ar and He and 1 to 3.5 ms for  $N_2$  was observed (unconfined). This is at least 10 times the RC time constant of the cw resistive impedance times the coupling capacitor. This refers to the fast part of the bias change; a slow part is also observed. On switch-off, again a fast decay depending on pressure and power plus a slow decay probably due to circuit time constants is observed for all three gases. The implications on modulated discharge processing are considered.

**DB-23** Optical Emission and Electrical Measurements on the NIST GEC RF Reference Cell,\* J. R. ROBERTS, S. DJUROVIĆ, J. K. OLTHOFF, and M. A. SOBOLEWSKI, NIST - Spatially and temporally resolved spectral emission data is presented for Ar discharges in the NIST GEC RF Reference Cell. These data are correlated to voltage and current measurements. These electrical measurements include the first three Fourier components of the amplitude of the voltage and current and phase angle between them. All of these data are taken at the prescribed Reference Cell conditions of pressure, flow rate and peak-to-peak voltage.

\* Work partially supported by SEMATECH.

**DB-24** Accurate Electrical Measurements of RF Glow Discharges in the NIST GEC Reference Cell. M. A. SOBOLEWSKI, J. K. OLTHOFF, J. R. WHETSTONE, and J. ROBERTS, NIST— Measurement of voltage and current waveforms is an important and convenient diagnostic tool for characterizing rf plasmas in etching and deposition systems. However, these measurements are often subject to large systematic errors. We have investigated Ar plasmas in the GEC reference cell and have found that simple models of the reactive parasitic elements in the cell are not sufficient to obtain accurate values of plasma impedance and other plasma parameters. Instead, we have applied a more general method to measure and account for these parasitics. Careful calibration of measuring instruments was also shown to be critical. To check these methods, the results were compared with data obtained simultaneously by other diagnostic techniques. The increases in the accuracy of electrical measurements should allow better comparison of results obtained on different cells and may eventually provide a means of testing plasma models or of accurately determining important processing parameters.

**DB-25** Ion Kinetic Energy Distributions in the GEC Reference Cell, J. K. OLTHOFF, R. J. VAN BRUNT, and M. A. SOBOLEWSKI, NIST — A quadrupole mass spectrometer with an electrostatic energy analyzer has been used to measure the kinetic energy distributions of ions sampled from Ar and Ar/O<sub>2</sub> discharges produced in the GEC rf Reference Cell. Ions are collected using a stainless steel sampling cone with an 0.2 mm aperture located midway between the electrodes, to the side of the plasma. When the cone is positioned near the edge of the electrodes a sheath forms at the cone surface and the cone behaves as part of the grounded electrode. The kinetic energy distributions for ions produced in the sheath (such as Ar<sup>+</sup> and Ar<sup>++</sup>) exhibit structure similar to those previously obtained by sampling through the grounded electrode. Ions produced in the bulk plasma that experience few interactions in the sheath (such as Ar<sub>2</sub><sup>+</sup> and ArH<sup>+</sup>) exhibit energy distributions with little or no structure. Small amounts of oxygen (2-20%) added to an argon discharge produce significant changes in the shape and mean energy of the ion kinetic energy distributions. Corresponding changes in the plasma voltage and current waveforms are observed.

**DB-26** Measurements on the Michigan GEC Reference Cell\* M. L. BRAKE, M. PASSOW\*\*, J. PENDER, A. LUJAN, M. BUJE, P. VENTZEK and M. ELTA, Dept. of Nuclear Eng., Univ. of Michigan- Measurements on the University of Michigan GEC Reference Cell will be presented. Baseline measurements include the following: A typical base pressure of  $< 1 \times 10^{-7}$  Torr is achieved with a cryopump and the leak-rate is  $< 1.0$  mTorr/hour. A turbo pump is used during operation. The measured capacitances and resonant frequencies at the top and bottom electrodes of the cell along with the calculated inductances are 84 pF and 85 pF, 62 MHz and 42 MHz, and 79 nH and 148 nH, respectively. The waveforms of the fundamental through to the fifth harmonic of the RF voltage and current including magnitude and phase during the presence of a plasma at 20 sccm, 0.1, 0.25, 0.5 and 1.0 Torr and measured peak-to-peak driving voltages of 75, 150, 200 and 250 V will be presented. Abel inverted radial emission profiles of argon discharges at the above conditions will be also be presented. Sheath thicknesses are estimated from photographs and found to be inversely proportional to the square root of the pressure.

\*Supported by NSF CTS-9009899 and SRC 90-MC-085

\*\*Current address: IBM East Fishkill, Hopewell Junction, New York 12550



**DB-27** Spatial and Temporal Resolution of Plasma-Induced Emission Measurements,\* M. J. COLGAN and D. E. MURNICK, Rutgers University, Newark, NJ 07102—The coupling of the time and position dependence of plasma-induced emission (PIE) in a parallel plate rf discharge demands stronger resolution criteria for measurements of time variations than are required to resolve static spatial features alone. As shown in a recent study,<sup>1</sup> previously unresolved features of PIE can be observed with a carefully designed optical system. The response function of a typical configuration used for PIE measurements has been determined by ray tracing calculations. The optical system (a condenser followed by a secondary focusing lens) images part of the discharge onto the entrance slit of a monochromator. The parameters varied in this study include the monochromator slit width and the focal length and f-number of the lenses. A simple system for measuring PIE in the GEC Reference Cell is described along with calculations of relevant response functions.

\*Work supported in part by the USARO.

<sup>1</sup>M. J. Colgan, *et al.*, Phys. Rev. Lett. **66**, 1858 (1991).

**DB-28** Modeling and Diagnostics of RF Glow Discharges in Ar T.Makabe N.Nakano, F.Tochikubo & S.Kakuta, Keio Univ.— In previous papers, we have proposed and developed the relaxation Continuum(RCT) model, considering the relaxation kinetics for momentum and energies of charged-particles. The diagnostic technique for the RF glow discharges has been also developed by the spatiotemporally resolved-optical emission spectroscopy(STR-OES). Absolute measurements of density and net-formation rate of excited-species in optically allowed-state are possible with resolutions,  $\Delta t < 0.2\text{ns}$  and  $\Delta z < 0.1\text{mm}$ . This paper discusses the quantitative comparison between theory and experiment of the RF discharge structures in Ar for 100kHz and 13.56MHz under the same external condition. Selected probe-particle is Ar( $3p_5$ ) with the excitation energy of 14.6eV. Essential and close agreement between both results has been shown. The theoretical spatiotemporal peaks of net-excitation rate with  $2.2 \times 10^{12}\text{cm}^{-3}\text{s}^{-1}$  at 28.7 and 64.5 ns in time, and at 17.6 and 2.4mm in space coincide with the experimental with relative differences within 2 and 3%, respectively, at  $f=13.56\text{MHz}$ ,  $V_0=50\text{V}$ ,  $p=1\text{Torr}$ ,  $d=2\text{cm}$  and  $8.4\text{mWcm}^{-2}$ . The influence of metastables Ar( $^3P_{0,2}$ ) on RF discharge structures is also discussed as a function of dissipated power by both procedures.

**DB-29** Electrical Measurements and Analysis of Ar and SF<sub>6</sub> RF Discharges, H. Shan, J. MCVITTIE, and S. SELF, Stanford U.- Using a commercial single wafer etch chamber operating at 13.56 MHz, current, voltage and impedance measurements were made on Ar and SF<sub>6</sub> discharges from 50 mT to 1 Torr. The impedance measurements were made at the electrodes with the RF off using the complex conjugate method, while the RF current and voltage measurements were made at an external point A near the electrodes. Through calibration and circuit analysis the parasitic circuit elements were derived for the circuit between point A and the electrodes. Excellent agreement was obtained for the plasma impedance from both types of measurements. At low pressures the sheath dominates with Ar and SF<sub>6</sub> both being capacitive. As the pressure increases, the Ar phase stays near -70° while the impedance gradually decreases by 2X. For SF<sub>6</sub> the negative ion concentration increases with pressure resulting in an inductive phase and a 5X increase in impedance. Effects of RF power and gas mixing will be shown along with derived electron and ion densities and sheath thicknesses.

**DB-30** The Parametric and Time Dependencies of Negative Ions from Pulsed RF Discharges,\* L.J. OVERZET, L. LUO, and Y. LIN, U. of Texas-DALLAS- Negative ion spectra have been measured from pulsed RF discharges in BCl<sub>3</sub>, Cl<sub>2</sub> and CCl<sub>2</sub>F<sub>2</sub> gas mixtures by direct ion mass spectrometry. It is found that Cl<sup>-</sup> has the highest signal intensity in BCl<sub>3</sub> discharges, with BCl<sub>4</sub><sup>-</sup>, B<sub>2</sub>Cl<sub>4</sub><sup>-</sup>, and B<sub>2</sub>Cl<sub>5</sub><sup>-</sup> present. Cl<sub>2</sub><sup>-</sup> signals were on the same order as that for Cl<sup>-</sup> in Cl<sub>2</sub> discharges. There were about 15 negative ions found in CCl<sub>2</sub>F<sub>2</sub> discharge, all of them are Cl-containing or F-containing. Heavy mass negative ions in these discharges show evidence of clustering with etching products such as SiF<sub>5</sub><sup>-</sup> and SiCF<sub>4</sub><sup>-</sup>. Pressure and time dependencies of negative ions in BCl<sub>3</sub> discharges have been determined. BCl<sub>4</sub><sup>-</sup> signals were found to increase with increasing pressure. They also exhibited an "onset" time which accounted for the approximate 5 minute time lag between discharge initiation and the detection of the ion signals. The effects of Ar gas addition were also investigated and possible correlation between negative ions and particulate formation will be discussed.

\*Work supported in part by National Science Foundation under ECS-9009662 and Texas Instruments.

**SESSION EA**

8:00AM - 10:00 AM, Wednesday, October 23

Ballroom A

**CATHODES IN DISCHARGES: A REVIEW**

Chair: J. F. Waymouth

**EA-1** Diagnostics and Modeling of the Cathode Fall and Negative Glow Regions of Cold Cathode Discharges, J. E. LAWLER and W. N. G. HITCHON, Univ. of Wisconsin, Madison, WI, 53706 - The application of various advanced laser diagnostics and computer simulations has led to more quantitative understanding of the cathode region of some simple cold cathode discharges. During the last decade laser optogalvanic and fluorescence techniques have been used to measure: electric field distributions, the current balance at the cathode, the density of metastable atoms, the gas temperature, the density and temperature of the trapped electrons in the negative glow, the location of field reversals in the negative glow, and other quantities.<sup>1</sup> Self-consistent kinetic models such as those based on the Convective Scheme are much more realistic than older models and compare favorably with experiment.<sup>2</sup> Future challenges include the application of these techniques to gases with more complex chemistry and the development of an understanding of the dynamic behavior of the cathode region.

<sup>1</sup>E. A. Den Hartog, et al., Phys. Rev. A 38, 2471 (1988); J. E. Lawler et al., Phys. Rev. A 43, 4427 (1991).

<sup>2</sup>T. J. Sommerer et al., Phys. Rev. A 39, 6356 (1989).

**EA-2** Diagnostics and Modelling of the Sheath and Negative Glow of Hot-Cathode Discharges, V. GODYAK, GTE Laboratories and R. LAGUSHENKO, GTE Lighting Products - Physical processes in plasma and the cathode sheath of low pressure negative glow are discussed. Special attention is paid to the mechanism of formation of the electron energy distribution function (EEDF). The role played by various collisional processes in the energy relaxation of primary electrons accelerated in the cathode sheath is evaluated in terms of corresponding characteristic lengths. Possibility of the energy relaxation of primary electron beam due to excitation of plasma waves is considered and evaluated. Methods and result of calculations of the EEDF and ionization rate are reviewed. Results of the probe measurement of the EEDF are presented and analyzed from the standpoint of the EEDF formation mechanism. Applications of the optical diagnostic methods for the measurement of the ion and excited atom number densities in the vicinity of thermoionic cathode are reviewed.

**EA-3 Diagnostics and Modeling of the Cathode Temperature Profile in Hot-Cathode Discharges,** ASHOK K. BHATTACHARYA and THOMAS F. SOULES, GE Lighting, Nela Park, Cleveland, OH 44112- Theoretical models and diagnostics of low pressure discharge lamp electrodes are reviewed. A self-consistent one-dimensional model for calculating the temperature distribution on an electrode will be discussed. The thermal model includes joule and ion bombardment heating and cooling due to conduction, radiation and electron emission. The model successfully describes the temperature profile along a linear electrode giving hot spot formation and transient temperature profiles during starting. Diagnostics which compliment such a model include photodiode-arrays for measuring the temperature profile and in-situ measurements of work function under the accelerating field of the sheath. Barium evaporation from the electrode can also be measured utilizing LIF and atomic absorption techniques.

**EA-4 Electron Emission in Hot-Cathode Discharges: Modelling and Paucity of Good Diagnostic Methods.** JOHN F. WAYMOUTH, 16 Bennett Rd, Marblehead MA, 01945. In hot cathode discharges, the cathode temperature is determined by a power balance including power deposited from the discharge, in large part from ion bombardment. The electron emission itself is determined by the cathode temperature and the electric field at the cathode surface, which is in turn primarily determined by the ion current to the cathode. The ion current is produced from the electron emission by ionization processes in the negative glow. Modelling of this complex feedback system has to date been the only way to estimate the internal variables. Although there are a number of methods to measure zero-field electron emission of cathodes in discharges, there has to date been no way to determine the emission at the accelerating field in the discharge, and no generally-applicable way to determine ion current to a cathode. These problems represent research opportunities.

**SESSION EB**

8:00 AM - 10:00 AM, Wednesday, October 23

Ballroom B

**IONIZATION & ELECTRON COLLISIONS**

Chair: R.A. Bonham, Indiana University

**EB-1** Partial Electron Ionization Cross Sections for Molecules.\* M. FOLTIN, C. WINKLER, V. GRILL, D. MARGREITER, H.U. POLL, and T.D. MÄRK, Inst. Ionenphysik, Univ. Innsbruck, Austria.-- Fragment ions produced by dissociative electron impact ionization often have large amounts of kinetic energy (up to several eV). Presently performed computer simulations of the ion trajectories in a Nier-type ion source show strong discrimination effects in the extraction characteristics of such ions. Using these results a correction function is calculated here for a given potential distribution of such a Nier type ion source extraction system. This correction function has been used to correct partial ionization cross sections measured with a modified Nier type ion source in combination with a double focusing sector field mass spectrometer. The obtained results for  $H_2$ ,  $N_2$ ,  $CF_4$ ,  $SF_6$  and  $C_3H_8$  will be presented and their accuracy will be discussed using selected previous data for comparison.

\* Work supported in part by the Öster. Fonds zur Förderung der Wissensch. Forschung and the BMWF, Wien.

**EB-2** Cross Sections for the Production of Positive Ions by Electron Impact on  $F_2$ : S.K.Srivastava and M.V.V.S. Rao<sup>#</sup>, Jet Propulsion Laboratory, California Institute of Technology. Normalized values of cross sections for the production of  $F_2^+$ ,  $F^+ + F_2^{2+}$ , and  $F^{2+}$  have been measured by utilizing a crossed electron beam-molecular beam collision geometry and the relative flow technique for electron impact energies ranging from 0 eV to 1 KeV. For  $F^+ + F_2^{2+}$  and  $F^{2+}$  present results are the first ones and their cross sections at 100 eV electron impact energy are  $1.4 \times 10^{-17} \text{ cm}^2$  and  $5.9 \times 10^{-21} \text{ cm}^2$ , respectively. Cross sections for the generation of all ions (total cross sections) from  $F_2$  have been measured previously by Center and Mandl<sup>1</sup> and by Stevie and Vasile<sup>2</sup>. Their values at 100 eV electron impact energy are  $1.5 \times 10^{-16} \text{ cm}^2$  and  $1.25 \times 10^{-16} \text{ cm}^2$ , respectively. Present measurements, at this energy, give a value of  $(9.9 \pm 1.5) \times 10^{-17} \text{ cm}^2$ .

\*Work supported by Air Force Wright Aeronautical Laboratories.  
<sup>#</sup>NRC-NASA Research Associate.

1. R.E. Center and A. Mandl, J. Chem. Phys. 57, 4104(1972).
2. F.A. Stevie and M.J. Visile, J. Chem. Phys. 74, 5106(1981).

**EB-3** Electron-Impact Ionization of Atoms and Molecules Using the Fast-Beam-Technique.\* V. TARNOVSKY and K. BECKER, City College of C.U.N.Y. --- The recently reported<sup>1</sup> 30% spread in the measured  $\text{Ar}^{2+}/\text{Ar}^+$  ionization cross section ratios motivated this new study of the measurement of double-to-single ionization cross section ratios for Kr and Ar using the fast-atom-beam technique. An attempt was made to identify and quantify all possible systematic uncertainties inherent to the fast-beam technique. Our results<sup>2</sup> confirm earlier measurements using the same technique<sup>3</sup>. We establish overall error limits of at least  $\pm 9\%$  for cross section ratios of single-to-multiple ionization for the same target and of  $\pm 10\%$  for ratios of single ionization cross sections for different target species. The error margins are dominated by systematic uncertainties which do not cancel when cross section ratios are measured in our apparatus, since the ratios are obtained under similar, but not identical experimental conditions. We also present result for the electron-impact ionization and dissociative ionization of some selected free plasma radicals.

\*Supported by the National Science Foundation.

1. C. Ma et al., Rev. Sci. Instrum. **62**, 909 (1991)
2. V. Tarnovsky and K. Becker, submitted to Z. Phys. D
3. R.C. Wetzel et al., Phys. Rev. A **35**, 559 (1987)

**EB-4** Why Are Multicharged Partial Ionization Cross Sections So Hard to Measure? An Analysis of Time-of-Flight Techniques.\* M. R. BRUCE and R. A. BONHAM, Argonne National Laboratory, Argonne, IL 60439 and Indiana University, Bloomington, IN 47405--Measurements of the ratio of the partial ionization cross sections for  $\text{Ar}^{2+}$  to  $\text{Ar}^+$  are carried out for both beam-beam and static-gas (absolute) scattering geometries by using a pulsed electron beam excitation source with time-of-flight analysis of the ion masses. The cross section ratio and, in the case of static gas, the individual absolute partial ionization cross sections were measured by using a wide variety of different experimental conditions to find a reason for the disagreement between cross sections from different laboratories. Conclusions drawn from this study may benefit future measurement attempts.

\* Work supported in part by the U.S. Department of Energy, Office of Energy Research, Office of Health and Environmental Research, under Contract W-31-109-Eng-38 (RAB).



**EB-5** Electron-H<sub>2</sub>S Collisions in an Exact Exchange Plus Parameter-Free Polarization Model\*, A. Jain and

K L Baluja, Phys. Dept., Florida A&M Univ., Tallahassee, Fl 32307, - The low-energy e-H<sub>2</sub>S scattering is treated in the static-exchange plus parameter-free polarization model. The exchange effects are included exactly by solving the inhomogeneous coupled differential equations iteratively. A recently proposed computationally optimized iterative scheme [1] is employed. The convergence of scattering parameters with respect to the number of iterations is checked for each symmetry and energy. We found significant differences between model and the exact exchange results, particularly around the B<sub>2</sub> shape resonance region. We compare our calculations (differential, integral and momentum transfer cross sections) with recent measurements and other calculations employing a local exchange model.

[1]. Jain *et al*, J. Phys. B24, L255 (1991)

\*Research supported by the US Dept. of Airforce, Wright-Patterson AFB

**EB-6** Metastable Fragmentation of Rare Gas Cluster Ions Initiated by Excimer Decay\* M. FOLTIN, G. WALDER, and T.D. MÄRK, *Inst. Ionenphysik, Univ. Innsbruck, Austria.*--

A new unusual metastable fragmentation channel of argon and neon cluster ions produced by electron impact ionization of a neutral cluster beam has been studied with a double focusing sector field mass spectrometer. In contrast to the usual case of statistical single monomer evaporation, in the new metastable fragmentation channel the number of ejected monomers is larger than one, e.g. in the case of argon cluster ions it rises from 2 for the Ar<sub>4</sub><sup>+</sup> up to 10 for the Ar<sub>30</sub><sup>+</sup> parent cluster ion. After studying the dependence of the fragment ion current on (i) the electron energy, (ii) the parent cluster size and the number of ejected monomers, and (iii) the time interval between ion formation and dissociation, we concluded that the radiative decay of a metastable excimer Ar<sub>2</sub><sup>\*(3Σ<sub>u</sub><sup>+</sup>)</sup> (resp. Ne<sub>2</sub><sup>\*(3Σ<sub>u</sub><sup>+</sup>)</sup>) localized inside the cluster ion leads to repulsion of Ar (resp. Ne) atoms in the ground state Ar<sub>2</sub>(<sup>1</sup>Σ<sub>g</sub><sup>+</sup>) (resp. Ne<sub>2</sub>(<sup>1</sup>Σ<sub>g</sub><sup>+</sup>)) and to subsequent disintegration of the cluster. Formation of the excimer is induced by one of two outgoing electrons originating from the previous successful ionization inside the same cluster.

\* Work supported in part by the Öster. Fonds zur Förderung der Wissensch. Forschung and the BMWF, Wien.

**EB-7** Low Energy e-Ar Momentum Transfer Cross-Section, M.J. BRENNAN, Electron Physics Group, Australian National University - Recent work<sup>1,2</sup> has shown that solutions of the Boltzmann equation which use the so called "two-term" approximation provide an inadequate description of the transverse diffusion of electrons in argon gas at low values of E/N, contrary to earlier evidence<sup>3</sup>. Previous determinations of the momentum transfer cross section for argon from the analysis of transport data<sup>4,5,6</sup> have used two-term codes in good faith. Progress towards the determination of a new cross section in the energy range 0 - 4 eV, including an analysis of the energy dependence of the uncertainty in the derived cross section is reported.

<sup>1</sup>G.L. Braglia, M. Diligenti, J. Wilhelm & R. Winkler, *Nuovo Cimento D*, 12, 975, (1990)

<sup>2</sup>M.J. Brennan and K.F. Ness, submitted to *Nuovo Cimento D*.

<sup>3</sup>H.B. Milloy & R.O. Watts, *Aust. J. Phys.* 30, 73 (1977)

<sup>4</sup>L.S. Frost & A.V. Phelps, *Phys Rev A* 136 1538 (1964)

<sup>5</sup>H.B. Milloy, R.W. Crompton, J.A. Rees & A.G. Robertson, *Aust. J. Phys.* 30, 61 (1977)

<sup>6</sup>G.N. Haddad & T.F. O'Malley, *Aust. J. Phys.* 35, 35 (1982)

**EB-8** Elastic Scattering of Low Energy Electrons from Ammonia, D.T. ALLE, R.J. GULLEY, M.J. BRUNGER and S.J. BUCKMAN, Electron Physics Group, Australian National University - We report absolute differential cross sections ( $E_0 = 2-50$  eV) for vibrationally elastic electron scattering from  $\text{NH}_3$ . The present measurements were conducted with a crossed electron-molecule beam apparatus<sup>1</sup> and the data placed on an absolute scale via the relative flow technique<sup>2</sup>. Our results are presented and compared against available theoretical calculations<sup>3,4</sup> and the only previous absolute experimental determination<sup>5</sup>. We would characterise the overall level of agreement between ourselves and references 3 and 4 as being fair, whilst the agreement with Ben Arfa and Tronc at 7.5 eV is good.

<sup>1</sup>M.J. Brunger et al. *J. Phys.* B24, 1435 (1991)

<sup>2</sup>J.C. Nickel et al. *J. Phys.* E22, 730 (1989)

<sup>3</sup>F. Gianturco, private communication

<sup>4</sup>H.P. Pritchard et al. *Phys. Rev.* A39, 2392 (1989)

<sup>5</sup>M. Ben Arfa and M. Tronc, *J. de Chemie Physique* 85, 879 (1988).

**SESSION F**

10:15 AM - 11:30 AM, Wednesday, October 23

Ballroom A

**PLENARY LECTURE**

Chair: J. Gerardo, Sandia National Laboratories

Welcoming Remarks:

Richard E. Peck, President - University of New Mexico

**F-1**      **Plasma Physics Issues for Inertial Fusion with Light Ion Beams**,\* J. P. VANDEVENDER, Sandia National Laboratories--Inertial confinement fusion driven by beams of low atomic mass ions offers the potential for megajoule-class ignition experiments in the near term, gigajoule thermonuclear yields in the midterm, and economic fusion power in the longer term. The recent study by the Fusion Policy Advisory Committee noted that "light ion drivers may actually be closest to meeting the needs of an inertial fusion energy driver for economic power production." However, the report also goes on to say that the ion beam program must still demonstrate the required beam intensity on target and resolve pulse shape and beam transport issues. The power generation, ion production, ion acceleration, focusing, and beam transport of these intense beams introduce new and challenging physics issues. The status of those issues and the progress in resolving them for the Particle Beam Fusion Accelerator II will be presented.

\*This work supported by the U. S. Department of Energy under contract DE-AC04-76DP00789.

**SESSION H**

1:30 PM - 3:30 PM, Wednesday, October 23

Ballroom C

**POSTERS**  
**Transport**  
**Electron & Photon Collisions**  
**Lamps**

**HA-1** Nonequilibrium Electron Transport: A Comparison of Approaches Based on a Finite Set of Moment Equations, J. H. INGOLD, GE Lighting, General Electric Co., and E. KUNHARDT, Weber Research Institute, Polytechnic University, - Macroscopic models for describing nonequilibrium electron transport that are based on moments of the distribution function are characterized by the number of moments that are used in the description and the method used for closing the resulting set of equations. In this presentation, four moment based descriptions are briefly reviewed: The Density Gradient Expansion (DGE), Modified Druyvesteyn Distribution (MDD), Macro-Kinetic Theory (MKT), and Momentum Transfer Approximation (MTA). These models have been used in the analysis of a model problem (namely, transport near absorbing boundaries) and the results compared to those obtained from solution of the Boltzmann equation. The adequacy of the various model for describing nonequilibrium transport is discussed.

**HA-2** Self-consistent Monte Carlo Simulation of RF Glow Discharges, \* J. H. TSAI and C. WU, Electrical Engineering Department, Auburn University, AL 36849. -- A self-consistent nonequilibrium model of RF glow discharges between parallel plates has been studied by Monte Carlo technique. Spatio-temporal variations of the space-charge fields, electron and ion densities, and several transport parameters e.g., the ionization coefficient, momentum and energy relaxation times, and electron velocities in multiple energy groups will be presented in this paper. Moreover, spatio-temporal variation of the ionization rate to the electron power deposition and the average electron energy has been used to illustrate a transition phenomenon of multiple energy groups for the electrons in the RF glow discharge.

\* This work is supported by NSF under ECS-9009395 and CRAY Research Inc.

**HA-3** Nonequilibrium Electron Transport near Absorbing Boundaries. JOHN INGOLD, GE Lighting, Cleveland, OH 44112—A modified moment method<sup>1</sup> is used to predict the effect of absorbing boundaries on a continuous stream of electrons traveling in a steady, uniform electric field. The method predicts nonequilibrium behavior of electron density and average energy near absorbing boundaries in good qualitative agreement with published Boltzmann and Monte Carlo calculations<sup>2</sup> for the same physical problems. The relation of this work to other moment methods<sup>3</sup> is discussed.

<sup>1</sup>J. H. Ingold, Phys. Rev. A **40**, 7158 (1989); **42**, 950 (1990).

<sup>2</sup>R. E. Robson, Aust. J. Phys. **34**, 223 (1981); J. J. Lowke, J. H. Parker, and C. A. Hall, Phys. Rev. A **15**, 1237 (1977); G. L. Braglia and J. J. Lowke, J. Phys. D: Appl. Phys. **12**, 1831 (1979).

<sup>3</sup>E. E. Kunhardt, J. Wu, and B. Penetrante, Phys. Rev. A **37**, 1654 (1988); G. Remouliotis and L. E. Cram, J. Phys. D: Appl. Phys. **22**, 113 (1988); L. E. Cram, Phys. Rev. A **43**, 4480 (1991).

**HA-4** Time Dependence of Swarm Parameters of Electrons in Argon. \*A. A. SEBASTIAN and J. M. WADEHRA, Wayne State University- Time-dependent swarm parameters (average energy, drift velocity etc.) have been computed for electrons in argon gas for E/N values of 283, 565, 1412 and 2825 Td using a modified version of the algorithm of Drallos and Wadehra<sup>1</sup>. The results obtained using a Maxwellian initial distribution function are compared to those using a delta-function initial distribution function. Although the transient behavior of the swarm parameters using the two functions differ, the equilibrium values agree as expected in a steady state Townsend type experiment. Also presented is a simplified version of the above algorithm which provides time-dependent swarm parameters for the case of zero external electric field. In particular, for a spherically symmetric delta -function initial distribution function, the zero field mobilities thus obtained are compared with the results of Shizgal and McMahon<sup>2</sup>. Our data exhibit a negative transient mobility for certain values of electron temperature and ambient gas density.

\*Support of the Air Force Office of Scientific Research is gratefully acknowledged.

<sup>1</sup>P.J.Drallos and J.M.Wadehra, Phys.Rev.A **40**, 1967 (1989).

<sup>2</sup>B.Shizgal and D.R.A.McMahon, Phys.Rev.A **32**, 3669 (1985).

**HA-5** Departures from Thermodynamic Equilibrium in Particle-Beam Generated Molecular Oxygen Plasma,  
N. PEYRAUD-CUENCA, Observatoire de la Côte d'Azur, Nice, France- Departures from Maxwellian behaviour have already been calculated analytically for the "tail"<sup>1</sup> and the "bulk"<sup>2</sup> of the electron distribution function (e.d.f.) in a general particle beam generated plasma. However the theory must be adapted<sup>3,2</sup> to the particular and interesting case of O<sub>2</sub> where, owing to low threshold metastable state excitations, the "bulk" and the "tail" of the e.d.f. are separated by an intermediate region with equal importance between elastic electron-electron collisions and inelastic processes. We obtain analytically<sup>3,2</sup> significant departures to the Maxwellian with an e.d.f. characterized by a "plateau" between the first metastable threshold (0.98 eV) and the third electronic threshold (4.5 eV) followed by a decreasing after 4.5 eV.

<sup>1</sup> N. Peyraud-Cuenca, J. Phys. B 21, 3311 (1988).

<sup>2</sup> N. Peyraud-Cuenca, J. Phys. B 23, 3729 (1990).

<sup>3</sup> N. Peyraud-Cuenca, J. Phys. B 23, 3709 (1990).

**HA-6** Multigroup Treatment of Electron Transport in Gases,\*  
E. KUNHARDT, Weber Research Institute, Polytechnic University, - Given initial and/or boundary conditions, the behavior of an assembly of electrons in a noble gas can be obtained from solution of the kinetic equation for the distribution function,  $f(v,r,t)$ . By expanding the distribution in terms of localized functions in  $v$ -space, an equivalent formulation can be obtained in terms of the expansion coefficients. These coefficients can be related to the density of "electron groups" associated with the localized functions. By partially summing over a finite number of groups, coarser representations involving fewer groups defined over different regions of velocity space (such as two group models) can be developed, with provisions for determining the transition rates between these groups. This approach is illustrated in the context of the Fokker-Planck kinetic equation.

\*Work supported by ONR.



**HA-7** An Analysis of Position-Dependent Electron Swarm Behavior in Steady-State Townsend Discharges by Convective-Scheme Technique, Y. Sakai, H. Sugawara and H. Tagashira, Department of Electrical Engineering, Hokkaido University - The position-dependent swarm parameters and energy distribution  $F(x, \epsilon)$  of electrons in argon gas were analysed using a convective-scheme technique in which a proper relation between the trajectories of electrons and the cells defined in energy  $\epsilon$  and  $x$  space was considered. The results showed the fine structures of damped fluctuation in the swarm parameters, which had been obtained by a Monte Carlo technique. When initial electrons with the zero energy were ejected from a cathode,  $F(\epsilon, x)$  at  $E/N=283$  Td could not reach the equilibrium condition even at the distance at which the equilibrium values of mean energy, drift velocity, etc. of electron seemed already obtained.

**HA-8** An Ion Transport Model for the Afterglow of Radio-Frequency Discharges.\* L. J. OVERZET AND L. LUO, University of Texas at Dallas— We are measuring the positive and negative ion flux as a function of time from amplitude modulated rf discharges and have noticed that the time dependencies of the flux from varying negative ions can be significantly different (on a 0.1 ms time scale). In order to better understand the cause of these differences we have developed an ion transport code for the late afterglow of an amplitude modulated rf discharge with multiple positive and negative ions. We have assumed constant mobilities and used a self consistent field distribution. In the simplest case, 1 positive and 2 negative ions, the transport in the presence of the applied dc bias was found to correspond remarkably well with measurements. The differences in the time dependent signals can be attributed to shielding by higher mobility negative ions, and, ion-ion mutual neutralization as well as diffusion loss rates have only small impacts on the time dependent flux. Additional results including estimates of the impact of electron attachment on the measured signal are also anticipated for the conference.

\* Work supported in part by the National Science Foundation ECS - 9009662 and Texas Instruments Inc.

**HA-9** Velocity Distributions of Na<sup>+</sup> Ions in Ne<sup>\*</sup>, M.J. HOGAN, P.P. ONG and K.Y. LAM, National University of Singapore, L.A. VIEHLAND, Parks College of Saint Louis University -- Calculations based on Monte-Carlo simulations, on three-temperature kinetic theory, and on bimaxwellian kinetic theory have found that the KMV<sup>1</sup> Na<sup>+</sup>-Ne interaction potential is a good representation of the true potential. Using this potential, velocity distribution functions of Na<sup>+</sup> ions in Ne at E/N = 5, 37.5, 100, and 200 Td were calculated. As E/N increased, the skewness of the distributions in the direction of the electric field initially increased rapidly, and then slowly decreased. The excess kurtosis both parallel and perpendicular to the electric field direction followed the same trend. Correlation between the perpendicular and parallel velocity component distribution functions was found.

<sup>1</sup>A.D. Koutselos, E.A. Mason and L.A. Viehland, J. Chem. Phys. 93, 7125 (1990).

\*Partially supported by NSF grant CHE-8814963.

**HA-10** Radial Distribution of the Plasma Density in the Positive Column of the High Current Stationary Glow Discharge, L. Pekker, U. of Minnesota - A model is presented which describes the plasma parameters in the positive column of a stationary self-maintained glow discharge not in contact with the longitudinal walls of the discharge chamber, such that the volume ionization and recombination processes balance each other. In this model, the compression of the positive column is provided by the azimuthal magnetic field created by charge current. We obtain the value of the discharge current  $I_0$  and the radial distributions of the plasma density, electrical potential, current density, and magnetic field strength for the case when charged-particle diffusion is exactly balanced by action of the electric and magnetic fields of the positive column. We also examine the situation where the current of glow discharge is much larger than  $I_0$ , such that charged-particle diffusion can be ignored.

**HA-11** Monte-Carlo Simulation of Electron Properties in an Electron Cyclotron Resonance Microwave Discharge, S. C. KUO and E. E. KUNHARDT, WRI, Polytechnic U. Electron properties of an electron cyclotron resonance (ECR) microwave discharge in a cylindrical waveguide are studied via a Monte-Carlo simulation. Temporally and spatially dependent TM wave solutions are obtained from the field analysis. The wave is strongly attenuated in the propagating direction. Space charge induced electric field in the plasma is solved via the Poisson equation using appropriate boundary condition and charge density. Time averaged, space dependent electron energy distributions are computed self-consistently by integrating, over time, electron trajectories subjected to the electromagnetic field, the space charge field and collisions with hydrogen molecules. Simulation results show that the thickness of ECR layer is on the order of a few millimeter. Near the ECR layer, the ponderomotive force exerted on electrons enhances the downstream plasma.

**HB-1** Angular Distribution of Electrons Elastically Scattered from Water Vapor, \* A. GRAFE and T. W. SHYN, Space Physics Research Laboratory, Univ. of Michigan — The angular distributions of electrons elastically scattered from H<sub>2</sub>O have been measured by electron impact using a modulated crossed-beam method. The incident energy and angular range measured were from 30 to 200 eV and from 12 to 156°, respectively. The present results show a large backward scattering for low incident energies, but this backward scattering falls off for high incident energies. The present results are in agreement in shape, but not in magnitude, with the measurements of Danjo and Nishimura<sup>1</sup> and are in quantitative agreement with the measurements of Katase et al.<sup>2</sup> Agreement with the SEP1 calculation of Jain et al.<sup>3</sup> is good, although some discrepancies were found at 200 eV.

\*This work was supported by NASA Grant No. NAGW-938.

<sup>1</sup>A. Danjo and H. Nishimura, J. Phys. Soc. Jpn. 54, 1224 (1985).

<sup>2</sup>A. Katase, K. Ishibashi, Y. Matsumoto, T. Sakae, S. Maezono, E. Murakami, K. Watanabe, and H. Maki, J. Phys. B 19, 2715 (1986).

<sup>3</sup>A. K. Jain, A. N. Tripathi, and A. Jain, Phys. Rev. A 37, 2893 (1988).

## HB-2

### *Electron CF<sub>4</sub> Scattering at Low and Intermediate Energies\**

H. Tanaka and L. Boesten, *Sophia University, Tokyo*, H. Sato, *Ochanomizu University, Tokyo* and M. Dillon, D. Spence and M. Kimura, *Argonne National Laboratory, USA*

Energy and angular distributions of electrons elastically scattered from CF<sub>4</sub> were recorded over a range of 20° to 120° for incident energies of 1 to 100 eV. These were supplemented by measurements of vibrational excitation functions for the anti stretching mode ν<sub>3</sub> which reveals the presence of two resonances located at 2 and 7 eV respectively. All determinations were made absolute by comparison with helium via the relative flow method.

Calculations employing the continuum multiple scattering were used to elucidate the mechanisms underlying the resonance structure.

---

\*Work supported by the U.S. Department of Energy, Assistant Secretary for Energy Research, Office of Health and Environmental Research under contract w-31-109-Eng-38 and by a Grant in Aid from the Ministry of Education, Science and Culture, Japan.

**HB-3** Electron Scattering on NO<sub>2</sub>: Vibrational Excitation at Low Energy (0.3 - 3eV). R. ABOUAF and C. BENOIT, LCAM Univ. Paris Sud Orsay, France.- Vibrational excitation of NO<sub>2</sub> via the formation of transitory anion states (resonances) is reported in the low energy scattering region (0.3 - 3eV). Differential energy loss spectra, angular analysis and vibrational excitation versus electron energy have been carried out using an electron crossed beams spectrometer equipped with 2 analysers in tandem<sup>1</sup>. Important excitation of the bending mode around  $E_i = 0.5\text{eV}$  suggests a substantial change in the NON angle and leads to the assignment X <sup>1</sup>A<sub>1</sub> (116°) for the NO<sub>2</sub><sup>-</sup> resonant state reached in this energy region. This is confirmed by the angular analysis. Above  $E_i = 1\text{eV}$ , excitation of the symmetric stretch mode series (up to  $n=5$ ) is dominant via the B<sub>1</sub> resonant state (<sup>1</sup>B<sub>1</sub> and /or <sup>3</sup>B<sub>1</sub>). The vibrational excitation cross sections of the bending mode series below 1eV shows some evidence of a long lived anion state, whereas excitation of the symmetric stretch seems to be relevant of an intermediate lifetime resonant state.

I.C. Benoit and R.Abouaf Chem. Phys. Lett. 123 134 (1986)

**HB-4** The Absolute Electron Impact Cross Sections for Double Cation Formation in CF<sub>4</sub>.\* M. R. BRUCE, CE MA, Indiana University, Bloomington, IN 47405 and R. A. BONHAM, Argonne National Laboratory, Argonne, IL 60439 and Indiana University, Bloomington, IN 47405--Double cation formation for electron impact on CF<sub>4</sub> has been measured in a coincidence experiment for electron energies from threshold to 500 eV. Only the four reactions  $e + \text{CF}_4 \rightarrow \text{CF}_n^+ + \text{F}^+ + 3e$ ,  $n = 0 - 3$ , have been observed to have an appreciable ( $>10^{-20} \text{cm}^2$ ) cross section. These results make it possible for the first time to make an accurate estimate of the counting cross section for the total ionization of CF<sub>4</sub> and lead to an upward revision of our previously estimated neutral dissociation cross section by a factor of two. These results also make it possible to obtain upper and lower bounds on the neutral fluorine production cross section which is found to be of the same magnitude as the total dissociation cross section.

\* Work supported in part by the U.S. Department of Energy, Office of Energy Research, Office of Health and Environmental Research, under Contract W-31-109-Eng-38 (RAB).

**HB-5** Direct Measurement of Ionization-Excitation Branching Ratios for N<sub>2</sub> using a Coincidence Ionization Technique. \* J. P. DOERING and L. GOEMBEL, Johns Hopkins U. -- Ionization-excitation branching ratios for N<sub>2</sub> have been measured for the X <sup>2</sup>Σ<sub>g</sub><sup>+</sup>, A <sup>2</sup>Π<sub>u</sub>, and B <sup>2</sup>Σ<sub>u</sub><sup>+</sup> states of N<sub>2</sub><sup>+</sup> ions produced by electron-impact ionization of N<sub>2</sub> at low to medium (~100 eV) energies. A coincidence technique in which the "scattered" and "secondary" electrons are energy analyzed and measured in coincidence was used. Data have been obtained for secondary electron energies of 2.5, 5.0, 10.0, and 15.0 eV at various combinations of scattered and secondary electron angles. Since the kinematics of the ionization collision are completely determined by the experiment, the final electronic state of the ion is known unambiguously. The relative fourfold differential cross sections produced by the experiment for each electronic state have been integrated over energy and angle variables to give branching ratios. The results are in good agreement with what has been deduced previously from other less direct techniques. This experiment offers a promising non-optical method for the determination of partial ionization cross sections and branching ratios.

\*Work supported by NSF Grant ATM-8915375.

**HB-6** Selective Detection of O<sup>1</sup>S by XeO Formation Following Electron Impact Dissociation of O<sub>2</sub> and N<sub>2</sub>O. \* L.R. LECLAIR, J.J. CORR, and J.W. McCONKEY, University of Windsor, Canada. - Time-of-flight (TOF) studies of metastable fragments from dissociated molecules have been ongoing for about 25 years, but are usually limited to fragments with excitation energies (E) greater than 5 eV because of experimental difficulties. We have constructed a TOF apparatus which employs a disc of frozen Xenon to monitor the production of O<sup>1</sup>S atoms (E=4.18eV) following electron impact dissociation of oxygen containing molecules of aeronomic interest. O<sup>1</sup>S metastables incident on the disc form XeO excimers which quickly decay and the resulting optical fluorescence is detected by a photomultiplier. Spectral analysis of the excimer radiation reveals a strong band centered at 375 nm, and a weaker one at 550 nm. This method has the advantage of discriminating against other metastable fragments like O<sup>3</sup>S<sup>0</sup>, or metastable N, as neither has produced a detectable signal in our experiments. Kinetic energy distributions of the O metastables derived from TOF data will be presented along with excitation functions.

\* Research supported by the Petroleum Research Fund administered by the American Chemical Society and the Natural Sciences and Engineering Research Council of Canada.

**HB-7** Production of Excited Helium Atoms in the Singlet Levels by Electron Collisions with Metastable Helium Atoms.\* R. B. LOCKWOOD, FRANCIS A. SHARPTON, L. W. ANDERSON, J. E. LAWLER, and Chun C. LIN, U. of Wisconsin—Cross sections for electron excitation out of the metastable levels into several singlet levels of He have been measured. A beam of He atoms containing a small fraction of metastables ( $10^{-5}$ ) is crossed by an electron beam. The intensities of several emission lines such as the  $4^1D \rightarrow 2^1P$  (492nm) or  $3^1S \rightarrow 2^1P$  (728nm) transitions are measured. For energies below 19 eV excitation out of the ground level is not possible. The emission is entirely due to electron excitation into  $He(n^1L)$  out of either the  $2^1S$  or  $2^3S$  metastable levels. The number density of each metastable is determined by a laser-induced fluorescence experiment. From the energy dependence of the observed emission, the individual cross sections for exciting  $3^1S$ ,  $3^1D$ , and  $4^1D$  from each metastable level are determined and the results are presented. To measure cross sections at higher energies, a different method for producing metastables is presented.

\*Supported by the National Science Foundation.

**HB-8** Threshold Behavior in Electron Excitation of Na. B. MARINKOVIC,\* P. WANG, and ALAN GALLAGHER,\*\* JILA, U. OF Colorado and NIST - We have measured the optical excitation functions of the 4D, 5D, and 4P states of sodium, in the threshold energy region with  $\sim 30$  meV energy resolution. At this resolution the D states appear as step functions at threshold, while the 4P state onset is considerably more gradual. Some structures are observed in the 4-6 eV region, but these are not very large in our data. A cylindrical trochoidal monochromator, a high density atomic beam and large-angle light collection are used to achieve useable S/N.

\* Present address: Institute of Physics, Belgrade, Yugoslavia.

\*\* Staff Member, Quantum Physics Division, National Institute of Standards and Technology.

**HB-9** Dissociative Photoionization Processes in Isolated Weakly-Bound Small Molecular Clusters. \* E.A. WALTERS, J.R. GROVER, J.T. CLAY, G. HAGENOW, and P.CID-AGUERO, BNL, U. of New Mexico and Frej U. Berlin - Photon-initiated chemical reactions within size-selected small clusters formed in free jet expansions of gas mixtures have been studied by mass spectrometry. The photon source is the tunable beam available at beamline U11 of the 750 MeV electron storage ring at NSLS.  $C_6H_6Cl^+$  is produced from  $(C_6H_6)_2HCl$  with an onset energy of 14.8eV, but is not formed from  $C_6H_6 \cdot HCl$  at any energy.  $C_2H_4Cl^+$  comes from dissociative ionization of both  $C_2H_4 \cdot HCl$  and  $(C_2H_4)_2HCl$ , but the yield is much higher in the latter case.  $C_6F_6O^+$  is generated from  $C_6F_6 \cdot O_2$  at a photon energy equal to the ionization energy of  $C_6F_6$  plus the dissociation energy of  $O_2$ . The yield of  $CF_3Br^+$  from  $CF_3Br$  is enormously increased by "solvent" stabilization of the ion with  $CH_3OH$ . Branching ratios for photofragmentation of  $C_4H_4S$  (thiophene) into  $C_4H_4S^+$  and  $C_2H_2S^+$  depend strongly on parent cluster size. A broad range of mechanisms is required to explain these results. Detailed mechanisms will be described for these cases.

\*Work supported in part by the U.S. Department of Energy and in part by the U.S. Air Force.

#### **HB-10**

Subexcitation Electrons in an  $O_2$  and  $N_2$  Mixture.\* MINEO KIMURA, M. A. ISHII, and MITIO INOKUTI, Argonne National Laboratory, Argonne, IL 60439--Subexcitation electrons, having energies below the first electronic excitation threshold, play an essential role by depositing their energies to vibrational and rotational excitations of molecules in a medium and, hence, are important for a fundamental understanding of the subsequent radiation chemistry and biology. We have conducted a systematic study of subexcitation electron behavior in gaseous mixtures of  $O_2$  and  $N_2$  by using the Spencer-Fano theory. One of the significant findings is that  $N_2$  is dominant in the energy loss process. The addition of a small amount of  $N_2$  causes a remarkable change in some of the yields of  $O_2$ .

\* Work supported in part by the U.S. Department of Energy, Office of Energy Research, Office of Health and Environmental Research, under Contract W-31-109-Eng-38.



**HB-11** The Mass Dependence of Cross Sections for Vibrational Excitation of Diatomic Molecules by Electron Impact, \* D. E. ATEMS and J. M. WADEHRA, Wayne State University- A new scaling law is presented for resonant vibrational excitation (VE) by electron impact in diatomic molecules. We show that the mass dependence of the resonant cross section for VE in the impulse limit is of the form  $M^{|v_f - v_i|/2}$ , where  $M$  is the reduced nuclear mass and  $v_i$  and  $v_f$  refer to the initial and final vibrational levels, and  $|v_f - v_i| \neq 1$ . This result was obtained by an analytic treatment of the local complex differential equation for the wave function describing the motion of the nuclei in the resonant anion state. The potential curves for both the neutral molecule and the anion were approximated as Morse oscillators, and for the decay width of the anion an exponential form was chosen. This scaling law is also well-satisfied by numerical cross sections for VE in molecular hydrogen and its isotopes, obtained using exact potentials.

\*Support of the Air Force Office of Scientific Research is gratefully acknowledged.

## HB-12

*Non Franck-Condon Effects in The Molecular Electronic Excitation of O<sub>2</sub> and CO.*

M. Dillon, D. Spence and M. Kimura, *Argonne National Laboratory, USA*  
R. J. Buenker, L. Chantranupong and G. Hirsch, *Bergische Universitat-Gesamthochschule, Wuppertal, Germany.*

Franck-Condon envelopes in *electron energy loss* spectra recorded for the  $X^1\Sigma^+ \rightarrow B^1\Sigma^+$  and  $X^+\Sigma_g^- \rightarrow B^3\Sigma_u^-$  transitions in CO and O<sub>2</sub> show a pronounced variation with scattering angle. This behavior is in sharp contrast with the results standard formulations confirmed by all previous studies of electron impact and optically induced molecular excitation. Underlying mechanisms revealed by a theoretical investigation employing *multi reference configuration interaction* suggest that such phenomena may be much more general than previously assumed.

---

\*Work supported by the U.S. Department of Energy, Assistant Secretary for Energy Research, Office of Health and Environmental Research under contract w-31-109-Eng-38.

**HB-13** A First Born Approximation Data Base for Excited state - Excited State Electron Impact Transitions in Alkali Atoms.\*. UMA KRISHNAN AND BERNHARD STUMPF, Dept. of Physics, University of Idaho. --- We present first Born electron impact cross sections for 120 P  $\rightarrow$  S and P  $\rightarrow$  D transitions between excited states of alkali atoms. Atomic states are represented by a Coulomb approximation. This allows a consistent and comprehensive treatment of a large number of states. Calculations are carried out for energies up to 1000 times threshold energy. In order to check the validity of our calculations oscillator strengths are deduced from these Born cross sections and compared to oscillator strengths given by Lindgard and Nielsen<sup>1</sup>. Agreement is within about 5 % for lithium and sodium, 10 % for potassium, 15 % for rubidium and 20 % for cesium. Agreement is poor for transitions that involve the low-lying D states in potassium, rubidium and cesium.

<sup>1</sup>A. Lindgard and S. E. Nielsen, *At. Nucl. Data Tables*, **19**, 533 (1977)

\*Supported by Idaho EPSCoR and NSF under grant RII-8902065.

**HB-14** Differential Cross Sections for Electron Collisions from H<sub>2</sub>O and NH<sub>3</sub> Molecules at 1-200 eV in a Multi-Potential Hybrid Approach, K L Baluja and A Jain, *Phys. Dept., Florida A&M Univ., Tallahassee, FL 32307*, - The differential cross sections (DCS) for e-H<sub>2</sub>O (NH<sub>3</sub>) are calculated at all angles (0<sup>0</sup>-180<sup>0</sup>) in the energy range of 1-200 eV. The DCS are defined as  $\frac{d\sigma}{d\Omega}(\theta) = \sum_j \frac{d\sigma}{d\Omega}^{0j}(\theta)$ , where  $\frac{d\sigma}{d\Omega}^{0j}(\theta)$  corresponds to rotationally elastic ( $j = 0$ ) and inelastic ( $j \neq 0$ ) channels. The full interaction potential,  $V(\mathbf{r})$  of the e-molecule system is expanded in terms of multipole moment tensors as  $V(\mathbf{r}) = \sum_{LM} v_{LM}(r) S_{LM}^{A_1}(\hat{\mathbf{r}})$ . If the coupling between multipole moments is weak, each term  $v_{LM}$  gives rise to a particular rotational excitation DCS as defined above. The first Born theory is used for inelastic part, while the  $\frac{d\sigma}{d\Omega}^{00}(\theta)$  is calculated via partial wave analysis. Results are compared with recent absolute measurements and *ab initio* close-coupling calculations. This simple approach is quite successful even at lower energies.

**HB-15** Low Energy electron-Ethylene Scattering T. N. RESCIGNO and B. H. LENGFIELD\* Lawrence Livermore National Laboratory and B. I. SCHNEIDER\* Los Alamos National Laboratory -- Elastic and inelastic cross sections for electron-ethylene scattering have been determined with the complex-Kohn method. Our earlier elastic scattering studies of this system focused on the Ramsauer-Townsend minimum and the  $\Pi^*$  shape resonance found in the total cross section. In this study we report the results of a more extensive set of elastic scattering calculations and we also present electron impact excitation cross sections to the low-lying excited states. The mixed, valence-rydberg character of the V-state of ethylene makes the theoretical determination of the electron impact excitation cross section to this state particularly interesting and we will discuss the determination of the trial wave function needed to obtain this cross section.

\* This work was performed under the auspices of the U.S. Department of Energy by the Los Alamos and Livermore National Laboratories under contract Nos. W-7405-ENG-36 and W-7405-ENG-48.

**HC-1 Argon Metastables in the Negative Glow of a Fluorescent Lamp Like Discharge**, K. Mitsuhashi, R. C. Wamsley, and J. E. Lawler, Univ. of Wisconsin, Madison, WI, 53706--Argon metastable density distributions are measured using absorption spectroscopy in the negative glow of a fluorescent lamp like discharge (2.5 Torr Ar, 3.5 cm i.d.). Absorption measurements provide an absolute number density for cords through the discharge. Using an Abelian inversion of off axis cords we make 3 dimensional density maps. The spatial maps have a sharp peaks within 2 mm of the cathode hot spot and a broad low pedestal extending throughout the negative glow. The peak density of  $^3P_2$  metastables is  $2 \times 10^{12} \text{ cm}^{-3}$ , and is almost independent of current. The metastables are produced by collisions between ground state argon and high energy electrons emitted from the cathode. They are lost mainly by collisions with electrons, by Penning and associative ionization collisions with Hg atoms, and by collisions between pairs of metastables. High rates of electron collisions lead to a coupling of the populations of metastable and resonant Ar levels. The low broad pedestal in the spatial distribution is probably due to transport of trapped resonant radiation from the region near the hot spot. The Ar metastables are important in the ionization balance of the negative glow.

**HC-2 Measuring Ion Current to the Cathode of a Mercury-Rare-Gas Discharge**. JOHN F. WAYMOUTH, 16 Bennett Rd, Marblehead MA, 01945. A method is proposed for determining the ion current to the hot cathode in a mercury-rare-gas discharge. First, measure the current to a negatively biased collector around the negative glow. This is equal to the fraction of the ion production in the negative glow that does not reach the cathode. Second, make a transient measurement of total ion charge and ambipolar diffusion loss time constant in the negative glow. This gives the total ion production in the negative glow. Combining these two results permits independent determination of the number of positive ions produced per primary electron and of the fraction of these that reach the cathode. Experimental problems to be overcome in making these measurements include means of cleaning the collector of deposits of evaporants from the cathode, and means of determining secondary emission coefficient of the collector.

**HC-3** Self-Consistent Cathode Fall study including Negative Glow Electrons, M. DALVIE, S. HAMAGUCHI, R. FAROUKI, IBM T. J. Watson Res. Ctr. — We present results of Monte Carlo simulations of the cathode fall (CF) of a glow discharge in a model gas. Non-equilibrium ion and electron motion is followed. The electric field is determined self-consistently in the CF. The assumption of a weakly positive Negative Glow (NG) field is evaluated by comparison to an explicit treatment of NG electrons. Assuming a NG field yields an electron density at the CF-NG boundary roughly two orders of magnitude lower than has been previously measured in the NG. This is the density of only the "beam" component of the electron distribution, since electrons trapped by the field reversal in the NG are ignored. The result is a too-high electric field gradient at the CF-NG boundary, leading to an ion density which peaks *inside* the CF. The accuracy of the self-consistent field calculation throughout the CF is therefore reduced. The weak NG field assumption is replaced by a parameterized (double-Maxwellian) description of the NG electron distribution. The scope of the field calculation now extends to the field reversal point. We can thus make a preliminary examination of the CF-NG boundary (Coulomb collisions and electron-ion recombination are not considered). For example, the growth of the ion flux is large relative to the electric field gradient between the field reversal point and the CF-NG boundary.

**HC-4** Model Calculations of the Isotope Effect in Hg-Ar Discharges. MARK DUFFY and JOHN INGOLD, GE Lighting, Cleveland, OH 44112—Isotopic composition of mercury in a low pressure Hg-Ar discharge affects UV efficiency, through dependence of UV output on effective lifetime of optically thick radiation. Measurements<sup>1</sup> show an increase of about 7% in UV efficiency with addition of 2-3% Hg196 to natural mercury, which decreases effective lifetime. Earlier measurements<sup>2</sup> show a decrease of 8% with addition of 92.8% Hg202 to natural mercury, which increases effective lifetime. Model calculations are presented for these and other compositions. The model<sup>3</sup> accurately predicts the decrease observed for the Hg202 measurements, but not the increase observed for the Hg196 measurements.

<sup>1</sup>M. Grossman, *et al.*, *Phys. Rev. A* **34**, 4094 (1986).

<sup>2</sup>G. Franck and F. Schipp, *Ltg. Res. Tech.* **7**, 49 (1975).

<sup>3</sup>J. T. Dakin, *J. Appl. Phys.* **60**, 563 (1986).

**HC-5** On the Importance of the Hg\*/Hg\* Inelastic Scattering in the Modeling of the Low Pressure Hg-Ar Discharges. G.ZISSIS, V.PLAGNOL, J.J.DAMELINCOURT, C.P.A.Toulouse.-- The modeling of the low pressure Hg-Ar positive column is sufficiently complex to necessitate the use of simplifying assumptions. A very common hypothesis is to neglect the inelastic scattering between excited Hg atoms. In fact, for Hg partial pressures less than 10 mTorr the atomic ratio [Hg\*]/[Hg] remains less than 1%, thus the probability of a Hg\*/Hg\* inelastic scattering seems to be negligible. However, we do not dispose precise informations on the nature of these interactions and the existent cross section data are very uncertain. Anyway, it is difficult to neglect these collisions when Hg partial pressure becomes important. In this work the reaction  $2\text{Hg}(6^3\text{P}_2) \rightarrow \text{Hg}(6^1\text{S}_0) + \text{Hg}^+ + e^-$  has been added in a self consistent collisional radiative model described elsewhere.<sup>1</sup> The cross section values found in the literature vary between  $1\text{\AA}^2$  and  $100\text{\AA}^2$ . In this work we adjust this value in order to minimize the deviations between the experimental data and calculations for the numeric Hg( $6^3\text{P}$ ) atomic state densities in a large range of Hg partial pressures. In fact the population density of these levels is found to be very sensitive to the above reaction. If we neglect these interactions the deviations between experimental data ( $0.83 \times 10^{18} \text{m}^{-3}$ ) and calculations for the density of the  $6^3\text{P}_2$  level (at  $p_{\text{Hg}}=36.1\text{mTorr}$ ) is found to be 115%. The same deviation becomes 31% if we take a cross section value of  $10\text{\AA}^2$ . Finally, the deviations have been found to be minimal for a cross section value of  $24\text{\AA}^2$  (less than 10%). The above results have been obtained in the case of Hg-Ar discharge with tube diameter 36mm, Ar pressure 3 Torr and discharge current 0.4A.

<sup>1</sup>G.Zissis, V.Plagnol, J.J.Damelincourt, XX-ICPIG, 8-12 July, Pise Italy (1991).

**HC-6** On the Influence of the Physical Plasma Parameters in the Modelling of the Low Pressure Hg-Ar Discharges V.PLAGNOL, G.ZISSIS, I.BERNAT, C.P.A.Toulouse.-- Our work<sup>1</sup> describes results of numerical calculations on the Hg-Ar positive column, based on a simplified model of discharge plasma with a six-level scheme of the Hg atom. The assumptions thus used, easily point out the role played by certain parameters and their direct consequences on the final results. Our main assumption concerns the radial concentration profiles of the excited states. Different density profiles have been tested and we have chosen the Bessel function which gives better agreement with experimental results. However it is interesting to see their influence on the 254nm flux energy. We have taken six different radial function, from a linear one to a sixth order polynomial one. Our results are obtained for a 36mm tube diameter filled with 3 Torr Ar and operating at a discharge current of 0.4 A. For a cold spot temperature of 20°C, the two extremum profiles stated above lead to a flux energy difference of about 23% whereas at 60°C the former is less than 1.5 %. The influence of the profile is negligible at high temperature, this phenomenon is due to the thermalisation of the system. At high Hg pressure the decrease of  $\Phi_{254\text{nm}}$  is essentially due to Hg\*/Hg\* inelastic scattering. The escape factors parameters are very important in the determination of the excited states' densities. We have used Bernat values<sup>2</sup> (in good accordance with  $\tau_{\text{exp}}$ ), relative to the 254nm line, which are different from those of Holstein theory (more than 30%). For the 185nm line we have taken experimental values for the imprisonment factor. The account for Ar excitation and ionisation in our calculations allows us to be in very good agreement with experimental data for very low Hg pressure. Excellent results are obtained with  $\tau_{105\text{nm}} = 5 \tau_{\text{exp}}$ .

<sup>1</sup>V.Plagnol, G.Zissis, M.Ziane, XX-ICPIG, 8-12 July, Pise Italy (1991).

<sup>2</sup>I.Bernat, J.L.Bonneval, J.J.Damelincourt, XX-ICPIG, 8-12 July, Pise Italy (1991).

**HC-7** Characteristics of HgBr in a Dielectric Barrier Discharge. H.-P. POPP and A. BEYING, U. of Karlsruhe (FRG).-- We have studied the characteristics of HgBr

in a high-pressure dielectric barrier discharge in the frequency range from 25 kHz to 13.5 MHz. We will report on the dependence of the output light intensity and the emission spectra on various parameters such as gas pressure, frequency, input voltage and discharge current. We will also present our results of gain and absorption measurements and optical pumping of the HgBr ( $X, \Sigma - B, \Sigma$ ) state.

**HC-8**

CONSTRICTED HIGH POWER MICROWAVE EXCITED KRYPTON ARC LAMP

G. LÖHMANN, H.-P. POPP, M. NEIGER, H. MERKEL  
L T I - UNIVERSITY OF KARLSRUHE / F R G

A Krypton high pressure discharge arc lamp within a cylindrical cavity is driven by a 2.45 GHz magnetron with input powers from 0.5 KW to several Kilowatts. High heat capacity silicon oil provides lamp cooling. By selection of proper cavity modes highly constricted arc plasmas were achieved. Efficiency of radiation output, plasma diagnostics and a simple model of the interaction of arc plasma and cavity field will be presented.

**HC-9** Chemical Nonequilibrium in a 0.1 Bar Hydrogen Arc, T. L. Eddy, INEL/EG&G Idaho - The deviation from local chemical equilibrium (LChE) in a flowing hydrogen arc is evaluated using de Donder's affinity.<sup>1</sup> Prior measurements<sup>2</sup> of 190 amp hydrogen arc in an arc tunnel at 0.1 bar were evaluated on the basis of thermal nonequilibrium (non-LThE).<sup>3</sup> High power experiments indicated that non-LThE alone is insufficient to describe the states.<sup>4</sup> The affinity is determined from the continuum given  $N_e$ . When both non-LChE & non-LThE analyses are applied to the H-arc,  $T_e$  is found to be closer to  $T_{LTE}$  from Balmer populations than with non-LThE only. The affinity is found to be about 10% of the ionization energy. In argon plasma jets<sup>5</sup> near 85 kPa, it has been found to be about 25% over various conditions and 20% in Ar/He:2/1 mixtures.<sup>6</sup>

\*Work sponsored by DOE Contract DE-AC07-76ID01570.

<sup>1</sup>T.L. Eddy & K.Y. Cho, Nat. Heat Transfer Conf. (1991).

<sup>2</sup>T.L. Eddy, et al., AIAA Paper 68-136 (1968).

<sup>3</sup>T.L. Eddy, Ph.D. Thesis, U. Minn., Mpls. (1972).

<sup>4</sup>B.A. Detering, et al., Nat. Heat Transfer Conf. (1991).

<sup>5</sup>T.L. Eddy, et al., Nat. Heat Transfer Conf. (1991).

<sup>6</sup>T.L. Eddy, et al., in Thermal Spray Research and Applications, pp.33-37, ASM Internat., Materials Park, OH (1991).

**HC-10** Effect of Hollow Cathode Cooling on Plasma Plume Emission Characteristics, W.L. Collett, S.M. Mahajan, and C.A. Ventrice, Tenn. Tech. Univ.--The emission spectrum from a hollow cathode argon plasma was used to detect trace elements such as, Cd, As, Cs, etc. in coal ash. The coal ash was embedded into the flat side of a copper cathode. Measurements were made at a gas pressure of 3 torr. A 0.5 meter spectrometer was used in the spectral analysis of the plasma plume. It was found that the temperature of the cathode played a critical role in the accuracy of the spectral intensity measurements. A special cathode was designed to eliminate these undesired heating effects. The cathode incorporated an internal cooling chamber through which a dielectric fluid was circulated. Measurements of the spectral intensity of coal ash trace elements will be compared with and without cooling of the cathode.



**HC-11** Some Important Properties of Arc Core, Zhong-Jie, Li, Huanghe University, ZHENGZHOU, P.R. China - A new definition of arc core based on the arc electrical properties in terms of shape factors<sup>1</sup> for arc core in this paper. The relationships between the parameters of arc core and that of external flow for nozzle arcs are derived empirically by this study. Both achievements form the basis for the predictive calculations of arc behaviour and improve measurements of arc core processes. Reckoning of shape factors dealt with by using Hermann's temperature profile<sup>2</sup> are examined. By solving the arc core transition layer equation, the net emitted radiation loss per unit length is formulated. The comparison of the radiation loss calculations in some arc models indicate the new method suggested in this paper yields the more accurate results.

1. H.L. Walmley, G.R. Jones, IEEE, PS-8, No. 1, 39-49, 1980
2. W. Hermann, K. Ragaller, IEEE, PAS-96, 1536-1552, 1977

**HC-12** A Model for Interaction of Arc and Gas Flow, Zhong-Jie, Li, Huanghe University, ZHENGZHOU, P.R. China - An approximate solution of governing equations for gas blast arcs has been developed to study interaction of arc with the gas flow in this paper. For the same purpose, momentum and energy conservations compared with Hermann's results are discussed. Also, the paper presents the error analysis of the simplifications concerned with shape factors which exists in most integrated arc models. The published results of the enthalpy flux shape factor has been corrected from this study. The laws of gas flow behaviour indicated by the gas pressure ratio, gas flow rate and velocity upon the arc thermal boundary are studied in detail. These studies provide the basis for calculation of arc-induced shock and arc clogging.

1. W. Hermann et al, J. Physics, D., 7, 607, 1974
2. H.L. Waimley et al, IEEE., PS-8, No. 1, 39-49, 1980

**SESSION J**

3:30 PM - 5:30 PM, Wednesday, October 23

Ballroom C

**POSTERS**  
**Optical & Probe Diagnostics**  
**Glows**  
**Particles in Plasmas**

**JA-1** What determines ion energy at an unbiased wafer in an ECR etching tool?\* N. HERSHKOWITZ, S.W. LAM, M. HUSSEIN, H. PERSING, E. DEN HARTOG, University of Wisconsin-Madison -- The UW etching tool has an unusual array of gas phase diagnostics including: Langmuir probes, LIF, IR absorption, PAD, VUV, and QMS. Results from three diagnostics -- probes, PAD, and LIF are combined with Monte-Carlo modeling to determine the functional dependence of ion energy at an unbiased wafer in the ECR tool. Ion  $E_{\parallel}$  and  $T_{\perp}/E_{\parallel}$  ( $\perp$  and  $\parallel$  to the magnetic field) are important parameters because a magnetic field is present at wafers being etched.  $T_{\perp}/E_{\parallel}$  is directly determined by PAD and inferred from LIF data. Potentials are determined with probes. It is shown that, except at very low pressures, ion energies are well below those predicted from the ambipolar potentials (usually  $< T_e/e$ ). It is shown the dominant contribution to the ion energy at the wafer comes from acceleration in the wafer-plasma sheath. The wafer floating potential is sensitive to the hot electron portion of the electron velocity distribution function. We conclude that etching does not take advantage of the ambipolar potential but is sensitive to the spatial distribution of hot electrons. There appears to be no ion energy advantage in placing the wafer far from the ECR source throat. Wafer location is determined by hot electron uniformity and uniformity of the magnetic field.

\*Supported by NSF grant ECD-8721545.

**JA-2** The Use of Faraday Rotation to Measure the Thickness and Polarization of an Alkali Vapor, M. Dulick, D.R. Swenson, D. Tupa, R.L. York, W.D. Cornelius, and O.B. van Dyck, Los Alamos National Laboratory --- We present a general method of calculating the Verdet and alpha constants for Faraday rotation in various alkali vapors. The theory gives the Faraday rotation as a function of the frequency of the probe light, the thickness and polarization of the vapor, and the applied magnetic field. We have developed a computer program to calculate the Faraday rotation as a function of these parameters; a copy of the program is available from the authors.

We describe various methods of measuring the Faraday rotation produced in an alkali vapor. These can be used to determine the thickness and polarization of the vapor. We have measured the Faraday rotation in a vapor for different magnetic fields, vapor thicknesses and polarizations, and probe frequencies. Measurements of the optical rotation near the D lines are consistent with the calculations to within 5%.

**JA-3 Wafer Temperature Measurement during Process by IR-Interferometry, C. F. A. VAN OS, and B.N. CHAPMAN, Lucas Labs, Sunnyvale, CA 94086 -** Infrared laser interferometry can accurately measure changes in temperature during processing by recording the variation in interference pattern between reflections from the front and rear wafer faces provided both are polished.<sup>1</sup> The optical path difference variation is mostly due to temperature dependence of the refractive index, but is also a direct effect of thermal expansion. Temperatures from below 100 to about 1000 Kelvins can be tracked within 2 degrees using this technique, whose practical application is reported in this paper.

---

<sup>1</sup> V.M. Donnelly and J.A. McGaulley, J. Vac. Sci. Technol. A 8 (1990) 84.

#### **JA-4**

**Laser Induced Fluorescence Temperature Measurements in a CH<sub>4</sub>-H<sub>2</sub> Discharge during the Growth of Diamond, H.N. CHU, E.A. DEN HARTOG, A.R. LEFKOW, L.W. ANDERSON, M.G. LAGALLY, and J.E. LAWLER, U. of Wisconsin-Madison-** The gas kinetic temperature in a DC hollow cathode CH<sub>4</sub>-H<sub>2</sub> discharge has been measured during the growth of diamond using laser induced fluorescence (LIF) on a CN impurity. Two different types of laser induced fluorescence (LIF) experiments have been carried out for total CH<sub>4</sub>-H<sub>2</sub> gas pressures between 10 and 90 Torr. In the traditional LIF experiment the laser is scanned to excite various ground rotational levels and all emitted radiation is detected. In the LIF "redistribution" experiment the laser wavelength is fixed to excite from a single ground rotational level and the fluorescence from all excited rotational levels is spectrally resolved with a scanned monochromator. The LIF temperature measurements agree with each other. The LIF redistribution measurements show that there are enough collisions to equilibrate the rotational levels during the lifetime of the excited levels. Optical emission intensities of either the R branch of the G  $1\Sigma \Rightarrow$  B  $1\Sigma$  (0-0) band of H<sub>2</sub> or the R branch of the B  $2\Sigma^+ \Rightarrow$  X  $2\Sigma^+$  (0-0) band of CN give the same temperature.

**JA-5** Spatial Profiles of Absolute H-atom Concentration in RF discharges,\* A.D. TSEREPI, J.R. DUNLOP, B.L. PREPPERNAU and T.A. MILLER, The Ohio State University-The technique of two-photon absorption laser-induced fluorescence (TALIF) has been used to measure non-intrusively the concentration of ground state hydrogen atoms of the inter-electrode space of a 10MHz hydrogen discharge. An absolute H-atom concentration of the order of  $10^{14}$  atoms/cm<sup>3</sup> is observed to be relatively constant over a region around the center of the discharge until it decreases at distances close to the stainless steel electrode surfaces, following an exponential law. When a GaAs wafer is placed on the electrode surface, the H-atom concentration changes significantly. Spatial profiles taken parallel to the electrode surface indicate that the concentration is increased over the GaAs wafer to levels comparable to those at the center of the discharge. Substitution of deuterium for hydrogen provides useful information concerning the possible mechanisms producing the observed surface-plasma interaction.

\*Work supported by Air Force Wright Research and Development Center via contract 722698.

**JA-6** RF Sheath Characteristics in a Plasma Sputtering System, K.F. AL-ASSADI and N.M.D. BROWN, JCRC, UUC, Coleraine, UK- The plasma potential of a 13.56 MHz argon glow discharge were measured using rf self-compensating Langmuir probe,<sup>(1)</sup> while the energy of ions striking the grounded electrode was measured by a retarding grid energy analyser<sup>(2)</sup> in a power range between 10-200 watts and at pressure of 13, 30 and 40 mTorr in an unconfined geometrically planar plasma system. The voltages on the excitation electrodes were carefully measured and related to the measured plasma potential and the energy of the ions. This reveals that the rf sheaf exhibited predominantly capacitive behaviour. In turn the grounded and the excitation electrodes sheath at a pressure of 13 mTorr is found to have relatively high voltage, while the excitation electrode sheath at pressures of 30 and 40 mTorr is found to have a higher voltage than that of the grounded electrode.

<sup>(1)</sup> P.A. Chatterton, J.A. Rees, W.V. Lu and K.F. Al-Assadi, Vacuum **42**, no. 7 pp.489, 1991.

<sup>(2)</sup> K.F. Al-Assadi, P.A. Chatterton and J.A. Rees, Vacuum **38** No. 8, pp.633, 1988.

**JA-7** A Micro-machined Sensor for In Situ Characterization of Plasma Sheath Potentials and Ion Energy Distributions. \*\*R. Jewett, M. Blain, H.M. Anderson, B. Smith, U. of New Mexico and Sandia National Laboratories

A micromachined array of ion lenses was fabricated and used to characterize several plasma chemistries. Although present measurement tools, such as Langmuir Probes, can provide insight into potentials present in laboratory plasmas, as well as useful density measurements, they also significantly change the characteristics of plasma around the probe. This unfortunate quality renders them unsuitable as a production diagnostics tool, and hinders their effectiveness as a laboratory instrument. The micromachined array of 2.5 million ion lenses provides a non-intrusive view of ion energy, current, and potential on plasma boundaries. Preliminary tests in argon and  $CF_4$  plasmas using the GEC Reference Cell are discussed. Applications such as examining recently proposed particle trapping mechanisms, and characterizing inhomogeneous electric field structures are discussed. Comparisons are made to a simple computer model and future changes to the measurement tool are suggested.

\*\* Work supported by Sandia National Laboratories-  
Contract # DE-AC04-76DP00789

**JA-8** Mass Spectra of Hydrocarbon DC Arcjet Plasmas Used in the Deposition of Polycrystalline Diamond\*, K. R. Stalder, W. Homs, SRI International--We report on measurements of the mass spectra obtained by sampling an arcjet plasma impinging upon a small aperture. The plasma jet typically operates with 1%  $CH_4$  in  $H_2$  gas at 200 Torr. Previous measurements of a free jet, determined from the optical emissions from  $C_2$ , indicate the temperature 10 mm from the arcjet orifice is approximately 4000 K.<sup>1</sup> Independent measurements of CH rotational distributions, determined by LIF techniques, indicate a significantly lower temperature.<sup>2</sup> Mass spectra, measured with a quadrupole mass spectrometer, will reflect the chemical species concentrations and temperatures present at the boundary where fast diamond growth has been demonstrated. These measurements, in progress, should help determine the critical conditions and gas-phase species that are present when diamond is growing rapidly.

\* Work Supported by ARO Contract No. DAAL03-89-K-0157

1. K. R. Stalder and R. L. Sharpless, J. Appl. Phys. **68**, 6187 (1990).
2. G. A. Raiche, G. P. Smith & J. B. Jeffries, Proc. ICNDST-2, p.251(1991)

**JA-9** Measurement of Electron Density in Methane/Hydrogen/Oxygen Plasmas, H. SNYDER and C. B. FLEDDERMANN, Center for High Technology Materials, U. of New Mexico- The electron density in methane/hydrogen/oxygen plasmas used for diamond thin film deposition has been measured using a microwave cavity. The plasma was established in a quartz tube inside an rf helical resonator operating at 13.6 MHz, which has previously been used to deposit diamond thin films. The empty microwave cavity resonates at 982.6 MHz operating in the  $TM_{011}$  mode; electron densities are determined by measuring the shift in the resonant frequency of the cavity. Electron density measurements were also made using argon for comparison. For pure argon discharges, electron densities of  $10^9/\text{cm}^3$  were measured. For the same rf power, the electron density in a 5%  $\text{CH}_4/\text{H}_2$  mixture is an order of magnitude less than for argon. Electron density measurements at pressures between 10 mTorr and 1 Torr will be presented for hydrogen with methane and oxygen concentrations varying between zero and 5%, the range of interest for diamond deposition. Measurements such as these are important for understanding and improving PECVD processes for diamond coatings.

**JA-10** Langmuir Probe Characterization of Drifting Electrons, T. E. SHERIDAN, Dept. of Physics, The University of Iowa - The electron current to a negatively-biased, cylindrical, Langmuir probe is computed for the case of drifting, Maxwellian electrons in a low-pressure discharge. The degree of drift is characterized by  $v_d/v_{th}$ , where  $v_d$  is the drift speed, and  $v_{th} = \sqrt{2kT_e/m_e}$  is the thermal speed. I find that the knee of the characteristic underestimates the plasma potential for  $v_d/v_{th} > 1.25$ . Further, for  $v_d/v_{th}$  greater than about 0.1, an analysis ignoring the drift will compute an erroneously high electron temperature.

**JA-11** Spatially Resolved Ion Velocity Distributions in Chlorine Electron Cyclotron Resonance Plasmas, TOSHIKI NAKANO\*, NADER SADEGHI#, DENNIS J. TREVOR, RICHARD A. GOTTSCHO, R. W. BOSWELL@, AT&T Bell Laboratories - The primary advantage of high density plasma sources rests in their provision of low but controllable ion energy bombardment. Our previous studies of ion transport in Ar plasmas using spatially resolved Doppler-shifted laser-induced fluorescence showed clearly that the ion velocity distribution function (ivdf) was not as cold nor as controllable as hoped.<sup>1</sup> In this work, we extend these measurements to chlorine plasmas and find only minor quantitative differences from Ar showing that geometric and electromagnetic design are the dominant factors in determining ivdfs in high density plasma systems at low pressure. We also extend our previous measurements to examine the effects of a cusp magnetic field and the influence of the electrode platen on ion transport.

\* National Defense Academy, Yokosuka, Japan

# Universite Joseph Fourier and CNRS, Grenoble, France

@ Australian National University, Canberra, Australia

<sup>1</sup> N. Sadeghi, T. Nakano, D. J. Trevor, and R. A. Gottscho, J. Appl. Phys. (in press).

**JA-12** Spatial Vibrational Population Profiles of the Ground State of N<sub>2</sub> in a Compact, Wall-Less DC Glow Discharge Using Coherent Anti-Stokes Raman Spectroscopy. P. P. YANEY and M. W. Millard\*, U. of Dayton;\*\* -- Rotational and "vibrational" temperatures were obtained from Raman spectra of the nitrogen Q-branch using scanning, folded-BOXCARS at axial and radial positions. The discharge was spatially confined by an insulating cathode cap machined from Microy with a 9-mm hole. The spatial resolution element was about 50  $\mu\text{m}$  dia. by 1 mm long. A normal-glow, parallel plate discharge was set up between molybdenum electrodes spaced 12 mm at a current density of 30 mA/cm<sup>2</sup>, a pressure of 20 Torr and E/N = 45 Td. A nitrogen flow rate of 80 SCCM was maintained. These conditions were chosen to minimize instabilities. Theoretical spectra were fit to the data by fitting separate rotational and vibrational temperatures from which the populations were determined. The v=0 population reveals a strong dependence on the spatial electron density function probably through the e<sup>-</sup>-N<sub>2</sub> interaction while the v>0 states appear populated more by anharmonic pumping.

\* In partial fulfillment of the requirements for the M.S. degree in Electro-Optics.

\*\* Supported by USAF Contract F33615-90-C-2036.



**JB-1** Self-consistent dc glow discharge simulations applied to diamond film deposition reactors, M. SURENDRA and D. B. GRAVES, University of California, Berkeley; and L. S. PLANO, Crystallume - Self-consistent particle-fluid hybrid simulations have been used to study the structure of hydrogen dc discharges between parallel plates. A particle approach is used to describe energetic electrons in the cathode region, while the electrons and ions in the low field region of the discharge are modeled fluids. Simulation results for pure H<sub>2</sub> discharges at conditions typical in diamond growth (approximately 20 - 30 torr at 1000 K, 100 - 200 Am<sup>-2</sup>) are in reasonable agreement with optical emission and Langmuir probe measurements. The plasma potential in these discharges is negative with respect to the anode, unlike discharges at lower pressures. Anode glows are also observed. Dissociation of H<sub>2</sub> in the anode region contributes significantly to the flux of atomic hydrogen to the anode, where diamond is typically grown.

**JB-2** An Efficient Algorithm for the study of Non-equilibrium Dynamics of Electrons from the solution of Boltzmann equation, S. SHANKAR, U of Minnesota and MSI and K.F.JENSEN, Massachusetts Institute of Technology - The Boltzmann equation for electrons is difficult to solve due to the many phase and space dimensions that are necessary to represent it. The hyperbolic nature and the complexity of the collision integral limit the time step in an explicit time integration method. We have solved the Boltzmann equation in the cathode fall of a radially symmetric glow discharge, using an implicit time integration technique with streamline upwinding as applied to Galerkin finite elements. The resulting Petrov-Galerkin formulation was modified to capture nonlinear and time dependent discontinuities. One of the key features of the numerical scheme is the fewer number of elements needed to resolve the solution in the spatial and velocity domain. The other key features are the efficient storing of collision kernel, optimal nature of algorithm, and extensibility to other systems like RF discharges.

**JB-3** Breakdown Characteristics of Non-Planar Plasma Sheaths,\* A. SYLJUASEN, E. E. KUNHARDT, J. BENTSON, S. POPOVIĆ, S. BARONE, Weber Research Institute, Polytechnic University, - The application of a positive voltage to a spherical electrode immersed in a background plasma results in the formation of a plasma sheath in which an ionization induced instability can lead to breakdown. In this paper, the conditions for the steady state breakdown are calculated for the case of spherical symmetry. The results are obtained for the case of a charged body in ionosphere. The critical sheath radius and anode potential are obtained. It is shown that the ratio of the total number of electrons to ions contained in the sheath is constant at breakdown. The effects of the superimposed homogeneous magnetic field are discussed.

\*Work supported by SDIO/IST.

**JB-4** Hydrogenated Amorphous Silicon Thin Film Deposition Using an Electron Beam Generated Disc Plasma,\* D. M. SHAW, T. Y. SHENG, Z. YU, and G. J. COLLINS, Colorado State University, N. ADACHI, ORC Manufacturing Co. Ltd. (Japan)- A large area disc-shaped hydrogen lamp has been used to deposit uniform hydrogenated amorphous silicon films on 7.5 cm wafers. The newly developed windowless disc plasma VUV lamp employs a ring-shaped cold cathode 19 cm in diameter by 1.5 cm high. Silane ( $\text{SiH}_4$ ) has been used as reactant with 121.5 nm vacuum ultraviolet (VUV) radiation to directly photodissociate  $\text{SiH}_4$ , as well as by means of sensitized reactions with excited atomic hydrogen. We achieved a deposition rate of 40 Å/min independent of substrate temperature, implying that little or no thermal decomposition of the  $\text{SiH}_4$  occurs. The films have an optical band-gap of 1.75 eV and good photoconductivity properties. Hydrogen content and bonding were investigated using infra-red spectroscopy.

\*Work supported in part by NSF US-JAPAN Cooperation Program(Dr.Alex De Angelis), and QRC (Fort Collins).

**JB-5 ANALYTICAL EXPRESSION OF THE IONIZATION SOURCE TERM IN ARGON, HELIUM AND NITROGEN - I.**

Pérès, N. Ouadoudi, L.C. Pitchford, and J.P. Boeuf, CNRS, Centre de Physique Atomique, Toulouse, FRANCE - An analytical expression of the ionization source term for quasi steady-state DC glow discharge conditions was derived from Monte Carlo simulations in argon, helium and nitrogen. In this formulation, the ionization source term normalized to pressure is expressed as a function of the position between anode and cathode, the sheath length (pdc) and the applied voltage (V). The analytical expressions are valid for the three gases, for the following conditions : Ar, pdc ranging from 0.05 to 0.25 cm.torr and V from 150 to 500 volts; He, 0-1.5 cm.torr and 100-300 volts; N<sub>2</sub>, 0.05-0.3 cm.torr and 150-400 volts. These ranges of parameters include typical DC discharge operating conditions. These expressions can easily be included in a one-dimension fluid model of the discharge.

**JB-6 Recombination Peaks in Pulsed Noble Gas-Cu Hollow Cathode Afterglow.** G.RUBIN, M.JANOSSY, P.MEZEI, P.APAI, K.ROZSA, Central Research Institute for Physics, Budapest. Current, voltage and intensity of He, Ne, Ar and Cu lines were measured during and after a rectangular current pulse. 4 mm diameter helical Cu tube was used with a length of 10 cm. The gas pressure was 3-25 mbar and the Cu vapour was introduced by sputtering. A pulsed current signal generator was used. Pulse width: 6-100  $\mu$ s, rising and falling time: 300 ns, current: up to 23 A. Strong recombination enhancement was observed at HeII 468.6, NeII 440.9 and ArII 358.2 nm lines in the afterglow. Smaller and long afterglow peaks were observed on some atomic transitions. No recombination peaks were found on copper ion lines, however, on CuII lines excited by charge transfer collisions with He and Ne ions a long decay up to 100  $\mu$ s was observed. The recombination enhancement had an optimum with the pulse width. The effect is explained by ions produced at the high voltage rising part of the pulse and recombined by the low energy electrons.

**JB-7 Monte Carlo Study of the Electron Swarm in a He Disc Plasma, \* B. SHI, T. SHENG, Z. YU and G. J. COLLINS, Colorado State University-** A disc plasma creates VUV radiation with high efficiency originating from helium ion state. The Monte Carlo method simulated the electron interaction with helium atoms to create excited He ions. The trace of the electron swarm trajectories in the helium shows how the ring-shape cathode and its electric field trap electrons inside the disc area. Electron trapping explains why the disc plasma has high efficiency in creating the output of VUV. The relation between ring cathode width and radiation output shows that smaller width increases electron energy loss via scattering outside the ring cathode, but it also increases the density of both electrons and helium ions, thereby increases the intensity of VUV radiation. As a consequence of these conflicting conditions an optimum ring cathode width exists. Theoretical and experimental values of optimum ring cathode width are quite similar.

\*Work supported by NSF (Grant INT-8913426, Dr. L Goldberg).

### **JB-8**

**Ionization and excitation rate coefficients in argon and helium over a wide range of E/N**,\* P. J. DRALLOS, G. N. HAYS, and M. E. RILEY, Sandia National Laboratories -- Experimentally and theoretically obtained ionization and excitation rate coefficients in helium and argon over a wide range of E/N are presented. The studies included E/N values from a few hundred to several thousand Td ( $1 \text{ Td} = 10^{-17} \text{ V cm}^2$ ). Measurements were made in an electrodeless cell contained in an S-band waveguide immersed in a dc magnetic field and subjected to a pulsed microwave field at cyclotron resonance. These measurements are equivalent to experiments in dc electric fields<sup>1</sup>, but avoid the complications that would result in a conventional cell due to electrode effects. The experiment is modeled by a time-dependent, spatially-independent Boltzmann calculation. The model incorporates a two-dimensional electron velocity distribution function and provides an exact numerical solution of the Boltzmann equation<sup>2</sup>.

\*This work performed at Sandia National Laboratories, supported by the U.S Department of Energy under Contract Number DE-AC04-76DP00789.

<sup>1</sup>G. N. Hays, L. C. Pitchford, J. B. Gerardo, J. T. Verdeyen and Y. M. Li, Phys. Rev. A 36, 2031 (1987).

<sup>2</sup>P. J. Drallos and J. M. Wadehra, Phys Rev. A 40, 1967 (1989).

**JB-9** Modeling of Magnetron Discharges, M. MEYYAPPAN and T.R. GOVINDAN, Scientific Research Associates - Magnetron discharges are receiving attention in etching semiconductors as they permit processing with low damage to the wafer and provide high etch rates. We present a discharge physics model for a 13.56 MHz planar magnetron discharge. The applied magnetic field is uniform and normal to the electric field. The model consists of the first three moments of the Boltzmann equation with proper description of the elastic and inelastic collision terms. The rate expressions were obtained<sup>1</sup> using a computer code by Morgan<sup>2</sup> which solves the Boltzmann equation to find the EEDF. The transport of electrons,  $\text{Cl}_2^+$  and  $\text{Cl}^-$  in a chlorine discharge is considered. Numerical solutions have been obtained using an efficient finite difference scheme. The study includes parametric variation of electrode gap, applied bias, pressure and magnetic field. The results show that the increase in electron and ion densities and ionization and attachment rates due to the magnetic field is significant ( $>5$ ). Qualitative and quantitative differences in density, electron temperature and electric field between magnetron and conventional ( $B = 0$ ) discharges will be presented. The model provides an understanding of the magnetron discharges and the information needed for computing etch rates.

<sup>1</sup>S.H. Park and D. Economou, *J. Appl. Phys.*, **68**, 3904 (1990)

<sup>2</sup>W.L. Morgan, *Comp. Phys. Commun.*, **58**, 127 (1990)

**JB-10** A Collisional-Radiative Model for Low-Pressure Microwave Discharges in Helium, L.L. ALVES, G. GOUSSET\*, C.M. FERREIRA, IST, Lisbon Tech. U. - A C-R model for *He* microwave discharges was developed by coupling the electron Boltzmann equation<sup>1</sup> (taking into account stepwise and superelastic processes, together with electron-electron collisions) to the rate balance equations for the  $n \leq 6$  excited states and the continuity and transport equations for the electrons, and atomic and molecular ions. The predicted characteristics for the maintenance electric field and for the mean absorbed power per electron agree well with experimental data from surface wave discharges for  $10^{15} \lesssim NR \lesssim 10^{17} \text{ cm}^2$ ,  $10^{-7} \lesssim \omega/N \lesssim 10^{-6} \text{ cm}^3\text{s}^{-1}$ ,  $6.10^{-5} \lesssim n_e/N \lesssim 2.10^{-4}$ . The predicted populations for the  $2^3S$  and  $2^3P$  states also agree well with experimental data. The dependence of the discharge characteristics on  $\omega/N$  and  $n_e/N$  is relatively small. The dependence on  $R$  is also much smaller than previously obtained, using a simplified model<sup>2</sup>. The molecular ions density predicted from the model, is much smaller than  $n_e$ , attaining a maximum of  $0.4n_e$  for the higher pressures considered in this work ( $\sim 25\text{ torr}$ ).

\*LPGP, Université Paris-Sud, Orsay

<sup>1</sup>L.L. Alves and C.M. Ferreira, *J. Phys. D*, **24**, 581 (1991)

<sup>2</sup>C.M. Ferreira et.al., *IEEE Trans. Plasma Sci.*, **19**, 229 (1991)

**JB-11** Optical Emission-based Measurements of Electric Fields in the Cathode Fall Region of He and CF<sub>4</sub>/He DC Glow Discharges. H. SHAN, S.A. SELF and M.A. CAPPELLI, Stanford University -- Electric field distributions in the cathode fall regions of He and CF<sub>4</sub>/He DC glow discharges have been measured by optical emission spectroscopy. We make use of Stark mixing in helium, and the strength of Stark-enhanced forbidden transitions relative to that of allowed transitions with common upper electronic states to infer the electric field strengths. Our experiments indicate that a resolution of approximately 250 V/m can be obtained with the 5<sup>1</sup>P<sup>0</sup>-2<sup>1</sup>P<sup>0</sup> and 5<sup>1</sup>P<sup>0</sup>-2<sup>1</sup>S transition pairs. Our calculations suggest that a significant increase in sensitivity and resolution can be obtained by use of transitions originating from higher lying electronic states. A further improvement in spatial resolution and sensitivity can be obtained by use of laser excitation from nearby metastable levels. The integration of the measured local electric field strength gives a discharge voltage that is found to be in good agreement with the applied voltage over a range of discharge conditions.

**JB-12** Particle-In-Cell Simulation of Plasma Immersion Ion Implantation. R.W.BOSWELL and M.A.JARNYK, P.R.L. Research School of Physical Sciences and Engineering, Australian National University -- Plasma Immersion Ion Implantation (PSII) is a process in which a substrate immersed in a plasma has a series of high negative voltage pulses applied to it in order to extract ions from the plasma and implant them into the substrate. A Particle-In-Cell (PIC) simulation of PSII in a parallel plate system has been performed with an ion mass representing hydrogen. When a -20 kV pulse is applied a rapidly expanding sheath heats the electrons to high energies (> 1000 eV) leading to an increase in the plasma density. Many of these energetic electrons are expelled from the plasma giving a high plasma potential (>5 kV).

**JB-13** Incorporation of Plasma Effects in the Modelling of Chemical Vapor Deposition of Diamond, E. MEEKS and M. A. CAPPELLI, Stanford University -- Plasma non-equilibrium effects have been incorporated into the chemical vapor deposition modelling of diamond deposition in a stagnation-flow reactor. The model includes an electron energy equation for tracking the electron temperature through the stagnation boundary layer. Results show that, with thermal equilibrium assumed at the reactor inlet, the electrons do not remain in thermal equilibrium with heavy species as the gas cools, due to the high thermal conductivity of the electrons. Finite rate electron chemistry with dependence on electron temperature is also included along with neutral H<sub>2</sub> third-body dissociation. A comparison of atomic hydrogen production rates for the case of thermal (Saha) equilibrium at the reactor inlet suggest that electron chemistry contribution of hydrogen dissociation is negligible. A more general formulation of the governing equations for the inclusion of substrate biasing is provided as a basis for future work.

**JB-14** Pressure Gradients and Flow Patterns in the DC Positive Column, D. W. ERNIE and L. PEKKER, U. of Minnesota - Taking into account both the charge imbalance volume force and charged-particle momentum divergence force components given by Leiby and Oskam<sup>1</sup>, an analytical expression is derived for the driving volume force in the dc positive column of a monoatomic gas. This expression is used to numerically solve for the axial neutral particle pressure gradients and flow patterns for both closed and by-pass discharge tube configurations. For discharges with sufficiently small current densities (e.g., a 0.1 mA, 3.0 mm diameter, 5 Torr He discharge), this model yields a reversal in the pressure gradient from that predicted by previous studies where the charge imbalance volume force had been neglected.<sup>1,2</sup> For by-pass tube configurations, this pressure reversal can result in a cathode directed neutral flow, as opposed to the previously predicted anode directed flow.

<sup>1</sup>C. C. Leiby, Jr. and H. J. Oskam, *Phys. Fluids* 10, 1992 (1967).

<sup>2</sup>J. H. Ingold and H. J. Oskam, *Phys. Fluids* 27, 214 (1984).

**JB-15** Analysis of the Transition to Chaos in a Glow Discharge, D. Hudson, Naval Surface Warfare Center/ White Oak Laboratory- Previous work has shown that dc glow discharges exhibit a transition to chaotic behavior if the gas possesses a metastable state. One way the transition to chaos displays itself is by the development of a small periodic current on top of dc component. In this paper, a tentative analysis from a kinetics point of view is given. A system of nonlinear rate equations similar to those of Robertson<sup>1</sup> are numerically solved for the case of He. This approach allows various reactions to be included or removed as desired. Both metastable states as well as various ionization processes and diffusion are included. Experimental are used if available otherwise they are calculated using Gryzinsky cross sections and a numerical energy distribution function. Results for the rate coefficients and the resulting current are presented. Indications for future work will be given.

<sup>1</sup>Robertson, H.S., Phys. Rev. 105, 368, (1957)

**JB-16** Simulations of Energetic Neutral Generation in Plasma Sheaths, J. REY and J. MCVITTIE, CIS, Stanford University. The sheath generation of energetic neutrals due to ion-neutral collisions was studied for weakly ionized plasmas such as are used in plasma etching. The Monte Carlo simulator implemented in SPEEDIE (the Stanford Profile Emulator for Etching and Deposition in IC Engineering) was used. Two idealized collision models were investigated, momentum transfer in which a hard ball collision mechanism is assumed and charge exchange in which no momentum transfer is assumed. The Knudsen number  $K$  (mean free path over sheath thickness) was used as the main parameter to characterize the different discharge conditions. For large  $K$  ( $K > 1$ , few collisions) the energy taken by the ions from the field is carried almost entirely by them to the electrode surface. When  $K$  is lowered so that there are several sheath collisions on average, the deposited energy on the surface is carried by both ions and neutrals. Their angular and energy distributions are quite different depending on the collision model and  $K$  assumed for the simulation. Of particular interest are the angle and energy distributions for momentum transfer collisions in the intermediate  $K$  regime ( $.1 < K < 1$ ) in which the neutrals show a broad angle distribution with low energies while ions present a strongly peaked angle distribution at high energies. It is also found that energetic neutrals can carry a large portion of the energy initially gained by the ions but lost by collisions. It is expected that these energetic neutrals can play an important role in profile evolution in both etching and PECVD.



**JC-1** Particle Detection and Electrostatic Trapping in Plasma Processes, J.E. HEIDENREICH and G.S. SELWYN, IBM Res. Div., Yorktown Heights, NY. -- The recent discovery of microscopic particles in plasmas used for etching, deposition and sputtering has generated much scientific and technological interest. Key issues involve the formation, transport and control of particles in plasmas. Laser light scattering studies have shown that suspension of particles is ubiquitous to all plasma processes. This result has been confirmed in both laboratory and manufacturing tools. Studies have also shown that suspended particles are negatively charged and are influenced by strong and weak electrical field effects in the plasma. One result of this is *particle trapping*, the electrostatic suspension and confinement of a charged particle. The presence of a silicon wafer on an electrode, a common configuration used in plasma processing, creates significant particle traps along the edges and center of the wafer. Often, the result is a high particle count around the edges of wafers or other trapping regions in the plasma tool. Frequently, these findings are inappropriately attributed to faulty handling or storage of wafers and the contribution of the tool is overlooked. This talk focuses on the new detection technique for observing this previously unknown phenomenon.

**JC-2** Simulation of Particle Confinement and Flux Penetration in dc Discharges. Seung J. Choi, Michael J. McCaughey, Timothy J. Sommerer and Mark J. Kushner, University of Illinois, Department of Electrical and Computer Engineering, Urbana, IL 61801 \* - Particulate contamination (dust) accumulates at sheath edges in dc and rf discharges. The profiles result from a balance of viscous ion drag and electrostatic confinement, and hence depend on current density and particle size. The dust accumulates where the high energy component of the electron flux from the cathode fall penetrates into the negative glow. A model has been developed to assess the regime in which particles are trapped at the sheath edge and the effect that the particles have on the penetration of the electron flux into the negative glow. A beam-bulk (b-b) model for the cathode fall is used to simulate plasma and dust transport. Electric fields and dust locations from the b-b model are used in a Monte Carlo simulation to assess the effect of the dust on excitation rates, and the models are iterated. Excitation rates decrease when the electron flux attempts to penetrate the particulate "wall", the result being that the cathode fall becomes thinner with a higher voltage.

\* Work supported by IBM E. Fishkill, NSF and ARO.

**JC-3 Model for Charging and Confinement of Particulates in a Plasma, J. Goree\*, Max-Planck Institut für extraterrestrische Physik, 8046 Garching b. München, Germany--**

Micron-size particulates can be confined in the inter-electrode region of an rf plasma. To understand how and where this confinement takes place, and how it can be controlled, I have developed a potential energy formalism, which is different from other models.<sup>1</sup> Stable confinement requires an absolute minimum in the potential energy,  $W$ . Taking into account only electrostatic charging and gravity,  $W = QV + Mgz$ , it is possible to explain most of the experimental results of Selwyn et al.<sup>2</sup> To develop a prescribed electric potential  $V$  and compute the charge  $Q$  on a dust grain, it helps to recognize that there are three time scales:  $\tau_{RF} \ll \tau_{RC} \ll \tau_{\text{bounce}}$ , where  $\tau_{RF}$  is the rf period,  $\tau_{RC}$  is the charging time, and  $\tau_{\text{bounce}}$  is the sheath transit time for a grain.

<sup>1</sup>Sommerer et al., "Monte-Carlo...", submitted to Appl. Phys. Lett.

<sup>2</sup>Selwyn et al., "Rastered Laser Light Scattering...", submitted to JVST

\*On leave from the Dept of Physics, Univ. Iowa, Iowa City, Iowa 52242

**JC-4 Dust in rf plasmas, B. N. Ganguly, P. D. Haaland, P. Bletzinger and A. Garscadden Wright-Patterson AFB, OH.--** Recent studies applying laser scattering to low pressure rf etching and deposition reactors have shown that particles often occur in these plasmas. Usually the particles are first observed at the sheath boundary and then slowly migrate into the bulk plasma. Our research has revealed different types of particles and dust depending on the plasma conditions. In gases such as carbon monoxide-argon mixtures, the particles occur essentially instantaneously on discharge ignition and they are dispersed reasonably uniformly throughout the discharge volume and boundary regions. If this discharge is run for a long time (hours), or after many on-off cycles, the particles become larger and then tend to concentrate outside the sheaths. We present data on the distributed dust form, collective effects and colloid-like structures; and microphotographs of the dust. The carbon dust particles appear porous and have only partial spherical symmetry.

**JC-5**      Modeling 2-D Electric Field Variations in a Parallel Plate RF Discharge using Particle-in-Cell Monte Carlo Techniques.

R. C. Sierocinski and H. M. Anderson, U. of New Mexico, R.K. Keinigs, T.A. Oliphant, Los Alamos National Laboratories

Variations in the plasma potential near the sheath/plasma interface of planar diode rf discharges have been implicated as electrostatic traps for particles which accumulate in the discharge during processing.<sup>1</sup> This study reports on the development of a first principle, two dimensional particle-in-cell Monte Carlo computer model which is capable of simulating axial and radial spatial variations in electric fields of rf discharges due to changes in surface characteristics of the electrode. Three idealized problems are treated involving perturbations in the electrode surface due to the physical presence of a wafer and the presence of materials on the electrode surface with varying dielectric properties. The effect of discharge operating parameters (power, pressure, etc) on the variation in depth of the potential wall of the electrostatic trap will be presented.

1) G.S. Selwyn, J. Singh and R.S. Bennett, *J. Vac. Sci. Tech. A* 7, 2758 (1989)

**JC-6**      Rotational relaxation molecules N<sub>2</sub> in free jet expansion. R.E. Mukhametzianov, Acad. Sci. SSSR Moldova, 11-226 prospekt Moscovsky, Kishinev, 277068, USSR---A method of receiving simple analytical expressions for cross-sections and rate constants for rotational excitation of diatomic molecules by atoms on the base of quasiclassical theory is proposed. All the considerations are carried out for a concrete Ar-N<sub>2</sub> system. Also, I calculate He-H<sub>2</sub>, Ar-LiH, Ar-Li<sub>2</sub> systems. The results of calculations according to the proposed analytical formulae are compared with some other calculations (1) and experimental data. They are convenient for use in various relaxation gasdynamics problems. Analytical expressions for RT- and RR-cross-sections of diatomics based on the such theory are proposed. The analytical approximations of complete scattering sections are obtained and used for calculations of rate constants of the RT processes, diffusion coefficients in the relaxation Fokker-Planck equations using the Ar-N<sub>2</sub> system and rotational relaxation time in N<sub>2</sub>. It have solved a gasdynamics problem about rotational relaxation in the free jet expansion on sonic nozzle for N<sub>2</sub> with RT and RR-transitions (3). The results are discussed.

1. Fack R.T. - Journal of Chemical Physics, 1975, V. 62, N8, p. 3143-3148. 2. Dubrovskii G.V., Pavlov V.A. Mukhametzianov R.E. - Soviet Physics-Engineering Physics, 1984, V. 47, N2, p. 301-310. 3. Dubrovskii G.V. Bogdanov A.V., Mukhametzianov R.E. - Soviet Physics Technical Physics, 1984, V. 54, N6, p. 1096-1099.

**JC-7      Process Induced Particulate Generation and Deposition During Single Wafer Reactive Ion Etching.** P.J. Resnick, H.M. Anderson, N.E. Brown, U. of New Mexico and Sandia National Laboratories

Particle generation during  $C_2F_6/CHF_3$  reactive ion etching of  $SiO_2$  has been studied using a particle flux monitor placed in the downstream pumping port of a production single wafer etcher. Particles in the size range of 0.38 - 0.5  $\mu m$  were detected emanating from the reactor chamber during the etch cycle. Downstream particle counts correlated with the appearance of 0.1  $\mu m$  diameter particles deposited in-situ on the wafer surface during etching. Particle generation, which begins rapidly after breakdown, is shown to strongly depend on process conditions. An areal particle distribution was observed on the wafer surface with the highest density occurring near the major flat of 150 mm wafers after etching. The particle distribution is explained in terms of a particle trapping phenomena which occurs due to material discontinuities of the electrode with a wafer present. Further observations also indicate that particle generation in  $C_2F_6/CHF_3$  oxide etch plasma is not the product of simple gas phase fluorocarbon polymerization and that surface-mediated events are involved in the initiation and/or in-situ growth of plasma particulates.

**SESSION K**

7:00 PM - 9:00 PM, Wednesday, October 23

Ballroom A

**WORKSHOP - GEC REFERENCE CELL ISSUES**

Co-Facilitators: J. Gerardo, Sandia National Laboratories  
H. Swain, MIT

## **SESSION LA**

8:00 AM - 10:00 AM, Thursday, October 24

Ballroom A

### **LAMPS & CATHODES**

Chair: J. Ingold, General Electric - Nela Park

**LA-1** X-Ray Measurement of Spatial Distribution of Mercury Gas Density and Temperature in Operating HID Lamps,\* T. FOHL, J. LESTER, and P. A. VICHARELLI, GTE Laboratories Incorporated, Waltham, MA— Using a collimated beam of x-rays from the National Synchrotron Light Source at Brookhaven National Laboratory, the spatial distribution of chordal absorption due to mercury vapor was measured in operating high intensity discharge lamps (HID). The chordal absorption is deconvolved to give distributions of absolute density. The density values yield the distribution of temperature. Measurements of radial distributions of density and temperature are presented with 0.5 mm resolution to radial values within 1.0 mm of the arc tube (13 mm diameter) wall and in the cool ends—regions which are inaccessible to most optical methods. Data are presented for two different temperature distributions.

\* Research carried out in part at NSLS BNL, which is supported by DOE.

**LA-2** Time Dependent x-Ray Measurements of Mercury Density in HID Lamps\*, J. LESTER, J. KRAMER, and T. FOHL, GTE Laboratories Incorporated, Waltham, MA— Absorption of x-rays was used to determine the mass of mercury intercepted by the beam in three types of high intensity discharge (HID) lamps. Measurements are reported for lamps warming up after start, during full power operation, and cooling down after extinguishing the arc. The x-ray beam is obtained from the National Synchrotron Light Source at Brookhaven National Laboratory. Time resolution is of the order of one second and spatial resolution of the order of 3 mm. During the cooling phase absolute values of mercury density are obtained which are used to determine the temperature of the cold spot in the lamp as a function of time.

\* Research carried out in part at NSLS BNL, which is supported by DOE.

**LA-3** Time Dependent Electron Energy Distribution Effects in the Low-Pressure Hg-Ar Positive Column, J.T. DAKIN, GE Lighting, Cleveland, OH 44112--Experimental data and a time dependent numerical model are used to study the Electron Energy Distribution Function (EEDF) in a low-pressure Hg-Ar positive column. Typical conditions are a tube diameter of 36 mm, an Ar pressure of 3 Torr, Hg vapor pressure in equilibrium with a 40° C wall, and current of order 0.4 A. The positive column voltage responses to current waveforms associated with dc, ac and pulsed excitation are explored. The numerical model solves time dependent equations for the Hg excited state and electron densities, the electric field, and the EEDF. Radial variations in the EEDF are neglected; radial variations in the excited state and electron densities are assumed represented by simple functions which are zero at the walls. Approaches to representing the EEDF, including one and two temperature models (1T and 2T), and a Boltzmann model (B) are compared. Time dependent EEDF solutions from the Boltzmann model are presented for various current waveforms and frequencies.

**LA-4** Current Dependence of Hg<sup>+</sup> Densities in the Cathode Region of a Hg-Ar Discharge, R. C. Wamsley, T. R. O'Brian, K. Mitsuhashi, and J. E. Lawler, Univ. of Wisconsin, Madison, WI, 53706--Single-photon LIF, at 194.2 nm, from the ground state of Hg<sup>+</sup> is used to measure the mercury ion density as a function of current from 20 to 400 mA in a fluorescent lamp like discharge (2.5 Torr Ar, 3.5 cm i.d.). An absorption experiment provides the absolute density calibration while the LIF provides better signal-to-noise, spatial resolution, and a larger dynamic range than the absorption experiment. The minimum density in the Faraday dark space (FDS) and the positive column (PC) density are shown to vary linearly with current. The minimum axial ion density in the FDS is ~50 % of the axial density in the PC at all currents. At 400 mA the respective axial densities are  $2.8 \times 10^{11} \text{ cm}^{-3}$  and  $4.6 \times 10^{11} \text{ cm}^{-3}$ . The density adjacent to the cathode in the negative glow (NG) is linear for currents above 250 mA but is nonlinear at lower currents. The peak axial density in the NG is  $2.4 \times 10^{12} \text{ cm}^{-3}$  at 400 mA.



**LA-5** Voltage-Current Characteristics in the Hot Cathode Glow Discharge, W. W. BYSZEWSKI, Y. M. LI, P. D. GREGOR and A. B. BUDINGER, GTE Laboratories- Voltage and current waveforms were measured during the hot cathode ac glow discharge. A negative slope in the V-I characteristic was observed during a portion of the ac cycle with rising current. The value of this negative differential plasma resistance depends upon the amplitude of the open circuit voltage and the impedance of the power controlling circuit. A theoretical model for the discharge phase with negative differential resistance has been developed. It comprises a modified cathode fall model of abnormal glow and the electrode energy balance. The hot cathode ac glow discharge is important in lighting applications. It appears during the starting phase of discharge lamps and often is associated with electrode sputtering which may limit transmittance of the arc tube wall. Experimental V-I characteristics of the complete ac cycle and the theoretical model for the portion with negative differential resistance will be presented.

**LA-6** Nonequilibrium cathode fall models, Y. M. Li, GTE Laboratories Inc., 40 Sylvan Rd., Waltham, MA. 02254. The most important nonequilibrium process in the cathode fall region is the ionization due to the electrons emitted from the cathode. The basic reason for such nonequilibrium behavior is due to the electron energy relaxation length is comparable or larger than the cathode fall thickness and the local electron energy distribution function cannot be prescribed by local E/n. In this work, the original von-Engel Steenbeck cathode fall model for the glow discharge is modified to incorporate variable ion mobility. Both the equilibrium and nonequilibrium models for the Townsend ionization coefficient are used in the calculations. Two simple nonequilibrium models are treated. In the first model, the cathode fall region is simply divided into nonequilibrium (next to the cathode) and equilibrium regions where the potential difference between the interface and the cathode is the ionization potential. No ionization is produced in the nonequilibrium region. In the second model, the moment equation for the average electron energy is solved and the ionization is assumed to be determined by the local average energy. Based on these modifications, the cathode fall thickness, electric field distribution and current density-voltage characteristics are derived. Using argon as an example, a detailed comparisons between the current density-voltage characteristics for both the equilibrium and nonequilibrium models will be presented.

LA-7 Investigation of the Arc Spot Formation on Cold Cathodes in Dependence on the Electrode Material, R. Bayer, J. Mentel, AEEO, Ruhr-Universität Bochum, FRG.

The column of a high current arc in air is magnetically blown against a cathode positioned perpendicularly to the arc axis. A linearly increasing voltage is applied to this electrode. The delay time of the arc spot formation on this electrode was measured for smooth electrodes made of 24 elements and 3 technical materials. The cumulative frequency distribution of this delay time was found to be a characteristic function of the bulk and surface properties of the electrode material. The average commutation time and its standard deviation are low for noble metals with a high electrical conductivity and a low work function and they are high for metals with a strong gas adsorbing capability at the surface; they are lower for technical than for pure metals. The spot traces shown by SEM micrographs are similar to that of vacuum arcs. Supported by DFG, grant SFB 191, A3.

LA-8 Continuous Phase Transition Model of an Arc Cathode Region at Atmospheric Pressure, H. MINOO and A. KADDANI, L. P. G.P., Univ. Paris - Sud, Orsay, C. DELALONDRE and O. SIMONIN, LNH, Chatou, France

- Continuous phase transition model is applied to the cathode region of an arc at atmospheric pressure in Argon (Ar) with a Tungsten (W) cathode. Following this model, variations of all thermodynamic functions and transport coefficients are continuous in the transition region between W cathode and Ar arc plasma. Different equations governing momentum and energy conservation laws and continuity conditions are solved numerically in one dimensional approximation. This local description of the cathode region leads to differential equations solved on one dimensional sub-grid on each wall point, used as boundary conditions in a two dimensional simulation of the whole arc column based on the numerical resolution of hydrodynamic transport equations coupled with density current conservation equation using Ohm's law.

**SESSION LB**

8:00 AM -10:00AM, Thursday, October 24

Ballroom B

**ELECTRON EXCITATION & IONIZATION**

Chair: Tom Rescigno, Lawrence Livermore National Laboratory

**LB-1** Electron Scattering at the Threshold Region, 2-4 eV, of Resonant Transition in Sodium,\* C. H. YING, L. VUŠKOVIĆ, and B. BEDERSON, New York U.— We are reporting the first measurements of small angle absolute differential cross sections for  $3S \rightarrow 3S$  and  $3S \rightarrow 3P$  for nine different electron energies in the range of 2-4 eV. Accurate cross sections over below and above excitation threshold are obtained for the 0.1 eV change of impact energy. Data, first of this kind for a metal atom scattering, will be compared with a close coupling calculation<sup>1</sup>. Basic information about experimental technique and data analyzes are explained in previous publication<sup>2</sup> and references within. Details of the present experiment and deconvolution procedures used to obtain absolute (i.e., not normalized) cross sections will available at the conference.

\* Research supported by U.S. National Science Foundation.

<sup>1</sup>H.L. Zhuo, D.W. Norcross, G. Snitchler, and D.A. Stauffer, *Bull. Am. Phys. Soc.* **35**, 1170 (1990).

<sup>2</sup>T.Y. Jiang, C.H. Ying, L. Vušković, and B. Bederson, *Phys. Rev. A* **42**, 3852 (1990).

**LB-2** Electron Impact Excitation of the Rare Gases.\* M.A.KHAKOO, T.TRAN and D.BORDELON, California State University, Fullerton.— Using electron energy loss spectroscopy, intensity ratios for the differential electron impact excitation of the  $(n+1)s[3/2]_2^0$  and  $(n+1)s'[1/2]_0^0$  metastable states of the heavy rare gases from the ground  $n^1S_0$  state are presented. Incident electron energies are 20eV and 30eV with scattering angles from  $10^\circ$  to  $120^\circ$ . These measurements are compared to previous experimental and theoretical data<sup>1,2</sup> and find that existing (first-order) theories may be inadequate for handling spin-exchange in these targets.

\* Supported by the Research Corporation (Cottrell Fund ) Grant # C-2954.

(1) First order many body theory, eg. N.T.Padial et al., *Phys.Rev.* **A23**, 2194 (1981).

(2) First order distorted wave approximation, D.Madison and K.Bartschat, (1991) Private Comm.

**LB-3** Non-Statistical Branching Ratios for Excitation of Metastable States in Noble Gases. K. BARTSCHAT, Drake University, D. H. MADISON and P. BURKE, University of Missouri-Rolla.---Previous relativistic distorted wave Born (DWBA) calculations<sup>1</sup> which were based on the Pauli form of the Schrödinger equation have been extended to excitation of the metastable  $np^5(n+1)s\ ^3P_{0,2}$  states of neon, argon, krypton, and xenon. According to statistical arguments, the ratio of cross sections for exciting the  $J = 2$  and  $J = 0$  states should be 5:1. However, both the DWBA calculations and recent experimental results<sup>2</sup> show strong deviations from this expected ratio. The results for several collision energies will be presented and compared with the available experimental data.

<sup>1</sup>K. Bartschat and D. H. Madison, J. Phys. B 20, 5839 (1987).

<sup>2</sup>M. A. Khakoo (1991), private communication.

Work supported by the National Science Foundation and the Research Corporation.

**LB-4** Electron Impact Excitation of Higher Rubidium States.\* CONNOR FLYNN, ZUYI WEI AND BERNHARD STUMPF, Dept. of Physics, University of Idaho. --- We have measured electron impact cross sections for the Rubidium 7S, 8S, 5D, and 6D states. Energies range from threshold to 1000 eV. Relative optical emission cross sections are obtained by measuring the impact produced  $nS_{1/2} \rightarrow 5P_{3/2}$  and  $nD_{3/2} \rightarrow 5P_{1/2}$  fluorescence at right angles to electron and atom beam. In order to obtain absolute cross section values we have calculated cross sections in First Born approximation for direct excitation and excitation by cascading and normalize the experimental data to theory at 1000 eV. The measured cross sections show a steep onset at threshold rising to a maximum within less than 1 eV. The peak value of the cross section is 12 times larger than the cross section at 100 eV for the Rb 7S and 8S states, and 16 times larger than the cross section at 100 eV for the 5D and 6D states.

\*Supported by Idaho EPSCoR and NSF under grant RII-8902065.

**LB-5** Electron Impact Excitation of the Copper Resonance Lines\*

CONNOR FLYNN, ZUYI WEI AND BERNHARD STUMPF, Dept. of Physics, University of Idaho. --- We have measured the electron impact cross section for excitation of the copper  $4P \rightarrow 4S$  resonance lines in the energy range from threshold to 500 eV. The measured relative optical emission cross section is normalized to first Born approximation at high energies. The cross section rises rapidly at threshold (3.8 eV), indicating some structure, in agreement with theoretical predictions<sup>1</sup>. The cross section has a rather flat maximum of about  $10 \pi a_0^2$  at around 10 eV, falling slowly to about  $5 \pi a_0^2$  at 100 eV. A Fano plot of the cross section is well approximated by a straight line over the entire energy range. Thus we show that the cross section, save for structures in the vicinity of threshold, may be represented by a  $\lg(E)/E$  dependence.

\*Supported in part by Idaho EPSCoR and NSF under grant RII-8902065 and by Westinghouse under contract C85-110544-046-0002.

<sup>1</sup>K. F. Scheibner, A. U. Hazi and R. J. Henry, Phys. Rev. A 35, 4869 (1987)

**LB-6** VUV Emission Cross Sections for OI Resonance Lines Following Electron Impact on Atomic Oxygen.\*

S. WANG and J.W. McCONKEY, University of Windsor, Canada. --The absolute emission cross sections for atomic oxygen resonance lines at 130.3 nm, 102.7 nm, 98.9 nm and 87.8 nm following electron impact on atomic oxygen have been established up to 100 eV. About 70% of NO molecules are dissociated by an r.f.-discharge source<sup>1</sup> to provide a high concentration of atomic oxygen in the target beam. Extreme care has been taken to measure the trapping reduction in the emission rate for these resonance lines. The emission cross section for OI 130.3 nm multiplet has been determined to be  $7.7 \times 10^{-18} \text{ cm}^2$  at 100 eV. This value has been used to normalize other cross sections. Present results will be compared with theory and other previous measurements.

\* Research supported by the Natural Sciences and Engineering Research Council of Canada.

1 J.L. Forand, S. Wang, J. Woolsey and J.W. McConkey, Can. J. Phys. 66, 349 (1988).

**LB-7** Electron-Impact Excitation from the Metastable States of Helium,\* D. C. CARTWRIGHT and G. CSANAK, Los Alamos National Laboratory— Electron-impact excitation and ionization from metastable states of the inert gases are believed to be important for certain conditions in partially ionized gases but little experimental data are available for these processes because of difficulties in performing the experiments. Differential and integral cross sections for excitation from the  $2^3S$  and  $2^1S$  states in He have been calculated using both First-Order Many-Body Theory and the Distorted Wave Approximation to evaluate the importance of incident channel distortion. Both sets of cross sections agree very well with the limited experimental data and differ from each other only at low energy and larger scattering angles. As was previously known, the integral cross sections are 2 to 3 orders of magnitude larger than corresponding processes from the ground state.

\*Supported by NSF/OIP, the DOE, and U. Calif./Los Alamos Collaboration (CALCOR)

**LB-8** Comparison of Electron and Positron Results for Scattering from Hydrogen, D. H. MADISON, M. WOODWARD, AND V. BUBELEV, University of Missouri-Rolla.---The elementary first order Born approximation predicts that the cross sections for electrons and positrons should be the same. Any improved theory, however, predicts that these cross sections should be different. Consequently, it is of interest to compare electron and positron results to determine both the extent of the breakdown of the Born approximation and the effects of identical versus non-identical particles. Electron and positron results calculated in the first and second order distorted wave approximation will be presented, discussed, and compared with previous calculations.

Work supported by the NSF.

**SESSION M**

10:15 AM - 12:15 PM, Thursday, October 24

Ballroom C

**POSTERS****Glows****Plasma Surface Interactions  
Heavy Particles & Negative Ions**



**MA-1** Wide Area Near Afterglow Oxygen Radical and VUV Source for Photoresist Ashing,\* Z. YU, G. J. COLLINS, Colorado State University, S. HATTORI, Nagoya Industrial Science Institute (Japan), D. SUGIMOTO, and M. SAITA, Nippon Seiko K.K. (Japan), J. D. MEYER, Quantum Research Corporation - An active oxygen plasma of disc shape is used to ash photoresist films with  $\pm 5\%$  non-uniformity over 15 cm diameter wafers located in a field free region downstream of the active plasma which we term the near afterglow. In the near afterglow the resist surface is exposed primarily to both an atomic oxygen flux ( $10^{18}$  atoms  $\text{cm}^{-2}$   $\text{sec}^{-1}$ ) as well as a flux of 130.6 nm oxygen resonance radiation ( $10^{-3}$   $\text{W cm}^{-2}$   $\text{Sr}^{-1}$ ). Under these conditions an ashing rate of 1.5 micrometer per minute is obtained at 100°C substrate temperature, with a rather low apparent excitation energy of 1.07 kcal per mol., for the Novolac resist (OFPR-800) as compared to ash rates achieved with conventional methods. Moreover, the dry development of silylated resist has been demonstrated using this source.

\*Work supported in part by NSF US-JAPAN Cooperation Program (Dr. Alex De Angelis).

**MA-2** VOLTAGE CURRENT CHARACTERISTICS OF LOW PRESSURE ARGON DISCHARGES - I. Pérès, L.C. Pitchford, and J.P. Boeuf, CNRS, Centre de Physique Atomique, Toulouse, FRANCE and H. Gielen, and P. Postma, Philips Lighting, Eindhoven, THE NETHERLANDS - Voltage-current characteristics have been measured in argon discharges with aluminum parallel plate electrodes of 4 cm diameter with a 1 cm spacing and for gas pressures of 1 to 10 torr. The experiment was carefully designed to avoid possible effects of gas heating. These measurements fall roughly in the middle of previous measurements which exhibit very large scatter. The V-I characteristics were also calculated from a self-consistent fluid model using ionization source terms derived from Monte Carlo simulations<sup>1</sup>. The predicted V-I characteristics agree well with the experiments if  $\gamma$ , the secondary electron emission coefficient for ion bombardment, is taken to be 0.07.

1. I. Pérès, et al, these proceedings

**MA-3** Multi-Dimensional Modeling of the Discharge Excited XeCl Laser, M.M. TURNER, DCU - A previously reported simulation<sup>1</sup> of the discharge excited XeCl laser has been further developed by incorporating a two dimensional solution of the electric field equations. A numerical coordinate transform<sup>2</sup> is used to compute the electric field accurately in complex geometries. This extended model has been used to study the effect of electrode design on the stability of long-pulse XeCl laser discharges. Compared with an ideal uniform field configuration, the use of Chang or Stappaerts electrodes can reduce pulse energy and duration by more than 50%. The results suggest that the standard electrode profiles are not optimum, and therefore that laser performance may be enhanced by further attention to discharge electrode design.

<sup>1</sup>M.M. Turner and P.W. Smith, IEEE Trans. Plas. Sci. 19(2), pp 350-360 (1991).

<sup>2</sup>J.F. Thompson, Z.U.A. Warsi and C.W. Mastin, J. Comp. Phys. 47(1), pp 1-108 (1982).

**MA-4** High Voltage Hollow Cathode Magnetron Discharge. K.ROZSA\*, L.LI, G.J.COLLINS, P.APAI\*,  
*Dept. of Electrical Engineering, Colorado State University, Fort Collins, CO 80523.*

Increased voltage due to the longitudinal magnetic field in a hollow cathode discharge laser tube was observed. The discharge tube had a diameter of 11 mm and a length of 350 mm. Anode grid was placed near the cathode surface in front of the hollow cathode cylinder forming a free aperture of 8.5 mm diameter. The discharge current was varied between 1-3 A, with 1-2 mbar He-Ar (100:1) gas filling. Around 700 Gauss a strong resonance-like increase of the voltage was observed accompanied with similar increase of the intensity of the spectral lines. We attribute the high voltage to an obstructed-like discharge formed by the magnetic field and the special anode geometry.

\* *Central Research Institute for Physics,  
Budapest, Hungary*

**MA-5 An Analytic Model of the Ion Angular Distribution Function in A Highly Collisional Sheath,**<sup>1</sup> M. A. LIEBERMAN, V. VAHEDI, R. A. STEWART, University of California, Berkeley - An analytic model is developed that predicts the ion angular distribution function in a highly collisional sheath. In a previous study<sup>2</sup>, the normal ion velocity distribution was obtained under the assumption that charge-exchange is the dominant ion-neutral collision mechanism. In the present model, we assume  $\lambda_s > \lambda_{cx}$ , where  $\lambda_s$  and  $\lambda_{cx}$  are the mean free paths for ion-neutral scattering and charge-exchange collisions, respectively. With this assumption, we consider the angular distribution to arise mainly from ions that strike the electrode after undergoing only one scattering collision following the last charge-exchange collision.

- 
1. Work supported in part by a gift from Applied Materials, Inc. and a grant from the California Office of Competitive Technology.
  2. V. Vahedi, M. A. Lieberman, M. A. Alves, J. P. Verboncoeur, and C. K. Birdsall, *J. Appl. Phys.*, **69** 2008 (1991).

**MA-6 Monte Carlo Study of Both Electron and Hydrogen Atom Swarms in a Hydrogen Molecule Disc Discharge System,** \* B. SHI, T. Y. SHENG, Z. YU and G. J. COLLINS, Colorado State University-Wide area (>50 cm<sup>2</sup>) VUV radiation was obtained from a hydrogen disc shaped discharge system with high efficiency (8%). For the calculation of the 121.5 nm radiation flux and its generation efficiency the Monte Carlo method was used to estimate both the electron and hydrogen atom swarm. We obtained theoretical estimates of the electron and atom density distribution, the electron energy distribution and the spacial distribution of radiation flux. It was found that about 15% of electric energy goes into the hydrogen molecule dissociation and about 47% of electric energy goes into hydrogen molecule ionization in a 1 Torr disc discharge system. Good agreement between experiment and theory as regards as the spacial distribution of the 121.5 nm photon flux and its variation versus pressure was obtained.

\*Work supported by NSF (Grant INT-8913426, Dr. L. Golderg).

**MA-7**

A Phenomenologically Developed Surface Kinetic Model for CF<sub>4</sub> and CF<sub>4</sub>/O<sub>2</sub> Etch of SiO<sub>2</sub>\*, V. Singh, A.K. Varnas and R.R. Rhinehart, Texas Tech University - A kinetic model was derived from a proposed mechanistic model to predict the etch rate of SiO<sub>2</sub> in CF<sub>4</sub> and CF<sub>4</sub>/O<sub>2</sub> plasmas. The kinetic model was parameterized using both literature<sup>1</sup> and our experimental data. The range of operating conditions investigated were from 200-400 in Torr pressure, 70-110 sccm flow rate, 200-700 Watts power and 0-24% oxygen. For this range of experimental operating conditions it was observed that F radicals assisted by ion bombardment of the water surface, are the active reactive species.

The proposed kinetic model is:

$$\text{Etch Rate} = \frac{K_1[F] + K_2[F][ION]}{1 + K_3[ION]}$$

This kinetic model was found to match both the literature and our own experimental data. The model will be useful in both reactor design and control.

\* Work supported by a State of Texas Advanced Technology Program.

<sup>1</sup> Donnelly, et. al., J. Appl. Phys. 55, 1 (1984).

**MA-8** Potential and ion energy distribution in the sheath, K.-U. RIEMANN, Institut für Theoretische Physik, Ruhr-Universität Bochum, D-4630 Bochum 1, Germany. The ion energy distribution of the ions bombarding a negative wall depends on the sheath potential and on the ion kinetics in the boundary layer. In most discharges the electron Debye length  $\lambda_D$  is small as compared with the ion mean free path  $\lambda_c$ . For weakly negative walls the sheath is, therefore, nearly collision free. In case of highly negative walls, however, the sheath thickness increases and collisions in the sheath may become important. We analyse the effect of collisions on the ion distribution function and on the selfconsistent sheath potential variation in the sheath. The theory starts from the charge exchange model of ion kinetics, presents a very simple formula for the potential of the unipolar ion sheath (covering the whole range from collision free to collision dominated sheaths) and extends a former asymptotic analysis [1]  $\lambda_D/\lambda_c \rightarrow 0$  to the Debye sheath.

[1] K.-U. Riemann, Phys. Fluids 24, 2163 (1981)

**MA-9** Electrical Breakdown in Partially Enclosed Structures.\*  
 E. E. KUNHARDT, S. BARONE, J. BENTSON, S. POPOVIC,  
 Weber Research Institute, Polytechnic University, - In this paper,  
 we present a theory for electrical breakdown in the regime  
 $Nd/(Nd)_m \ll 1$  and  $B \neq 0$ , in partially enclosed structures, where  
 the effect of the "ground" electrode (i.e., the enclosing structure)  
 needs to be taken into account. We considered the electrode  
 geometries for the stressed electrode to be either cylinders of  
 infinite length or spheres. The radius of the stressed electrode is  
 assumed to be much smaller than the interelectrode separation.  
 Breakdown characteristics are found to have two branches. One  
 branch corresponds to a high current discharge at large anode  
 voltage, the other corresponds to a complex set of low current  
 toroidal discharges at relatively low anode voltage. A value for  
 magnetic field strength  $B_{crit}$  is found to exist below which the  
 considered breakdown mechanism cannot exist. A scaling law for  
 $B_{crit}$  with respect to the electrode dimensions was obtained.

\*Work supported by SDIO/IST.

**MA-10** Plasma Stoichiometry and Reaction Rate Constants  
 in a Continuous Flow Stirred-Tank Reactor.\* Fred V.  
 Wells, Rene Rodriguez, Doug Warner and Pat Woodward,  
 Idaho State University, Pocatello, ID, 83209.--Quantitative  
 mass spectroscopic measurements on the effluent gas in rf  
 excited halocarbon plasmas were performed. The  
 plasmas studied were  $CCl_4$ ,  $CF_4$ ,  $CX_4/He$ , and  $CX_4/Ar$   
 where  $X = Cl, F$  in the pressure range of 0.10 to 0.60 torr  
 with rf power between 0.15 and 0.60 W/cm<sup>2</sup>. The  
 electrodes were maintained at a constant temperature of  
 296 K. Modeling the mass spectroscopic data was ac-  
 complished using a continuous flow stirred-tank reactor  
 model to provide the reaction stoichiometry and overall  
 rate constant. This model provided remarkably good fits  
 to the experimental data with errors generally less than  
 5%. Reaction rate constants and stoichiometric coef-  
 ficients were found to be a function of gas pressure and rf  
 power. The extent of reaction was primarily a function of  
 flow and rf power.

\*Work supported by Gould Electronics, Semiconductor  
 Division.

**MA-11**

Investigation of Discharge Impedance and Spectral Emission in a Cylindrical Magnetron with an Internal Axial Anode Grid \* L.LI, Z.YU B.SHI, G.J.COLLINS, Colorado State University K.ROZSA, Central Research Institute for Physics, Hungary, and J.D.MEYER, Quantum Research Corporation - A cylindrical magnetron with an axial anode grid structure was designed for metal ion lasers. The internal anode grid allows one to increase electric potential of the cylindrical magnetron discharge. The higher voltage operation allows for thereby increasing the production of metal ions by cathode sputtering. A dramatic variation at the discharge impedance with the axial magnetic field has been observed and the spectral emissions of CuI, CuII, HeI, and HeII transitions have been studied. The dependence of discharge impedance on magnetic field has been plotted for different geometrical configurations of the internal grid structure, and as a function of ambient gas type, pressure, and gas composition. The high voltage cylindrical magnetron discharge can also be used to increase the electron temperature for laser excitation, and for metal sputtering and thin film deposition. A computer model is proposed to simulate the introduction of anode structure into the cylindrical magnetron cathode.

\*Work supported in part by National Science Foundation (#ECS-8815051 and #INT-8913426)

**MA-12** The Solar Array module Plasma Interactions Experiment (SAMPIE), G.B. Hillard, NASA Lewis Research Center - The SAMPIE flight experiment, scheduled for shuttle launch in 1994, will explore a variety of interactions between high voltage space power systems and the ionospheric plasma. The specific experiments generally concern both arcing from high voltage components and current collection through plasma sheaths. Included will be a number of solar cell technologies of current interest as well as idealized experiments designed to explore basic phenomena. The rationale for the flight experiment, current design status, and a discussion of the significance of the expected data will be presented.

**MA-13 Dissociation and Chemiluminescence of Silane in Active Nitrogen**, C. A. DeJoseph, Jr., Wright-Patterson A.F.B. - The reaction of silane with active nitrogen has been studied in a small flowing afterglow system over a pressure range of 0.5 to 10 torr. Infrared, visible, and u.v. emission spectroscopy has been used to study chemiluminescence from the reaction, while tunable diode laser spectroscopy has been used to measure silane density downstream of the reaction zone. At higher pressures, the dominant emitters in the visible/u.v. region are  $\text{Si}^*$  and  $\text{SiN}^*$ . Silane dissociation has been measured by titrating a known silane mass flow while observing the density end point downstream of the reaction. Under these conditions, silane dissociation is proportional to the N-atom density in the afterglow, but does not appear to result from direct reaction of N-atoms with silane. The data indicate a chemical chain reaction is involved in both chemiluminescence production and silane dissociation. Emission and dissociation measurements will be presented along with a reaction model developed to describe the observed results.

**MA-14 Particle Simulation of a Narrow-Gap Symmetric Malter Gas Diode\*** R.W. SCHMIEDER, R.T. MCGRATH, R.B. CAMPBELL *Sandia National Laboratories* , —A symmetric Malter gas diode consists of a pair of electrodes covered with a thin film of dielectric, separated by a gas-filled gap. Application of a voltage to the electrodes produces breakdown in the gas, resulting in the charging of the dielectric. Under certain conditions, the surface charge is quasi-stable, and produces a high electric field on the metal electrodes, sufficient to cause field emission from the metal and a self-sustained discharge in the gas. Thus, once the diode is switched on, it stays on. We are simulating these devices using 1D2v planar particle-in-cell codes that include atomic data for electron-neutral elastic, excitation, and ionization collisions, ion-neutral scattering and charge exchange, and various surface emission processes. We have studied a narrow (0.01cm) gap diode with either 100 torr argon or helium gas. In this device, multiplication in the gas is insufficient to sustain the discharge. We find that anomalous electron emission from the surfaces due to the Malter Effect and field-enhanced secondary emission from rough and porous dielectric surfaces appear to be both necessary and sufficient for a self-sustained discharge. Simulations incorporating these models will be reported.

\*This work was supported by the U.S. Department of Energy under Contract DE-AC04-76DP00789.

**MA-15** Kinetics of Polythiophene Deposition in an Argon Afterglow, P. Haaland and J. Targove, Air Force Institute of Technology—Polythiophene,  $(C_4H_2S)_n$ , has emerged as a material with promising non-linear optical properties. However the conventional synthetic routes produce films with nonuniform morphology and composition that restricts optical applications. <sup>a</sup> Injection of thiophene into an active plasma results in very many reactions, the products of which may or may not be of interest. Addition of the organic precursor to the afterglow permits better control of the chemical kinetics. The decomposition of thiophene in the afterglow of an RF argon plasma has been examined with a view to understanding the mechanism of polythiophene film formation. While  $C_2H_2$ ,  $C_4H_2$ ,  $H_2S$ , and  $C_2H_4$  are prominent neutral products observed by quadrupole mass spectrometry, the deposited film accounts for less than one percent of the observed thiophene loss. The deposition rate decreases linearly with the amount of  $H_2$  added to the plasma, suggesting a role for the Ar metastable which is quenched by hydrogen. This role is confirmed by the electrostatic modulation of film deposition and probe measurements which correlate deposition with Penning ionization of  $C_4H_4S$  in the afterglow. The dense, uniform films which result from the ambipolar flux of thiophene cations have been examined by spectroscopic ellipsometry, Rutherford backscattering, infrared spectroscopy, and atomic force microscopy.

<sup>a</sup>T. Skotheim, ed., Handbook of Conducting Polymers, (NY:Marcel Dekker), chapter 9, 1986

**MA-16** New Hollow Cathode Contours for Superior Performance. W. L. COLLETT and S. M. MAHAJAN, Tennessee Tech Univ.—A Hollow Cathode geometry in a glow discharge is traditionally used for the elemental analysis. A small hole in the flat side of the hollow cathode produces an intense plasma plume [1]. Sputtering from the cathode produces emission signals thereby allowing an analysis of the cathode material. The inside contour of the hollow cathode plays a tremendous part in the determination of sputter efficiency. The finite difference method was used to obtain potential distribution around various inside contours such as converging, converging-diverging, converging-converging, spherical, etc. Axial potential gradient was then used as a guideline for the interpretation of sputter efficiency in various contours. Experiments were conducted with copper cathodes in an argon gas discharge. Intensities of prominent emission lines of copper were recorded with the hollow cathodes having various inside contours. Results indicate that the converging contours have a higher sputter efficiency than the other contours which were analyzed. Comparison between the results of finite difference method and emission spectroscopy will also be presented.

[1] R. K. Marcus and W. W. Harrison, "Analysis of Geological Samples by Hollow Cathode Plume Atomic Emission Spectrometry," Analytical Chemistry, Vol. 59, pp. 2369-2373, 1987.



**MB-1** Efficient Sputtering and Deposition by a Flat-Cathode DC Glow Discharge \* KORALY ROZRA, GEOFFREY STUTZIN, and ALAN GALLAGHER, JILA, Univ. of Colorado and NIST- High sputtering yields and substrate deposition rates have been obtained from operation of a unique DC glow discharge. A grid of thin wires is placed very close and parallel to the cathode. The wires are mounted on a cap which surrounds the cathode but is electrically isolated from it. The wires behave as anodes and artificially contract the cathode sheath, reducing the charge-exchange-collision energy loss by ions accelerating in the sheath. As a result, the effective sputtering yield is dramatically increased because the average ion impact energy at the cathode is increased towards full discharge voltage. The value of  $Pg$ , where  $P$  is pressure and  $g$  is the gap between adjacent wires, has a strong effect on the V-I characteristic, sputtering yield, and deposition rate on a substrate positioned in front of the cathode. Data for silicon, copper, tungsten, and molybdenum targets are presented.

\* Work supported in part by Solar Energy Research Institute.

**MB-2** Surface Charge Deposition and its Influence on the Stochastic Behavior of Pulsating Dielectric Barrier Discharges, R. J. VAN BRUNT and E. W. CERNYAR, NIST

— It is shown from measurements made using a real-time stochastic analyzer<sup>1</sup> that phase-to-phase propagation of memory about charge deposited on a dielectric surface significantly influences the stochastic behavior of a pulsating dielectric-barrier discharge. The measurements were made with a point-to-solid dielectric discharge gap in air for applied voltages at frequencies in the range of 60 to 300 Hz. From data on phase-restricted conditional discharge pulse phase-of-occurrence and amplitude distributions, it is evident that the most probable amplitude and phase-of-occurrence of a discharge pulse are strongly dependent on the amount of charge deposited on the dielectric surface by previous discharge events. The observed distributions are consistent with the predictions of a simplified model that considers effects of surface charge on the time-dependent mean electric-field strength in the discharge gap.

<sup>1</sup>R. J. Van Brunt and S. V. Kulkarni, Phys. Rev. A 42, 4908 (1990).

**MB-3** Vibrational Relaxation and Dissociation of D<sub>2</sub>(v,j) on Cu(111), M.CACCIATORE, P.DE FELICE, M. CAPITELLI and G.D.BILLING\*, Centro Chimica Plasmici Bari-Italy and (\*)H.C. Ørsted Institute, U. of Copenhagen-Denmark -The dissociative chemisorption of H<sub>2</sub>/D<sub>2</sub> with single crystal Cu surface has recently been the object of experimental<sup>1</sup> and theoretical<sup>2</sup> investigations. Here we present our results for the D<sub>2</sub>(v,j)/Cu(111) system obtained within a semiclassical model developed for the interaction of molecules with non-rigid surfaces. The dissociation probability for D<sub>2</sub> in a specific initial (v,j) state has been computed as a function of the impact energy and the surface temperature set to 300K. The quantum tunneling probability through the potential barriers has also been evaluated. The results show that the D<sub>2</sub> dissociation probability is smaller when compared to that of H<sub>2</sub>. The D<sub>2</sub> absorption probability, as well as the energy transferred to the surface phonons, is higher than that found for H<sub>2</sub>.

<sup>1</sup>B.F.Hayden, C.L.A.Lamont Surf.Sci. 243,31(1991)

<sup>2</sup>M.Cacciatore, G.D.Billing Surf.Sci. 232,35(1990)  
D. Halstead, S. Holloway J.Chem.Phys. 93, 2859 (1990)

**MB-4** Evidence for Above- and Sub-Surface Neutralization during Interactions of Highly Charged Ions with a Metal Surface.\* F.W. MEYER, S.H. OVERBURY, C.C. HAVENER, P.A. ZEIJLMANS VAN EMMICHOVEN, and D.M. ZEHNER, ORNL -- Projectile K-Auger have been studied for 60-keV N<sup>6+</sup> ions incident on Au and Cu single crystal targets in the range of angles 0.20 to 20°. The shape of the observed projectile K-Auger emission is characterized by two resolvable components with strikingly different dependences on perpendicular velocity. A "fast" component, limited by the rate of K-Auger decay in the essentially neutralized projectile, dominates and is ascribed to "sub-surface" emission. This component was satisfactorily modelled using a Monte Carlo simulation of the detailed projectile trajectories and close binary encounters with target atoms inside the bulk after surface penetration. The simulation was able to reproduce reasonably well the experimentally observed dependences on projectile incidence angle, target crystal azimuth, and observation angle. A much weaker "slow" component appears at very small angles and has a time dependence characteristic of the neutralization-deexcitation cascade predicted to occur above the surface prior to surface penetration.

\*Research sponsored by the Office of Basic Energy Sciences, U.S. DOE, under contract DE-AC05-84OR21400 with Martin Marietta Energy Systems, Inc., and the Joint Institute for Heavy Ion Research under contract DE-FG05-87ER40361 with the University of Tennessee.

**MB-5** Electron Scattering as a Probe of Adsorbate/Surface Interactions: Low-Energy  $e$ -BeCO and  $e$ -Be<sub>3</sub>CO Elastic Scattering, J. A. Sheehy<sup>a</sup> and Winifred M. Huo, NASA Ames Research Center — The low-energy elastic scattering of electrons by BeCO and Be<sub>3</sub>CO is examined employing the Schwinger multi-channel method to explore the relationship of features in electron-scattering cross sections with various types of adsorbate/surface interactions and orientations. Beryllium is chosen as the initial substrate since it is feasible to treat relatively large Be clusters with *ab initio* methods, and CO is taken as the adsorbate because the well-known  $\Pi$ -symmetry resonance in free CO is not seen in experimental studies of CO adsorbed to a number of transition-metal surfaces. The  $X^1\Sigma^+$  state of BeCO has a long Be-C bond distance, thereby being an analogue of physisorption, and its electron-scattering cross section has a  $\Pi$ -symmetry resonance at an energy nearly identical to that of free CO. By contrast, this feature is not evident in the cross section for the first excited  $^1\Sigma^+$  state of BeCO, which has a short Be-C distance analogous to chemisorption. Be<sub>3</sub>CO is studied to determine the resonance behavior of the cross section for various adsorption sites of CO to the Be cluster, as well as the effects of neighboring atoms.

<sup>a</sup> NRC/NASA Research Associate

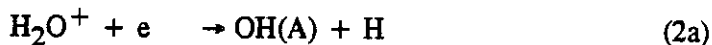
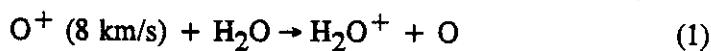
**MB-6** LIF characterisation of a magnetron discharge used in preparing high temperature superconducting thin films, W G GRAHAM, B F BURNS and T MORROW, Queen's University, Belfast BT7 1NN, N Ireland — Since the discovery of high temperature superconductivity there has been extensive interest in the preparation of thin films of such materials for both scientific and technological purposes. We have been using a magnetron discharge system, with a single, composite target to produce YBaCuO films and using plasma induced emission (PIE) and laser induced fluorescence (LIF) to characterize the discharge. These measurements are correlated with measurements of the elemental composition and quality of the films. Based on these PIE and LIF measurements we have been able to adjust the stoichiometry of a single target to produce homogeneous thin films with the correct stoichiometry.

These measurements also give an insight into the basic processes in the discharge. For example it is found that the ratio of barium to barium oxide in the discharge is sensitive to the magnetron power and that this ratio has a significant effect on the film stoichiometry. Measurements with O<sub>2</sub> added to the Ar discharge indicate that elemental oxides are produced in the discharge volume and that the oxygen influences the character of the target.

**MC-1** Ar<sub>2</sub> Second Continuum Emission in a Pulsed Discharge Excited Pulsed Supersonic Gas Expansion, M. F. MASTERS\*, J. E. TUCKER, B. L. WEXLER, and S. K. SEARLES, Laser Physics Branch, NRL.-- We have observed Ar<sub>2</sub>\* in a pulsed supersonic expansion jet with pulsed discharge excitation through the expansion nozzle. This emission extends from 115 to 140 nm peaking at 128 nm, and arises from transitions of low lying ro-vibrational levels of the A<sup>3</sup>Σ<sub>u</sub><sup>+</sup>, B<sup>1</sup>Σ<sub>u</sub><sup>+</sup>→X<sup>1</sup>Σ<sub>g</sub><sup>+</sup> bands. Ar<sub>2</sub>\* emission is strongly dependent upon the pressure upstream of the nozzle, and the onset of the observed fluorescence occurs when this pressure reaches approximately 2.5 atm prior to firing the discharge. Possible Ar<sub>2</sub>\* formation mechanisms strongly favor higher pressures. We will present a parametric study of the excimer emission as a function of gas pressure, discharge voltage, and position within the nozzle-ground rod gap.

\* National Research Council Postdoctoral Fellow.

**MC-2** Visible Emissions Produced in the Reaction of 8 km/s O/O<sup>+</sup> with H<sub>2</sub>O, \* D.M. SONNENFROH AND G.E. CALEDONIA, Physical Sciences Inc. - The interaction of water vapor with a partially ionized beam of oxygen atoms traveling at a velocity of 8 km/s has been investigated under single collision conditions. OH(A) emission has been observed in the Δv=0,1 sequences. The emission intensity is found to scale as the square of the charge density as the ionization level is varied between 10<sup>-3</sup> to 10<sup>-2</sup> of the total density. The emission is interpreted to arise from the reaction sequence



The measurements are interpreted to provide an evaluation of the efficiency of reaction (2a).

\*Work supported through the Lincoln Laboratory.

**MC-3** Ion Motion in an Ion Cyclotron Resonance Trap, K. Riehl, D. Determan, L. Pachter, and P. Haaland, Air Force Institute of Technology-Fourier Transform Mass Spectrometry has emerged as an important tool for characterizing the cross-sections for generation and reaction of charged species. Ions are formed in a cubic trap in a strong magnetic field. Conventional approaches to the excitation and detection either assume infinite parallel plate boundary conditions or perform a quadrupolar expansion of the electric field. We report here an adaptive multipolar expansion of the trap electric field and the detailed relationship of the rf excitation to the ion trajectories. The spatial boundary conditions are shown to cause motion parallel to the magnetic field axis and a dependence of the final cyclotron radius on the initial ions' axial locations. This axial excitation can change the ion kinetic energy and the image current induced in the detection circuit, both effects which influence measurements of ion-molecule reaction rates and ionization cross-sections. Experimental observation of the dependence of the ICR signal on excitation voltage confirms the role of axial excitation and ejection. The role of discretized as opposed to continuous wave excitation and the importance of the phase modulation in Selected Waveform Inverse Fourier Transform excitation is also explored.

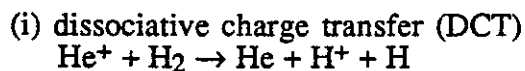
**MC-4** Rotational excitation of  $N_2^+$  in collisions with  $N_2$ , Jacek Borysow, Physics Department, Michigan Tech. University and A.V. Phelps, JILA, U. Colorado and NIST - We have reported measurements of populations of several rotational levels of  $N_2^+$  in a positive column of pulsed pure nitrogen plasma [1]. The model of the kinetics of the rotational excitation for molecular ions based on an anisotropic two temperature velocity distribution of  $N_2^+$  is presented. Excitation cross sections are assumed to be energy independent above the threshold. The steady state ratio of populations between two levels can be then expressed as a product of ratios of rate coefficients ,e.g. for the measured [1]  $p_4/p_{14}$  is

$$\frac{p_4}{p_{14}} = \frac{k_{46} k_{68} \dots k_{1214}}{k_{64} k_{86} \dots k_{1412}} \quad (1)$$

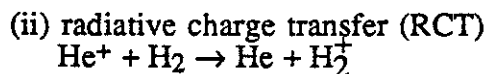
Calculated rate coefficients, based on the Monte Carlo integration give good agreement between experiment and model computation. The computational uncertainty is  $\pm 8\%$  after  $10^5$  steps of integration. Computations used experimental velocity distribution for molecular ions.

1. Jacek Borysow and A.V. Phelps, *Bull. Am. Soc.* **35**, 1837 (1990).

**MC-5** Radiative and Nonradiative Charge Transfer in  $\text{He}^+ + \text{H}_2$  Collisions in the meV Regime.\* MINEO KIMURA and N. F. LANE, Argonne National Laboratory, Argonne, IL 60439 and Rice U., Houston, TX 77251--Schauer et al.<sup>1</sup> recently measured absolute rate constants at ultra-low energy in an experiment for:



and



at  $T = 15$  K. We proposed that exoergic inelastic processes proceed via tunneling for DCT and dipole coupling for RCT. The present findings are in reasonable accord with the measurement.

\* Work supported in part by the U.S. Department of Energy, Office of Energy Research, Office of Health and Environmental Research, under Contract W-31-109-Eng-38 (MK), and by the Office of Basic Energy Sciences (NFL).

<sup>1</sup> Schauer et al., J. Chem. Phys. 91, 4593 (1989).

**MC-6** Diatomic Interaction Potentials for Rare Gas-Rare Gas and Rare Gas-Halide Systems\* E. J. Mansky, School of Physics, Georgia Tech. In excimer laser research a large number of two and three body reaction rates are required to accurately model the kinetics of the plasma which is created transiently in the discharge. To compute accurately the required reaction rates (eg. ion-ion recombination rates, ion-atom association rates), knowledge of the diatomic interaction potentials for a number of dimer positive and negative ions as well as some neutral diatomics is needed. This includes not only knowledge of the interaction potentials in the equilibrium geometry configuration, but also at larger internuclear distances.

Simple analytical formula based on the dipole polarizabilities, ionization energies and equilibrium geometry of the constituent atoms, which well reproduces the known *ab-initio* results for  $Rg - Rg$ ,  $Rg - Rg'$ ,  $Rg - Rg^+$ ,  $Rg - Hl$  (ionic channels only) and  $Rg - Hl^-$  systems (where  $Rg$  represents one of the rare gases  $Ne - Xe$  and  $Hl$  represents a halide:  $F, Cl, Br, I$ ), will be presented at the conference. Figures for a large number of diatomic interaction potentials of interest in current excimer laser research (eg.  $\text{KrF}$ ,  $\text{XeCl}$ ,  $\text{XeBr}$ ) will be presented at the meeting. In addition, in view of their importance in theories of electron capture in heavy particle collisions, cross sections for orbiting versus impact energy will also be presented.

\* Work supported by AFOSR grant no. 89-0426.

**MC-7** Vibrational Energy Exchanges in H<sub>2</sub> and D<sub>2</sub> Collisions: the Effect of Rotational Coupling, M. CACCIATORE, R.A. CAPORUSSO and G.D. BILLING\*, Centro Chimica Plasmi Bari Italy and (\*)H.C. Ørsted Institute U.of Copenhagen-Denmark-

The importance of the Coriolis coupling term in vibration-to-translation (V-T/R) energy exchange in collisions between vibrational excited H<sub>2</sub> and D<sub>2</sub> molecules has been pointed out within a semiclassical "coupled state" method<sup>1</sup>. According this model the quantum equations of motion for the vibrational amplitudes are solved numerically by expanding the total wave function in the basis of the centrifugally distorted Morse wave functions. It turns out that the inclusion of the centrifugal force in the quantum equations has a significant effect on the vibrational energy transferred during the collision and, in turn, on the V-T/R cross-sections. Furthermore, this effect critically depends both on the vibrational energy contents of the colliding molecules and the impact energy at which the collision takes place.

<sup>1</sup> M.Cacciatore et al., Chem.Phys.Lett. 157, 305 (1989), J.Phys.Chem., to be published.

**MC-8** Calculations of fine-structure changing collisions of excited Xe\* A.P.HICKMAN, D.L.HUESTIS, and R.P.SAXON, SRI International--Calculations of cross sections for mixing of Xe(5p<sup>5</sup>nl) (nl=6s,6p,5d) by thermal collisions with He and Ar are reported. Ab initio structure calculations have been performed using the COLUMBUS codes,<sup>1</sup> which include spin orbit effects and relativistic effects in the heavy atom core. A model Hamiltonian approach has been developed that allows the necessary nonadiabatic coupling matrix elements to be determined. The dynamics equations are solved using the coupled channel method, and calculated mixing rates are compared with recent experiments.<sup>2,3</sup> The mixing rates depend strongly on the particular transition and on the collision partner (He or Ar). The calculations provide an explanation for most of the state-to-state rates in terms of the features of the potential curves.

\* Work supported by Sandia National Laboratories

1. A.H.H.Chang and R.M.Pitzer, J.Am.Chem.Soc.111, 2500 (1989) and references therein.
2. J. Xu and D.W.Setser, J.Chem.Phys. 92, 4191 (1990).
3. W.J.Alford, IEEE J.Quant.Elec. 26, 1633 (1990).

**MC-9** Temporary Negative Ion States of CN-bearing Compounds,\* P.D. BURROW, A.E. HOWARD, A.R. JOHNSTON and K.D. JORDAN, U. of Nebraska, Lincoln, - The energies of the temporary negative ion states of HCN, CH<sub>3</sub>CN, CH<sub>2</sub>(CN)<sub>2</sub>, acrylonitrile, fumeronitrile, benzonitrile, TCNE and TCNQ have been determined using electron transmission spectroscopy.<sup>1</sup> The resonances associated with temporary occupation of the in-plane and out-of-plane antibonding pi orbitals were observed, and the symmetries were assigned with the aid of MO calculations. Crude stabilization calculations were also carried out in fumeronitrile and TCNE to verify the assignments.

\*Supported by NSF.

<sup>1</sup>L. Sanche and G.J. Schulz, Phys. Rev. A 5, 1672 (1972).

**MC-10** Dissociative Attachment in Monochloroalkanes,\* D.M. PEARL and P.D. BURROW, U. of Nebraska, Lincoln-The characteristics of the temporary negative ion states in these compounds are not fully understood with regard to their role in the dissociative attachment (DA) process. To augment measurements<sup>1,2</sup> of the energies of the transient anions by electron transmission spectroscopy, we are carrying out a study of the total DA cross sections. A new apparatus has been constructed featuring a trochoidal electron monochromator, a collision region consisting of a long gas cell (10 cm) to minimize end effects, and provisions for accurate pressure and current measurements. Preliminary results in the n-compounds with 2 to 4 C atoms show DA cross sections in the 1.7 - 0.5x10<sup>-19</sup> cm<sup>2</sup> range respectively. The cross section for isopropyl Cl is 24 times larger than that for n-propyl-Cl.

\*Supported by NSF.

<sup>1</sup>P.D. Burrow, A. Modelli, N.S. Chiu and K.D. Jordan, JCP 77, 2699 (1982).

<sup>2</sup>M. Guerra, D. Jones, G. Distefano, F. Scagnolari and A. Modelli, JCP 94, 484 (1991).



**MC-11** Photodetachment of Ca<sup>-</sup> near the Ca(<sup>1</sup>P) Threshold\* C. W. Walter and J. R. Peterson, SRI International -- We have used a fast ion beam-coaxial laser beam technique to investigate the photophysics of Ca<sup>-</sup>. Measurements of the photodetachment spectrum over the photon energy range 2.7-3.0 eV reveal a large resonance near 2.95 eV resulting from the threshold for Ca(4s<sup>2</sup>4p <sup>2</sup>P)->Ca(4s4p <sup>1</sup>P)+kp transitions strongly influenced by a nearby negative ion resonance. Analysis of the data using a modified form of the p-wave Wigner threshold law<sup>1</sup> provides both the resonance energy and the photodetachment threshold. The resonance is located ~17 meV above the Ca(<sup>1</sup>P) energy level and is identified as the <sup>2</sup>D shape resonance observed in electron scattering studies.<sup>2</sup> The measured threshold energy yields an electron affinity of 18± 2 meV for Ca(<sup>1</sup>S), substantially lower than previous values.<sup>3</sup> The present results will be compared with theoretical calculations of the electron affinity of Ca.

\*Research supported by AFOSR and NSF.

1. J.R. Peterson, et al., Phys. Rev. Lett. **55**, 692 (1985).
2. A.R. Johnston, et al., Phys. Rev. A **40**, 4770 (1989).
3. D.J. Pegg, et al., Phys. Rev. Lett. **59**, 2267 (1987).

**MC-12** Extraction of Negative Ions from a Pulsed Modulated Volume Source, K.N. MELLON and M.B. HOPKINS, Physics Dept., DCU, Ireland - There has been much interest in the development of a low pressure, high efficiency volume source for the production of negative deuterium ion beams for use in Neutral Beam Injection systems. Volume production of negative ions requires control of the bulk electron energy to optimize dissociative attachment, and fast electrons to pump the vibrational levels of D<sub>2</sub>. These requirements can be achieved in a low pressure discharge, by rapid modulation of the discharge current. This phenomenon is known as the temporal filter. When the discharge has reached steady state conditions and is switched off, a dramatic increase in the D<sup>-</sup> extracted current is observed. This increase is due to the continued D<sup>-</sup> production coupled with reduced losses from electron detachment. Furthermore, at high frequencies (10kHz), and on/off duty factor of 35%, an unmodulated D<sup>-</sup> current is extracted, which is five times greater than in the steady state discharge.

**MC-13 The Optically Pumped Polarized H<sup>-</sup> Ion Source at LAMPF**, R.L. York, D. Tupa, D.R. Swenson, and O.B. van Dyck, Los Alamos National Laboratory --- We describe the design and operation of a polarized H<sup>-</sup> ion source which is in operation for nuclear physics experiments at LAMPF. The beam is polarized by charge capture by H<sup>+</sup> ions from laser optically pumped polarized alkali atoms, as proposed by Anderson.<sup>1</sup> The LAMPF source has introduced several unique features: it uses K vapor polarized by Ti:Sapphire lasers, a simple frequency automation system for the lasers, a superconducting magnet for the ECR ion source, accel-accel biasing for the ECR source extraction electrodes, and a bending magnet/spin precessor which facilitates the alignment of the laser beam into the alkali vapor target. During a 5 month production run in 1990, the typical performance was 25  $\mu$ A of current with 55% polarization or 15  $\mu$ A of current with 62% polarization with source availability of greater than 90%. Optimization of the ion beam extraction optics and the optical pumping efficiency have lead to improvements in source performance. Our experiments indicate that doubling the Ti:Sapphire laser optical pumping power should allow us to achieve 28  $\mu$ A and 65% polarization during beam production in 1991.<sup>2</sup>

<sup>1</sup>L.W. Anderson, Nucl. Instr. and Meth. 167 (1979) p. 363

<sup>2</sup>R.L York et al., and D.R. Swenson et al., Proceedings of 1991 IEEE Particle Accelerator Conference, San Francisco

#### **MC-14**

Dissociative recombination of N<sub>4</sub><sup>+</sup> ions with electrons. Y.S. CAO and R. JOHNSEN, University of Pittsburgh---Spectroscopic observations of N<sub>2</sub> second-positive band emissions from photoionized afterglow plasmas containing predominantly N<sub>4</sub><sup>+</sup> ions indicate that electron recombination leads to dissociation of the N<sub>4</sub><sup>+</sup> ion into a ground state N<sub>2</sub> and an excited C<sup>3</sup>Π<sub>u</sub> (v=0,1,2) N<sub>2</sub> molecule. This observation supports a recent suggestion by D.R. Bates<sup>1</sup> that molecular dimer ions of this type recombine into excited molecules, a process that he referred to as "super-dissociative recombination" We measured a total recombination coefficient of 2.6 x10<sup>-6</sup> cm<sup>3</sup>/s at T=300K, larger by nearly a factor of two than a previous microwave-afterglow result <sup>2</sup>. The experimental method employed in this work makes use of high-pressure (300 to 800 Torr of He with traces of N<sub>2</sub>) afterglow plasmas produced by uv ionization from a spark, radio-frequency probes, mass spectrometry, and optical spectroscopy.

Work supported, in part by ARO and NASA.

1. D.R. Bates, J.Phys. B, 24, 703 (1991)

2. M. Whitaker, M.A. Biondi, and R. Johnsen, Phys. Rev. A 24, 743 (1981)

**MC-15** Dissociative Recombination of TMAE Ions,\* K. R. Stalder, D. J. Eckstrom and R. J. Vidmar, SRI International--Experiments on microwave absorption in highly collisional plasmas created by the photoionization of tetrakis-dimethylamino ethylene (TMAE) vapor in atmospheric pressure helium are being conducted. The lifetime of the plasma, approximately 20  $\mu$ s, is controlled by dissociative recombination of electrons with the TMAE ions. Electrons are quickly thermalized to 300 K. The plasma is fairly large (10's of cm) and nonuniform with an approximate Gaussian density profile. Microwave transmission experiments probing the plasma density profile have been conducted. Peak plasma densities as high as  $1.6 \times 10^{11} \text{ cm}^{-3}$  have been observed. The dissociative recombination coefficient of TMAE ions with 300 K electrons in this nonuniform plasma has thus been determined to be  $(9.7 \pm 0.6) \times 10^{-6} \text{ cm}^3 \text{ s}^{-1}$ .

\*Work supported by AFOSR Contract No. F49620-90-C-0041.

**MC-16** Product States of  $\text{Ar}_2^+$  Dissociative Recombination\* J. R. Peterson, SRI International--The excited  $\text{Ar}^*$  product states of  $\text{Ar}_2^+$  dissociative recombination (DR) are commonly believed to be in  $3p^5 4p$  configurations, based on optical emissions in afterglows.<sup>1</sup> However, time-of-flight measurements of metastable  $\text{Ar}^*$  produced in a discharge, reported by Hardy et al.,<sup>2</sup> show a superthermal component. An analysis of the data strongly indicates that this peak results from  $\text{Ar}^*$  ( $3p^5 4s$ ) states as direct products of  $\text{Ar}_2^+$  DR. The data are apparently the first evidence that the primary (>90%) excited products are in 4s states. A similar superthermal peak of  $\text{Kr}^*$  is observed from Kr discharges.<sup>3</sup>

\*Supported by NSF and AFOSR.

1. Articles by D. L. Huestis and M. H. Biondi in *Applied Atomic Collision Physics*, Vol. 3, "Gas Lasers," McDaniel and Nighan, Eds. (Academic Press, 1982).
2. K. A. Hardy, E. Gillman, and J. W. Sheldon, *J. Appl. Phys.* **67**, 7240 (1990).
3. Data kindly provided by J. W. Sheldon (1990).

**SESSION NA**

1:30 PM - 3:30 PM, Thursday, October 24

Ballroom A

**ALTERNATIVE APPLICATIONS FOR PLASMA PROCESSING**

Chair: M. Moisan, Universite de Montreal

**NA-1** Review of Thermal Plasma Chemical Vapor Deposition, J.V.R. HEBERLEIN, University of Minnesota -  
Thermal plasma chemical vapor deposition (TPCVD) is a technique in which the high density of vapor phase deposition precursors can result in high film deposition rates with little loss in film quality. A thermal plasma serves as the source of dissociated deposition precursor species, and a non-equilibrium boundary layer exists between the plasma and the cooled substrate which is brought into the immediate vicinity of the plasma. The kinetics of the chemical reactions in the boundary layer and on the surface determine the film characteristics. This deposition technique is particularly valuable for the deposition of thick films of materials which do not possess a liquid phase, such as SiC and diamond. Several different approaches to control the boundary layer conditions and, therefore, the film characteristics are discussed, including those which have resulted in the growth of highly textured YBCO films and in homo-epitaxial growth of diamond.

**NA-2** Plasmas and Their Adaptation to Biomedical Applications: The Example of Sterilization, J. PELLETIER, LCP3, UJF and CNRS, Grenoble, France- Applications of plasmas to the biomedical field are rapidly growing. Surface treatments of biomaterials are expected to improve their biocompatibility and biofunctionality in specific areas such as chemical inertness (e.g., blood compatibility), non-toxicity (allergic reactions) and long term stability (implants). As an example, the plasma sterilization of heat sensitive materials would be an attractive substitute for ethylene oxide processing which leaves adsorbed toxic residues. In oxygen-based plasmas, the de-activation of pathogenic organisms is assumed to be due (near ambient temperature) to their slow combustion with the active species. In the absence of ion bombardment, the concentration of oxygen atoms is an important parameter entering the plasma sterilization efficiency. Means for achieving high production and low loss rates of oxygen atoms are reviewed and discussed. In particular, an initial improvement would be to generate the plasma in the sterilization volume itself. Uniform plasma excitation at electron cyclotron resonance (ECR) which allows resonant coupling in the whole treatment volume (no shadowing) and requires reduced electric fields to sustain the discharge (no heating of biomaterials) is particularly adapted to this purpose. Permanent magnet structures developed for nuclear magnetic resonance (NMR) imaging can be usefully employed to produce the intense magnetic fields which would be required for large volume, uniform ECR plasmas.

**NA-3** Radical Production in Coronal Discharges for Air Cleaning\*

B. M. PENETRANTE, J. N. BARDSLEY, P. A. VITELLO, G. E. VOGTLIN and W. W. HOFER, Lawrence Livermore National Laboratory - Coronal discharges formed by submicrosecond pulses lead to the destruction of many pollutant molecules<sup>1,2</sup>, such as NO, SO<sub>2</sub> and CFC-113, through reactions of radicals that are created by electron impact dissociation or ionization. Two-dimensional models of streamer formation and propagation are used to study the density and energy distribution of the electrons in the streamer head and stem during the initial transit between coaxial cylindrical electrodes. Radical production is very efficient in this stage, provided that the average applied field exceeds about 20kV/cm. Further calculations are underway to ascertain whether the efficiency falls during later stages of the discharge and to determine the factors that control the number of coexisting streamers. The analysis will be used to predict the optimal pulse length, and to explore the sensitivity of the radical production rate to the levels of O<sub>2</sub> and H<sub>2</sub>O in the air. The results will be compared with experiments at LLNL and elsewhere.

\*Work performed under the auspices of the U. S. Department of Energy under Contract No. W-7405-ENG-48.

<sup>1</sup>G. Dinelli, L. Civitano and M. Rea, IEEE Ind. Appl. Soc.(1988)1621.

<sup>2</sup>S. Masuda and H. Nakao, IEEE Trans. Ind. Appl. 26, 374 (1990)

**NA-4** Magnetron Enhanced Reactive Ion Etching of

GaAs, M. MEYYAPPAN, Scientific Research Associates, Inc., and G. F. MCLANE, U.S. Army ETDL - A magnetron discharge has been used to etch GaAs in SiCl<sub>4</sub> and BCl<sub>3</sub> plasmas. The band magnetron cathode (Materials Research Corporation) has two permanent magnets located within the body of the cathode with two more at the top of the chamber cover to ensure a uniform magnetic field (100-150 G). The reactor which operates at 13.56 MHz is characterized by a high degree of ionization and a low self bias critical in reducing wafer damage. Etch rates of 1.6 μm/min were achieved with a control of side wall angle of the via hole and selectivity. Patterned samples with varying line widths down to 0.25 μm were etched. The side walls are vertical as revealed by SEM. Etched surfaces were characterized using XPS and AUGER to study the surface chemistry. Plasma diagnostics using emission spectroscopy and microwave interferometry will be discussed.

**NA-5**      Characterization of a Compact RF Induction Plasma Source and the Extracted Neutral Beam, L. Chen and A. Sekiguchi, IBM General Technology Division, Hopewell Junction, NY 12533

We present a neutral beam apparatus designed to generate a high-flux low-energy neutral beam. The neutral beam is extracted from a plasma source into a UHV equipment via a neutralizer. The plasma source is a magnetic mirror confined RF induction source with an induced electric field ( $E_\theta$ ) which is perpendicular to the background magnetic field ( $B_z$ ). The plasma source can be operated at low gas pressures ( $10^{-4}$  Torr and lower) and can produce a wide range of plasma densities ( $10^9 \text{ cm}^{-3}$  to  $10^{12} \text{ cm}^{-3}$ ) and electron temperatures ( $3 \text{ eV} < T_e < 50 \text{ eV}$ ) depending on the mode of operation. When this plasma source is operated in conjunction with a neutralizer, the apparatus produces neutral beams. Evidence of neutral beam production has been obtained and full characterization of the extracted neutral beam (using a chopper and a UTI mass spectrum analyzer) is currently in progress. We will present detailed characterization of the plasma source and the extracted neutral beam during the conference.

**NA-6**      Investigation of ECR discharge mechanisms based on the study of surface-wave sustained magnetoplasmas: a systematic approach, J. MARGOT and M. MOISAN, U. de Montréal - This approach considers the methodology and the formalism of the modelling of cylindrical plasma columns sustained by electromagnetic surface waves and extends them to the case where these discharges are submitted to an axial, static magnetic field  $B_0$ . It leads to a variety of waves that are guided by the plasma column, these waves differing in particular by the spatial distribution of their electric field intensity. This distribution, as we show, plays on the power transfer from the HF field to the plasma and it influences the spatial density distribution of excited atoms. This led us to analyse, as a function of  $B_0$ , the respective rôles of the wave attenuation coefficient, wave polarisation and HF power required to maintain an electron-ion pair in the discharge upon the plasma density and upon the electric field for the gas breakdown. In the latter case, we have introduced<sup>1</sup> the novel concept of effective electric conductivity that appears to be more instructive here than that of the effective electric field.

<sup>1</sup> J. Margot and M. Moisan to appear in J. Phys. D (1991)

**SESSION NB**

1:30 PM - 3:30 PM, Thursday, October 24

Ballroom B

**DISCHARGE MODELS**

Chair: J. P. Boeuf, CNRS - Toulouse



**NB-1** Model Calculations of Hot F Atom Energy

Distribution in Low Pressure Plasma Reactors.<sup>1</sup> A.S. Clarke, B. Shizgal, Dept. of Chemistry, Univ. of British Columbia —

Hot neutral atoms that are not completely thermalized in low pressure reactors may activate non-thermal gas phase and surface reactions for which the corresponding thermal reaction rates are very small. In this paper, the non-equilibrium energy distribution function of hot F atoms is determined from the Boltzmann equation which describes the production of hot atoms by electron dissociation of  $CF_4$  and the thermalization via elastic collisions with  $CF_4$ . The electron distribution function which determines the production rate of hot F atoms is modelled appropriately. The F-atom energy distribution function is assumed to be time-independent and spatially homogeneous. The details of the hot atom energy distribution function and the enhancement of non-thermal reaction rates relative to the thermal values are reported.

<sup>1</sup>Research supported by a grant from the Natural Sciences and Engineering Research Council of Canada

**NB-2** Charging of Pattern Features During Plasma Etching, J. C.

Arnold and H. H. Sawin, Department of Chemical Engineering, MIT,

Cambridge, MA 02139. The localized charging of a recessed step during

the plasma etching of a perfectly insulating surface was modelled

assuming an isotropic electron flux and monodirectional ion

bombardment. The field set up by the localized charging acts to deflect

arriving ions, modifying the ion flux densities within the feature, and

thus, etching rates. Preliminary simulations indicate that this may be

important in the shaping of etching profiles.

**NB-3** TRANSIENT AND STEADY-STATE HOLLOW CATHODE DISCHARGES: MODEL

- L.C. Pitchford and J.-P. Boeuf, CNRS, Centre de Physique Atomique, Toulouse, FRANCE - We report model results of electric field distributions in transient and steady-state hollow cathode (HC) discharges for comparison with experiments<sup>1</sup>. The purpose of this work is to provide a better understanding of the onset of the pseudospark discharge. The model is a 2-D, hybrid fluid-particle description of the electric field and charged particle distributions. The electron impact ionization terms appearing in the electron and ion fluid equations are determined by a Monte Carlo simulation in order to account for the nonequilibrium between high energy electrons and the electric field. The model predictions for steady-state discharge voltage-current characteristics (on the order of 200 V and 1-10 mA) and for the transient electric field are in agreement with the experimental results.

1. J.P. Booth, et al these proceedings.

**NB-4** Steady state and transient hollow cathode discharges: Experiments

J. P. BOOTH, M.P. ALBERTA and J. DEROUARD, Univ. GRENOBLE I, France. - Time and space resolved electric field and optical emission measurements have been performed in a transparent walled hollow cathode discharge cell whose geometry resembles pseudospark devices. The electric field was determined (amplitude and direction) using laser Stark mixing spectroscopy of NaK<sup>1</sup>. Measurements were made in discharges of Ar-K mixtures (at about 0.5 Torr, 10 mA). The space charge penetrates inside the (initially equipotential) volume of the hollow cathode through a small hole (3 mm diameter) on the axis of the device. The resulting space charge field is clearly seen, as well as the distortion of the field lines close to the axis. Pulsed operation allowed us to determine the characteristic time for the space charge to build up in the hollow cathode, which is a fraction of a microsecond, and to observe the onset of the charge multiplication. Our observations are in good agreement with numerical simulations<sup>2</sup>.

1. M.P. Alberta and J. Derouard, J. Phys. D 24, 904 (1991)
2. L.C. Pitchford and J.P. Boeuf, companion contribution

**NB-5** Temporal Relaxation of Electrons in Nitrogen, E.E. Kunhardt and P. Hui, Weber Research Institute, Polytechnic University, -- We have examined the temporal relaxations of the mean energy, drift velocity, and rate coefficients in nitrogen after a fixed step change of  $E/N$  with various initial conditions using the Monte Carlo Flux method [1]. We have found that although the initial responses of all quantities can be quite different, they all approach the steady state exponentially at the same rate and with the same dependence on  $E/N$ . It has been found that the exponential time constant is determined by the largest nonzero eigenvalue and the corresponding eigenvector of the transport matrix. The characterization of the relaxation during the early (non-exponential) time will be discussed.

\* Work supported by the National Science Foundation

I. G. Schaefer and P. Hui, J. Comput. Phys. 130(1990)

**NB-6** Electron Drift Velocity and Net Ionization Coefficient at High  $E/N$  in  $\text{SiH}_4$ , L. E. KLINE and D. K. DAVIES, Westinghouse STC -- Electron drift velocity and net ionization coefficient values have been measured in swarm experiments and calculated using Monte Carlo simulations in order to derive a set of  $\text{SiH}_4$  cross sections. The cross section determinations of Ohmori et al.<sup>1</sup> were hampered by a lack of high  $E/n$  drift velocity data. Our new experimental data has allowed us to obtain improved  $\text{SiH}_4$  cross sections. We found that predictions made using the cross sections of Ref. 1 agree well with experiment for  $E/n \leq 100$  Td. For higher  $E/n$  values we obtained good agreement with our measured drift velocity and ionization coefficient data by replacing the vibrational cross sections given in Ref 1 with the vibrational cross sections of Kurachi and Nakamura.<sup>2</sup> We also used the dissociation cross section of Ref. 2 from the threshold at 8.4 eV to 30 eV. The dissociation cross section of Ref. 1 was used for electron energies above 50 eV, with the two cross sections connected by a straight line between 30 eV and 50 eV. The resulting cross section set gives good agreement between measured and predicted drift velocities for  $1 \leq E/n \leq 1000$  Td. Predicted net ionization coefficient values are in reasonable agreement with experiment from the ionization threshold to 1400 Td.

1. Y. Ohmori, M. Shimosuma and H. Tagashira, J. Phys. D. 19, 1029 (1986).
2. M. Kurachi and Y. Nakamura, J. Phys. D. 22, 107 (1989).

**NB-7** Comparison Between Nonequilibrium and Equilibrium Fluid Models of RF Glow Discharges, F. YOUNG and C. WU, EE Dept. Auburn U. - A nonequilibrium fluid model is obtained by interpolating between a kinetic and a three-moment nonequilibrium formulation of Boltzmann equation in the time scale of the moment relaxation time. Whereas the single-moment equilibrium model assumes that the energy and velocity relax to the equilibrium state. To compare the difference between these two models, a self-consistent rf glow discharge simulation by the fluid (solved by MAFCT<sup>2</sup>) and Poisson's equations is used. A major difference is that the sheath width is reduced by 20% for the case that the amplitude of the applied rf field equals 45 V/cm at 1 torr background pressure. Moreover, the comparisons of charged particle density, space-charge field, power deposition and ionization rate between these two models will be reported in this paper. The results are compared with those from self-consistent Monte Carlo simulation.

\*This work is supported by NSF under ECS-9009395 and CRAY Research, Inc.

1E.E.Kunhardt, J.Wu, B. Penetrante, *Phys. Rev. A* **37**, 1654 (1988)

2E.E.Kunhardt, C.Wu, *J. Comput. Phys.* **68**, 127 (1987)

**NB-8** The Bohm criterion and the ion acoustic sound barrier, K.-U. RIEMANN, *Inst. f. Theoretische Physik, Ruhr-Universität Bochum*, D-4630 Bochum 1, Germany. In the limit of a small Debye length  $\lambda_D$  the plasma boundary layer is split up into a thin space charge region (sheath) and a quasineutral plasma region (presheath). Necessary condition for the formation of a stationary sheath is the validity of Bohm's sheath criterion. In its most simple form it requires that the ions enter the sheath region at least with ion sound velocity  $v_B$ . On the other hand the sonic point  $v = v_B$  results in a singularity terminating the quasineutral plasma approximation. Thus Bohm's criterion is usually fulfilled in the equality form. However, in widening geometries, the flow may become supersonic within the plasma. In this case the Bohm criterion is oversatisfied and the sheath edge exhibits no singularity. This hydrodynamic result is in apparent contradiction to kinetic results indicating that the validity of Bohm's criterion and the structure of the sheath edge depend exclusively on the elementary processes of the plasma ions and not on the geometry [1]. The contradiction is demonstrated and resolved with the example of a collisionless cylindrical column, where ionization is restricted to a small region near the axis.

[1] K.-U. Riemann, *J. Phys. D* **24**, 493-518 (1991)

**SESSION P**

3:30 PM - 5:30 PM, Thursday, October 24

Ballroom C

**POSTERS**

**Collisions in Plasmas**

**Emission Spectroscopy**

**Pulsed Power**

**Alternative Applications for Plasma Processing**

**PA-1** Stark Broadening in Laser-Produced Oxygen Plasmas,\*  
 L.S. Dzelzkalns and W.A.M. Blumberg, Phillips Laboratory (AFSC), P.C.F. Ip, V. Eccles, and R.A. Armstrong, Mission Research Corp. - The IR line emissions from OI Rydberg states have been measured in a recombining oxygen plasma produced by laser-induced breakdown. Spectral emission measurements for the wavelength range of 3.5 to 8.0 microns have been analysed using Stark broadening theory. Semi-classical line broadening calculations were performed using quasi-static ion broadening theory and the impact approximation to describe electron broadening. OI line emission spectra were calculated for different electron densities, electron temperatures, and electronic temperatures to determine the sensitivity of the line profiles to these parameters. Comparisons of these calculations to the O plasma emission spectra have been made to obtain best fits to the experimental data. The application of this method to the determination of plasma parameters will be presented.

\* Work supported by the Air Force Office of Scientific Research and the Defense Nuclear Agency.

**PA-2** CH Emission from Low Current, CH<sub>4</sub> - Ar Discharges at High E/n.\* Z. Lj. PETROVIĆ\*\* and A. V. PHELPS, JILA, University of Colorado and NIST. - Measurements were made of CH(A→X) band emission at 430 nm using a high E/n drift tube. For E/n = 2 kTd and p = 100 mTorr and 2 to 90% CH<sub>4</sub> in CH<sub>4</sub> - Ar mixtures, the CH emission peaks near the cathode indicating heavy particle excitation. This CH signal increases linearly with Ar for ≤ 50% Ar and linearly with CH<sub>4</sub> for ≤ 10% CH<sub>4</sub>. Also, the CH emission increases linearly with distance from the anode. A consistent reaction sequence begins with the CH<sub>3</sub><sup>+</sup> ion, which is known to be formed efficiently in collisions of electrons and of Ar<sup>+</sup> with CH<sub>4</sub>. As for fast H production in H<sub>2</sub>,<sup>1</sup> the CH<sub>3</sub><sup>+</sup> ions gain > 20 eV before they collide with Ar or CH<sub>4</sub> to produce fast CH. Fast CH - Ar collisions then excite the CH(A) state. In contrast to H<sub>2</sub> discharges,<sup>1</sup> the small change in CH emission with cathode material suggests backscattering of CH is unimportant in our experiments.

\* Work supported in part by Air Force Wright Laboratories.

\*\* Permanent address: Institute of Physics, Belgrade, Yugoslavia.  
 1. Z. Lj. Petrović, B. M. Jelenković, and A. V. Phelps, Phys. Rev. Letters (submitted).

**PA-3** Breakdown Delay Times in Photo-triggered Discharges, M. LEGENTIL, S. PASQUIERS, V. PUECH and R. RIVA, U. Paris-Sud, Orsay, France- The breakdown delay times (BDT) are characteristic parameters of photoswitched discharges<sup>1</sup>. We present experimental and theoretical investigations of the BDT in high pressure Ne/Xe, Ne/HCl and Ne/Xe/HCl mixtures for  $0.01 < E/N < 50$  Td and for Xenon and HCl concentrations in the range 0.01-10 %. The predicted BDT values result from a model coupling the Boltzmann equation to the kinetics and circuit equations. These values agree very well with the experiments. The evolution, versus E/N and gas mixture, is discussed. As a result, it is shown that the BDT heavily depends on the microscopic processes and are rather insensitive to the circuit parameters.

<sup>1</sup>H. Brunet et al, J. Appl. Phys. 68, 4474 (1990).

**PA-4** Electron Excitation Temperature and Density Measurements in Non-equilibrium, Low-pressure, Cs-Ar Plasmas\* - S. D. MARCUM and T. M. CIFERNO, Miami University, Oxford, Oh 45056 -- Electron excitation temperature and density have been measured in a low pressure (0.05 Torr Cs, 2 Torr total pressure) cesium-argon discharge that uses a heated cathode (1500 K). The temperature and density values result from a comparison of measured and calculated absolute spontaneous emission intensities of 26 lines in the Cs I spectrum. Calculated spectra are derived from a model<sup>1</sup> that allows prediction of absolute cesium excited state densities and emission intensities in such plasmas, as functions of electron temperature and density. The best fit between measured and calculated spectra give an excitation temperature near 6000 K and an electron density of roughly  $5 \times 10^7$  cm<sup>-3</sup>. The density value is more than an order of magnitude lower than that estimated from current continuity. The disagreement can be understood in terms of the non-equilibrium nature of such low density plasmas.

\*Work supported in part by U.S. Air Force (WPAFB).  
<sup>1</sup>S.D. Marcum, J.L. Myers, M.A. Gieske, M. Tackett and B.N. Ganguly, J. Appl. Phys. 69, 27 (1991).

**PA-5** Characterization of a Flowing Afterglow in an Electronegative Plasma. D. E. BELL and WM. F. BAILEY, Air Force Institute of Technology, WPAFB, OH — In non-equilibrium electronegative plasmas, a steady state is achieved in which a radial segregation of plasma constituents into a positive-negative ion region and an electron-positive ion region occurs. The negative ion density is determined by volumetric processes and is trapped by the radial ampipolar field. In contrast, for a simple two component ion plasma, the limiting Schottky profile is achieved. Here the temporal evolution of the plasma density and radial profiles are investigated in order to characterize the transition from the segregated to proportional mode using a flowing afterglow model as a vehicle. The time-dependent fluid moment equations are solved, assuming radially uniform temperature profiles, using the Crank-Nicolson method. The transition is parameterized in terms of discharge current, and pressure. Comparisons are made to the effective diffusion coefficients of Rogoff<sup>1</sup>.

<sup>1</sup>G.I. Rogoff, J. Phys. D 18, 1533 (1985).

**PA-6** Modeling of Magnetic Multicusp Deuterium Plasmas for Negative Ion Production. C. GORSE, M. CAPITELLI, and M. BACAL<sup>+</sup>, University of Bri and Centro Studio Chimica Plasm (CNR) Italy and Ecole Polytechnique<sup>+</sup> France - The selfconsistent model, which solves at the same time the vibrational kinetics, the electron energy distribution function, the dissociation and the negative ion kinetics in magnetic multicusp plasmas, developed for H<sub>2</sub><sup>1</sup> has been extended to D<sub>2</sub> plasmas. The input data involving each vibrational level of D<sub>2</sub> (e-V, E-V, V-T, electronic excitation and dissociation, interaction of D<sub>2</sub> (v) with metallic walls and so on) are those discussed in ref. 2. In this communication, we present results for vibrational distributions, electron energy distribution functions, electron temperature and electron number density, D and D concentrations as a function of current intensity, pressure and applied voltage for the same experimental conditions previously discussed for H<sub>2</sub><sup>1</sup>.

<sup>1</sup>C. Gorse, R. Celiberto, M. Cacciatore, M. Bacal and M. Capitelli, GEC '90 R-14, 154

<sup>2</sup>M. Cacciatore, M. Capitelli and R. Celiberto, Nuclear Fusion 1991, in press.



**PA-7** Oscillations in Pulsed, Parallel-Plane Hydrogen Discharges.\* B. M. JELENKOVIĆ,\*\* Z. Lj. PETROVIĆ,\*\* K. ROZSA,\*\*\* and A. V. PHELPS, JILA, University of Colorado and NIST. - Measurements were made of damped oscillations in the current, voltage, and light emission induced by a voltage pulse applied to the stabilizing resistor of discharges in H<sub>2</sub> at pd of 0.3 to 1 cm Torr operating at voltages of 300 to 700 V. Single pulses  $\approx$  1 ms long resulted in low ion bombardment. For pulse currents  $I$  of 0.01 to 5 mA ( $2 \times 10^{-7}$  to  $10^{-4}$  A/cm<sup>2</sup>), the frequencies and damping constants were 5 to 200 kHz and  $2 \times 10^3$  to  $10^5$  s<sup>-1</sup>. At currents below those for oscillation growth, the steady-state voltage decreased as  $-4000 \times I$ . Transient models relate the frequencies, damping constants, and onset of oscillation growth to ion transit times, electron ionization, and ion-induced secondary electron yields. For 0.5 Torr, the voltage decreases agree with models of space-charge field induced changes in secondary electron yields.

\* Work supported in part by Air Force Wright Laboratories.

\*\* Permanent address: Institute of Physics, Belgrade, Yugoslavia.

\*\*\*Permanent address: Central Research Institute of Physics, Budapest, Hungary.

**PA-8** Excitation by Fast Hydrogen Atoms in H<sub>2</sub> Discharges at High E/n.\* Z. Lj. PETROVIĆ,\*\* B. M. JELENKOVIĆ,\*\* and A. V. PHELPS, JILA, University of Colorado and NIST. - Fast excited H atoms produced in collisions of fast H atoms with H<sub>2</sub> and observed by Doppler spectroscopy and quantitative radiometry are shown to dominate the production of H $\alpha$  emission in low-current, low-pressure H<sub>2</sub> discharges. Backscattered fast H atoms resulting from H<sup>+</sup> ions and H atoms incident on the cathode excite most of the H $\alpha$  for a heavy metal cathode (AuPd), but excite much less H $\alpha$  for a graphite cathode. Other collisions producing H $\alpha$  are: electron-H<sub>2</sub>  $\leq$  25%, H<sup>+</sup>-H<sub>2</sub>  $\leq$  10%, and H<sup>+</sup>-cathode - negligible. The models use data on the energy distribution of backscattered H atoms. Excitation by backscattered H atoms explains H atom emission previously attributed to excitation at the cathode surface.<sup>1</sup>

\* Work supported in part by National Science Foundation, by US-Yugoslavia Joint Board (Project 924), and by NIST.

\*\* Permanent address: Institute of Physics, Belgrade, Yugoslavia.

1. A. Cappelli, R. A. Gottscho, and T. Miller, Plasma Chem. Plasma Proc. 5, 317 (1985); C. Barbeau and J. Jolly, J. Phys. D 23, 1168 (1990).

**PA-9**      Model Simulations of He rf Discharges and the Importance of Including Ionization from Metastables. R. C. Sierocinski and H. M. Anderson, U. of New Mexico

A particle-in-cell Monte Carlo simulation model<sup>1</sup> has been used to study He discharges under conditions characteristically used in the GEC Reference Cell calibration (pressure 200-500 mTorr, 200-500 V peak-to-peak applied voltage). Model calculations are compared assuming first that the major features of He discharges can be modeled with a single composite cross section for ionization, excitation and metastable production and secondly assuming that additional cross sections for ionization from the 1s2s composite singlet and triplet metastable states are needed. Model predictions for plasma density and energy are compared against experimental data obtained from the Reference Cell.

1) M. Surendra and D.B. Graves, *Phys. Rev. Lett.* **66**, 1469 (1991)

**PA-10**

Boundary dominated high field low pressure deuterium discharges, B. N. Ganguly and Alan Garscadden, Wright-Patterson AFB, OH - Spatially resolved electric field, Doppler width and emission intensity profiles have been measured in a low current, low nd ( $\leq 0.3$  Torr cm) D<sub>2</sub> dc discharge. The axial electric field measurement, obtained from the D <sub>$\beta$</sub>  Stark splittings, indicates the entire interelectrode volume, except for the anode edge, is a collisional sheath. The D <sub>$\alpha$</sub>  and D <sub>$\beta$</sub>  emission linewidth profiles from the interelectrode volume show that, for this high E/n ( $> 35$  kTd) discharge condition, the heavy particle excitation dominates over the electron impact process. This type of discharge usually has a positive characteristic, it exhibit current-voltage oscillation whose amplitude is strongly dependent on the circuit parameters. The voltage-current measurements of D<sub>2</sub> and H<sub>2</sub> discharges, at 0.3 Torr cm, show the discharge maintenance voltage is significantly higher for the D<sub>2</sub> compared to the H<sub>2</sub> discharge which also indicates the importance of heavy particle impact ionization for low nd discharges.

**PB-1** CT Measurement of DC-Magnetron Discharges in ArA.Itoh\*, N.Shimura, T.Koike and T.Makabe, Keio Univ.—

Emission Selected-Computer Tomography (ESCT) system has been constructed to investigate the structure in magnetron discharges in Ar. Photons from the discharge are detected by two identical scanning mirror systems, movable parallel and perpendicular to electrodes, positioned outside the two orthogonal small windows on the chamber.

Measurements by ESCT have been performed in a planar DC magnetron, made of Al target with a 100 mm diameter and a 20 mm spacing, with maximum magnetic field of 1000G. Magnetron is operated at 10 W for (a)0.3 Pa,295 V, (b)1.0 Pa,260 V and (c)10 Pa,195 V, respectively. Three emission lines, ArI(419.8nm;14.6eV), ArII(433.7nm; 41.2eV) and AlI(396.2nm;3.15eV), are selectively observed. After the reconstruction of the observed data by Radon transform using ART, tomographic picture gives two dimensional intensity profile of the excited species as a function of axial distance. It is visualized in detail that the peak of the intensity expands to radial direction with increasing pressure.

\*Permanent address;Shibaura Engineering works Co.Ltd.

**PB-2** Spectroscopic Determination of Level Populations in aPositive Column HeSe<sup>+</sup>-Laser, R.NENTWIG and J.MENTEL,A.EEO,Ruhr-Universität Bochum, FRG— For Doppler broadened

lines with known transition probabilities the population densities of the upper levels are calculated from the line intensities and the effective absorption coefficients, which have been measured end-on for the selenium and helium lines emitted by the positive column of a HeSe<sup>+</sup>-Laser. The population densities of the lower levels as well as of most of the remaining neutral and ionized Selenium and Helium levels are calculated by the application of Kirchhoff's law in a generalized form. Under optimal lasing conditions the population densities of the laser levels and their difference are of the order of  $10^9 \text{ cm}^{-3}$ . The density of the neutral selenium is less than  $10^{11} \text{ cm}^{-3}$ . The electron density is calculated to be  $10^{13} \text{ cm}^{-3}$ . By Fabry-Perot measurements of the Doppler shift of the emitted lines the selenium ions have been shown to drift in the axial electric field of the discharge. The drift velocity is estimated to be of the order of 50 - 100 m/s and seems to be correlated to the lifetime of the corresponding upper level. With the particle densities obtained a detailed picture of the elementary processes responsible for the population inversion and their performance limiting impact for the HeSe<sup>+</sup>-Laser is given.

**PB-3** Study of Optical Emission Spectra in the Microwave Plasma Assisted Diamond Deposition Environment, S. C. KUO and E. E. KUNHARDT, WRI Polytechnic U.- In diamond film deposition using  $\text{CH}_4/\text{H}_2$  plasmas, the quality of the film is influenced strongly by the  $\text{CH}_4/\text{H}_2$  ratio. We have studied the optical emission spectra in the microwave plasma assisted diamond deposition environment. The spectrum detected in the  $\text{CH}_4/\text{H}_2$  plasma were  $\text{CH}(4315 \text{ \AA})$ ,  $\text{C}_2(5165 \text{ \AA})$ ,  $\text{C}_2(5625 \text{ \AA})$  and the hydrogen Balmer line series  $\text{H}_\alpha(6563 \text{ \AA})$ ,  $\text{H}_\beta(4861 \text{ \AA})$  and  $\text{H}_\gamma(4341 \text{ \AA})$ . The molecular hydrogen emission spectrum was also detected. The temperature of hydrogen atoms in the plasma was estimated to be 2200 K by the two-line radiance ratio method<sup>1</sup>. It is well known that  $\text{C}_2$  contributes mainly to the growth of graphite, while high density of atomic hydrogen is the major contributing factor in the production of high quality diamond films. The relation between the  $\text{C}_2/\text{H}_\alpha$  ratio and the  $\text{CH}_4/\text{H}_2$  ratio will be presented.

<sup>1</sup>R. H. Tourin, *Spectroscopic Gas Temperature Measurement* (Elsevier, Amsterdam, 1966), p. 46.

**PB-4** Dependence of  $\text{O}(^1\text{S})\text{Ar}$  decaytime on  $\text{O}_2$  Content, K. YUASA, Toshiba Lighting and Technology Coporation- To detect the amount of  $\text{O}_2$  existing in  $\text{Ar-N}_2$  plasma as impurity, we have investigated the light spectra from it. Total pressure of the plasma is 93000 Pa ( $\text{Ar } 90\%$ ,  $\text{N}_2$  10%) and  $\text{O}_2$  content is less than 250 PPM. Though any significant dependence of spectrum decaytime on the  $\text{O}_2$  content is not found from  $\text{Ar, N}_2$ , large dependence on the  $\text{O}_2$  is found from  $\text{O}(^1\text{S})\text{Ar}$  excimer formed in pulse like discharge, i.e., while  $\text{O}_2$  content is less than 50 PPM,  $1/D$  ( $D$ ; decaytime) of the excimer increases in proportion to  $\text{O}_2$  content ( $1/D=20 \times \text{O}_2$  where  $\text{O}_2$  is in PPM). The measured decaytime fits the calculation using the equation of Welge and Atkinson.<sup>1</sup> While  $\text{O}_2$  content becomes more than 50 PPM,  $1/D$  increases with higher rate. It is possible, for example, to detect the amount of  $\text{O}_2$  in incandescent lamps which contain the gases without destruction of envelopes.

<sup>1</sup> K.H. Welge and R. Atkinson, . Ch. Phys. 64, 531 (1976)

**PB-5** Vacuum Ultraviolet (VUV) Measurements on an ECR Plasma Using  $CF_4$  and  $CHF_3$ ,\* JYH-SHYANG JENQ and JAMES W. TAYLOR, Materials Science Program, Department of Chemistry and the Engineering Research Center, University of Wisconsin-Madison - The vacuum ultraviolet (VUV) emission from ECR plasmas of  $CF_4$  and  $CHF_3$  has been related to the emitting species over the range of 80 nm to 200 nm, such as fluorine (95.5 and 97.4 nm), hydrogen (121.6) and carbon (156.1, 165.7 and 193.1 nm). The variation of emitting species intensity with process variables, flow, and gas composition have been studied. Preliminary conclusions are reached concerning the dominant species and their energetics. The VUV spectra are very sensitive to impurities in ECR etching plasmas, providing a diagnostic for controlling the variability of the etching.

\*This work was supported by the Engineering Research Center for Plasma-Aided Manufacturing under grant ECD-8721545 from the National Science Foundation.

**PB-6** Measurement of X-rays Emitted from ECR Processing Plasmas,\* J. L. SHOHET, T. J. CASTAGNA, K. A. ASHTIANI, and N. HERSHKOWITZ, ERC for Plasma-Aided Manufacturing, U. of Wisconsin-Madison- X-rays produced in electron-cyclotron-resonance (ECR) processing plasmas have been detected and measured. X-ray production has several important aspects. X radiation may result in damage to substrates. It can also be of concern to operating personnel. Finally, information about the X radiation spectrum can be used as a plasma diagnostic, yielding information about the electron energy distribution. We report measurements of X radiation from argon and nitrogen ECR plasmas which were generated in a magnetic mirror geometry which was modified for downstream processing. The neutral gas pressure was varied between 0.5 and 2.0 mTorr. The 2.45 GHz microwave power (ASTeX S-1000) was varied between 800 and 1000 watts. The X-rays were measured using a liquid-nitrogen-cooled lithium drifted silicon crystal detector covered with an 8-micron thick beryllium window (EDAX AMR 1200-169-5 energy dispersive analyzer). The detector was placed inside the vacuum system at the mirror mid-plane and was oriented so as to detect X-rays which were produced in this region, primarily in a direction perpendicular to the d.c. magnetic field. The detector could measure X-ray energies from 1 keV to 40 keV. Measurable X-rays were observed within 5-10 minutes of operation. In particular, X-rays appeared when the resonant layer intersected the vacuum chamber within the acceptance angle of the detector. The X-ray spectra also exhibited a strong dependence on the neutral gas pressure.

\*This is based on work supported by the National Science Foundation Grant No. ECD-8721545.

**PB-7** Study of the Soft X-Ray Emission from Carbon Plasmas Excited by Fast Capillary Discharges. B. SZAPIRO, J.J. ROCCA, M.C. MARCONI, D. CORTAZAR and F. TOMASEL. Colorado State University. The possibility of developing a soft X-Ray recombination laser based on a capillary discharge has been proposed [1]. We report the study of the soft X-Ray emission from highly ionized carbon plasmas created in polyethylene capillary discharges. Our initial experiments were conducted in 1 mm diam. capillaries excited by 100 ns current pulses from a table-top discharge with  $V \leq 40$  kV. C VI lines were observed to dominate the spectra for excitation energies above 20 J, peaking at 35-50 ns after the maximum of the current pulse and rapidly decaying.  $N_e$  was estimated from Stark broadening to be approximately  $1 \times 10^{19} \text{ cm}^{-3}$  and  $T_e$  in the core at least 70 eV. To produce initially hotter and more rapidly cooled plasmas we constructed an 800 kV pulser that generates 150 kA current pulses with 11 ns 10-90% risetime and 25 ns FWHM. In this discharge strong emission from the 18.2 nm line of C VI was observed both during and at the end of the current pulse. We present time resolved spectra for different capillary geometries designed to optimize plasma cooling.

1. J.J. Rocca, D.C. Beethe, M.C. Marconi. *Optics Letters* **13**, 505, 1988.

-- Work supported by N.S.F and U.S. D.o.E.

**PB-8** Time Resolved Electric Field Measurements in Hydrogen RF Plasmas by Stark Emission Spectroscopy, J.P. BOOTH, J. DEROUARD and N. SADEGHI, Laboratoire de Spectrométrie Physique, Université Grenoble 1, France- Temporally and spatially resolved measurements of the electric field have been made in a 30 kHz parallel plate discharge in hydrogen at 1 and 2 Torr. In this technique the Stark splitting of Rydberg states ( $n = 6$  in this case) of H atoms is determined from the spectral line profile of Balmer series emission induced by the plasma<sup>1</sup>. The line profiles also show large Doppler broadening due the complex mechanisms of excited state atom production<sup>2</sup>, but this can be allowed for by measuring the profile of the H $\alpha$  emission, which is not significantly perturbed by the Stark effect. Fields up to 2 kV/cm were observed close to the electrodes during the cathodic period of the cycle, with a precision of  $\pm 100$  V and a spatial resolution of 1mm. Measurements were impossible in higher frequency (4 MHz) plasmas due to lack of signal: large sheath potentials, causing energetic ion bombardment, are necessary to produce the emitting atoms by backscattering of neutralised ions<sup>2</sup>. A laser excitation method is under development to allow measurements over a wider range of conditions with increased sensitivity and spatio-temporal resolution.

<sup>1</sup> C.Barbeau and J.Jolly, *Appl.Phys.Lett.* **58**, 237, (1991)

<sup>2</sup> C.Barbeau and J.Jolly, *J.Phys.D*, **23**, 1168, (1990)

**PB-9** Comparison of the Stark Broadening of Hydrogen Balmer and Neutral Helium Lines in a High Pressure, Low Electron Temperature Helium Plasma, L. W. Downes, S. D. Marcum and W. E. Wells, Miami University, Oxford, OH and J. Stevefelt, GREMI, Université d'Orléans, France. In our most recent studies of high-pressure (500 - 5000 Torr), electron-beam-pumped (900 ns, 10 A/cm<sup>2</sup>, 250 keV) helium plasmas, the use of Stark-broadened linewidths as a measure of electron density gives widely varying values depending on the line used. For example, using the quasi-static approximation, the Stark-broadened linewidths of the group of lines including the neutral helium lines at 388.9 nm, 501.5 nm, 587.6 nm, 728.1 nm, and the hydrogen Balmer- $\alpha$  (656.3 nm) line, indicates an electron density of the order 10<sup>16</sup> cm<sup>-3</sup>. Similar measurements of the H $\beta$  line give a density of only 10<sup>14</sup> cm<sup>-3</sup>. The latter value is much more reasonable and is in excellent agreement with calculation<sup>1</sup>. Since such measurements based on the H $\beta$  linewidth are known<sup>2</sup> to be relatively insensitive to electron temperature, our results suggest a more significant electron temperature effect for the other studied lines than previously known<sup>2</sup>.

<sup>1</sup>"Estimation of Electron Densities in <sup>3</sup>He Dominated Plasmas," by B.D. Depaola, S.D. Marcum, H.K. Wrench, B.L. Whitten and W.E. Wells in *Proceedings of the First International Symposium on Nuclear Induced Plasmas and Nuclear Pumped LASERS*, M. Fitare, ed., Les Editions de Physique, 91402 Orsay, France, 1978.

<sup>2</sup>*Spectral Line Broadening by Plasmas*, H.R. Griem, Academic Press, New York, 1974

**PB-10** Optical absorption spectroscopy study of the role of plasma chemistry in YBCO pulsed laser deposition, W G GRAHAM, H F SAKEEK, T MORROW and D G WALMSLEY, Queen's University, Belfast BT7 1NN, N Ireland - Excimer laser ablation is increasingly recognized as a successful method for the deposition of oxide superconductor thin films. Various diagnostic techniques have been used to elucidate the basic mechanisms of the laser ablation process. Optical emission spectroscopy is often used but is difficult to interpret since observed intensities depend on both number densities and local excitation mechanisms. Here time-resolved optical absorption spectroscopy techniques have been used to study Ba, Ba<sup>+</sup> and YO absorptions in the laser-produced plasma plume from a YBCO target. This provides quantitative information on the spatial and temporal behaviour of the plume. Results obtained indicate an initial explosive removal of material from the target surface followed by a subsequent diffusion-controlled evaporation process. Some YO is ejected from the target in molecular form, particularly at laser fluence < 6J/cm<sup>2</sup>, whilst additional YO is formed in subsequent reaction of Y with oxygen at the plasma plume edges. The formation of metastable Ba<sup>+</sup> (5<sup>2</sup>D<sub>5/2</sub>) is also observed in the outer reactive layers of the plasma plume.

**PB-11** Time and space resolved optical emission and electron energy distribution function measurements in rf plasmas, W G GRAHAM<sup>1</sup>, C A ANDERSON<sup>2</sup> and K R STALDER<sup>3</sup>, <sup>1</sup>Queen's University, Belfast BT7 1NN, N Ireland, <sup>2</sup>University of Ulster, Coleraine BT52 1SA, N Ireland, <sup>3</sup>SRI International, Menlo Park, CA 94025, USA - There is currently much interest in the mechanisms which generate and sustain rf glow discharges both for intrinsic reasons and because of their technological applications. Observation of the optical emission from the discharge is often used for diagnostic and process control purposes. While this technique is nonintrusive it is difficult to interpret since the emission intensity depends not only on the radiating species density but also on the density and energy distribution of the exciting electrons. These latter parameters can be measured using a suitable Langmuir probe technique<sup>1</sup>.

We have measured the spatial variation of both the optical emission and the plasma parameters in a parallel plate discharge capacitively driven at frequencies from 100 to 400 kHz. The measurements were made at specific times during the rf cycles<sup>1</sup>. The electron energy distribution function show changes in shape as the electrodes are approached. Optical emission can be interpreted in terms of these changes.

1 C A Anderson, W G Graham and M B Hopkins, Appl Phys Lett 52, 783 (1988).

**PB-12** Elementary processes in He-N<sub>2</sub> RF pulsed discharges. S. DE BENEDICTIS, G. DILECCE AND M. SIMEK(++), Centro Studio Chimica Plasmi CNR Bari Italy - Continuous and pulsed rf discharges have been investigated in a parallel plate reactor fed with He-N<sub>2</sub> mixture. Since He and N<sub>2</sub> have metastable states at very different energy thresholds both the bulk and the tail of eedf could be affected by superelastic collisions if they predominate with respect to the physics of the discharge. Langmuir probe, Optical Emission Spectroscopy as well as LIF techniques have been used to monitor the decay of eedf as well as that of the electronically excited states of He, N<sub>2</sub>(A, B, C) and N<sub>2</sub><sup>+</sup>(B) as the pressure and composition of mixture are varied. The experiments performed under conditions typically used for testing devices dedicated to plasma technology does not seem to evidence during the discharge regime effects due to superelastic collisions while the post discharge regime results to be very rich of kinetic couplings. The results of the measurements are discussed on the basis of relaxation processes.

Work supported by P.F. on Electrooptical Technologies (CNR)

(++) P.A. Inst. of Plasma Physics Czechoslovak Ac. of Science Prague.



**PC-1**

Glow Voltage Reduction By Gas Kinetics Engineering In Atmospheric Pressure Pulsed Glow Discharges For Pulsed Power Switches, W. M. MOENY, J. M. ELIZONDO, A. E. RODRIGUEZ, and M. G. WHITE Tetra Corporation, Albuquerque, NM— A major difficulty with using atmospheric pressure self sustained glow discharges for switching applications has been the high switch loss due to high glow voltage. Typically the glow voltage on a self sustained discharge is 70 to 90 percent of the breakdown voltage. This paper describes modeling, analysis, and experiments that have resulted in a development of self sustained glow discharge gas mixtures with high breakdown voltage and low glow voltage. Gas mixtures have been developed where the breakdown voltage is six times the glow voltage. This development was achieved through "engineering" the gas mixtures to control the power flow through the excited states into processes that provide excited state ionization. Experimental results of switch experiments achieving breakdown voltages of 16 kV/cm and glow voltages of 2.7 kV/cm will be shown.

\*This work was supported by SDI and monitored by DNA.

**PC-2** Ionization Coefficients and Sparking Potentials in Ternary Mixtures of SF<sub>6</sub>-CCl<sub>2</sub>F<sub>2</sub>-N<sub>2</sub> and SF<sub>6</sub>-CCl<sub>2</sub>F<sub>2</sub>-CO<sub>2</sub>  
G.R.VENKATESHAIAH and M.S.NAIDU, Indian Institute of Science, Inida— Ionization and attachment coefficients ( $\alpha, \eta$ ) have been measured and the critical E/P (at  $\alpha = \eta$ ) are evaluated from the steady-state Townsend current growth curves in the ternary mixtures over the range of  $100 \leq E/P \leq 240 \text{ Vcm}^{-1} \text{ Torr}^{-1}$  in 22 suitably selected gas mixtures in which each component gas concentration was varied from 0% to 80%. Breakdown voltage were also measured in a few selected mixtures of practical importance with 60% N<sub>2</sub> and 60% CO<sub>2</sub>. The results exhibit a characteristic non-linearity with the increase in the concentration of CCl<sub>2</sub>F<sub>2</sub>. The degree of non-linearity decreases with increasing N<sub>2</sub>/CO<sub>2</sub> concentration. Gas mixtures containing 10% SF<sub>6</sub>, 50% - 70% CCl<sub>2</sub>F<sub>2</sub> and the rest N<sub>2</sub>/CO<sub>2</sub> appear to constitute an optimum mixture for use in practical devices. Most of the results constitute first of their kind and no comparison has been made.

**PC-3** Time-Dependent Boltzmann Analysis of Relaxation of Kinetic Coefficients in Air,\*

A. E. Rodriguez, Tetra Corporation 3701 Hawkins St. NE, Albuquerque, NM 87109—We have used numerical solutions to the time-dependent Boltzmann equation to characterize the relaxation of non-equilibrium transport and kinetic coefficients in dry air. Time steps follow a geometric progression until a steady-state is achieved; then the E/N value is changed, simulating a stair-step E vs time function. At each time step, we calculate the instantaneous non-equilibrium transport and kinetic coefficients. It is often assumed that the non-equilibrium coefficients can be approximated by interpolating equilibrium coefficient vs mean energy curves. Our plots of non-equilibrium coefficients vs mean energy for E/N up-steps compared to down-steps show that the coefficients relax faster than mean energy does. An alternative methodology is discussed, based on a characteristic relaxation time independent of energy relaxation.

\* Work supported by Harry Diamond Labs

**PC-4**

Non-Equilibrium Electron Transport in Dry Air\* A.  
E. Rodríguez Tetra Corporation 3701 Hawkins NE Albuquerque, New Mexico 87109—We examine the non-equilibrium behavior of an electron fluid subjected to an E-field step-function. Integration of the momentum conservation equation yields electron velocity vs time. The solutions show a peculiar overshoot of the equilibrium value, and a relaxation toward it from the high side. This is interpreted as a relaxation toward a sliding quasi-equilibrium given by the ratio of the driving force and the friction-like collision term. The error in an equilibrium treatment is shown to produce a charge-separation error corresponding to a space-charge field error comparable to the total E-field. A similar order-of-magnitude analysis of electron multiplication (Townsend avalanche) shows that non-equilibrium effects are probably negligible.

\*Work supported by Harry Diamond Labs

**PC-5** The Effect of Water Vapour on Impulse Breakdown of Air,\* J.DUTTON, A.J.DAVIES, M. MATALLAH, Department of Physics, U.Wales,Swansea,UK, and R.T.WATERS, ELSYM, U.Wales,Cardiff,UK.-Measurements, under strictly-controlled conditions in a large sealed ionization chamber, have been made on discharges developing in humid air under positive impulse voltages in 20cm-long sphere-plane (sp) and rod-plane (rp) gaps, for a range of pressures from 600 to 900 torr at 32 C and water vapour concentrations between 2.5 and 30g m<sup>-3</sup>. The variation of breakdown voltage with humidity indicated that a humidity correction factor of +1% per g m<sup>-3</sup> relative to the value at 11g m<sup>-3</sup> was appropriate for both geometries. These results agree with the new IEC Standards for the rp configuration but are slightly higher for the sp system. The influence of water vapour on space-charge development and streamer propagation was also studied by measuring the field distribution and the conducted charge at each electrode, together with the light emission from the discharge. The results show a one-to-one correspondence between the injected charge and breakdown voltage and are explained in terms of negative-ion clustering and electron attachment/detachment reactions.

\*Work supported by the UK Science and Engineering Research Council and National Grid PLC.

**PC-6** Interaction of Microwaves with Gaseous Plasmas Formed by Abrupt Laser-Induced Ionization\*, P.R.BOLTON and J.E.SWAIN, LLNL.- We have investigated microwave characteristics of plasmas produced by laser-induced ionization with intense, short pulse. Localized critical electron densities can be reached within time intervals shorter than microwave periods. Focusing pulse energy into a section of 'S'band waveguide containing air at atmospheric density facilitated our study of microwave interactions without limitations imposed by window requirements. We noted the rapid onset of significant microwave reflectivity from the plasma. However, in the absence of any probe the laser plasma itself is a significant microwave source. For a 120 picosecond FWHM, pulse energies above 800 mJoules produced observable microwave power corresponding to peak fields of a few V/cm for ultra-short durations representing only 2 or 3 cycles. Results using a 1064 nm wavelength will be presented for laser pulse energies up to 2 Joules, (focussed intensities up to 10<sup>14</sup> W/cm<sup>2</sup>). This work has general application to pulsed power generation and to related pulse compression using rapid cavity switching. \* This work was performed under the auspices of the U.S. Department of Energy by the Lawrence Livermore National Laboratory under contract number W-7405-ENG-48

**PC-7** Cathode Heating Mechanisms in Hollow Cathode Pseudospark Thyratrons. Timothy J. Sommerer, Hoyoung Pak and Mark J. Kushner, University of Illinois, Department of Electrical and Computer Engineering, Urbana, IL 61801

\* - Pseudospark thyratrons are presently being developed as low pressure plasma switches due to their high cathode current densities and small size. Current densities in excess of  $10 \text{ kA-cm}^{-2}$  are obtained from a small area of the cathode which melts during the current pulse. It has been hypothesized that electric field enhanced thermionic emission is responsible. We have developed a computer model to assess cathode heating during commutation to investigate the onset of thermionic emission. The 2-dimensional model includes transport equations for charged species, solution of Poisson's equation and an integral sheath model. We track the power flux due to ion bombardment as a function of position on the cathode to determine its rate of heating. We find that the power flux to the cathode is insufficient for melting unless the current is distributed in a filamentary fashion, as opposed to microscopically uniform, or that the cathode displays film-like thermal conductivities.

\* Work supported by SDIO/IST through ONR, and NSF

**PC-8** Glow Discharge Opening and Closing Plasma Switch Scheme. J.J.ROCCA, F.GONZALEZ and K.FLOYD. Colorado State University.---A plasma switch based on shifting a hollow cathode glow discharge (HCD) from the low impedance mode to the high impedance electron beam mode by means of a magnetic field has been investigated at Old Dominion University (1). Current modulation was observed applying a field of up to  $H=1$  Tesla. Herein we describe a plasma switch scheme in which the current in a cold cathode glow discharge is turned off and on following the application or interruption of a small (0.01 Tesla) magnetic field. In this scheme the field quenches the oscillation of the beam electrons in a low pressure HCD, decreasing the ionization efficiency by approximately the ratio between the reaching distance of the beam electrons to the cathode-anode distance, and opening the discharge. Virtually total current interruption of a dc He discharge was demonstrated during the time a pulsed H field was applied to a HCD of rectangular cross section having a pair of parallel planar cathodes perpendicular to a pair of parallel plate anodes. Discharge configurations in which the switch is normally open or normally closed for  $H=0$  can be implemented.

1. Mai T. Nyo, K.H. Schoenbach, G.A. Gerdin and J.A.H. Lee. IEEE Trans. Plasma Science, 18, 669, 1990.

**PC-9** Kinetic Model of a Thermionic Direct Energy Converter. W.N.G. Hitchon, J.E. Lawler and G.J. Parker, University of Wisconsin-Madison, J.B. McVey, Rasor Associates, Sunnyvale, CA. Thermionic direct energy conversion in a very high density Cesium plasma is not adequately described by approximate methods, so a kinetic description using a "Convective Scheme" (CS)<sup>1</sup> has been developed. The time-scales of the system vary over a huge range, from the plasma period  $T_p \sim 10^{-12}$  s to ion loss times  $\tau_i \sim 10^{-5}$  s.

An implicit scheme allows the integration step to be increased beyond the plasma period, however, and techniques have been developed to allow the behavior on a relatively short time-scale to be extrapolated to the ion time-scale. V-I characteristics of the energy converter will be discussed.

<sup>1</sup> T.J. Sommerer, W.N.G. Hitchon and J.E. Lawler, Phys. Rev. Lett. 63, (1989)2361.

**PD-1** Experimental study of magnetoplasmas sustained by electromagnetic guided waves at or close to electron cyclotron resonance (ECR), J. MARGOT, M. MOISAN and R. GRENIER, U. de Montréal - This communication reports experimental results on a new kind of ECR-type plasma, that is sustained by the propagation of electromagnetic guided waves (surface wave modified by the presence of a static, longitudinal magnetic field  $B_0$ ). The experiments are performed in a large cylindrical plasma vessel (30 cm i.d., 300 cm long). Operation at two different frequencies (2450 and 600 MHz) and at low gas pressure (argon 0.5 - 4 mTorr) shows the possibility of achieving wave mode selection ( $m = 0$ ,  $|m| = 1$  where  $m$  is the azimuthal wavenumber) as well as an excellent wave-plasma coupling. The plasma produced is stable and perfectly reproducible. By using electrostatic probes, we measure plasma characteristics (density and electron temperature or electron energy distribution function) and examine the influence of the wave frequency and of the wave mode electric field configuration on the spatial distribution of the plasma density and electron energy as well as on the power balance of the discharge.

**PD-2** Contamination by Sputtering in Mirror Field Electron Cyclotron Resonance Microwave Ion Plasma.\* S. M. Gorbatiuk and L.A. Berry, Oak Ridge National Laboratory-Langmuir probe measurements, visual observation, and Rutherford backscattering spectrometry (RBS) have been used to investigate source chamber sputtering for electron cyclotron resonance (ECR) plasma systems operated with Ar, N<sub>2</sub>, and Cl<sub>2</sub>. Potentials in the source  $>20\text{eV}$  combined with high plasma densities ( $>10^{12}\text{cm}^{-3}$ ) led to source chamber sputtering and coating of the microwave entrance window. During Ar operation, the microwave entrance window coating caused significant absorption of incident microwave power and decreased source efficiency by as much as 40% in  $<5$  min. The contamination levels found on samples placed downstream of the plasma source were consistent with (Fe+Ni) fluxes up to  $3.8 \times 10^{11}\text{cm}^2\text{sec}^{-1}$ . Cl<sub>2</sub> operation did not result in microwave entrance window coating, however surface contamination from sputtering was detected.

Operation of the source with an anodized aluminum liner was effective in reducing microwave entrance window coating but resulted in some heavy metal contamination due to sputtering of impurities in the liner itself. Also, checks with secondary ion mass spectrometry (SIMS) indicated some Al contamination from sputtering of the anodized aluminum liner material. Finally, a technique for in situ cleaning of the microwave entrance window was developed and expedited source contamination studies.

\*Research sponsored by the Division of Materials Sciences, U.S. Department of Energy under contract DE-AC05-84OR21400 with Martin Marietta Energy Systems, Inc. and with SEMATECH.

**PD-3** An Improved Spiral Loop Antenna for Inductively Coupled Plasma Sources, <sup>1</sup> T. INTRATOR, J. MENARD and N. HERSHKOWITZ, Dep't Nuclear Engin. and Engin. Physics, Univ. of Wisconsin

We have developed and characterized a metal enamel coated spiral loop antenna that is useful as an inductively coupled plasma source. It has enhanced plasma confinement due to multi-dipole magnetic cusp fields on the boundary, and is very efficient. Operation is possible at low neutral pressures, with various working gases such as Ar, He, N<sub>2</sub> discharges at ( $P_0 > 6 \times 10^{-5} \text{ Torr}$ ), with a range of background magnetic field from 0 - 150 Gauss. The hardware and a wideband tunable matching network will be described. In order to learn how to optimize the source uniformity for plasma processing applications, we are trying to isolate the various features, such as gas choice, line cusp confinement, RF frequency, etc. Data for different working gases, magnetic line cusp configurations, and background magnetic fields will be shown.

<sup>1</sup>supported by NSF Grant ECD-8721545

**PD-4** Experimental Characterization of a Chlorine Helicon Plasma, TOSHIKI NAKANO\*, NADER SADEGHI#, DENNIS J. TREVOR, RICHARD A. GOTTSCHO, R. W. BOSWELL@, J. MARGOT-CHAKER%, and A. PERRY@, AT&T Bell Laboratories - Radio frequency excited helicon plasmas show promise for processing of electronic and photonic materials because of their high density and low plasma potential. In this work, we use Doppler-shifted laser-induced fluorescence to measure metastable ion velocity distribution functions, microwave interferometry to measure electron density, and Langmuir probes to estimate ion current density. Measurements are made both in the source and downstream as a function of magnetic field, power, and pressure. In addition, the effect of a wafer platen downstream from the source on the ion transport is investigated and compared to our recent measurements on a similar ECR reactor.<sup>1</sup>

\* National Defense Academy, Yokosuka, Japan

# Universite Joseph Fourier and CNRS, Grenoble, France

@ Australian National University, Canberra, Australia

% University of Montreal

<sup>1</sup> N. Sadeghi, T. Nakano, D. J. Trevor, and R. A. Gottscho, J. Appl. Phys. (in press).

**PD-5** Simple and Inexpensive Microwave Plasma Assisted CVD Facility,\* M. A. BREWER, I. G. BROWN, M. R. DICKINSON, J. E. GALVIN, R. A. MACGILL and M. C. SALVADORI, Lawrence Berkeley Laboratory, U. of California, Berkeley, CA 94720 - A simple and inexpensive microwave plasma assisted CVD facility has been developed and used for synthesis of diamond thin films. The system is similar to those developed by others but includes several unique features that make it particularly economical and safe, yet capable of producing high quality diamond films. A 2.45 GHz magnetron from a commercial microwave oven is used as the microwave power source. A conventional mixture of 0.5% methane in hydrogen is ionized in a bell jar reaction chamber located within a simple microwave cavity. By using a small hydrogen reservoir adjacent to the gas supply, an empty hydrogen tank can be replaced without interrupting film synthesis or causing any drift in plasma characteristics. Hence, films can be grown continuously while storing only a 24-hour supply of explosive gases. System interlocks provide safe start-up and shut-down, and allow unsupervised operation. Here we describe the electrical, microwave and mechanical aspects of the system, and summarize the performance of the facility as used to reproducibly synthesize high quality diamond thin films.

\*Supported by U.S. D.O.E. under contract number ACO3 76SF-00098.

**PD-6** A Recirculating Coronal Discharge System for Air Cleaning\*, G. E. VOGTLIN, W. W. HOFER, B. M. PENETRANTE and J. N. BARDSLEY, Lawrence Livermore National Laboratory - A recirculating gas cleaning system has been constructed incorporating a pulsed plasma reactor in coaxial cylinder geometry, with a wire of diameter 1.59mm inside a stainless steel cylinder of inner radius 20.6mm. Positive corona are formed by the application of pulses of up to 45 kV with rise times of 10-20 ns, pulse lengths of 50-200 ns and peak currents up to 500 A. Higher voltages lead to premature arc formation. Flow rates of up to 2 liters per second can be achieved in the 4.6 liter gas system, and filters are included to remove the acids formed from the pollutant molecules. First tests of the system using NO at initial levels around 100 ppm show that 99% destruction can be achieved with approximately 250 pulses. No NO removal is seen if the air is replaced by dry nitrogen, showing the crucial role of radicals produced from O<sub>2</sub> and/or H<sub>2</sub>O. Further experiments are underway to determine the dependence of the process efficiency on the electrical characteristics, and on the humidity level of the air, and to check the predictions of discharge simulations described elsewhere at this meeting.

\*Work performed under the auspices of the U. S. Department of Energy under Contract No. W-7405-ENG-48.



**PD-7** **Multidipole-RF Electrode Experiments<sup>a</sup>**, R. Breun, C. Lai, N. Hershkowitz, A. Wendt, C. Woods University of Wisconsin - Madison. Multidipole systems allow one to use localized electron energy sources to create a large uniform plasma at low neutral density. In order to effectively use this system as a plasma etching device, we initiated studies in a bell jar system with a single planar RF powered electrode inserted at one end of the 'magnetic bucket'. We found that the powered electrode must be designed properly or impurity(metal) deposition occurs along with photo-resist reticulation and reduced etching. It has become clear that optimization requires an adequate global model of the sheath dynamics, gas flow, impurity generation as well as the effects of localized plasma sources. As we formulate this model we are designing a new configuration. We plan to test salient features of the model in the present configuration and as confidence increases build the new configuration. We will present our model and our latest design.

---

<sup>a</sup>Supported by U.S. NSF Grant ECD-8721545.

**SESSION QA**

8:00 AM - 10:00 AM, Friday, October 25

Ballroom A

**IONIZED GAS PHYSICS IN PULSED POWER**

Chair: W. M. Moeny, Tetra Corporation

**QA-1 MODELING A KrF LASER-TRIGGERED SF<sub>6</sub> SPARK GAP,\*** A. E. RODRIGUEZ, Tetra Corporation Albuquerque, New Mexico — We have modeled a KrF laser-triggered SF<sub>6</sub> spark gap at various levels of detail. A one-dimensional model of the laser-SF<sub>6</sub> interaction includes the focused beam geometry, the laser pulse shape, nonlinear absorption of the laser, and multi-photon interactions with the SF<sub>6</sub> and trace hydrocarbons. The dominant ionization mechanism is 2-photon excitation followed by 2-photon ionization. This model is incorporated in a one-dimensional model of the Formation and Propagation Streamers (FPS), which shows how streamers propagate from the laser-generated spark. Finally, a zero-dimensional analysis of the local kinetics at a critical point along the laser path showed that the laser not only triggers a streamer, but its photodetachment sustains the discharge which would otherwise be quenched by the strong attachment in SF<sub>6</sub>.

\* Work supported by Sandia National Laboratories.

**QA-2 Magnetic Control of Hollow Cathode Discharges\***, K.H. SCHOENBACH, G.A. GERDIN, T. TESSNOW, J. PIEKAREK and R. JOSHI, Physical Electronics Research Institute, ODU, Norfolk, VA - The results of electrical and optical measurements on pulsed hollow cathode discharges indicate that their low resistance compared to glow discharges between plane parallel electrodes is due to enhanced secondary ionization by electrons which oscillate between opposite walls of the hollow cathode ("pendel" electrons). Calculations of the electron kinetics in cylindrical hollow cathode discharges by means of a Monte-Carlo code showed that the application of axial magnetic fields causes a drastic reduction of the electron density on the axis of the discharge, an effect which was used to modulate the resistance of a hollow cathode discharge in He. Most recently switching out of the hollow cathode mode into a low current glow mode was achieved with magnetic field intensities of less than 100 G (1). The possibility to operate hollow cathode discharge switches in parallel permits the use of arrays of such discharges as magnetically controlled pulsed power modulators and opening switches.

\*Work supported by SDIO/IST and managed by ONR.

(1) J. Rocca, CSU, Ft. Collins, CO, private communication.

**QA-3** Hollow and Super-emissive Cathode Processes in the Pseudospark and Back-lighted Thyatron, M. A. GUNDERSEN, G. KIRKMAN\*, and W. HARTMANN†, Univ. of Southern California, Los Angeles, CA, - The pseudospark and the closely-related back-lighted thyatron conduct high current and have additional properties that are useful for pulsed power switching and the production of uniform, high density plasmas. These properties are related to the cathode emission processes of these devices. These processes occur in several phases, including a hollow cathode phase, and a super-emissive phase. The distinction between these processes will be reviewed. Several new applications, including electron beam generation and plasma lenses for linear colliders, will be discussed.

\*now with Integrated Applied Physics, Waltham, MA

†now with Siemens, Erlangen, Germany

**QA-4** The Tacitron. A Low Noise Thyatron Capable of Current Interruption by Grid Action\*...40 Years Later G. MCDUFF, T. R. BURKES, and V. KAIBESHEV. PPE and IAE - After World War II the group of researchers E.O. Johnson, W. M. Webster, J. Olmstead, and L. Malter at the RCA Laboratories in Princeton, New Jersey began a comprehensive investigation into the operation of gas discharge devices. Great interest in inverters that operated off of 28 VDC for airborne power conditioning application spawned a multiyear research effort into low voltage gas discharge tube with extremely low conduction drop for high efficiencies. During this time, many new characteristics of gas discharge devices were discovered. One, that under certain conditions, the current in a thyatron type discharge could be interrupted by grid control. This device was named the tacitron. By the mid to late 50's, solid state devices began to appear and emphasis was directed toward this technology and gas discharge tubes became "old stuff". In Europe, researchers diligently continued working on developing this technology. This paper summarizes the development of the tacitron from its origin in the US, development in Europe from 1960 till present, and the current state-of-the-art in commercial tacitron technology in the USSR.

\*Taken from Proceedings of the IRE September 1954

**SESSION QB**

8:00 AM - 10:00 AM, Friday, October 25

Ballroom B

**GLOWS II**

Chair: M. Lieberman, University of California - Berkeley

**QB-1** A Plasma Kinetics and Surface Deposition Model for the Deposition of SiO<sub>2</sub> from O<sub>2</sub>/TEOS rf Discharges.

Mark J. Kushner, Phillip J. Stout and Timothy J. Sommerer, University of Illinois, Department of Electrical and Computer Engineering, Urbana, IL 61801 \*  
 - TEOS (tetraethoxysilane) is an attractive source gas for SiO<sub>2</sub> deposition compared to SiH<sub>4</sub> due to safety considerations and the highly conformal films which can be obtained. We have developed a plasma kinetics and surface deposition model to investigate the plasma decomposition of TEOS in rf discharges, and the manner in which TEOS fragments are incorporated in the film. The model consists of a self consistent Monte Carlo -fluid hybrid model for plasma transport coupled to a 2-dimensional plasma chemistry model. Fluxes from plasma chemistry model are used as input to a surface kinetics model. The decomposition of TEOS into Si(C<sub>2</sub>H<sub>5</sub>O)<sub>x</sub>(OH)<sub>4-x</sub> complexes, believed to be the deposition precursor, is thought to proceed by O atom oxidation. The rate coefficients for this process are derived based on the observed deposition rates. We also predict that large fluxes of hydrocarbon species and may contribute to carbon contamination of the films.

\* Work supported by IBM E. Fishkill and NSF.

**QB-2** Nonequilibrium Plasma Destruction of Hazardous Organic Compounds Using Silent Electrical Discharges, L.A.

ROSOCHA AND W.H. MCCULLA, University of California, Los Alamos National Laboratory - Nonequilibrium plasmas created by silent (dielectric barrier) electrical discharges can efficiently create copious quantities of reactive free radicals in gases from the dissociation of molecular oxygen by energetic electrons in the discharge. With some water present, the primary radicals are O(<sup>3</sup>P) and OH. This process provides a viable alternative to incineration of toxic materials because it allows effective channeling of electrical energy into chemical processes through electrons rather than increasing the enthalpy of the waste stream. We are engaged in research to develop this silent discharge plasma (SDP) process as an effective means of destroying hazardous organic compounds, particularly halogenated and non-halogenated hydrocarbons in gaseous media. An overview of the process, discussion of representative plasma chemistry, a description of apparatus, data on the destruction of selected compounds, and relationships to other key efforts at Auburn University and the University of Illinois will be presented.

**QB-3** Modeling and Simulation of Plasma Enhanced Chemical Vapor Deposition, \* M. MAZHAR ISLAMRAJA, C. CHANG, J.P. MCVITTIE, M.C. CAPPELLI and K.C. SARASWAT, Stanford University- An analytical model has been developed to simulate profile evolution during plasma enhanced chemical vapor deposition (PECVD). The model takes into account adsorption and re-emission at the surface and a spatially varying reaction probability (sticking coefficient). The reaction probability of the rate limiting species is found to be a function of the incident ion energy. The ions, being very energetic, break surface bonds upon impingement, thus creating more reaction sites. This leads to higher reaction rates of the rate limiting species at places of ion bombardment, leading to higher deposition rates at these places. The simulated results are compared to experimental profile evolution in trenches and test structures of varying geometries for plasma enhanced chemical vapor deposition of silicon dioxide and silicon nitride used for passivation in semiconductor devices.

\* This work was supported by SRC and DARPA

**QB-4** Optimization of Deposition Fluxes in Remote Plasma Enhanced Chemical Vapor Deposition, Mark J. Kushner, University of Illinois, Department of Electrical and Computer Engineering, Urbana, IL 61801 \* - Remote Plasma Enhanced Chemical Vapor Deposition (RPECVD) is a method whereby thin films may be deposited with the substrate located outside of the plasma zone. This allows a higher degree of control of the flux of radicals incident onto the substrate than in conventional PECVD where the substrate is immersed in the plasma. A computer model for the RPECVD of silicon alloys has been developed to investigate methods to selectively optimize the flux of radicals to the substrate during deposition of a-Si:H,  $\mu\text{c-Si}$  and  $\text{Si}_3\text{N}_4$ , and results from that study will be presented. In most cases, the mixing of gases in the reactor makes it difficult to prevent generation of undesirable deposition precursors, however isolating the substrate far downstream allows many of the species to react away before striking the substrate. Conditions optimizing the production of  $\text{SiH}_x(\text{NH}_2)_{4-x}$  complexes, believed to be the precursor for deposition of  $\text{Si}_3\text{N}_4$ , will be discussed.

\* Work supported by Semiconductor Research Corporation and the National Science Foundation.

**QB-5** Chemistry and Kinetics of Plasma Deposition of SiO<sub>2</sub> films from TEOS and mixtures of TEOS with O<sub>2</sub> and rare gases, C. CHARLES, P.GARCIA and Y.CATHERINE, Institut des matériaux de Nantes / CNRS, LPCM, Nantes, FRANCE.

Interlayer dielectrics used in advanced semiconductor devices must have good electrical properties, fill narrow spaces without voids and present good step coverage. A organic silicon compound is used as silicon source for deposition of SiO<sub>2</sub> films in a conventional planar rf plasma reactor: tetraethoxysilane (TEOS, Si(OC<sub>2</sub>H<sub>5</sub>)<sub>4</sub>) is non-explosive, non-toxic and presents a high surface mobility. Thence no special safety installation is required as it is the case with silane.

The plasma chemistry is studied by quadrupole mass spectrometry and the properties of the SiO<sub>2</sub> deposited films are obtained by ellipsometry, FTIR and MEB methods. Results on deposition kinetics, films properties and step coverage are presented for different mixtures of TEOS with rare gases and oxygen.

The influence of reactor configuration (gas equipment, earthed grid between electrodes) and substrate temperature is investigated.

**QB-6** Variation of Voltage, Ion Flux, and Other Plasma Properties as a Function of Pressure and Power in a Confined Argon Discharge, J. LIU and H.H. SAWIN, M.I.T. -- Plasma properties have been measured in a confined, geometrically symmetric, argon discharge. The properties measured include voltage, current, power, ion flux, ion energy, and sheath width. Power is calculated using the stray impedance de-embedding technique reported by Butterbaugh *et al.*<sup>1</sup> and measured voltage and current waveforms. The ion flux and ion energy was measured using the apparatus detailed in a previous paper<sup>2</sup>. The sheath width was determined using spatial and temporal scans of the 7506Å emission line. Argon pressure used range from 0.2 Torr to 1.0 Torr. Electrode separation was kept constant at 1 inch, while electrode diameter varied from 3" to 6".

1. J.W.Butterbaugh, L.D.Baston, and H.H.Sawin, J.Vac.Sci.Technol. A8, 916 (1990).

2. J.Liu, G.L.Huppert, and H.H.Sawin, J.Appl.Phys. 68, 3916 (1990).



**QB-7** A Study of Collisions in the Cathode Fall of Glow Discharges from a numerical solution of the Boltzmann equation for Electrons. S. SHANKAR, U of Minnesota and MSI and K.F.JENSEN, Massachusetts Institute of Technology - We have studied the collisional frequencies and mean free paths for various gas pressures (1 MTorr-1Torr) in a glow discharge and have observed the change of behavior of electrons from a *particle-like behavior to fluid-like behavior*. We have been able to describe the discharge in terms of the various *characteristic length* and *time* scales which are inherently present in the plasma. The Boltzmann equation simulation has allowed us to study the range of applicability of other models that are used study glow discharges such as *fluid flow models* and *spherical harmonic approximations*. We have observed that the distribution function does not follow any proposed functions. We have evaluated the coefficients of the spherical harmonic series for the electron distribution function (EDF) and found that it is necessary to include more than two terms to accurately represent the EDF.

**QB-8** Toroidal Discharges in Superimposed Electrical and Magnetic Fields. S. POPOVIC, E. KUNHARDT, J. BENTSON, S. BARONE, Weber Research Institute, Polytechnic University, - The results of the study of a series of DC discharges around a charged spherical anode in the presence of axial magnetic field are presented. The discharges were generated at conditions where the background ( $p_0 = 10^{-6} - 10^{-2}$ Torr) was lower than the magnetic "pressure". The analysis of electron motion in this field distribution shows that there is a region of initial conditions which lead to chaotic behavior. This has direct consequences on the avalanche process and the structures of the discharges which are found to be toroidal in shape. Transitions between the discharge modes are marked by sharp cascades in volt-ampere characteristics. The relation of these phenomena to the density distribution of the trapped space-charge around the anode is discussed. The results are applied to the case of a charged body surrounded by the ionospheric plasma and by an induced discharge in the space environment.

\*Work supported by SDIO/IST.

**SESSION RA**

10:15 AM - 12:15 PM, Friday, October 25

Ballroom A

**LASERS & SWITCHING**

Chair: C. Young, Tetra Corporation

**RA-1** Characterization of the Fission-Fragment Excited Helium/Argon Laser at 1.79  $\mu\text{m}$ ,\* G. A. HEBNER and G. N. HAYS, Sandia National Laboratories--Characteristics of the fission-fragment excited helium/argon laser operating on the 1.79  $\mu\text{m}$  ( $3d[1/2]_{3/2} - 4p[3/2]_{1,2}$ ) argon transition are presented. Fission-fragment excitation utilizes the highly energetic particles (70-90 MeV) created when the neutron flux from the reactor strikes the  $^{235}\text{U}$  coating on the inside of the laser cell to produce ionization and excitation in the laser gas. Laser output occurs for approximately 90 percent of the 0.9 to 3 millisecond FWHM thermal neutron pump pulse. Output power efficiency optimizes for a total gas pressure of 760 torr and argon concentration of 0.3 to 2.0 percent. Power efficiency was 1.6 percent for instantaneous pump rates of 45 to 230  $\text{W}/\text{cm}^3$ . The small signal gain and saturation intensity for instantaneous pump rates of 30 to 90  $\text{W}/\text{cm}^3$  are 0.55 to 1.05  $\%/ \text{cm}$  and 70 to 110  $\text{W}/\text{cm}^2$  respectively. The laser threshold as a function of helium pressure and argon concentration will be presented. The advantages of fission-fragment excitation over electron beam excitation in predominantly helium gas mixtures will be discussed.

\*This work was performed at Sandia National Laboratories and supported by the U.S. Department of Energy under DE-AC04-76DP00789.

**RA-2** Long Pulse (100  $\mu\text{s}$ ) Ar-Xe Laser Pumped by an Electron-beam-controlled discharge\*, T.T. Perkins and J.H. Jacob, Science Research Laboratory, Inc. - The output power and intrinsic efficiency of a 1.73  $\mu\text{m}$  Ar-Xe laser pumped by an electron-beam-controlled discharge have been measured. A 200 keV electron beam generated by a thermionic cathode was used to create uniform ionization in a 5.5 X 40 X 2.5  $\text{cm}^3$  volume for the full duration of the discharge pulse. A lumped-element transmission line, matched to the 0.1  $\Omega$  discharge impedance, generated rectangular pump pulses with durations of 25, 50 or 100  $\mu\text{s}$ . Power deposition into the discharge was varied from 100 to 1000  $\text{W}\text{-cm}^{-3}$ . Stable operation of the discharge was observed for a 100  $\mu\text{s}$  pulse. Intrinsic efficiencies of greater than 2% have been measured.

\*This work was sponsored by the Army/SDIO under contract #DASG60-89-C-0073.

**RA-3** Modeling of the Microwave and Discharge Excited Atomic Xe Laser. Jong W. Shon and Mark J. Kushner, University of Illinois, Department of Electrical and Computer Engineering, Urbana, IL 61801 \* - The high pressure ( $\geq 0.5$  atm) atomic Xe laser oscillates on at least 5 infrared transitions ( $1.73 \mu\text{m} - 3.51 \mu\text{m}$ ), and operates at high intrinsic efficiencies ( $\leq 5\%$ ) using a variety of excitation sources. Recently pulsed electric discharge and microwave excitation has been experimentally investigated<sup>1,2</sup>. We have developed computer models of those lasers to study scaling of the laser at high pump rates and energy deposition. A new modeling technique was developed which extends the use of the local field approximation for high pressure discharges to conditions where zero-crossings in the electric field occur. We find that microwave excitation is nearly equivalent to particle beam excitation when compared on the basis of power deposition, and exhibits similar high gas temperature effects. Pumping the Xe laser using a TEA discharge optimizes at lower Xe concentrations than using microwave or particle beam excitation.

\* Work supported by Sandia National Laboratory

<sup>1</sup> G. Hebner, 43rd Gas. Electr. Conf., Paper D-2, 1990.

<sup>2</sup> K. Komatsu, et al., J. Quant. Elect. 27, 90 (1991)

**RA-4** Visible Recombination Laser Using Electron Beam Pumping\*, R.L. RHOADES and J.T. VERDEYEN, U. of Illinois, Dept. of Electrical Engineering, 1406 W. Green St., Urbana, IL 61801. We have observed lasing on the 585.2 nm transition of neon in various He:Ne:Ar mixtures [1,2]. Parametric studies have shown that maximum peak power is obtained with a mix of approximately 10:2:1 and a total system pressure of 2-3 atmospheres. These experiments were performed in a coaxial diode chamber with a thin-walled aluminum anode driven by a Febetron 706 pulse-forming line. The resulting laser pulse has a duration of about 75 nsec and a peak power of nearly 5 watts. Peak gains approaching 3% per cm have been observed. Studies of other possible recombination lasers will also be reported.

[1] N.G. Basov, et al, Sov. Tech. Phys. Lett., 11(4), 181, (1985).

[2] G.A. Hebner and G.N. Hays, Appl. Phys. Lett., 57(21), 2175, (1990).

\* Work supported by Sandia National Laboratory.

**RA-5**

Modeling of a Low Pressure Cesium-Barium Discharge for Switch Applications, \* C. M. YOUNG and A. E. RODRIGUEZ, Tetra Corporation, Albuquerque, NM— We are developing a model of a low pressure Cesium-Barium discharge in order to understand the operation of a tacitron switch. The tacitron is a high temperature (1500 degrees K, nominal) switch capable of operating in a nuclear environment with very low conduction drop (volts). Our model uses a zero dimensional Boltzmann solver to generate time and field dependent transport coefficients which are then used in a fluid model to describe the motion of both the electrons and the ions in the discharge. We will describe both the physics related issues and the modeling issues. Preliminary computational results will be presented.

\*This research is funded by SDIO/IST and managed by AFWAL.

**RA-6** Simulation of Holdoff in Nonplanar Geometries and Hollow Cathode Switches. Hoyoung Pak and Mark J. Kushner, University of Illinois, Department of Electrical and Computer Engineering, University of Illinois, Urbana, IL 61801 \* - Paschen's law relates the holdoff, or breakdown, voltage between plane parallel electrodes as a function of  $pd$  (gas pressure  $\times$  electrode separation). In nonplanar geometries, Paschen's law is difficult to apply due to ambiguity in the electron path length, nonuniform electric fields and nonequilibrium of the electron swarm. We have developed a Monte Carlo simulation of electron and ion transport, and applied it to assessing low pressure holdoff in nonplanar geometries, and the hollow cathode pseudospark switch in particular. We find that holdoff decreases under conditions which allow potential penetration into the hollow cathode. We also find that for typical conditions (He, 0.1 - 2 Torr, 10s kV holdoff) the majority of electron production during holdoff is a consequence of ion impact, of which half is a result of ion impact ionization in the gas phase. Ion energies striking the cathode average many 100s eV to a few keV, with maximum values approaching the anode potential.

\* Work supported by SDIO/IST through ONR, and NSF

**RA-7** Ion Source Spectroscopy on PBFA II,\* J.E. BAILEY, A.L. CARLSON, A.B. FILUK, T. NASH, and Y. MARON, Sandia National Laboratories and Weizmann Institute of Science - Light-ion ICF experiments on the PBFA II accelerator provide a unique opportunity to investigate ion beam source physics at the anode of an applied-B ion diode. Spectroscopic observations of the anode plasma have been made in the visible; various atoms and ions, including C II, C III, C IV, and Li I have been identified. The spectral line profiles show strong broadening and shifting. A line-fitting code that accounts for Zeeman splitting, Stark shifting, and instrumental, Doppler, and Stark broadening has been used to analyze these profiles. Calculations have been done to check that the lines analyzed are optically thin. An electron density of  $\sim 2 \times 10^{23} \text{ m}^{-3}$  in the anode plasma is measured from Stark broadening of the C IV 5f-6g transition. The electric field in the accelerating gap reaches  $\sim 800 \text{ MV/m}$ , as determined from Stark shifts of Li I 2s-2p (6708 Å). This is the largest electric field ever measured with spectroscopic methods. The C IV ion temperature, as derived from deconvolved Doppler broadening, is 0.5-2.5 keV. The mechanism responsible for generating the unexpected high source temperature is under investigation. Evidence for the high temperature, and further spectroscopic results, will be presented.

\*Work supported in part by the U.S. Dept. of Energy

**RA-8** Radial Structure of Kilobar-Pressure Plasma Discharges\* S. N. KEMPKA and D. A. BENSON, Sandia National Laboratories, Albuquerque, NM, 87111. Experimental and numerical techniques are used to characterize the radial structure of plasmas (250 MPa, 5 eV) generated in a high-pressure vessel. Such plasmas have been proposed to improve control of combustion in gun ballistic cycles by possibly controlling the mixing of fuel and oxidizer. In the experiments, the plasma is generated in a capillary (0.25 cm radius) lined with polyethylene which ablates and forms a dense mixture of ionized carbon and hydrogen. Measured values of peak power dissipation and electrical current are 100 MW and 40 kA. In the pressure and temperature range of interest, the plasma is optically thick (Rosseland mean free path is 10  $\mu\text{m}$ ) which precludes the use of optical diagnostic techniques to examine the radial structure of the plasma, so a numerical model is used. The model is based on conservation of continuum mass, momentum, and energy, and assumes the radiative diffusion approximation and a classical electrical conductivity derived from electron-ion and electron-neutral collisions. Numerical results will be presented which exhibit strong radial variations in the plasma temperature and species, and match measured power and electrical current.

\*This work was performed at Sandia National Laboratories, which is operated for the U. S. Department of Energy, under contract number DE-AC04-76DP00789.

**SESSION RB**

10:15 AM - 12:15 PM, Friday, October 25

Ballroom B

**ECR & INDUCTION PLASMAS**

Chair: M. Barnes, IBM - East Fishkill

**RB-1** Electron Densities in the diffusion space of a helical resonator plasma. Peter Bletzinger, Aero Propulsion and Power Directorate, WPAFB, Ohio.--Electron densities ( $N_e$ ) were measured using a 35 GHz microwave interferometer at various distances downstream of a discharge generated by a helical resonator. The resonance frequency of the resonator was 10.4 MHz, varying slightly with power into the plasma. Gases used were argon,  $SF_6$  and  $CF_4$  at pressures from 0.01 to 0.2 Torr. In argon integrated line electron densities (LINE) ranged from  $10^{10} \text{ cm}^{-2}$  at 0.01 Torr to  $8 \cdot 10^{10} \text{ cm}^{-2}$  at 0.2 Torr and 80 Watts of input power 1" downstream of the resonator. Assuming a uniform distribution in the 2" diameter tube, this corresponds to an  $N_e$  of about  $5 \cdot 10^9$  to  $4 \cdot 10^{10} \text{ cm}^{-3}$ . In  $SF_6$  the LINE ranged from 1 to  $8 \cdot 10^9 \text{ cm}^{-2}$  at 0.1 Torr and 5 to 70 W input power to  $2 \cdot 10^{10} \text{ cm}^{-2}$  at 0.025 Torr. The variation of the LINE with pressure was opposite of that of argon. A similar trend was observed for  $CF_4$ , where the LINE ranged from  $1 \cdot 10^9$  to  $1.5 \cdot 10^{10} \text{ cm}^{-2}$  at 0.2 Torr to a maximum of  $2.5 \cdot 10^{10} \text{ cm}^{-2}$  at 0.025 Torr.

**RB-2** Microwave Impedance Matching in an E.C.R. Plasma Etch Tool. \* J.E.STEVENS, Princeton Plasma Physics Laboratory, and J.L.CECCHI, Dept. of Chemical Engineering, Princeton Univ.- Impedance matching between the microwave circuit and the plasma in an ECR plasma etch tool can be accomplished using a fixed impedance transformer where the reflected power is low enough to eliminate the need for additional matching. We use a quarter wave vacuum window to match a right hand polarized  $TE_{11}$  waveguide mode to the ECR plasma impedance. The density,  $n_e$ , and magnetic field, B, at the window and the window dielectric constant all affect the impedance match. It is often desirable to vary the window dielectric constant in order to operate over a wider range of B and  $n_e$ . Such a variation can be achieved with an additional quarter wave slab of teflon. For increasing magnetic field, matching improves when the window dielectric constant is lowered or the density is raised. The experimental results agree with a model for the plasma impedance.

\*Work supported by SRC/SEMATECH within the New Jersey SEMATECH Center of Excellence for Plasma Etching.



**RB-3** Relative Fluorine Concentrations in RF and (ECR) Microwave/RF Hybrid Glow Discharges\* J. PENDER, M. PASSOW\*\*, K. SUNG, Y. LIU, S. PANG, M. BRAKE AND M. ELTA, Univ. of Michigan- The relative concentration of atomic fluorine was measured in a CF<sub>4</sub> rf glow discharge (SEMI Group) and a modified ECR microwave/rf hybrid discharge (Wavemat microwave cavity on a SEMI Group PE/PECVD) using the actinometric technique. The dependence of fluorine concentration on RF and microwave power, pressure, flow and microwave cavity length were investigated in both the pure RF and the hybrid system. As expected the F concentration decreased with increasing CF<sub>4</sub> flow and increased with pressure in both the pure RF and hybrid systems. The F concentration also increased in both systems when powered by only RF power. When microwave power was added to the hybrid system the F concentration was enhanced by as much as a factor of 60. An anomalous behavior was observed when the RF power was varied in the hybrid system. The F concentration (i.e. the ratio of F 704 nm to Ar 750 nm) decreased with increasing RF when the microwave power was held constant. This may be due to the different excitation threshold energies of the lines. When the 703 Ar line was used, the F concentration did increase with increasing RF power. Si etch rates followed F trends.

\*Supported by SRC 90-MC-085

\*\*Current address: IBM East Fishkill, Hopewell Junction, NY

**RB-4** Depositing Thick SiO<sub>2</sub> Layers with the Helicon Diffusion Reactor, R. Boswell, A. Durandet, G. Giroult-Matlakowski and H. Persing, Plasma Research Laboratory, Research School of Physical Sciences and Engineering, The Australian National University, Canberra ACT 2601, Australia - A helicon diffusion reactor employing silane and oxygen chemistry is used to deposit thick ( $\approx 5$  microns) layers of SiO<sub>2</sub> on silicon wafers which are not externally biased nor heated. Deposition rates are roughly 40-70 nm per minute, contingent on rf power and feed gas flow rates. An *in situ* ellipsometer allows for the real time monitoring and control of film thickness and index of refraction. Data pertaining to the optical and physical characteristics of the deposited layers will also be presented.

**RB-5** A Network Model of the Helical Resonator, K. NIAZI, D. L. FLAMM, M. A. LIEBERMAN, U. C. Berkeley--- The Helical Resonator is a plasma source currently being developed for the patterning of sub-micron IC features. Preliminary studies have yielded a predictive model for understanding the dependence of the resonant frequency and power absorbed by the plasma on the device parameters.<sup>1</sup> Experimental studies of this model are complicated by the sensitivity of the power network to the state of the plasma, and to the configuration of the device as represented by the position of the power tap. To help clarify the coupling between the power source and the resonator we have modeled the power-resonator system as a transmission line network in which the resonator itself is viewed as a parallel combination of two helical transmission lines. We present results on standing wave ratio versus frequency for various plasma dissipation models and tap positions.

<sup>1</sup>M. A. Lieberman, A. J. Lichtenberg, and D. L. Flamm, Memorandum No. UCB/ERL M90/10 (1990).

**RB-6** 2D Modeling of a Low Pressure Plasma in a Non-uniform Magnetic Field, R.K.PORTEOUS and D.B.GRAVES, U.C. Berkeley - A 2D model of a cylindrically symmetric ecr argon plasma has been developed. The plasma chamber is 60 cm long and up to 30 cm in diameter. The chamber walls consist of regions which may be independently insulating, floating or biased. The magnetic field profile can be adjusted through the currents to external solenoidal coils. The ions are weakly magnetized and are modeled using a 2D3V particle-in-cell technique. The ion trajectories in the applied magnetic and self-consistent electric field are followed taking into account the charge exchange collisions with neutrals. The electrons are represented as a two-dimensional fluid with conservation equations for both mass and energy. The fluid is strongly magnetized; i.e. the transport coefficients are highly anisotropic. The ecr power input is localized to the resonance region in the source, with an assumed radial profile.

Results showing plasma density, potential, electron temperature, and ion flux profiles will be presented for different configurations of grounded and floating surfaces in the source region.

**RB-7** A WKB Approach to Electron Transport Problems.<sup>1</sup>

L. Demeio, B. Shizgal, Dept. of Chemistry, Univ. of British Columbia — This paper considers the calculation of electron transport properties in molecular gases with a WKB solution of the Boltzmann equation. The two-term approximation is adopted and elastic collisions are represented by the Fokker-Planck collision operator, while inelastic processes are described by a difference operator. We expand the difference operator to second order in the inelastic threshold energy and obtain a partial differential equation which can be transformed to Schrödinger form. The steady-state electron distribution is determined from the ground-state eigenfunction of the Schrödinger equation with the WKB approach. Electron transport properties in  $\text{CH}_4$  as well as for a model system are studied. The time-dependent approach to equilibrium is also considered.

<sup>1</sup> Research supported by a grant from the Natural Sciences and Engineering Research Council of Canada.

# **44th Annual Gaseous Electronics Conference**

## **EXHIBITOR PROGRAM**

### **Ballroom C**

1:30 PM - 5:30 PM - Wednesday, October 23

10:15 AM - 5:30 PM - Thursday, October 24

### American Institute of Physics

335 East 45th Street  
New York, NY 10017-3483  
Phone: (212) 661-9260  
Fax: (212) 661-2036  
Contact: Michael Hennelly

The American Institute of Physics will display recent AIP conference Proceedings and AIP books and journals on plasmas and related areas, including the Physics of Fluids A and B and the Soviet Journal of Plasma Physics. Copies of Physics Today and Computers in Physics will also be available.

### Balzers

46249 Warm Springs Blvd.  
Fremont, CA 94539  
Phone: (415) 651-3303  
Fax: (415) 651-0657  
Phone: (505) 892-4166 (New Mexico)  
Contact: Rick Von Vorous

Balzers is a manufacturer of high and ultra-high vacuum products. Products include turbo-molecular, cryogenic, rotary vane pumps. Standard turbopumps designed for corrosive radioactive service are available. Balzers extensive line of turbopumps come in standard, magnetically suspended and wide range with dry roughing pump versions.

Balzers has an extensive line of measurement instruments including leak detectors, magnetron gauges, and quadrupole mass spectrometers. Balzers also manufactures a plasma monitor for monitoring positive and negative ions and neutrals using a quadrupole mass spectrometer. Other unique mass spectromoter systems for CVD and etching systems, thin film sputter systems, and SIMS applications. Balzers manufactures cryostat and liquefaction systems capable of reaching 6.5 K using two stage closed cycle refrigerators.

### Chromex

2705-B Pan American NE  
Albuquerque, NM 87107  
Phone: (505) 344-6270  
Fax: (505) 344-6095

Spectral Emission Monitoring of a GEC RF Reference Cell

A demonstration of PARALLEL SPECTROSCOPY™ will show how the method can provide real-time simultaneous multi-channel spectral emission monitoring and analysis of the plasma discharge of a GEC Reference Cell. The demonstration consists of multi-channel optical fibers delivering spectral information from a source to a CHROMEX Imaging Spectrograph. The dispersed multi-channel spectra are imaged onto a two-dimensional CCD array detector with the resulting spectra being displayed simultaneously in real-time and analyzed with CHROMEX proprietary PLS multivariate software.

### Coherent Laser Group

1755 Montezuma Road  
Colorado Springs, CO 80920  
Phone: (719) 531-6656  
Fax: (719) 599-5816  
Contact: Salvatore Balsamo

Coherent Laser Group supports critical applications in the areas of scientific research and industrial testing, measuring and processing. The company manufactures the most diversified selection of lasers from a single source, including tunable-dye, ion, CW, YAG, YLF, ultrafast, and diode-pumped solid-state systems. To support customers in their work, a wide range of user-training courses and service-training courses are available. Both service engineers and applications engineers are on call to offer assistance, via toll free "800" numbers: Sales support is 1-800-527-3786, and service support is 1-800-367-7890. The company also maintains an in-stock supply of IonPure™ metal-ceramic replacement tubes for all its ion laser systems.

## COMDEL, Inc.

126 Sohler Rd.  
Beverly, MA 01915  
Phone: (508) 927-3144  
Fax: (508) 922-8205  
Contact: Ted Johnson

COMDEL offers a full line of RF delivery equipment.

CPS Series HF Solid State Power Supplies, 5-60 MHz - 200W-5KW.

CMS Series Solid State 915 MHz Power Supplies, 50-1200W.

CLF Series LF Solid State Power supplies 20KHz-450KHz - 500W-5KW.

CHS Series HF Hybrid Power Supplies - 12, 25 & 50KW.

MATCH PRO Series Automatic Matching Networks. Fast, precision tuning at all power levels.

RPM-1 Real Power Monitor: A load invariant power monitor and control tool provides unsurpassed process accuracy, repeatability and diagnostics.

WATTPAP Low Frequency Power Monitor: Measures delivered power in any impedance transmission line. 20KHz-1MHz

Custom configurations and requirements are welcomed.

COMDEL's 50 affiliates world-wide comprise the world's most experienced and responsive power conversion corporation.

## Commonwealth Scientific

500 Pendleton Street  
Alexandria, VA 22314  
Phone: (703) 548-0800  
Contact: Colin Quinn (Technical Department)

Permanent Magnet Ion sources arranging in size from 1 cm to 38 cm. ECR sources, linear gridless sources. The Mark I, II, and III gridless ion sources. All sources are easily retrofitted. Options include variable angle load-lock capabilities. Full computer control.

Commonwealth Scientific was founded in 1966.

## CVI Laser Corporation

200 Dorado Pl. SE  
Albuquerque, NM 87123  
Phone: (505) 296-9541

Laser Optics, Lasers, Monochromators and Interferometers.

## E G & G Instruments, Inc.

23575 Cabot Blvd. #204  
Hayward, CA 94545  
Phone: 1-800-729-7271

Electro-Optical instrumentation for optical emission spectroscopy.

## EEV, Inc.

4 Westchester Plaza  
Elmsford, NY 10523  
Phone: (914) 592-6050  
Fax: (914) 682-8922  
Contact: Ann Sayers

EEV will exhibit state of the art Hydrogen Thyratrons. Literature will be available describing tubes capable of switching 100 KA at 100 KV.

Also available will be Ignitron data, featuring low voltage, high current switching with a large coulomb transfer.

## ENI

100 Highpower Rd.  
Rochester, NY 14623-3498  
Phone: (716) 427-8300  
Fax: (716) 427-7839

Products displayed will be bench-mount radio frequency plasma generators and matching networks.

# GEC '91 Exhibitors

## Extrel Corporation

575 Epsilon Drive  
Pittsburgh, PA 15238  
Phone: (412) 963-7530  
Fax: (412) 963-6578

Extrel Corporation, formerly Extranuclear Laboratories, is the premier manufacturer of Quadrupole Mass Spectrometers Systems and Parts. Since its beginning in 1964, its product line has grown from the original Research Components to include a full range of mass spectrometers.

Extrel's Research Components systems and parts include: Quadrupole Power Supplies with mass ranges up to 4000 amu; Quadrupole Mass Filters - 9.5 mm, 16mm and 19 mm diameter quadrupole rods; Electron Impact Ionizers - axial, crossbeam and direct inlet; and the Electronics of Quadrupole Mass Spectrometers. All are used in applications such as Thermal Desorption, High Performance RGA, Surface Analysis, Molecular Beam and Cluster Chemistry.

## Granville-Phillips Company

5675 Arapahoe  
Boulder, CO 80303  
Phone: (303) 443-7660  
Fax: (303) 443-2546

Productivity Enhancing Vacuum Measurement and Control:

Granville-Phillips Company (GPC) designs, manufactures and markets instrumentation designed to help increase vacuum system productivity. GPC vacuum gauges and controllers can be configured to measure and control pressure from 1000 Torr to  $5 \times 10^{-12}$  Torr with a large variety of display types, set points, and output options to fit specific application needs. GPC's all-metal valves include precision gas flow control valves for contamination-free operation from atmosphere to ultra-high vacuum, and a one-inch gold seal UHV shut-off valve.

## Huntington Mechanical Laboratories

1040 L'Avenida  
Mountainview, CA 94043  
Phone: (415) 964-3323

Huntington Mechanical Laboratories will exhibit a GEC Cell, UHV components and photos. Literature will be available.

## IBM Corporation

6001 Indian School NE  
Albuquerque, NM 87110  
Phone: (505) 888-2321  
Fax: (505) 888-2709  
Contact: David Moffatt

IBM RS/6000 RISC Workstation

Workstations offer a cost effective solution for both numerically intensive and more traditional computing applications. They are ideally suited for scientific and technological modeling, CAD/CAM, and many other applications.

The RS/6000 family of workstations from IBM provides a wide range of computing power for both single and multiuser environments, suitable for academic, industrial and business users. We will demonstrate the computational, graphic and communications capability of this family of systems.

## IOP Publishing, LTD

1411 Walnut Street, Suite 200  
Philadelphia, PA 19102  
Phone: (215) 569-2988  
Fax: (215) 569-8911  
Email [pidgeon@a1.relay.upenn.edu](mailto:pidgeon@a1.relay.upenn.edu)

IOP Publishing LTD is a division of the Institute of Physics, UK, publishing books and journals in physics and associated sciences and technologies under the "Adam Hilger" and "Institute of Physics" imprints.

IOP is announcing a new journal for 1991: Plasma Sources Science & Technology, a major new forum for the publication of research papers in this rapidly developing field.

## Key High Vacuum Products

36 Southern Blvd.  
Nesconset, NY 11767  
Phone: (516) 360-3970

Key High Vacuum Products' exhibit will consist of various high vacuum valves in stainless steel and brass, butterfly valves, KF Fittings, clamps and components. Also on display will be various photo displays of chambers, including GEC chambers manufactured by Key High Vacuum Products.

## LUCAS LABS

470B Lakeside Drive  
Sunnyvale, CA 94086  
Phone: (408) 732-3280  
Fax: (408) 732-0102  
Contact: Stefano Mangano or David Gray

LUCAS LABS Offers:  
Process Diagnostic Cart  
Process Monitor  
Wafer Temperature Monitor

The most advanced, most complete, most sophisticated computer-based diagnostic products for plasma systems.

LUCAS LABS Offers:  
R&D Plasma Systems (Vortex-V2)

The most advanced, most flexible, computer-based multiple chamber cluster architecture with the latest state of the art HELICON source.

## MCNC

P.O. Box 12899  
Research Triangle Park, NC 27709  
Phone: (919) 248-1436  
Contact: Steve Bobbio

MCNC (formerly the Microelectronics Center of North Carolina) will be exhibiting information on their newest design of a split cathode magnetron plasma etch reactor. The system uses a magnetic field parallel to the cathode to confine the plasma and couple it to the substrate being processed. A remote plasma source is incorporated within the same ExB drift region as the substrate. The remote source helps build plasma density and allows process optimization. This system has been used to uniformly etch polymer at 2  $\mu\text{m}/\text{min}$ . and it routinely achieves SiO<sub>2</sub> selectivities of 400 to 1 over polysilicon using bromine chemistry.

## MDC Vacuum Products Corporation

23842 Cabot Boulevard  
Hayward, CA 94545  
Phone: (510) 887-6100  
Fax: (510) 887-0626

MDC offers a complete line of UHV components including: flanges and fittings, valves, roughing components, Instrumentation, electrical feedthroughs, XYZ manipulators, rotary and linear feedthroughs and fast entry load-lock systems.

Featured products will be all-metal sealed right angle valves and M.E.S.A. compatible rectangular gate valves.

## Melles Griot

2251 Rutherford Road  
Carlsbad, CA  
Phone: (619) 438-2131  
Fax: (619) 438-5208  
Contact: Carrie L. Moore

The Melles Griot exhibit at GEC '91 will display our range of instrumentation designed specifically for laser and plasma tube beam diagnostics. Active demonstrations of our optical beam profiling and power measuring instruments will be presented. Literature describing our new Spectrum Analyzer, our range of Detector products, and the Melles Griot general catalog, Optics Guide 5, will also be available for attendees. The catalog describes our complete range of optical products and instruments such as spatial filter, beam expanders and microscopes.

## MKS Instruments

5330 Sterling Drive  
Boulder, CO 80301  
Phone: (303) 449-6841  
Fax: (303) 449-4721

MKS will exhibit its full line of Baratron® capacitance manometers; upstream and downstream pressure control systems; MassFlo® flow meters and controllers; SensaVac® thermocouple, Pirani, and hot and cold cathode ionization vacuum gauges; CalStand® calibration systems and components; and NGS partial pressure analysis instrumentation.



# GEC '91 Exhibitors

## Nor-Cal Products

1967 South Oregon Street  
 P.O. Box 518  
 Yreka, CA 96097  
 Phone: (916) 842-4457 inside CA  
 1-800-824-4166  
 Fax: (916) 842-9130

Nor-Cal will be exhibiting samples of its standard vacuum components, such as valves, foreline traps, flanges, fittings, flexible stainless steel hoses, electrical and liquid feedthroughs and viewports. Custom vacuum components, possibly including a GEC Reference Cell, will also be exhibited. A nine-minute video will show the company's facilities and describe in detail particular aspects of its manufacturing process, such as material selection, welding, machining, cleaning and inspection. Nor-Cal will be distributing its facilities brochure and will take requests for its 200-page binder catalog.

## Princeton Instruments, Inc.

3660 Quakerbridge Road  
 Trenton, NJ 08619  
 Phone: (609) 587-9797  
 Fax: (609) 587-1970

Princeton Instruments Inc., will show its LN cooled CCD detector system, part of its complete line of slow-scan, high dynamic range CCD camera systems. Detectors are available with up to 18 bits, 1242 X 1152 pixel resolution, shutter times as short as 5 nanoseconds, and low light level detectability down to single photon sensitivity. These complete systems can be interfaced to AT type machines using DMA, or to any other computers using GPIB. Bundled image acquisition/processing software support is available for AT and Macintosh machines.

Also shown will be a thermoelectrically-cooled CCD detector mounted on an Chromex/Aries 250IS. This incredibly flexible combination of complete Optical Spectrometric Multichannel Analyzer and imaging spectrograph has already proven itself in the field to be capable of collecting remarkable spectroscopic and spectral/spatial data from plasma and other systems.

## Springer-Verlag

175 Fifth Avenue  
 New York, NY 10010  
 Phone: (Orders) 1-800-SPRINGE(R)  
 Fax: (Orders) (201) 348-4505  
 Info: (212) 460-1577  
 Contact: Ken Quinn, Physics Product Manager

Springer's publishing programs in physics and engineering combine to offer you a broad selection of books on the theory and applications of plasma science, surface science, and laser materials processing. Important new and recent titles on display include Nishikawa's Plasma Physics, Drobot's Computer Applications in Plasma Science, Raizer's Atomic and Electronic Structure of Surfaces, and Svanberg's Atomic and Molecular Spectroscopy.

Please also stop by to enter your name into our mailing list system.

## Tektronix

1258 Ortiz SE  
 Albuquerque, NM 87108  
 Phone: (505) 265-5541

Optical sampling to 6 GHz  
 Electrical sampling to 50 GHz  
 Portable digitizers to 1 G sample/second  
 Transient digitizers to 4.5 GHz, single shot

"Tektronix is the industry leader in Test and Measurement equipment across a broad range of frequencies. Visit Tektronix's booth for a demonstration of new instrumentation for your laboratory."

## THT Sales Company

7216-D Washington NE  
Albuquerque, NM 87109  
Phone: (505) 344-6441  
Fax: (505) 344-0599  
Contact: John Barnes

THT Sales Company is currently in its 12th year of providing high vacuum components and systems to the semiconductor industry, private and national laboratories, universities and consortium groups. The following companies will be represented at the THT Sales Exhibit.

**APD CRYOGENICS:** Cryogenic Pumps and Helium Refrigeration Lab Systems.

**ASTEX:** Microwave Plasma Systems (Diamond Film, Etch, CVD, MBE, etc.)

**ADVANCED ENERGY:** DC Magnetron Drives, RF Generators, Ion Source Drives

**PERKIN ELMER:** Ion Pumps and UHV Systems.

**PLASMQUEST:** Microwave plasma systems for etching, deposition, CVD processes.

**SPECTRA INSTRUMENTS:** Quadrupole Residual Gas Analyzers. Single-head and multi-tasking units.

**XINIX:** Plasma Etch End Point Controllers and Deposition Rate Monitors.

## UNM College of Engineering

College of Engineering - Univ. of New Mexico  
Albuquerque, NM 87131  
Phone: (505) 277-4354  
Contact: Gail Ward

The College of Engineering at the University of New Mexico offers graduate educational and research programs for students wishing to pursue studies in applied plasma physics and related ionized gas physics applications. A description of coursework and research provided through the departments of Chemical, Nuclear and Electrical Engineering will be provided.

Emphases in research and studies include: low temperature plasma processing, high temperature plasma fusion, and pulsed power applications.

## UNM

### Center for High Technology Materials

CHTM, University of New Mexico  
Albuquerque, NM 87131  
Phone: (505) 277-3317  
Fax: (505) 277-6433  
Contact: Steve Brueck

The Center for High Technology Materials (CHTM) at the University of New Mexico is a major university research center with programs in optoelectronics and microelectronics. The center features a vertically integrated structure that includes: materials growth, processing device development and integration. A sensitivity to manufacturing possibilities and constraints is maintained thru a SEMATECH program in *metrology for semiconductor manufacturing*. Major thrusts in optoelectronics include MOCVD growth of III-V materials, nonlinear optical thin films, nanostructure fabrication, high-power diode lasers and arrays, surface emitting-lasers, two-dimensional interconnects, high-speed optoelectronics, and diode-based visible sources. The focus of the microelectronics program is the development of metrology and on-line analysis tools for monitoring the semiconductor manufacturing process. Emphases include: chemometrics for thin films and for plasma processes, scanning force microscopy, scatterometry and alignment and overlay measurement.

**44th Annual  
Gaseous Electronics Conference**

**SCIENCE TEACHERS DAY  
PROGRAM**

**Picuris Room**

( lower level - convention center)

8:30 AM - 3:30 PM - Thursday, October 24

## NEW FRONTIERS IN PHYSICS AND CHEMISTRY

sponsored by  
 44th Annual Gaseous Electronics Conference  
 The American Physical Society  
 American Vacuum Society: New Mexico Chapter

Science Teacher's Day  
 Thursday, October 24, 1991 – Picuris Room Albuquerque Convention Center  
 Program Agenda

- 8:30 – 8:40      **Welcome by Dr. Harold M. Anderson**  
 The University of New Mexico, Secretary GEC '91  
 Dr. Brian B. Schwartz, American Physical Society  
 Dr. Chuck Peden, American Vacuum Society: NM Chapter
- 8:40 – 9:50      ***The Preparation of Diamond Films and their Applications***  
 Dr. L. W. Anderson, University of Wisconsin
- 10:10 – 11:45    ***Using Microcomputer Based Laboratories in Science Instruction***  
 Dr. Nancy Bell, University of Houston  
 Assisted by:    Tim Black, La Cueva High School, Albuquerque  
                      Bruce Bell, Sandia High School, Albuquerque
- 12:30 – 1:30    ***Fractals in the the Classroom***  
 Speakers:        Dr. Eugene Stanley, Boston University  
                      Paul Hickman, Recipient of the Presidential Medal for  
                                  Excellence in Science Teaching, 1990
- 1:30 – 3:00      ***A New Mexico Science Teacher's Resource Council***  
 Los Alamos National Laboratory – Judith Kay  
 Sandia National Laboratories – Steve Ortiz  
 UNM, College of Engineering – Gail Ward  
 IBM – Chuck Brink, Nancy Bell  
 Intel – Karen Sibbett  
 American Physical Society – Brian Schwartz  
 American Vacuum Society: NM Chapter – Chuck Peden
- 3:00 – 3:30      Discussion of Local Physics Alliances for New Mexico Teachers
- 3:30 – 5:00      Open Attendance to Gaseous Electronics Conference  
 Poster Paper Session//Scientific Equipment and Literature Exhibit

## INDEX OF AUTHORS

<b>A</b>		Belenguer, P.	AA-4
Abouaf, R.	HB-3	Bell, D.E.	PA-5
Adachi, N.	JB-4	Benjamin, N.M.P.	CA-5, DA-7
Al-Assadi, K.F.	JA-6	Benoit, C.	HB-3
Alberta, M.P.	NB-4	Benson, D.A.	RA-8
Alexandrovich, B.M.	AA-3, DB-2	Bentson, J.	JB-3, MA-9, QB-8
Alle, D.T.	EB-8	Bernat, I.	HC-6
Alves, L.L.	JB-10	Berry, L.A.	PD-2
Anderson, C.A.	PB-11	Beying, A.	HC-7
Anderson, H.M.	BB-2, DB-17, DB-18, JA-7, JC-5, JC-7	Bhattacharya, A.K.	EA-3
Anderson, L.W.	HB-7, JA-4	Bierbaum, V.M.	CB-2
Apai, P.	JB-6, MA-4	Billing, G.D.	MB-3, MC-7
Armstrong, R.A.	PA-1	Birdsall, C.K.	DB-8, DB-9
Arnold, J.C.	NB-2	Blain, M.	JA-7
Ashtiani, K.A.	PB-6	Bletzinger, P.	DB-22, JC-4, RB-1
Atems, D.E.	HB-11	Blondeau, J. Ph.	BA-5
<b>B</b>		Blumberg, W.A.M.	PA-1
Bacal, M.	PA-6	Blumer, W.	BB-5
Bailey, J.E.	RA-7	Boesten, L.	HB-2
Bailey, Wm. F.	PA-5	Boeuf, J. P.	AA-4, JB-5, MA-2, NB-3
Baluja, K.L.	EB-5, HB-14	Bohm, C.	AA-4
Bannister, M.	BB-4	Bolton, P.R.	PC-6
Bardsley, J.N.	NA-3	Bonham, R.A.	EB-4, HB-4
Barnes, M.S.	BA-7	Booth, J.P.	NB-4, PB-8
Barone, S.	JB-3, MA-9, QB-8	Bordelon, D.	LB-2
Bartschat, K.	LB-3	Borysow, J.	MC-4
Bayer, R.	LA-7	Boswell, R.W.	AA-7, CA-3, JA-11, JB-12, PD-4, RB-4
Beck, S.E.	BA-3	Bouchoule, A.	BA-5
Becker, K.H.	AB-4, EB-3		
Bederson, B.	LB-1		

Boufendi, L.	BA-5	Cecchi, J.L.	BB-4, RB-2
Brake, M.L.	DB-26, RB-3	Cernyar, E.W.	MB-2
Brennan, M.J.	EB-7	Chang, C.	QB-3
Breun, R.	PD-7	Chantranupong, L.	HB-12
Brewer, M.A.	PD-5	Chapman, B.N.	CA-5, DA-7, JA-13
Brown, I.G.	PD-5	Charles, C.	QB-5
Brown, N.E.	JC-7	Chen, C.	CA-6
Brown N.M.D.	JA-6	Chen, F.F.	CA-4
Bruce, M.R.	EB-4, HB-4	Chen, L.	NA-5
Brunger, M.J.	EB-8	Choi, S.J.	JC-2
Bryant, H.C.	AB-3	Christophorou, L.G.	AB-5
Bubelev, V.	LB-8	Chu, H.N.	JA-4
Buckman, S.J.	EB-8	Cid-Aguero, P.	HB-9
Budinger, A.B.	LA-5	Ciferno, T.M.	PA-4
Buenker, R.J.	HB-12	Clarke, A.S.	NB-1
Buie, M.	DB-26	Clay, J.T.	HB-9
Burke, P.	LB-3	Cohen, R.H.	DB-8
Burkes, T.R.	QA-4	Colgan, M.J.	DB-27
Burns, B.F.	MB-6	Collett, W.L.	HC-10, MA-16,
Burrow, P.D.	MC-9, MC-10	Collins, G.J.	JB-4, JB-7, MA-1, MA-4, MA-6
Byszewski, W.W.	LA-5		
<b>C</b>			
Cacciatore, M.	MB-3, MC-7	Cook, J.M.	CA-2
Caledonia, G.E.	MC-2	Cornelius, W.D.	JA-2
Campbell, R.B.	MA-14	Corr, J.J.	HB-6
Cao, Y.S.	MC-14	Cortazar, D.	PB-7
Capitelli, M.	MB-3, PA-6	Coultas, D.K.	BA-7
Caporusso, R.A.	MC-7	Csanak, G.	LB-7
Cappelli, M.A.	JB-11, JB-13		
Cappelli, M.C.	QB-3	<b>D</b>	
Carlile, R.N.	BA-2, BA-3	Dakin, J.T.	LA-3
Carlson, A.L.	RA-7	Dalvie, M.	HC-3
Cartwright, D.C.	LB-7	Damelincourt, J.J.	HC-5
Castagna, T.J.	PB-6	Daugherty, J.E.	BA-6
Catherine, Y.	QB-5	Davies, A.J.	PC-5

Davies, D.K. NB-5  
 De Benedictis, S. PB-12  
 De Felice, P. MB-3  
 DeJoseph, Jr., C.A. MA-13  
 Delalondre, C. LA-8  
 Demeio, L. RB-7  
 Den Hartog, E.A. DA-1, JA-1, JA-4

Derouard, J. NB-4, PB-8  
 Determan, D. MC-3  
 Dickinson, M.R. PD-5  
 Dilecce, G. PB-12  
 Dillon, M. HB-2, HB-12  
 Dipeso, G. DB-8  
 Djurovic, S. DB-23  
 Doering, J.P. DB-5  
 Downes, L.W. PB-9  
 Drallos, P.J. DB-16, JB-8  
 Dressler, R.A. CB-3  
 Duffy, M. HC-4  
 Dulick, M. JA-2  
 Dunlop, J.R. JA-5  
 Durandet, A. RB-4  
 Dutton, J. PC-5  
 Dye, R.C. BB-7  
 Dzelzhalns, L.S. PA-1

## E

Eccles, V. PA-1  
 Eckstrom, D.J. MC-15  
 Eddy, Jr., C.R. DA-6  
 Eddy, T.L. HC-9  
 Elizondo, J.M. PC-1  
 Elta, M. DB-26, RB-3  
 Emmert, G.A. BB-8  
 Ernie, D.W. JB-14

## F

Farouki, R. HC-3  
 Ferrerira, C.M. JB-10  
 Filuk, A.B. RA-7  
 Flamm, D.L. RB-5  
 Fleddermann, C.B. JA-9  
 Floyd, K. PC-8  
 Flynn, C. LB-4, LB-5  
 Fohl, T. LA-1, LA-2  
 Foltin, M. EB-1, EB-6  
 Foltyn, S.R. BB-7  
 Forster, J.C. BA-7, CA-8  
 Friedman, J.R. AB-4

## G

Gallagher, A. HB-8, MB-1  
 Galvin, J.E. PD-5  
 Ganguly, B.N. JA-3, JC-4  
 Garcia, P. QB-5  
 Gardner, J.A. CB-3  
 Garscadden, A. DB-22, JA-3, JC-4

Gates, D. CA-7  
 Geha, S. BA-2, BA-3  
 Gerdin, G.A. QA-2  
 Gielen, H. MA-2  
 Giroult-Matlakowski, G. RB-4  
 Godyak, V.A. AA-3, DB-1, DB-2, EA-2

Goembel, L. HB-5  
 Goertz, C.K. BA-1  
 Gonzalez, F. PC-8  
 Gorbatkin, S.M. PD-2  
 Goree, J. JC-3  
 Gorse, C. PA-6  
 Goto, T. DA-8





**J**

Jacob, J.H. RA-2  
 Jain, A. EB-5, HB-14  
 Janossy, M. JB-6  
 Jarnyk, M.A. JB-12  
 Jelenkovic, B.M. PA-7, PA-8  
 Jenq, J.S. PB-5  
 Jensen, K.F. JB-2, QB-7  
 Jewett, R. JA-7  
 Johnsen, R. CB-6, MC-14  
 Johnston, A.R. MC-9  
 Jordan, K.D. MC-9  
 Joshi, R. QA-2

**K**

Kaddani, A. CA-8  
 Kaibeshev, V. QA-4  
 Kakuta, S. DB-28  
 Keinigs, R.K. JC-5  
 Keller, J.H. BA-7, CA-8  
 Kempka, S.N. RA-8  
 Khakoo, M.A. LB-2  
 Kilgore, M.D. BA-6  
 Kimura, M. HB-2, HB-10,  
 HB-12, MC-5  
 Kirkman, G. QA-3  
 Kline, L.E. NB-5  
 Knutsen, K. CB-2  
 Koike, T. PB-1  
 Kovall, G. CA-6  
 Kramer, J. LA-2  
 Kreig, K.R. DA-7  
 Krishnan, U. HB-13  
 Kumar, D. DA-3

Kunhardt, E.E.

HA-1, HA-6,  
 HA-11, JB-3,  
 MA-9, NB-6,  
 PB-3, QB-8,  
 RB-8  
 HA-11, PB-3  
 AA-8, BA-4,  
 BB-1, DB-13,  
 JC-2, PC-7,  
 QB-1, QB-4,  
 RA-3, RA-6

Kuo, S.C.

Kushner, M.J.

**L**

Lagally, M.G. JA-4  
 Lagushenko R. EA-2  
 Lai, C. PD-7  
 Lam, K.Y. HA-9  
 Lam, S.W. DA-5, JA-1  
 Lamm, A. CA-6  
 Lampe, F.W. CB-7  
 Lane, N.F. MC-5  
 Laure, C. BA-5  
 Lawler, J.E. EA-1, HB-7,  
 HC-1, JA-4,  
 LA-4, PC-9  
 LeClair, L.R. HB-6  
 Lefkow, A.R. JA-4  
 Legentil, M. PA-3  
 Lengsfield, B.H. HB-15  
 Leone, S.R. CB-2  
 Lester, J. LA-1, LA-2  
 Li, C. DB-14  
 Li, L. MA-4, MA-11  
 Li, Y.M. LA-5, LA-6  
 Li, Z. HC-11, HC-12  
 Lichtenberg, A.J. AA-6, DB-10

Lieberman, M.A.	AA-6, DB-8, DB-9, DB-10, DB-12, MA-5, RB-5	McCaughey, M.J.	BA-4, JC-2
Lim, K.P.	CB-7	McClain, R.L.	DA-2
Lin, C.C.	HB-7	McConkey, J.W.	HB-6, LB-6
Lin, Y.	DB-30	McCulla, W.H.	QB-2
Liu, J.	QB-6	McDuff, G.	QA-4
Liu, Y.	RB-3	McGlynn, S.P.	DA-3
Lockwood, R.B.	HB-7	McGrath, R.T.	DB-16, MA-14
Lohmann, G.	HC-8	McLane, G.F.	NA-4
Lubell, M.S.	AB-4	McVey, J.B.	PC-9
Lujan, A.	DB-26	McVittie, J.P.	DB-29, JB-16
Luo, L.	DB-30, HA-8	Meeks, E.	JB-13
<b>M</b>		Mellon, K.N.	MC-12
Ma, C.	HB-4	Menard, J.	PD-3
MacAdam, K.B.	CB-1	Mentel, J.	LA-7, PB-2
MacGill, R.A.	PD-5	Merkel, H.	HC-8
Madison, D.H.	LB-3, LB-8	Meyer, F.W.	MB-4
Mahajan, S.M.	MC-10, MA-16	Meyer, J.D.	MA-1, MA-11
Mahoney, L.J.	DA-2	Meyyappan, M.	JB-9, NA-4
Makabe, T.	AA-5, DB-28, PB-1	Mezei, P.	JB-6
Mansky, E.J.	MC-6	Michels, H.H.	CB-5
Mantei, T.D.	CA-1	Millard, M.W.	JA-12
Marconi, M.C.	PB-7	Miller, P.A.	DB-17, DB-19
Marcum, S.D.	PA-4, PB-9		DB-20
Margot, J.	NA-6, PD-1	Miller, T.A.	JA-5
Margot-Chaker, J.	PD-4	Minoos, H.	LA-8
Margreiter, D.	EB-1	Mirrashidi, P.	DB-9
Marinkovic, B.	HB-8	Mitsubishi, K.	HC-1, LA-4
Mark, T.D.	EB-1, EB-6	Mock, J.L.	DB-18
Maron, Y.	RA-7	Moeny, W.M.	PC-1
Masters, M.F.	MC-1	Moisan, M.	NA-6, PD-1
Matallah, M.	PC-5	Morris, R.A.	CB-5
		Morrow, T.	MB-6, PB-10
		Muenshausen R.E.	BB-7
		Mukhametzianov, R.E.	JC-6
		Murad, E.	CB-3
		Murnick, D.E.	DB-27

**N**

Naidu, M.S. PC-2  
 Naito, M. DA-8  
 Nakano, N. AA-5, DB-28  
 Nakano, T. JA-11, PD-4  
 Nash, T. RA-7  
 Neiger, M. HC-8  
 Nentwig, R. PB-2  
 Nguyen, H. CA-7  
 Niazi, K. RB-5  
 Nitschke, T.E. DB-5  
 Nogar, N.S. BB-7

**O**

O'Brien, T.R. LA-4  
 O'Neill, J.A. BA-7  
 Oliphant, T.A. JC-5  
 Olthoff, J.K. DB-23, DB-24,  
 DB-25  
 Ong, P.P. HA-9  
 Orel, A.E. CB-4  
 Ouadoudi, N. JB-5  
 Overbury, S.H. MB-4  
 Overzet, L.J. DB-30, HA-8

**P**

Pachter, L. MC-3  
 Pak, H. PC-7, RA-6  
 Pang, S. RB-3  
 Parker, G.J. PC-9  
 Pasquiers, S. PA-3  
 Passow, M. DB-26, RB-3  
 Paulson, J.F. CB-5  
 Pearl, D.M. MC-10  
 Pekker, L. HA-10, JB-14  
 Pelletier, J. NA-2

Peltzer, E. CA-7  
 Pender, J. DB-26, RB-3  
 Penetrante, B.M. NA-3  
 Peres, I. JB-5, MA-2  
 Perkins, T.T. RA-2  
 Perrin, J. AA-4  
 Perry, A.J. CA-3, PD-4  
 Persing, H. DA-1, JA-1,  
 RB-4  
 Peterson, J.R. MC-11, MC-16  
 Petrovic, Z.Lj. PA-2, PA-7,  
 PA-8  
 Peyraud-Cuenca, N. HA-5  
 Phelps, A.V. MC-4, PA-2,  
 PA-7, PA-8  
 Piejak, R.B. AA-3, DB-2  
 Piekarek, J. QA-2  
 Pinnaduwege, L.A. AB-5  
 Pitchford, L.C. JB-5, MA-2,  
 NB-3  
 Plagnol, V. HC-5, HC-6  
 Plain, A. BA-5  
 Plano, L.S. JB-1  
 Pochan, P.D. DB-19  
 Poll, H.U. EB-1  
 Popovic, S. JB-3, MA-9,  
 QB-8  
 Popp, H.P. HC-7, HC-8  
 Porteous, R.K. BA-6, RB-6  
 Postma, P. MA-2  
 Preppernau, B.L. JA-5  
 Puech, V. PA-3

**R**

Rao, M.V.V.S. AB-6, EB-2  
 Rescigno, T.N. HB-15

Resnick, P.J.	JC-7	Saxon, R.P.	MC-8
Rey, J.	JB-16	Scanlan, J.V.	AA-2
Rhinehart, R.R.	MA-7	Schamiloglu, E.	AB-2
Rhoades, R.L.	RA-4	Schmieder, R.W.	MA-14
Riehl, K.	MC-3	Schneider, B.I.	HB-15
Riemann, K.U.	MA-8, NB-8	Schoenbach, K.H.	QA-2
Riley, M.E.	JB-8, DB-16	Scholes, G.	BB-4
Riva, R.	PA-3	Searles, S.K.	MC-1
Roberts, J.	DB-24	Sebastian, A.A.	HA-4
Roberts, J.R.	DB-23	Sekiguchi, A.	NA-5
Rocca, J.J.	PB-7, PC-8	Self, S.A.	DB-29, JB-11
Rodriguez, A.E.	PC-1, PC-3, PC-4, QA-1, RA-5	Selwyn, G.S.	JC-1
Rodriguez, R.	MA-10	Shan, H.	DB-29, JB-11
Rognlien, T.D.	DB-8	Shankar, S.	JB-2, QB-7
Rosocha, L.A.	QB-2	Sharpton, F.A.	HB-7
Rozsa, K.	JB-6, MA-4, MA-11, MB-1	Shaw, D.M.	JB-4
Rubin, G.	JB-6	Sheehy, J.A.	MB-5
		Sheng, T.	JB-7
		Sheng, T.Y.	JB-4, MA-6
		Sheridan, T.E.	JA-10
		Shi, B.	JB-7, MA-6, MA-11
<b>S</b>		Shimura, N.	AA-5, PB-1
Sadeghi, N.	JA-11, PD-4	Shizgal, B.	NB-1, RB-7
Sadeghi, N.	PB-8	Shohet, J.L.	PB-6
Saita, M.	MA-1	Shon, J.W.	RA-3
Sakai, A.	DA-8	Shyn, T.W.	HB-1
Sakai, Y.	HA-7	Sierocinski, R.C.	BB-2, JC-5
Sakeek, H.F.	PB-10	Simek, M.	PB-12
Salter, R.H.	CB-3	Simonin, O.	LA-8
Salvadori, M.C.	PD-5	Singh, V.	MA-7
Saraswat, K.C.	QB-3	Slanger, T.G.	BB-6
Sartwell, B.D.	DA-6	Smith, B.	JA-7
Sata, H.	HB-2	Smith, H.	AA-7
Sato, A.H.	DB-12	Snyder, H.	JA-9
Sawin, H.H.	DB-4, NB-2, QB-6		

Sobolewski, M.A.	DB-23, DB-24, DB-25	Teich, T.H.	BB-5
Sommerer, T.J.	AA-8, BA-4, DB-13, JC-2, PC-7, QB-1	Tessnow, T.	QA-2
Sonnenfroh, D.M.	MC-2	Tochikubo, F.	DB-28
Soules, T.F.	EA-3	Tomasei, F.	PB-7
Spence, D.	HB-2, HB-12	Toogood, M.	BA-5
Splichal, M.P.	DB-17, DB-18	Tosh, R.E.	CB-6
Srivastava, S.K.	AB-6, EB-2	Tran, T.	LB-2
Stalder, K.R.	JA-8, MC-15, PB-11	Trevor, D.J.	JA-11, PD-4
Stevelfelt, J.	PB-9	Trow, J.R.	CA-2
Stevens, J.E.	RB-2	Tsai, J.H.	DB-15,, HA-2
Stewart, R.A.	MA-5	Tserepi, A.D.	JA-5
Stout, P.J.	QB-1	Tucker, J.E.	MC-1
Stumpf, B.	HB-13, LB-4, LB-5	Tupa, D.	JA-2, MC-13
Stutzin, G.	MB-1	Turner, M.M.	DB-3, MA-3
Sugawara, H.	HA-7		
Sugimoto, D.	MA-1	V	
Sung, K.	RB-3	Vahedi, V.	DB-8, DB-9, MA-5
Surendra, M.	DB-5, DB-7, JB-1	Van Brunt, R.J.	DB-25, MB-2
Surrey, E.	BB-3	Van Os, C.F.	JA-13
Swain, J.E.	PC-6	Van Os, R.	CA-5
Swenson, D.R.	JA-2, MC-13	van Dyck, O.B.	JA-2, MC-13
Syljuasen, A.	JB-3	VanDevender, J.P.	F-1
Szapiro, B.	PB-7	Varnas, A.K.	MA-7
T		Venkateshaiah, G.R.	PC-2
Tagashira, H.	HA-7	Ventrice, C.A.	HC-10
Tanaka, H.	HB-2	Ventzek, P.	DB-26
Targove, J.	MA-15	Verdeyen, J.T.	DB-20, RA-4
Tarnovsky, V.	EB-3	Vicharelli, P.A.	LA-1
Taylor, J.W.	PB-5	Vidmar, R.J.	MC-15
		Viggiano, A.A.	CB-5
		Vitello, P.A.	NA-3
		Vogtlin, G.E.	NA-3, PD-6
		Vuskovic, L.	LB-1

**W**

Wadehra, J.M.	HA-4, HB-11	Young, C.M.	RA-5
Walder, G.	EB-6	Young, F.	NB-7
Walmsley, D.G.	PB-10	Yu, Z.	JB-4,
Walter, C.W.	MC-11		JB-7,
Walters, E.A.	HB-9		MA-1,
Wamsley, R.C.	HC-1, LA-4		MA-6,
Wang, P.	HB-8	Yuasa, K.	MA-11
Wang, S.	LB-6		PB-4
Warner, D.	MA-10	<b>Z</b>	
Waters, R.	PC-5	Zehner, D.M.	MB-4
Waymouth, J.F.	EA-4, HC-2	ZeijlmansVanEmmichoven,P.A.	MB-4
Wei, Z.	LB-4, LB-5	Zissis, G.	HC-5,
Wells, F.V.	DB-22, MA-10		HC-6
Wells, W.E.	PB-9		
Wendt, A.	DB-11, PD-7		
Werner, P.W.	AB-2		
Wexler, B.L.	MC-1		
Whetstone, J.R.	DB-24		
White, M.G.	PC-1		
Winkler, C.	EB-1		
Wood, B.P.	AA-6, DB-9,		
	DB-10		
Woods, C.	PD-7		
Woods, R.C.	DA-1, DA-2		
Woodward, P.	MA-10		
Woodward, M.	LB-8		
Wu, C.	DB-14, DB-15,		
	HA-2, NB-7		
Wu, X.D.	BB-7		

**Y**

Yaney, P.P.	JA-12
Ying, C.H.	LB-1
York, R.L.	JA-2, MC-13
Youchison, D.L.	DA-6

# 44th Annual Gaseous Electronics Conference

October 22 - 25, 1991

Albuquerque Convention Center  
Albuquerque, New Mexico

Tuesday, October 22		Wednesday, October 23		Thursday, October 24		Friday, October 25	
AA. 0800-1000 Glows I  Ballroom A	AB. 0800-1000 Multiphoton Processes and Negative Ions  Ballroom B	EA. 0800-1000 Cathodes in Discharges: A Review  Ballroom A	EB. 0800-1000 Ionization and Electron Collisions  Ballroom B	LA. 0800-1000 Lamps and Cathodes  Ballroom A	LB. 0800-1000 Electron Excitation and Ionization  Ballroom B	QA. 0800-1000 Ionized Gas Physics in Pulsed Power  Ballroom A	QB. 0800-1000 Glows II  Ballroom B
Break							
BA. 1015-1215 Particulates in RF Discharges  Ballroom A	BB. 1015-1215 Collision Processes in Discharges  Ballroom B	Welcome		M. 1015-1215 - Posters Glows, Plasma Surface Interactions, Heavy Particles and Negative Ions  Ballroom C	RA. 1015-1215 Lasers and Switching  Ballroom A	RB. 1015-1215 ECR and Induction Plasmas  Ballroom B	
		F. 1030-1130 Plenary Lecture					
		G. 1130-1200 Business Meeting  Ballroom A					
Lunch							
CA. 1330-1530 Comparison Session on High Density Plasmas  Ballroom A	CB. 1330-1530 Dissociation and Heavy Particle Collisions  Ballroom B	H. 1330-1530 - Posters Transport, Electron and Photon Collisions, Lamps  Ballroom C		NA. 1330-1530 Alternative Applications for Plasma Processing  Ballroom A	NB. 1330-1530 Discharge Models  Ballroom B	Adjourn	
Break							
D. 1530-1730 - Posters Diagnostics, GEC Reference Cell and Related RF Discharge Measurements and Modelling  Ballroom C		J. 1530-1730 - Posters Optical and Probe Diagnostics, Glows, Particles in Plasmas  Ballroom C		P. 1530-1730 - Posters Collisions in Plasmas, Emission Spectroscopy, Pulsed Power, Alternative Applications for Plasma Processing  Ballroom C			
		K. 1900-2100 Workshop on GEC Reference Cell Issues  Ballroom A		Social Hour 1830-1930 Banquet 1930-2130 Hyatt Regency Grand Pavilion			